High Temperature Stress on Cereal Photosynthesis: a Re-evaluation

By

Najla Abdullah Almalki

Submitted in Fulfilment of the Requirement for the Degree of Doctor of Philosophy

School of Life Sciences
College Medical Veterinary and Life Sciences
University of Glasgow,
U.K.

July, 2014

N. A. Almalki

Abstract

Under natural conditions, crop plants are likely to experience high leaf temperatures that reduce plant growth, reproduction, and photosynthesis, which impact dramatically on crop yield. Some wild plants such as Agave can withstand prolonged periods of T_{leaf} in excess of 55^0C but the mechanisms of thermotolerance are unclear at present. To establish whether there is sufficient genetic diversity to be exploited for developing heat tolerant crops, a comparative study was conducted to assess the effects of high leaf temperatures (T_{leaf}) on two barley lines (C3, Optic and Local) and two maize lines (C4, Sundance and Katumani) that are routinely grown in temperate and sub-tropical regions, respectively, in addition to the obligate C3 plant *Yucca filimentosa* that is endemic to hot arid habitats. Gas exchange measurements show light saturated CO_2 assimilation rates ($\mathbf{A_{sat}}$) and the carboxylation coefficient (the efficiency of CO_2 fixation, $\mathbf{\Phi CO_2}$) were irreversibly suppressed to approximately 20% of their pre-treatment levels immediately after raising T_{leaf} to 38.0 (± 0.2 ^{0}C) for 3 hours in all lines regardless of their origins (temperate or sub-tropical), and this inhibition was not attributed to stomatal closure. In contrast, *Y. filimentosa* showed a close correspondence between $\mathbf{A_{sat}}$ and stomatal conductance ($\mathbf{g_s}$) in response to leaf temperatures between 36° to 40°C with a marked suppression immediately after heat stress and rapid full recovery following one hour of release from stress. Above 40°C however, stomata respond differently by opening and increase $\mathbf{g_s}$. This pattern suggested the response of stomata in *Y. filimentosa* is regulated by temperature.

There is a general consensus that the primary site of thermal injury to CO_2 assimilation is RuBisCO Activase but this is contentious. In this study the effects of high leaf temperatures (T_{leaf}) on photosynthetic efficiency of barley were re-investigated. Parallel measurements using a range of techniques confirmed that the suppression of $\mathbf{A_{sat}}$ was not attributable to Maximum Quantum Efficiency of PSII (**ΦPSII**), or changes in the light harvesting capacity (leaf absorbance, Chl*a* fluorescence excitation spectra), or *in vitro* electron transport rates. Metabolomics profiling of heat stressed and control leaves showed that carbon flow between Ribose 5-phosphate (Ri5P) and 3-phosphoglycerate (3-PGA) was severely impaired by heat stress, consistent with the assertion that $\mathbf{A_{sat}}$ was suppressed by inhibition of RuBisCO activity. Surprisingly, enzyme-linked assays on RuBisCO prepared from leaves exposed to 38.0° (± 0.2°C) for 3 hours showed unequivocally that RuBisCO activity was not affected suggesting the substrates for RuBisCO (CO_2 and/or RuBP), rather than RuBisCO activity itself, accounted for the decrease in carbon flow from Ri5P to 3-PGA. These studies also showed that the standard procedures for isolating RuBisCO from

cereal leaves lead to a partial re-activation of RuBisCO resulting in false conclusions on the *in vivo* activation state of the enzyme. The implications of these results are discussed. In intact barley leaves, the suppression in $\mathbf{A_{sat}}$ was not reversed by increasing external CO_2 (**Ca**) to 1000 μmol CO_2. mol^{-1} air suggesting chloroplast CO_2 levels were not limiting. *In vitro* assays demonstrated the activities of Ri5P isomerase and phosphoribulose kinase (PRK) were not affected by these heat stress treatments. In contrast, measurements on leaf ATP levels and *in vivo* electron transport rate (ETR) showed a parallel and dramatic decline (>75%).

Post-illumination chlorophyll fluorescence relaxation (light-to-dark transition) was used to assess the magnitude of the proton motive force (pmf) across the thylakoid membrane of control and heat stressed leaves. Heat stress increased the relaxation half time (t½) from 45 to 180 seconds suggesting a decrease in proton conductance through the ATP synthase, and thus a decrease in leaf ATP levels[1].

Taken together these results suggest high leaf temperatures lead to a decrease in chloroplast ATP levels and this suppresses the synthesis of Ribulose 1,5-Bisphosphate by the C3 Cycle; carbon flow through RuBisCO is impaired and thus whole leaf photosynthesis rates decline severely.

[1] Some of the work in this thesis has been presented in two scientific meetings as:

1. Poster at Society for Experimental Biology (SEB), annual main meeting in Glasgow from 1st to 4th July 2011.
2. Oral presentation at Mini-Symposium on Photosynthesis by The Rank Prize Funds in Wordsworth Hotel, Grasmere, Cumbria, UK from 8th to 11th October 2012.
3. Poster at Society for Experimental Biology (SEB), annual main meeting in Manchester from 1st to 4th July 2014.

Table of Contents

List of Tables

List of Figures

Acknowledgements

بسم الله الرحمن الرحيم

In the name of God, the most merciful, the most kind.

I would like to express my sincere gratitude to my supervisor/friend Dr. Pere Dominy for his endless encouragement and support in all the time of research and writing of this thesis, for his patience, motivation, enthusiasm, and immense knowledge. He was always there to listen with care to my problems as if they were his and answer all my questions with a smile. Thank you for inspiring me to challenge myself and be a better scientist.

I would like also to thank all my colleagues in Arrnot lab and Bower building group for their help, encouragement and comments. Thank you for providing such a friendly, dynamic and supportive research environment.

My sincere thanks also go to Prof Martin Parry from Rothamsted Research for providing me with Purified wheat RuBisCO.

I wish to thank all my colleagues at my home university: King Abdulaziz University for their support. Funding for this project was provided by the Ministry of Higher Education of Saudi Arabia, and for that I am thankful.

I have been blessed with an incredibly supportive family; thank you my lovely parents for encouraging me to follow my dreams, brothers, sisters, beautiful niece and aunts for supporting me spiritually throughout my life. Special thanks to my best friend Dr. Mabrouka Altowati for her well-wishes and being there whenever I need a friend.

Finally, the ability and motivation required to complete this thesis are a gift from God, and for that I will always be grateful. I would like to end these acknowledgements with a quote from the 'Quran':

"وما توفيقي الا بالله عليه توكلت واليه انيب".

"My success can only come from Allah: in Him I trust and unto Him I turn".

Declaration

I declare that the work presented in this thesis is my own work, with the exception of the data that are presented in Table 4-1, which was pooled, with permission, from work obtained during previous studies in our laboratory and submitted by Shahwani, M. N. (2011) for a PhD degree in the University of Glasgow and carried out by Dr. Stéphanie Arrivault at the Max Planck Institute of Molecular Plant Physiology, Germany. This thesis has not been submitted in any previous application for any other degree in the University of Glasgow or any other institution.

Dedication

This thesis is dedicated to my family, this journey would not have been possible without you and especially for you father, you always said: **Be Brave**.

Abbreviations

A	CO_2 Assimilation Rate
A_{max}	Maximum CO_2 Assimilation Rate
A_{sat}	Light Saturated CO_2 Assimilation Rates at 380 µmol CO_2 mol^{-1}air.
ADP	Adenosine diphosphate
ADPG	ADP-glucose
AMP	Adenosine monophosphate
anti-*rbc*S	Anti RuBisCO small subunit
ATP	Adenosine Tri Phosphate
AtpC	ATP-Synthase γ-Subunit
C_a	Air CO_2 Concentration
C_c	Chloroplast CO_2 Concentration
C_i	Internal CO_2 Concentration
C_{ref}	Chamber CO_2
CA1P	2-Carboxyarabinitol 1-Phosphate
Chl*a* and Chl*b*	Chlorophyll a and b
DAP	dihydroxyacetone-Phosphate
DCMU	3-(3,4-Dichlorophenyl)-1,1-Dimethylurea
DHAP	Di Hydrogen Adenosine Phosphate
DTT	Dithiothreitol.
DW	Deionized Water
E	Transpiration Rate
E_{ref}	Chamber Humidity
ECS	Electrochromic Absorption Shift
EDTA	Ethylenediamine tetra acetic acid.
EGTA	Ethylene glycolbis(betaaminoethyl ether)-N,N,N′,N′-tetraacetic acid
ETR	Photosynthetic Electron Transport Rate
F′	Light Levels of Fluorescence
F_0 & F'_0	Minimal Fluorescence Level in the Dark and Light
F_m & F_m'	Maximum Fluorescence in the Dark and Light
F_q'	Difference in Fluorescence between F_m' and F'
***F*s′**	Steady State Level of Fluorescence
F_v	Variable Fluorescence
F6P	Fructose 6 Phosphate

FBP	Fructose Bisphosphate
FW	Fresh Weight
G1P and G6P	Glucose 1, 3 and 6 Phosphate
G3P	Glycerol 3-Phosphate
G3PDH	Glycerol 3-Phosphate Dehydrogenase
G3POX	Glycerol 3-Phosphate Oxidase
GAP	Glyceraldehyde 3-Phosphate
GAPDH	Glyceraldehyde 3-Phosphate Dehydrogenase
g_s	Stomatal Conductance
g_m	Mesophyll Conductance
HEPES	4-(2-Hydroxyethyl)-1-piperazineethanesulfonic acid
HS	Heat Stress
HSPs	Heat-Shock Proteins
IPCC	The Intergovernmental Panel on Climate Change
IRGA	Infra-Red Gas Analyzers
K_m	Michaelis Constant
K_m'	Apparent Michaelis Constant
LC-MS	Liquid Chromatography–Mass Spectrometry
LHCs	Light Harvesting Chlorophyll–Protein Complexes
mAU	Milli Absorbance Unit
Mg^{2+}	Magnesium Ion
$MgSO_4$	Magnesium Sulfate
MSD	Minimum Significant Difference
$NADP^+$	Nicotinamide Adenine Dinucleotide Phosphate- Reductase
NADPH	Nicotinamide Adenine Dinucleotide Phosphate-Oxidase
NPQ	Non-Photochemical Quenching
PAR	Photosynthetic Active Radiation.
PGA	Phosphoglyceric Acid
PGK	Phosphoglycerokinase
pH	Hydrogen Ion Concentration Unit
pmf	Proton Motive Force
PMSF	ε-Aminocapronic acid, 1 mM phenylmethanesulphonyl fluoride
PPFD	Photosynthetic Photon Flux Density
PRK	Phosphoribulokinase
PSII	Photosystem 2

Q_A	Primary Quinone Electron Acceptor of PSII
***q*E**	High-Energy State Quenching
***q*I**	Photoinhibition Quenching
***q*T**	State Transition Quenching
R^2	Linear Regression
$^{mit}R_L$ & $^{mit}R_D$	Mitochondrial Photorespiration in the Light and Dark
$^{Tot}R_L$	Total Photorespiration
RCI & RCII	PSI and PSII reaction centres
Ri5P	Ribose-5-phosphate
Ri5PI	Ribose 5 Phosphate Isomerase
Ru5P	ribulose-5-phosphate
RuBP	ribulose-1,5-bisphosphate
RuBisCO	Ribulose 1,5-bisphosphate carboxylase/oxygenase
S7P	Sedhabtulose 7 Phosphate
t½	Fluorescence Relaxation Half Time
T_{leaf} , T_{air} & T_{ch}	Leaf, Air and Chamber Temperature, respectively
TPI	Triose-Phosphate Isomerase
UDPG	Uridine Diphosphate Glucose
V_0	Apparent Photorespiration
V_0 max	Maximum Photorespiration
var	Variety
Vmax	Maximum Reaction Velocity of the Enzyme
VPD	Vapour Pressure Deficits
WT	wild type
X5P	Xylulose 5-phosphate
Γ	CO_2 Compensation Point
ΦCO_2	Carboxylation Efficiency
ΦPSII	Maximum Quantum Efficiency of PSII (F_v/F_m)

1 Chapter 1: Introduction

1.1 Global Temperature and Food Supply: Serious Problems in Agriculture.

Food security is considered one of the major international concerns now as rising population, lack of water, climate change, *etc.* are predicted to suppress crop production in the future. By the end of the 21st Century, the annual temperatures are predicted to warm by an average of 2–4°C in the important crop-growing regions of the world according to the Intergovernmental Panel on Climate Change (IPCC 2007b). Thus, most of the world's crops will be exposed to heat stress during some stages of their life cycle which could lead to yield suppression. Decreases in agricultural yield are already linked to rising global temperature and more frequent droughts (Peng, Huang *et al.* 2004; Long and Ort 2010; Teixeira, Fischer *et al.* 2013). Currently, most crops are grown in regions where current temperatures are already close to optimum for their production. Therefore, any further increases beyond these optimum temperatures may result in reduced grain production. The production of rice and maize, two of the most important cereals grown across the world, could be reduced by 50% by 2080 as a result of increases in global mean temperatures (Ceccarelli, Grando *et al.* 2010) .

In addition to the loss of production, rising mean temperature may have a negative impact on food prices. In 2010, wheat prices increased by up to 50% in the international market when Russian production was affected by unprecedented extreme high temperatures (FAO 2010; NOAA 2011). The Intergovernmental Panel on Climate Change (IPCC) predicted that if global mean temperature rises by more than 5.5 °C then global food prices will increase because of the failure of supply to keep pace with food demand (Easterling, Aggarwal *et al.* 2007). Therefore, the fourth assessment report of (IPCC) has acknowledged heat stress as an important threat to global food supply (IPCC 2007a).

To meet the challenges of increased global food demand due to rapid population growth, the grain production per unit land area (yield) will need to increase by more than double over this century (FAO 2009). The increase in production per decade of the two most important grains, wheat and rice, has declined 1% over the past two decades (Lobell, Schlenker *et al.* 2011). Clearly, this continuing trend suggests that production is approaching a ceiling. A considerable increase in the area used for arable farming will be required. Land expansion will take place mostly in arid and semi-arid regions (FAO 2009).

In addition, improved crops adapted to rising temperatures will also be required for further substantial improvements in yield potential (Evans 2013).

1.2 Heat stress

Heat stress is defined as the increases in temperature above the optimum growth temperature for a period such that plant performance is suppressed (Wahid, Gelani *et al.* 2007). Usually, a 10-15°C rapid rise above ambient temperature may be considered as heat stress. Generally, optimum growth temperatures differ for different plant species and genotypes within a species. Cool season and temperate crops often have lower threshold temperature values compared to tropical crops (Tay, Abdullah *et al.* 2007). There is great variation among plant species in terms of their response and tolerance to heat stress. On this basis, plants have been broadly classified into three groups according to their ability to cope with high temperatures (Larcher 2003): (1) the heat-sensitive species: (2) the relatively heat-resistant species: (3) the heat-tolerant species.

1.3 Effect of Heat Stress on Crops

1.3.1 Morpho-Anatomical Changes

High temperatures can cause considerable changes in morpho-anatomical structures of plants (Wahid, Gelani *et al.* 2007). Reduced germination and plant emergence, abnormal seedling form, poor seedling vigor, reduced radicle and plumule growth of seedlings are all major perturbations caused by heat stress documented in various cultivated plant species (Assmann and Shimazaki 1999; Dunwell 2000; Feller 2006). Furthermore, reduced plant height, number of tillers and total biomass have been observed in rice due to high temperature (Medlyn, Barton *et al.* 2001). The morphological symptoms of heat stress also include scorching and sunburn of leaves and twigs, branches and stems, leaf senescence and abscission, shoot and root growth inhibition, fruit discoloration and damage (Mott, Denne *et al.* 1997).

Anatomical changes in response to high temperature include reduced cell size, closure of stomata, increased stomatal and trichomatous densities, and larger xylem vessels of both root and shoot (Pons and Welschen 2003). In addition to the effect of heat stress on the cellular levels, the sub-cellular processes are also affected by high temperature. Major

modifications occur in the shape of chloroplasts leading to significant changes in photosynthesis (Wang, Vinocur *et al.* 2004). Changes in thylakoid function following heat stress was observed as a direct effect on the structure of the thylakoid membrane (Nobel and Smith 1983). Studies on effects of high temperatures on grape plants showed chloroplasts in the mesophyll cells became round in shape, the stromal lamellae became swollen, and the contents of vacuoles formed clumps, whilst the cristae were disrupted and mitochondria became empty (Zhang, Huang *et al.* 2005; Flood, Harbinson *et al.* 2011). The cumulative effects of all these changes under high temperature stress may be responsible for poor plant growth and productivity.

1.3.2 Physiological Responses

Heat stress causes alterations to the growth and production of crop plants by affecting many physiological processes. Although some plant processes might be affected more than others (Sharkey and Schrader 2006), the most important processes are those that are first affected when temperatures rise above the optimum for plant growth. Two plant processes have been identified as the most sensitive processes to heat stress, reproduction and photosynthesis (Berry and Bjorkman 1980; Peet, Sato *et al.* 1998).

Photosynthesis

Photosynthesis is commonly reported as the most heat sensitive physiological process in plants (Berry and Bjorkman 1980; Crafts-Brandner and Salvucci 2002). Carbon assimilation rates can be disrupted through perturbation of the light reactions, the enzyme kinetics of the Calvin cycle, or the supply of CO_2 to the chloroplast. It has been suggested that high temperatures affect all three of these critical processes of photosynthesis.

Components of the thylakoid membranes have been recognized as being particularly sensitive to heat stress (Berry and Bjorkman 1980; Yordanov, Dilova *et al.* 1986). For instance, grana become unstacked at high temperature due to the dissociation of the light-harvesting complexes from the core complex (Schreiber and Berry 1977; Armond, Björkman *et al.* 1980). Actually, Photosystem II (PSII) has long been recognized as the most temperature sensitive step in photosynthesis (Berry and Bjorkman 1980), although it appears from numerous reports that PSII inhibition is not observed until leaf temperature exceeds 40°C (Havaux 1993; Al-Khatib and Paulsen 1999). Chlorophyll fluorescence measurement of maize leaves showed that the maximum quantum efficiency of PSII

(**ΦPSII**; *i.e.* $\boldsymbol{F_v/F_m}$ of fully dark adapted leaves) decreased to below 80% relative to controls at leaf temperatures of 42.5°C, suggesting that inhibition of photosynthesis is likely to be caused by damage to PSII at this temperature (Crafts-Brandner and Salvucci 2002). It has been documented that heat stress affects PSII activity not only by an inactivation of the oxygen evolving complex (Nash, Miyao *et al.* 1985; Enami, Kitamura *et al.* 1994) but also by perturbations of electron transport within the PSII reaction centres (Bukhov, Sabat *et al.* 1990).

Furthermore, an increase in the permeability of the thylakoid membranes leading to proton leakage has been observed at temperatures lower than those required for PSII activity inhibition (Pastenes and Horton 1996; Bukhov, Wiese *et al.* 1999b). The role of the thylakoid membranes in the thermal damage to photosynthesis is also supported by work showing that heating caused increased thylakoid proton permeability in cotton leaves at temperatures as low as 36°C (Schrader, Wise *et al.* 2004). Increased proton leakiness, however, is believed to induce cyclic electron transport around PSI to maintain ATP content (Schrader, Wise *et al.* 2004).

It has also been proposed that deactivation of RuBisCO is the primary constraint to photosynthesis at moderately high leaf temperatures (Crafts-Brandner and Salvucci 2000; Haldimann and Feller 2004; Salvucci and Crafts-Brandner 2004b; Kim and Portis 2005; Hozain, Salvucci *et al.* 2010), and this generally occurs at temperatures that cause no damage to PSII (Feller, Crafts-Brandner *et al.* 1998). This deactivation was assumed to result from a loss of activity of RuBisCO Activase, which is very sensitive to denaturation by high temperatures (Salvucci, Osteryoung *et al.* 2001) or perhaps the binding of Activase to the thylakoid membrane (Rokka, Zhang *et al.* 2001). Although RuBisCO deactivation is confirmed at high temperatures, it is still not clear whether it is the cause or a consequence of the reduction of photosynthesis (Sharkey and Schrader 2006).

In plants, the ability to sustain leaf gas exchange and CO_2 assimilation rates under heat stress is directly linked with heat tolerance (Yang, Chen *et al.* 2006). In fact, it has been shown for cotton that greater transpirational cooling correlates with greater yields (Radin, Lu *et al.* 1994; Lu, Chen *et al.* 1997), implying that heat-stress-induced reductions of photosynthesis limits overall yield. Heat markedly affects the leaf water status, leaf stomatal conductance ($\mathbf{g_s}$) and intercellular CO_2 concentration (Greer and Weedon 2012). Stomatal closure under heat stress has been implicated in the impairment of photosynthesis by affecting intercellular CO_2 levels (Ashraf and Hafeez 2004).

1.4 What Limits Photosynthesis at Elevated Temperature?

The negative effects of heat stress on plants are well known, and photosynthesis is thought to be among the most thermosensitive processes in plants. Although both the light (electron transport) and dark (Calvin cycle) reactions of photosynthesis have been implicated as thermolabile components, the limiting processes controlling the response of CO_2 assimilation rate (A) to elevated temperatures remain unclear and controversial (Crafts-Brandner and Law 2000; Schrader, Wise *et al.* 2004). Several hypotheses have been proposed to explain the reduction in photosynthesis at elevated temperature. The leading hypotheses for photosynthetic limitation are either the decline in the capacity of electron transport to regenerate RuBP (Wise, Olson *et al.* 2004; Cen and Sage 2005; Makino and Sage 2007) or a reduction in the capacity of RuBisCO Activase to maintain RuBisCO in an active form (Crafts-Brandner and Salvucci 2000; Salvucci and Crafts-Brandner 2004b; Kim and Portis 2005; Hozain, Salvucci *et al.* 2010). Other possibilities have been suggested but these have not been fully evaluated; for example, the diffusion of CO_2 into the chloroplast (Rokka, Zhang *et al.* 2001; Salvucci, Osteryoung *et al.* 2001). The following sections will describe further these leading hypotheses.

1.4.1 RuBisCO Activase

Ribulose 1,5-bisphosphate carboxylase/oxygenase (RuBisCO) exists in higher plants as a large macromolecular complex of eight large and eight small subunits (Knight, Andersson *et al.* 1990) (Figure 1-1). The enzyme is involved in the first step of carbon fixation by catalyzing the carboxylation of ribulose-1,5-bisphosphate (RuBP) with CO_2. In the simplest case, the enzyme exists either in the active form with catalytic potential or as an inactive form. When RuBisCO is in the active form, the active site is carbamylated by the spontaneous addition of CO_2 in the presence of Mg^{2+} and then RuBP binds followed by the catalytic formation of 3-PGA (the first step in carbon fixation). RuBisCO must be carbamylated by the addition of a CO_2 molecule to an ε-amino group of a lysine located in the active-site in order to have activity (Lorimer, Badger *et al.* 1976; Cleland, Andrews *et al.* 1998; Portis Jr 2003). However, RuBP also binds to the decarbamylated site and switches RuBisCO to an inactive form. To overcome this inhibition of RuBisCO, plants contain the enzyme RuBisCO Activase, an ATPase that releases tightly bound pentose sugar-P from the active sites of RuBisCO making it free for carbamylation **(**Figure 1-2;

reviewed in Spreitzer and Salvucci 2002). Thus, the *in vivo* activation state of RuBisCO in leaves represents the steady state between the rate of deactivation and the rate of Activase-promoted activation.

RuBisCO Activase **(RCA)** is a nuclear-encoded chloroplast enzyme which comprises two isoforms generated from alternative splicing of pre-mRNAs: a large isoform of 45–48 kDa (RCA_L) and a small isoform of 41–43 kDa (RCA_S). The two isoforms are found in most species studied, for example, in spinach and Arabidopsis (Werneke, Chatfield *et al.* 1989), barley (Rundle and Zielinski 1991) and rice (Zhang and Komatsu 2000). The activity of Activase is regulated by redox changes in the carboxy-terminus of the larger isoform, mediated by thioredoxin-f, which alters the response of Activase to the ratio of ADP to ATP in the stroma (Zhang and Portis 1999; Zhang, Schürmann *et al.* 2001; Portis Jr 2003).

RuBisCO Activase in barley is encoded by two nuclear genes, RcaA and RcaB. The RuBisCO Activase gene A **(RcaA)** produces two mRNAs, which encode the two isoforms of Activase by an alternative splicing mechanism identical to that previously reported for spinach and Arabidopsis Rca genes. The RuBisCO Activase gene B **(RcaB)** is transcribed to produce a single mRNA, which encodes a mature peptide of 42 kDa (Rundle and Zielinski 1991). RuBisCO Activase encoded by RcaA is reported to be heat inactivated when temperature increased to 35 °C (Crafts-Brandner, van de Loo *et al.* 1997). In contrast, the thermostability of RuBisCO Activase encoded by RcaB is currently unexamined (Rollins, Habte *et al.* 2013). Some evidence, however, has suggested the upregulation of RuBisCO Activase encoded by RcaB under heat treatment implicating a specific role for RuBisCO Activase B in maintaining the activity of RuBisCO under high temperature conditions, possibly by being more thermostable than RuBisCO Activase encoded by RcaA (Rollins, Habte *et al.* 2013).

A general concept that RuBisCO activity is the main cause of photosynthetic inhibition under heat stress emerged from the early work of Weis (1981) and later by Ashraf and Hafeez (2004). The original idea was that the activation state of RuBisCO declined as a direct consequence of failure to carbamylate which was thought to be due to changes in stromal pH and Mg^{2+} concentration at high temperature. Since then, however, a much better understanding of the biochemical basis for changes in RuBisCO activation state has emerged. The observation has been made that plants exposed to elevated temperature show a parallel reduction in the activation state of RuBisCO and photosynthetic capacity leading to conclusions that the decline in photosynthesis above the thermal optimum is a consequence of RuBisCO deactivation (Law and Crafts-Brandner 1999; Salvucci and Crafts-Brandner 2004a; Yamori, Noguchi *et al.* 2005). Deactivation of RuBisCO above the

thermal optimum has been observed in many plants, for example in *Arabidopsis* (Kim and Portis 2005; Salvucci, DeRidder *et al.* 2006), spinach (Yamori, Suzuki *et al.* 2006) , cotton (Crafts-Brandner and Salvucci 2000), wheat (Kobza and Edwards 1987; Law and Crafts-Brandner 1999) and tobacco (Crafts-Brandner and Salvucci 2000).

Several different mechanisms for the decrease in RuBisCO activation in response to increased temperatures have been proposed. One suggested that the ability of Activase to maintain RuBisCO in the active form was reduced because its activity did not continue to increase with temperature to match the faster rates of RuBisCO de-activation (Crafts-Brandner and Salvucci 2000). Previous studies have documented that the deactivation of RuBisCO is not due to the heat lability of RuBisCO, which is heat stable to at least 50°C (Crafts-Brandner and Salvucci 2000). Instead, it is attributed to the relatively low temperature optimum of Activase and its marked lability at high temperatures (Robinson and Portis Jr 1989; Crafts-Brandner, van de Loo *et al.* 1997; Crafts-Brandner and Salvucci 2000). It is feasible that the deactivation of RuBisCO at high temperature is related to the aggregation of Activase into large molecular mass complexes that are inactive (Feller, Crafts-Brandner *et al.* 1998). Generally, a direct or an indirect effect of high temperature on one or more of these possibilities could reduce the overall activation state of RuBisCO.

Evidence supporting the hypothesis that reducing the deactivation of RuBisCO through improvements in RuBisCO Activase will lead to improved tolerance to moderate heat stress emerged from the natural variations of thermal stability of RuBisCO Activase and transgenic plants with improved Activase. It has been shown that thermal properties of Activase in species from contrasting thermal environments differed and correlate with temperature response of RuBisCO activation and photosynthesis, while the temperature response of their RuBisCO was remarkably similar (Salvucci and Crafts-Brandner 2004b). Transgenic *Arabidopsis* with more heat stable Activase produced by DNA shuffling showed higher photosynthetic rates, higher biomass and increased seed yields compared with the wild-type lines (Kurek, Chang *et al.* 2007). Also, more thermostable *Arabidopsis* RuBisCO Activase was generated by introducing a more heat stable chimeric RuBisCO Activase made from tobacco Activase with the sensor II region from *Arabidopsis* and transgenic plants expressing these Activases had higher rates of photosynthesis, biomass and seed yield after a short exposure to high temperatures compared with the wild type plants (Kumar, Li *et al.* 2009).

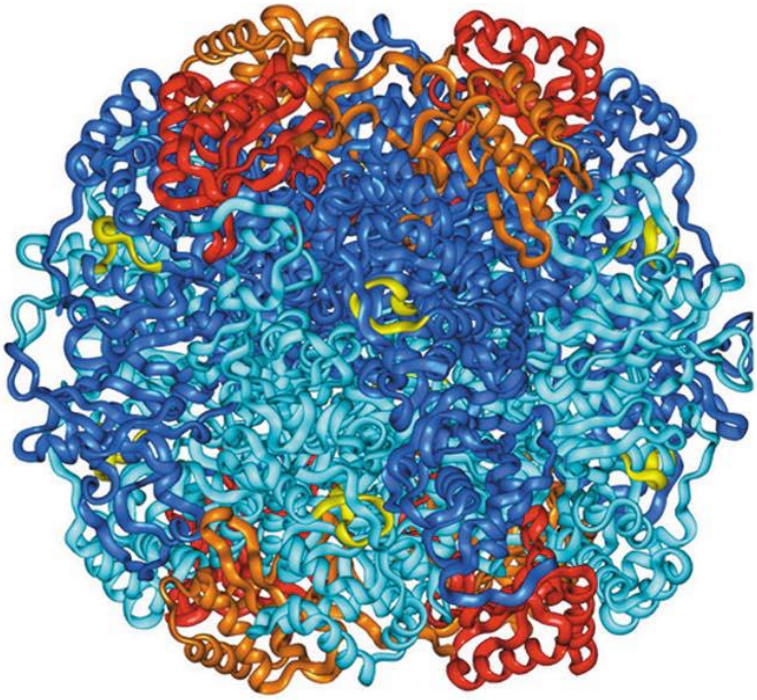

Figure 1-1 : Crystal Structure of Spinach RuBisCO.

The holoenzyme is composed of eight large subunits (*dark blue*, *light blue*) and eight small subunits (*red*, *orange*). Active sites that form between two neighboring large subunits are denoted by loop 6 (*yellow*; Protein Data Bank, entry number 8RUC).

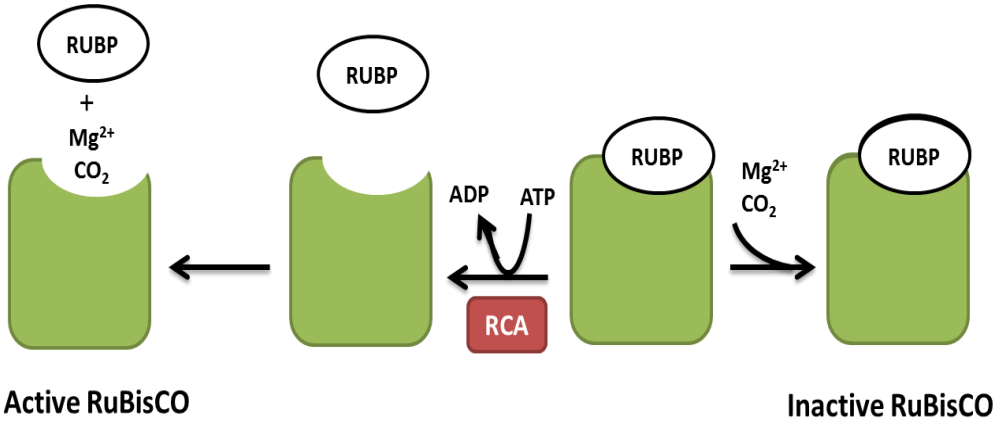

Figure 1-2 : Scheme for De-activation and Re-activation of RuBisCO.

When RuBisCO (Green) is in active form, the active site is carbamylated by CO_2 in the presence of Mg^{2+} and then binds RuBP followed by formation of 3-PGA (the first step in CO_2 fixation). RuBP could bind to the decarbamylated site first and then switch RuBisCO to an inactive form. Activase (red) physically interacts with inactivated RuBisCO to release RuBP from the active site of RuBisCO. These conformational changes require ATP hydrolysis by Activase. The active site then becomes free for carbamylation or rebinding of RuBP.

1.4.2 RuBP Regeneration

The capacity of RuBP regeneration has also been proposed as a limiting step for the decline in CO_2 assimilation rate at high temperatures instead of RuBisCO deactivation (Schrader, Wise *et al.* 2004; Cen and Sage 2005; Makino and Sage 2007). These groups suggested that the activation state of RuBisCO at high temperatures is a regulated response to other limitations imposed by electron transport capacity (Cen and Sage 2005; Sharkey 2005). Generally, the regeneration of RuBP is assumed to be determined by the whole-chain ETR in thylakoid membranes, since RuBP regeneration is dependent on the supply of ATP and NADPH (Von Caemmerer 2000). The reason for the decline in the electron transport capacity above the thermal optimum remains uncertain (Sage, Way *et al.* 2008). However, increased proton leakiness across the thylakoid membrane, impairing the coupling of ATP synthesis to electron transport, has been implicated as a cause of heat-induced reductions in electron transport capacity, particularly at high temperatures (Bukhov, Wiese *et al.* 1999a; Sharkey and Schrader 2006). In response to these effects, ATP/ADP ratios and the redox potential of the chloroplast decline leading to loss of RuBisCO Activase activity and in turn, a reduction in the RuBisCO activation state (Zhang, Kallis *et al.* 2002; Sage and Kubien 2007). Based on this understanding, it was assumed the decline in RuBisCO activation state at high temperatures is part of a regulated response to a limitation in other photosynthetic processes.

Further evidence supporting this hypothesis was apparent from experiments with antisense plants which provided the ability to distinguish the limitation on A between electron transport capacity and RuBisCO activity by altering the ratio of RuBisCO to RuBisCO Activase. Antisense tobacco and rice lines with reduced amount of RuBisCO relative to RuBisCO Activase (the RuBisCO content of the anti-*rbc*S lines was 30% and 35% of WT), showed the activation state of RuBisCO does not decline at moderately high temperatures (Makino and Sage 2007; Kubien and Sage 2008).

Additional support for this possibility was obtained from the work of (Cen and Sage 2005), who evaluated the limiting role of RuBisCO activation *versus* RuBP regeneration capacity by altering CO_2 levels to manipulate the activation state of RuBisCO. They argue that if the reduction in the activation state of RuBisCO is part of a regulated response to an electron transport limitation, then reducing CO_2 levels should balance the light and carboxylation reaction and allow for an increase in the activation state of RuBisCO. In contrast, if the activation state of RuBisCO at elevated temperature is reduced because RuBisCO Activase is heat labile, then CO_2 reduction should have no or little effect on the

activation state of RuBisCO. Their results showed a high activation state of RuBisCO at elevated temperatures and reduced CO_2 levels in sweet potatoes. All these findings support the view that the decline in RuBisCO activation above the thermal optima is due to a reduction in RuBisCO Activase activity as a result of limitation in electron transport capacity rather than a consequence of a direct effect of heat on the RuBisCO Activase.

1.4.3 CO_2 Diffusion

The diffusion of CO_2 into the leaf and chloroplast is also recognized as a potential limitation on the CO_2 assimilation rate (A) at high temperature. The diffusion of CO_2 from the atmosphere and through the boundary layer and stomatal pore to the intercellular spaces is defined as stomatal conductance ($\mathbf{g_s}$). Heat stress is considered one of the important factors affecting stomatal opening. It was suggested that as long as sufficient water is available for the plants in the soil, stomatal opening and transpiration may be high allowing for an efficient cooling of the leaf. On the other hand, however, limited water availability will induce stomatal closure to prevent water loss; it seems heat stress is inextricably linked with drought stress (Feller 2006). It was also suggested that as temperatures increase, the vapour pressure difference (VPD) between leaf and air rises exponentially leading to reduced stomatal conductance which in turn causes a reduction in intercellular CO_2 and **A** (Berry and Bjorkman 1980). Declines in **A** due to VPD-induced stomatal closure are common in hot conditions and explain much of the phenomenon known as midday stomatal closure (Pons and Welschen 2003; Tay, Abdullah *et al.* 2007).

Stomatal responses to temperatures are highly variable and depend upon the species and growth conditions. Stomata can open with rising temperature (a common response when vapor pressure deficit is low), close (often in response to increasing vapor pressure deficit with rising temperature) or remain unaffected (Kemp and Williams III 1980; Sage and Sharkey 1987; Yamori, Noguchi *et al.* 2006). Although the effects of light, external CO_2 concentration and water status on stomata are well documented (Mott, Denne *et al.* 1997; Assmann and Shimazaki 1999; Medlyn, Barton *et al.* 2001), knowledge of how stomata respond to elevated temperature remains limited (Feller 2006). However, evidence from various reports has suggested the low activation state of RuBisCO at elevated temperatures is caused by the thermosensitivity of RuBisCO Activase and this is the primary constraint on the rate of CO_2 assimilation. In these studies, stomata were opened and most likely not

limiting photosynthesis (Law and Crafts-Brandner 1999; Crafts-Brandner and Law 2000; Crafts-Brandner and Salvucci 2002).

Mesophyll conductance ($\mathbf{g_m}$), is defined as the conductance of CO_2 transfer from the intercellular leaf airspaces to the site of carboxylation (Farquhar and Sharkey 1982). Mesophyll conductance was initially thought to be large enough to have only a minor influence on photosynthesis rates (Farquhar, von Caemmerer *et al.* 1980). Other research suggests that $\mathbf{g}_m$ may be sufficiently small to cause a significant decrease in the concentration of CO_2 at the site of carboxylation ($\boldsymbol{C_c}$) relative to that in the intercellular space ($\boldsymbol{C_i}$), and consequently limit photosynthesis (Loreto, Harley *et al.* 1992; Evans, Caemmerer *et al.* 1994; von Caemmerer, Evans *et al.* 1994). However, this view has been challenged (Evans and Loreto 2000), as mesophyll conductance might potentially contribute to the thermal response of A by affecting the stromal CO_2 levels. The involvement of mesophyll conductance on photosynthesis rates at high temperature was evaluated for different species. For example, the decline in mesophyll conductance above the optimum temperature of photosynthesis was observed in tobacco and cool grown spinach (Bernacchi, Portis *et al.* 2002; Warren and Dreyer 2006). However, no such declines occurred in oak or warm-grown spinach between 25 and 35 °C (Warren and Dreyer 2006). No study has examined the response of mesophyll conductance above 40 °C, where electron transport or RuBisCO Activase was implicated as a major limitation on photosynthesis. Given the lack of evidence for temperature responses of mesophyll conductance above this temperature, it is unknown if the decline in photosynthesis is due to major limitation with mesophyll conductance.

1.5 Genetic Improvement for Heat-Stress Tolerance

The negative impact of heat stress can be reduced by developing crop plants with improved thermotolerance using various approaches including traditional and contemporary molecular breeding protocol and genetic engineering (Mittler and Blumwald 2010). Most traditional plant breeding programs have focused on the development of cultivars with high yield potential in non-stress environments. Such approaches have successfully increased crop yields (Warren 1998). Breeding plants for heat-stress tolerance however, requires growing plants in a hot environment and identification of the lines with greatest yield potential (Ehlers and Hall 1998). A major challenge in traditional breeding for heat tolerance under such conditions, however, is the impact of other environment stresses which makes the selection process very difficult.

Development of plants with enhanced stress tolerance has also been attempted by manipulation of the expression of identified proteins using a transgenic approach. For example, Heat-shock proteins (HSPs) are involved in plant abiotic stress tolerance by protecting proteins from denaturation (Wang, Vinocur *et al.* 2004). In fact, the stress tolerance of plants was found to be correlated positively with the level of HSPs (Sun, Van Montagu *et al.* 2002; LujÁN, LledÍAs *et al.* 2009). Overexpression of HSP101 from *Arabidopsis* in rice plants resulted in a significant improvement in growth performance during recovery from heat stress (Katiyar-Agarwal, Agarwal *et al.* 2003). Also, *Arabidopsis* plants have been engineered to prevent them from making trienoic fatty acids in their chloroplasts which has resulted in improvement of the ability to survive heat stress (Murakami, Tsuyama *et al.* 2000).

The thermal stability of RuBisCO Activase has been implicated as a limiting factor for photosynthesis (Crafts-Brandner and Salvucci 2000; Salvucci and Crafts-Brandner 2004b; Kim and Portis 2005; Hozain, Salvucci *et al.* 2010). Engineering plants to over-express RuBisCO Activase could be a promising approach to improve photosynthesis rates and as a result crop growth and production should increase. Rice plants over-expressing RuBisCO Activase have been produced (Wu, Li *et al.* 2007), but the effect of heat stress on these plants has not been examined. Alternatively transgenic tobacco plants with reduced amount of RuBisCO (anti-*rbc*S) that have higher ratios of RuBisCO Activase : RuBisCO than WT have been generated. Improving the temperature response of photosynthesis by this approach has so far yielded poor results (Kubien and Sage 2008; Yamori and von Caemmerer 2009).

The application of transgene technology for the improvement of crops for stress tolerance is a relatively new approach that has been attempted only in the last decade (Wahid, Gelani *et al.* 2007). The progress in engineering crop plants for stress tolerance is still slow due to insufficient knowledge of the critical proteins responsible for enhancement of temperature tolerance in higher plants. Therefore, an understanding of the physiological mechanisms and genetic basis of stress tolerance at the whole plant level, and the identification of the primary site of injury that affects plant growth under heat stress are required.

1.6 How Can Crop Production in Warm Climates be Improved?

Agaves are widely distributed in the New World deserts and well adapted to arid and semi-arid regions. These plants have shown a great ability to cope with extremely high temperatures and low rainfall conditions (LujÁN, LledÍAs *et al.* 2009). It was reported that the tolerance of different Agave species to high temperature is within the range of 57 to 65 °C (Nobel and Smith 1983). In addition, the ability of three Yucca species in arid South-Western USA to tolerate extremes of temperature was determined using gas exchange and chlorophyll fluorescence techniques. The results showed assimilation rate and Maximum Quantum Efficiency of PSII were maintained at high temperatures up to 53°C (Huxman, Hamerlynck *et al.* 1998).

Leaf temperatures of Agaves and other wild plants were recorded in desert habitat at a site near Jeddah, Saudi Arabia by a thermal imaging camera during the hottest part of the day (12.28 pm) where the air temperature was 38°C under full sunlight (approximately 2000 μmol photons. m^{-2}. s^{-1}). Leaf temperature in excess of 55.3°C was recorded (Figure 1-3). Despite the extreme leaf temperature and lack of water, these plants tolerate the high T_{leaf} and thrive in such conditions. These observations strongly indicated that Agave plants have distinct physiological adaptations allowing them to thrive where most C3 crop plants could not grow. The adaptive potential of plants to grow in such environments is due to the level of genetic variation (Flood, Harbinson *et al.* 2011). The increase in temperature in temperate regions as a result of climatic change may lead to conditions that plants in arid geographical areas regularly experience. Therefore, the thermotolerance features of Agaves offer an attractive avenue for studying the heat tolerance mechanism and provide opportunities for manipulation in crops. Desert plants, like the Agaves, are likely to have key physiological mechanisms that would benefit C3 crops in temperate regions in the future. For example, if the widely accepted view that deactivation of RuBisCO by heat stress arises from the thermolability of RuBisCO Activase, this suggests that the thermal properties of Activase from Agave plants are different from crop plants and should be studied. Engineering RuBisCO Activase from these plants into crops would be a promising strategy to enhance RuBisCO activity and photosynthetic performance under moderate temperatures. However, the main factor limiting photosynthesis under heat stress remains subject to debate (Salvucci and Crafts-Brandner 2004a; Schrader, Wise *et al.* 2004). Therefore, exploitation of this natural variation first requires the identification of the critical components of photosynthesis that are impaired by heat stress. Further basic research, particularly to outline the targets for improving crop photosynthesis under high

temperature, is critical before these opportunities can be adequately understood and validated.

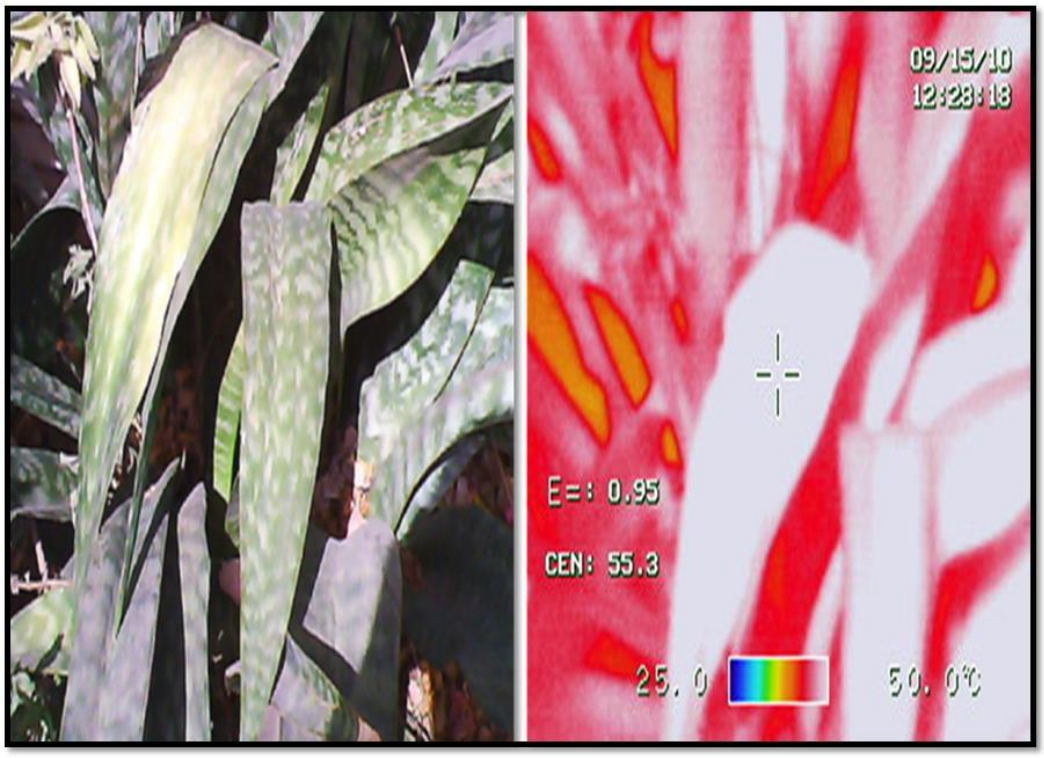

Figure 1-3: Visible and Thermal Image of Agave Plant Growing in a Natural Habitat in Saudi Arabia.

Agave plant located in natural habitat in Saudi Arabia; T_{air} was 38°C, full sunlight (approximately 2000 µmol photons. m^{-2}. s^{-1}) and T_{leaf} was 55.3°C.

1.7 Aim and Objectives of this Study

Photosynthesis is considered a major target for improving crop productivity using crop transgenic approaches (Dunwell 2000). As mentioned earlier, however, more basic research is critical before opportunities to improve photosynthesis by genetic engineering can be adequately applied. The aim of this study is to identify the potential target sites for thermal injury of CO_2 assimilation on cereals and to find whether there is sufficient genetic diversity to be exploited for developing heat tolerant crops.

To evaluate this possibility, experiments were conducted first to assess the effect of high leaf temperature on photosynthetic processes that are known to be heat sensitive using C3 (barley) and C4 (maize) plants from temperate and sub-tropical regions. In addition, the thermotolerant obligate C3 plant *Yucca filimentosa* was used to provide a comparison with a true xerophyte. Second, the leading hypotheses for thermal suppression of photosynthesis above the optimum leaf temperature were re-evalutated in the C3 crop barley to identify the possible site of thermal damage.

2 Chapter 2: Materials and Methods

2.1 Plant Material

Two barley lines (C3, *Hordeum vulgare cv.* Optic and landrace Local) and two Maize lines (C4, *Zea mays cv.* Sundance and Katumani) were studied as they are grown in temperate and tropical/sub-tropical regions, respectively. Optic is an elite European line (http://www3.syngenta.com/country/uk/en/Brochures/Optic_uk_brochure.pdf), with seeds procured from Syngenta Seeds Limited, Cambridge, UK: Local is a landrace selected from Balochistan, Pakistan; Sundance is a line that has been bred for the cooler UK weather with seeds procured from Suttons Consumer Products Ltd, Devon, UK: and Katumani is reported to be drought tolerant with seeds procured from Kenya Seed Company LTD, Nairobi, Kenya. Seeds from both temperate and subtropical lines were germinated on damp paper towels and after one week shifted to 2 liter pots containing a mixture of top soil and sand (1:3) and placed in a controlled environment growth room (09/15 hour Day/Night photoperiod, light intensity 150 µmoles.m^{-2}.s^{-1}, 23/20 °C temperature, humidity 60%). For comparison, *Yucca filimentosa*, an obligate C3 plant endemic to arid regions of tropical Central America, was also used; these were supplied by a commercial garden center.

2.2 Exposure to Heat Stress

The experimental approach used in this study was designed to circumvent some of the difficulties encountered with controlling leaf temperature (T_{leaf}). Confusion has arisen because often air temperature (T_{air}) not (T_{leaf}) is controlled and reported, but it is (T_{leaf}) that is of prime importance. T_{leaf} is dependent on the processes that heat (T_{air} and light intensity) and cool (transpiration and reflectance/emissivity) of the leaf (Monteith and Unsworth 2007). It is the rate of transpiration in particular that is difficult to control experimentally as this is determined by the water supply to the leaf and stomatal conductance (**g_s**, itself dependent on leaf temperature).

Instead of attempting to induce high leaf temperatures by increasing irradiance and/or (T_{air}), attached leaves were wrapped in cling film to reduce transpiration, and then placed on a temperature controlled thermal block in the dark. In this way (T_{leaf}) could be controlled very precisely (± 0.2°C) generating reproducible thermal stress events that do not arise from the generation of light-dependent reactive oxygen species. An appropriate

section of (fully expanded 4th) attached leaf (~80 mm from the base of the leaf blade) was lightly marked with a fine indelible marker pen, wrapped in cling film to prevent transpirational cooling, and placed on an aluminum plate laid upon the heating block of a MJ Machines PTC-200 PCR thermal cycler. The metal plate was thermally insulated with a neoprene gasket to prevent heat loss from the edges, and a neoprene pad to prevent heat loss from the upper leaf surface. Unless stated otherwise, the leaves were heated to 25.0, 30.0, 36.0, 38.0, 40.0 and 45.0°C (±0.2°C) for three hours. Lower and upper surface leaf temperatures were continuously monitored by using bead thermocouples (± 0.2°C) and data were recorded throughout the experiment. Heat stress treatment was conducted in the dark to prevent heat-induced photoinhibition as well as minimize leaf cooling due to transpiration.

2.3 Gas Exchange Measurements

2.3.1 Measurement of CO_2 Assimilation Rates

Light saturated CO_2 assimilation rates ($\mathbf{A_{sat}}$), carboxylation efficiency ($\mathbf{\Phi CO_2}$), transpiration (**E**), and stomatal conductance ($\mathbf{g_s}$) were measured using Infra-Red Gas Analyzers (IRGA) model and a LCpro+ portable photosynthesis system (ADC Bioscientific Ltd., Hoddesdon, Herts., UK), fitted with a rectangular narrow leaf chamber (window area of 5.8 cm^2). The LCpro+ instruments are fully programmable IRGAs that control temperature, incident light levels, humidity, and CO_2 concentration. A portion of the fully expanded fourth leaf was enclosed in the LCpro+ leaf chamber ensuring the leaf completely filled the chamber area. The chamber was illuminated with the adjustable LCpro+ LED unit; chamber CO_2 (*i.e.* $\mathbf{C_{air}}$ or $\mathbf{C_a}$), chamber humidity, and temperature (*i.e.* T_{ch}) were controlled by the LCpro+ console.

The most frequently used model for leaf gas exchange is that proposed by (Farquhar, Caemmerer *et al.* 1980) where CO_2 assimilation rates in response to carbon dioxide concentration provide a number of important parameters related to leaf photosynthesis. $\mathbf{A_{sat}}$ can be estimated from plots of CO_2 assimilation rates (**A**) *versus* external CO_2 concentrations ($\mathbf{C_a}$, $\mathbf{A/C_a}$ plots). Only a limited amount of information can be derived directly from A/C_a curves. However, it has been shown (Farquhar, Caemmerer *et al.* 1980; Farquhar and Sharkey 1982) that useful photosynthetic parameters can be extracted from plots of assimilation rate (**A**) against the CO_2 concentration in the intra cellular leaf space

($\mathbf{C_i}$, $\mathbf{A/C_i}$ plots), which can be constructed from $\mathbf{A/C_a}$ plots using simple calculations (Farquhar et al., 1980). Simply put, the $\mathbf{A/C_i}$ plot of a sample represents the CO_2 response when stomatal and boundary layer conductance to CO_2 diffusion have been removed, and thus the assimilation rate is limited by the kinetics of the carboxylation processes and mesophyll conductance ($\mathbf{g_m}$), which impairs CO_2 diffusion into the chloroplast from the intra cellular spaces. Mesophyll conductance ($\mathbf{g_m}$) is often considered to be large and to exert little influence on **A** (Farquhar, von Caemmerer *et al.* 1980), but recently this view has been challenged (Evans and Loreto 2000).

A region of attached leaf (~80 mm from the base of the leaf) was identified, marked and placed in a narrow leaf chamber of an IRGA (normally set at 25.0°C ±0.5°C) and CO_2 response curves were determined ($\mathbf{A/C_a}$ and $\mathbf{A/C_i}$) along with the corresponding transpiration (**E**) and stomatal conductance ($\mathbf{g_s}$). In barley and maize, these experiments were conducted immediately after; and 5 days after treatment (25.0, 30.0, 36.0, 38.0, 40.0 and 45.0°C ±0.2°C for 3 hours; see Section 2.2). In *Y. filimentosa* however, experiments were conducted immediately after; and 3 days after treatment (25.0, 38.0, 40.0 and 45.0°C ±0.2°C for 3 hours; see Section 2.2). The following conditions were routinely used unless stated otherwise. Samples were illuminated at 487 µmol photons $.m^{-2}$ $.s^{-1}$ (PPFD) for barley and 870 µmol photons $.m^{-2}$ $.s^{-1}$ (PPFD) for maize and Yucca, and exposed to 400 µmol CO_2 $.mol^{-1}$ air ($\mathbf{C_a}$), 5 mmol $.mol^{-1}$ humidity, for 10 minutes to ensure that selected leaves attained high photosynthesis rate, typically 15 µmol. $m^{-2}.s^{-1}$ for barley lines and 20 µmol. $m^{-2}.s^{-1}$ for maize lines. The leaves were then exposed to 0 µmol CO_2 $.mol^{-1}$ air ($\mathbf{C_a}$) for 15 minutes. After this period, the leaf samples attained a steady state of gas exchange and $\mathbf{C_a}$ levels were then increased incrementally every 20 minutes (0, 10, 20, 50, µmol CO_2 $.mol^{-1}$ air). After this period, the $\mathbf{C_a}$ levels were increased every 15 minutes (100, 200, 300, 400, 500, 600, 800 and 1000 µmol CO_2 $.mol^{-1}$ air). Gas exchange measurements on *Y. filimentosa* were determined at 380 µmol CO_2 $.mol^{-1}$ air and $\mathbf{A_{sat}}$, $\mathbf{g_s}$ and **E** were recorded for one hour with values obtained from steady state readings.

To ensure that any suppression in $\mathbf{A_{sat}}$ and $\mathbf{\Phi CO_2}$ was attributable to T_{leaf} itself and not due to the experimental setup, measurements were made on the same piece of attached leaf immediately before and immediately after exposing the leaf for 3 hours at room temperature *i.e.* T_{leaf} 25 ºC (± 0.2 ºC) using a modified thermal cycler (see Section 2.2). Preliminary experiments indicated keeping the leaf at 25.0 (± 0.2 ºC) for 3 hours did not have any significant effect on $\mathbf{A_{sat}}$, **E** or $\mathbf{g_s}$ (Figure 2-1). A profile of the typical chamber conditions used is presented in Figure 2-2. At low $\mathbf{C_i}$ the $\mathbf{A/C_i}$ curve is linear and the slope is an estimate of the carboxylation efficiency ($\mathbf{\Phi CO_2}$), while the Y intercept estimates the

sum of the rates of photorespiration and mitochondrial respiration in the light in a zero CO_2 atmosphere ($^{Tot}R_L = V_0 + {}^{mit}R_L$) where V_0 is the apparent photorespiration rate. The contribution of mitochondrial respiration in the light is assumed to be the same as that in the dark ($^{mit}R_D$; Figure 2-3).

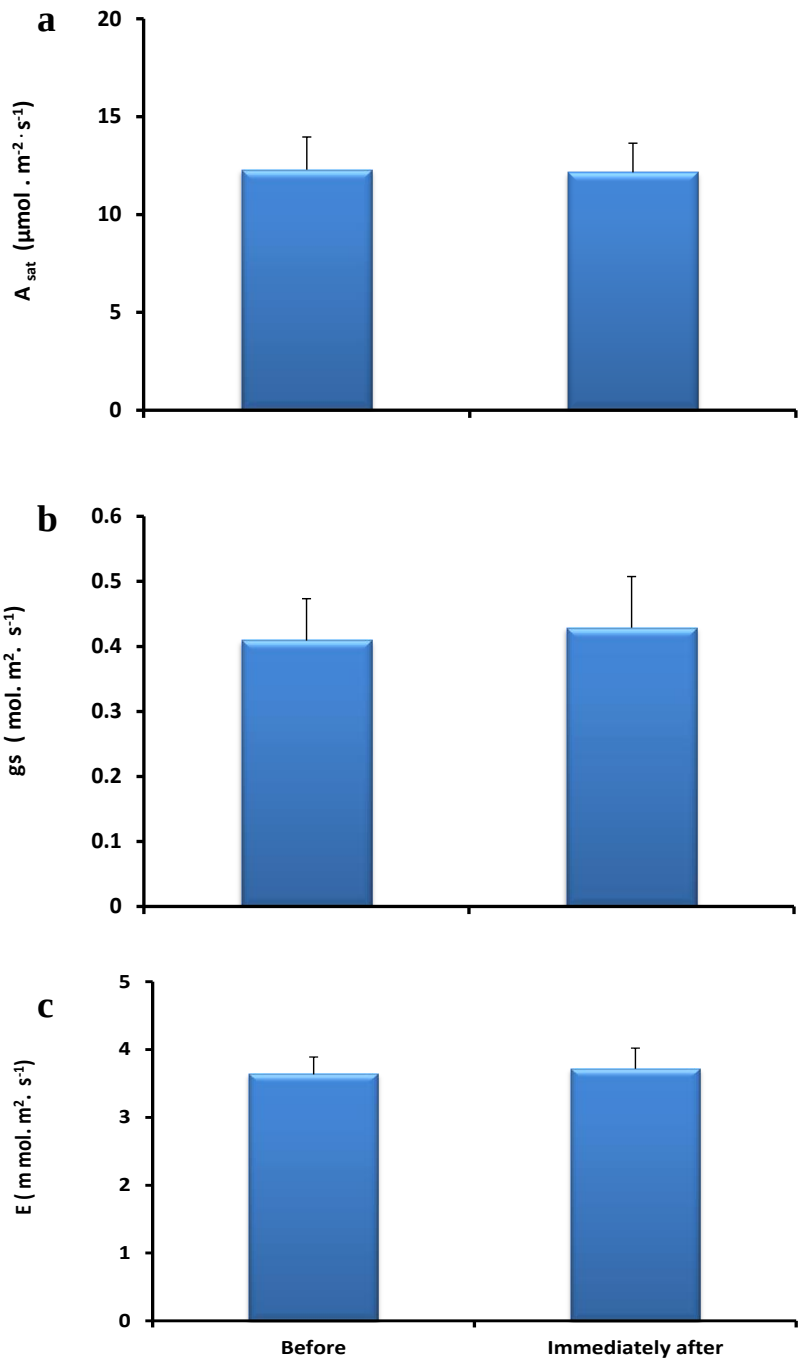

Figure 2-1: Effects of Three Hours (T_{leaf} 25ºC) on Barley Leaf Function.

(a): Light Saturated CO_2 Assimilation rates (**A_{sat}**); **(b):** Stomatal Conductance (**g_s**) ; **(c):** Transpiration Rate (**E**). Parameters were measured with IRGAs and extracted from CO_2 response curves (see Section 2.1.3.1.1) at T_{leaf} 25ºC (± 0.2ºC) and saturating light levels (560 µmol .m^{-2} .s^{-1} PAR) immediately before, immediately after subjecting a marked region of an attached barley to 25.0ºC (± 0.2 ºC) for three hours using a modified thermal cycler (see Section 2.2.2.2). The presented values are the Averages and Standard Errors of 3 replicates. ANOVA tests were performed by using a General Linear Model and different letter codes indicate Tukey's significant differences at $p<0.05$.

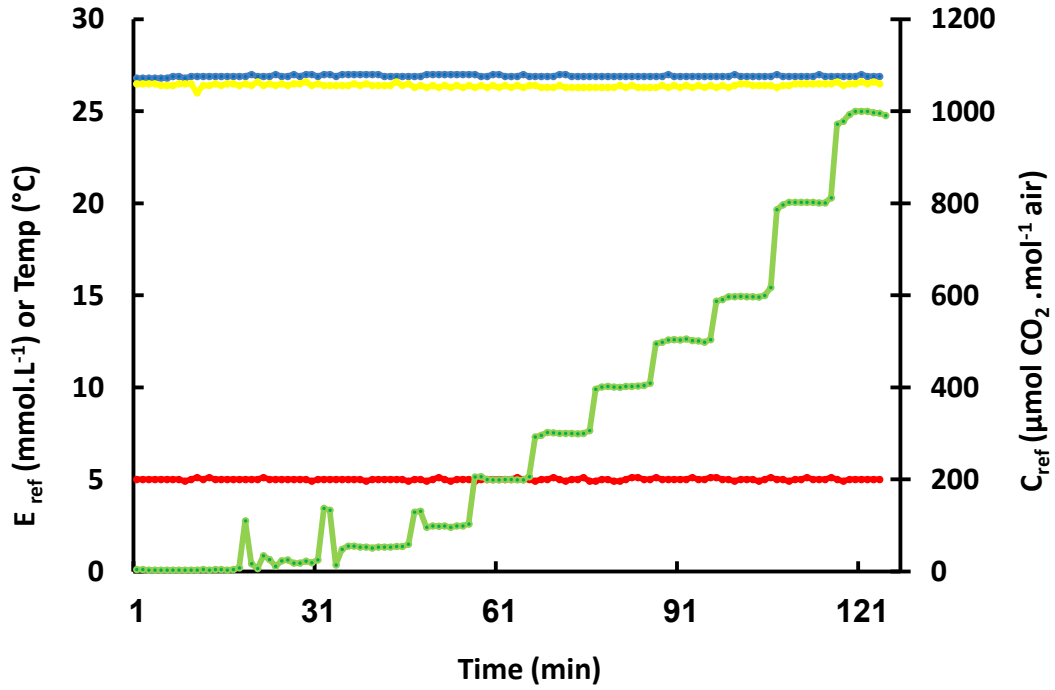

Figure 2-2: Profile of Leaf Chamber Conditions Used to Estimate CO_2 Response Curves.

(●),**C_{ref}** (**C_a**) chamber CO_2 controlled by the LCpro+ console. C_a levels increased incrementally every 20 minutes as follows (0, 10, 20, 50, µmol CO_2 .mol^{-1} air). After this period, the C_a levels were increased every 15 minutes (100, 200, 300, 400, 500, 600, 800 and 1000 µmol CO_2 .mol^{-1} air). (●), **E_{ref}** chamber humidity typically set to 5 mmol .mol^{-1}. (●), **T_{air}** chamber temperature typically set to 25.0°C. (●),**T_{leaf}** leaf temperature. Readings were taken every minute. During the course of these experiments light levels were maintained at 487 or 870 µmol photons .m^{-2} .s^{-1} (PPFD) using the LCpro+ light emitting diode unit; these light levels saturated photosynthesis rates in barley and maize, respectively.

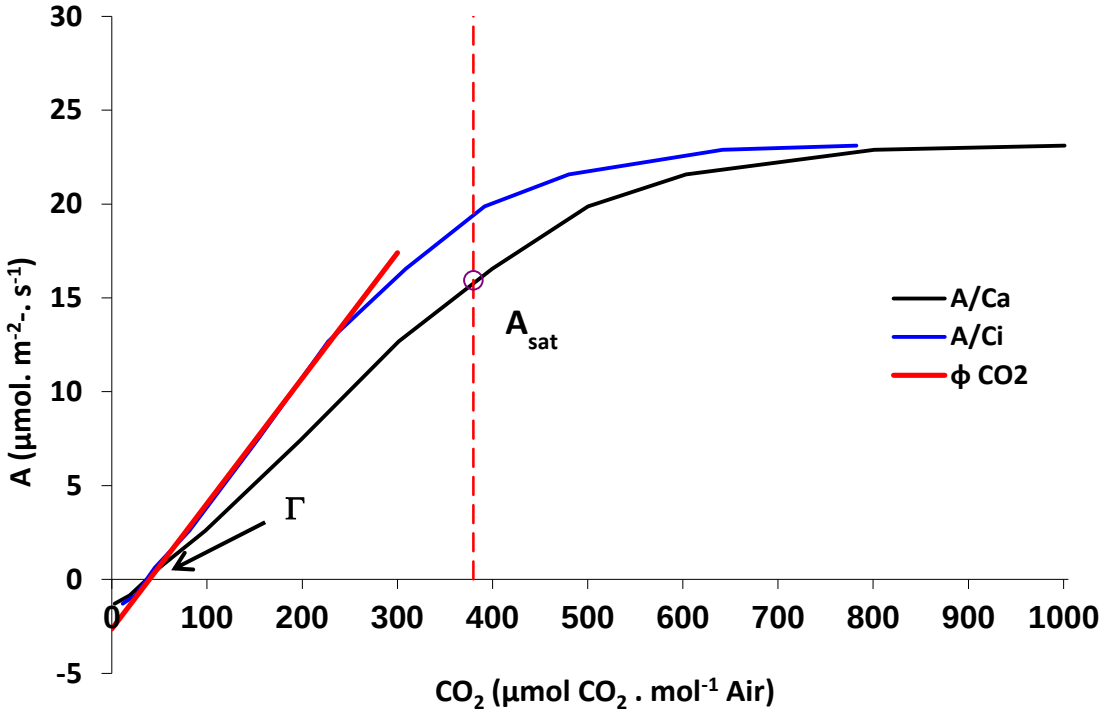

Figure 2-3: CO_2 Response Curves (A/C_a and A/C_i) of a Barley Leaf.

Leaves were sealed in the LCpro+ Narrow Leaf Chamber taking care to avoid damage; leaves were chosen that completely filled the chamber area (5.8 cm^2). Samples were dark adapted in conditioned air (0 µmol CO_2 $.mol^{-1}$ air, 5 µmol $.mol^{-1}$ humidity, and 25.0°C T_{ch}) for 10 minutes prior to running the program shown in Figure 2-1. Blue solid line (—) is the relationship between CO_2 assimilation (**A**) and the internal CO_2 concentration ($\mathbf{C_i}$). Black solid line (—) is the relationship between CO_2 assimilation (**A**) and the air CO_2 concentration (C_a). Red solid line (—) is carboxylation efficiency ($\mathbf{\Phi CO_2}$) from initial slope of the A/C_i curve. Red vertical dashed line (¦) is ambient CO_2 (380 µmol CO_2 $.mol^{-1}$ air); Γ is the CO_2 Compensation Point. Extrapolation of the initial slope of the $\mathbf{A/C_i}$ curve to the abscissa gives the total respiration rate (maximum apparent photorespiration V_0max plus mitochondrial respiration in the light, R_L). These data were collected using the program described in Figure 2-2.

2.3.2 Estimation of Mesophyll Conductance (g_m)

Mesophyll conductance (**g_m**) was estimated from gas exchange data using the 'Constant J' (electron transport) method (Loreto, Harley *et al.* 1992). The limitation of CO_2 assimilation rate (**A**) by the diffusion of CO_2 from the intracellular leaf space to the chloroplast stromal was also examined by measuring (**A**) at ambient and elevated CO_2 levels to overcome limiting (**g_m**) using IRGA as described in Section 2.3.1. This experiment was conducted before at 25.0°C and immediately after heat stressing the leaves at 38.0°C ±0.2°C for 3 hours, (see Section 2.2). Attached barley leaves were illuminated at 487 µmol photons $.m^{-2} .s^{-1}$ (PPFD), and exposed to 400 µmol CO_2 $.mol^{-1}$ air (**C_a**), 5 mmol $.mol^{-1}$ humidity, for 15 minutes. After this period, **A_{sat}** was determined when the leaf samples had attained a steady state. The **C_a** level was then increased to 1000 µmol CO_2 $.mol^{-1}$ air and the steady state maximum CO_2 assimilation rate (**A_{max}**) was determined.

2.3.3 Dark Respiration Measurements on Attached Leaves

Dark Respiration was measured using IRGAs. Attached barley leaves were incubated in the dark for 3 hours at 25.0 or 38.0°C (± 0.2°C; see section 2.2). Leaves were then sealed in the leaf chamber illuminated at 487 µmol photons $.m^{-2} .s^{-1}$ (PPFD) and exposed to 380 µmol CO_2 $.mol^{-1}$ air (**C_a**), 5 mmol $.mol^{-1}$ humidity. After 20 minutes, light was turned off and steady state dark respiration was measured in terms of CO_2 uptake for 40 minutes as described in Section 2.3.1.

2.4 Modulated Chlorophyll Fluorescence Measurements

2.4.1 ΦPSII, *in vivo* ETR and NPQ

Chlorophyll fluorescence measurements are used widely to investigate photosynthetic performance under different environmental conditions. From these measurements, estimates of the maximum quantum efficiency of photosystem II photochemistry ($\boldsymbol{F_v/F_m}$ of dark adapted leaves, *i.e.* **ΦPSII**), steady state rates of photosynthetic electron transport (ETR) and non-photochemical quenching (**NPQ**) during light induction can be calculated (Baker 2008).

Modulated chlorophyll fluorescence measurements were made on barley and maize leaves immediately after and 5 days after treatments at 25.0 and 38.0°C ±0.2°C for 3 hours, and in *Y. filimentosa*, immediately after and 3 days after treatments (25.0, 38.0, 40.0 and 45.0°C ±0.2°C for 3 hours; see Section 2.2). Intact leaves at 23°C were placed in 2030-B Leaf-Clip Holder of a MINI-PAM fluorimeter (PAM 2000H Walz, Effeltrich, Germany) connected to a PC and WinControl software, and irradiated with an external actinic light (550 µmol .m^{-2}.s^{-1} for barley and 800 µmol .m^{-2}.s^{-1} for maize and *Y. filimentosa*) delivered by a 150W quartz halogen bulb. Before the start of each experiment the leaf was fully dark-adapted for 20 minutes, before the measuring beam was switched on to determine the minimal fluorescence level in the dark ($\boldsymbol{F_0}$). Maximum fluorescence level in the dark ($\boldsymbol{F_m}$) was then determined at 100 kHz by providing a 0.4 s saturating pulse of white light (9000 µmol.m^{-2}.s^{-1} PPFD). After determination of 'dark' levels of $\boldsymbol{F_0}$ and $\boldsymbol{F_m}$ (*i.e.* determination of **ΦPSII** from $(\boldsymbol{F_m}-\boldsymbol{F_0})/\boldsymbol{F_m}$), the actinic light was switched on to drive photosynthesis and the resulting 'light' levels of fluorescence $\boldsymbol{F'}$ measured. Saturating light pulses were then applied every 60s to determine the maximal fluorescence in the light ($\boldsymbol{F_m'}$). Once a steady state level of fluorescence ($\boldsymbol{Fs'}$) was achieved, ETR and NPQ were recorded and the actinic light was switched off (see Figure 2-4).

The important parameters calculated were as follows:

ΦPSII= $(\boldsymbol{F_v/F_m})$, where $\boldsymbol{F_v}$= $\boldsymbol{F_m}$-$\boldsymbol{F_o}$ (maximum quantum efficiency of PSII)

NPQ= $(\boldsymbol{F_m/F_m'})$ -1 (Non-photochemical quenching)

ETR = $\boldsymbol{I.A_{leaf}}$.$\boldsymbol{fraction_{PSII}}$. PSII operating efficiency (Electron transport rate)

Where I is the irradiance [µmol .m^{-2}.s^{-1} PPFD] supplied to a leaf, $fraction_{PSII}$ is the fraction of absorbed energy distributed to photosystems II (taken as 0.5). A_{leaf} is the fraction of

absorbed energy frequently assumed to be 0.84, *i.e.*, 84% of incident PPFD is assumed to be absorbed by leaves. The PSII operating efficiency is the efficiency at which light absorbed by PSII is used for primary quinone electron acceptor of PSII (Q_A) reduction = ($\boldsymbol{F_q'/F_m'}$), where $\boldsymbol{F_q'}$ is the difference in fluorescence between $\boldsymbol{F_m'}$ and $\boldsymbol{F'}$ (see Figure 2-4).

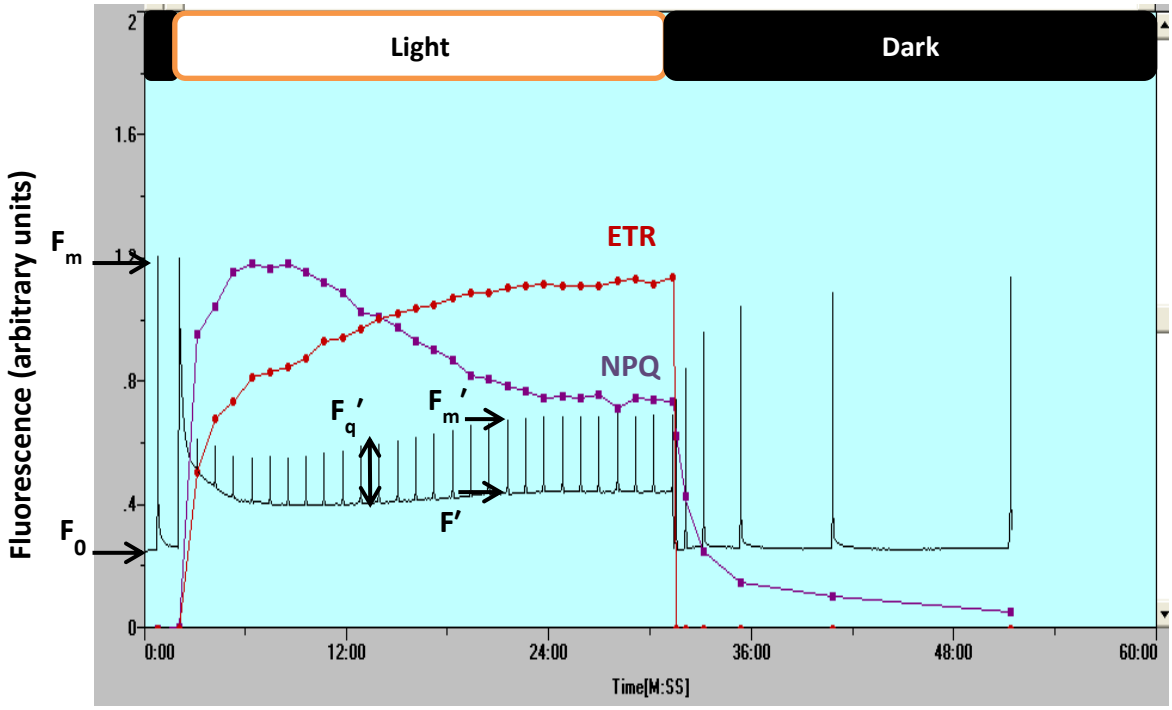

Figure 2-4: Typical Fluorescence Trace from Intact Barley Leaves Determined with a WALZ-PAM Fluorimeter.

Attached 4th emergent leaves were placed in the 2030-B Leaf- Clip Holder of PAM fluorimeter (PAM2000H Walz, Effeltrich, Germany) and data were collected to calculate several photosynthetic parameters including the maximum quantum yield of PSII Photochemistry (**ΦPSII**; *i.e.* $\boldsymbol{F_v/F_m}$) of fully dark adapted leaves, steady state ETR and the Non-Photochemical Quenching (**NPQ**) in the light and dark. 'Light bar', actinic light on; white light 550 or 800 µmol $.m^{-2}.s^{-1}$: 'Dark bar', actinic light off.

$\boldsymbol{F_0}$, minimal fluorescence level in the dark.

$\boldsymbol{F_m}$, maximum fluorescence level in the dark.

$\boldsymbol{F_m'}$, maximal fluorescence in the light.

$\boldsymbol{F'}$, fluorescence level in the light.

$\boldsymbol{F_q'}$, $F_m' - F'$.

2.4.2 Analysis of NPQ Fluorescence Dark Relaxation

Determination of **NPQ** fluorescence during the dark relaxation period was performed as described in section 2.4.1. After 20 minutes the actinic light was switched off and saturation pulses were applied in the dark (at 0, 30, 60, 150, 210, 330, 450, 750, 1050 and 1350 seconds); the dark induced relaxation phase was recorded for 20 minutes. For the effect of pulse frequency on **NPQ** fluorescence dark relaxation experiments, two different pulse frequency regimes were used. The first one, Reduced Pulse Frequency experiment, where a standard Induction Curve Program of the PAM fluorimeter was run with saturating pulses applied (at 0, 30, 90, 210, 510 and 1110 seconds) after switching off the actinic light. In the second regime, Increased Pulse Frequency experiment, the saturation pulses were applied (at 0, 30, 60, 90,120, 150, 180, 210, 300, 420, 730, and 1330 seconds). Dark relaxation of **NPQ** was resolved to three components using a theoretical model as described by (Horton and Hague 1988; Baker 2008). The three phases were resolved from plots of log (**NPQ**) as a function of 'dark' relaxation time by applying the relationship NPQ = (qE[1-e$^{-kE \cdot t}$]) + (qT[1-e$^{-kT \cdot t}$]) + (qI[1-e$^{-kI \cdot t}$]) where qE, qT and qI are relative sizes of fluorescence quenching attributable to the qE, qT and qI components, kE, kT and kI are the respective rate constants for relaxation, and t is time. The model is the sum of three exponential decay terms.

2.4.3 Fluorescence Relaxation of Thylakoid Proton Gradient

The recovery of $\boldsymbol{F'}$ to $\boldsymbol{F_o}$ (the fluorescence at steady state in the light and dark respectively), can also be used to estimate **NPQ** relaxation in the dark without requiring saturating light pulses. After steady state was achieved in the light, as described in section 2.4.1, the actinic beam was turned off and changes in fluorescence signal recorded in the dark for 20 minutes. The resulting changes in fluorescence signal were analysed using an Excel spreadsheet written to resolve the kinetic properties of **NPQ** relaxation. Relaxation half time (t½) was estimated by calculating the time required for minimum fluorescence level recorded in the dark to reach the final steady state level.

2.5 Measurements on Leaf Light Harvesting Capacity

Leaf absorbance was measured using a Perkin Elmer λ800 spectrophotometer fitted with a Lab-sphere PELA-1020 Integrated Sphere (2 nm slit widths) after incubating leaves at a temperature of 25.0 or 38.0ºC (± 0.2°C) for 3 hours (see section 2.2).

In addition to measurements on light absorbance, the efficiency of exciton delivery to PSII reaction centres was assessed from Chl*a* excitation spectra preformed at room temperature using a Perkin Elmer LS55 fluorimeter fitted with a fiber-optic attachment (excitation 350-600 nm with 5 nm slit widths; emission, 680 nm with 10 nm slit widths). Fluorescence changes arising from photochemical quenching were prevented by pre-treatment of 10 mm leaf discs for 30 minutes with aqueous solution of 50µM DCMU (3-(3,4-dichlorophenyl)-1,1-dimethylurea) to block photosynthetic electron transport and attain the maximal level of fluorescence ($\boldsymbol{F_m}$).

2.6 Electron Transport Rates (ETR) of Isolated Thylakoid Membranes (*in vitro*)

Measurements of the electron transport rates in the isolated thylakoid membrane were performed essentially as described by (Allen, Holmes *et al.* 1986) using a Clark-type oxygen electrode (Rank Brothers, Cambridge, UK) connected to an A/D converter and software (Picoscope 6 Oscilloscope, Pico Technology, Cambridgeshire, UK). Barley Leaves were incubated at 25.0, 36.0, 38.0 and 40ºC (± 0.2°C) for 3 hours as described in section 2.2. Leaves were rapidly homogenized with a blender in a solution containing 0.4 M sorbitol, 20 mM TES-KOH (pH 6.8), 10 mM NaCl and 1.0 mM $MgCl_2$. The homogenate was filtered through a layer of 200 µm nylon mesh and the filtrate was centrifuged at 3,000g at 4^0C for 1 min. The pellet was suspended in a 1.0 ml solution containing 0.2M sorbitol, 10 mM TES-KOH (pH 7.6), 0.1 mM NaCl and 1.0 mM $MgCl_2$. Immediately before the measurements of the ETR, 100 µl of chloroplasts were subjected to osmotic shock in 2 ml of buffer containing 50 mM HEPES-KOH (pH 7.6), 5 mM NaCl and 5 mM $MgCl_2$ in the cuvette of an oxygen electrode. The ETR in the thylakoid membranes was measured at saturating light (550 µmol m^{-2} s^{-1}) before and after the addition of 20 µM DCMU (Diuron3-(3,4-dichlorophenyl)-1,1-di-methylurea) as an electron transport inhibitor. For measurements of the whole-chain ETR (H_2O→methyl viologen), 5 mM sodium azide and 0.5 mM methyl viologen were added to the buffer. ETR was measured in the dark and light until reaching a steady rate (at least 5 min).

2.7 Analysis of Metabolite Pools

Leaf samples were prepared at the University of Glasgow (Shahwani 2011), but metabolite pool analysis was performed by Dr. Stéphanie Arrivault, Max Planck Institute of Molecular Plant Physiology, Am Muehlenberg, Germany, using 2D liquid chromatography (LC) linked to a triple mass spectrometer (Arrivault, Guenther *et al.* 2009). Metabolites were extracted using a modification of the method described in (Crafts-Brandner, van de Loo *et al.* 1997). Metabolite levels were quantified by comparison with authentic standards, and were corrected for ion suppression when internal standards were available. Some metabolites such as 3-PGA, glucose, fructose, sucrose and starch could not be reliably measured, and were determined by coupled enzymatic assays as described in a number of studies (Robinson and Portis Jr 1989; Von Caemmerer 2000; Sharkey, Badger *et al.* 2001; Gibon, Vigeolas *et al.* 2002). Full details of all the procedures can be found in (Arrivault, Guenther *et al.* 2009).

2.8 RuBisCO Activity

2.8.1 Preparation and Extraction of Leaf Samples

Metabolite fluxes during photosynthesis are often high and many metabolites, including NADP, ATP, ADP, AMP, DHAP, RuBP and FBP, often have turnover rates of the order of seconds or less (Stitt, Wirtz *et al.* 1980; 1983). It is imperative, therefore, that samples adapted to a steady rate of CO_2 assimilation are frozen rapidly. To achieve this, a system was built where a 500W quartz halogen lamp was used to irradiate attached barley leaves at 580 µmoles. $m^{-2}.s^{-1}$ (saturating light) delivered through a circulating cold water flask to remove infra-red heat. The leaf was kept at 22 °C (± 2 °C) and ambient air (380 µmoles CO_2 $.mol^{-1}$ air) was continuously flushed over the leaf (2 liters $.min^{-1}$). A Walz PAM fluorimeter was used to measure *in vivo* ETR as an estimate of the rate of CO_2 assimilation. When electron transport rate was at its steady state level for at least 20 minutes, the portion of attached leaf was frozen by submerging rapidly in a pool of liquid nitrogen in a polystyrene container and stored at -80°C until required. Measurements with a thermal imaging camera showed leaf temperature declined from 22°C to < -30°C in less than 1s. A heat stress temperature regime was applied to barley leaves just prior to the procedure described above. Leaves were incubated for 3 hours at 25.0, 38.0, 40.0 or 42.0°C (±0.2°C) as described in Section 2.2. Samples were prepared according to the method of (Sulpice, Tschoep *et al.* 2007) with some modifications. Leaf extracts were

prepared by grinding frozen leaf material at 4°C in a pre-cooled mortar and pestle and then approximately 20 mg of grounded leaf material was placed in a pre-weighed and pre-cooled and 1 ml Eppendorf tubes. The tubes containing leaf sample were re-weighted (±0.0001g) and the volume of extraction buffer was adjusted to produce 50 fold (w/v) dilutions. The entire procedure of grinding and extraction was carefully performed at <4°C. The composition of the extraction buffer was 20% (v/v) glycerol, 0.25% (w/v) bovine serum albumin, 1% (v/v) Triton-X100 (Sigma), 50 mM 4-(2-hydroxyethyl)-1-piperazineethanesulfonic acid (HEPES)/ KOH pH 7.5, 10 mM $MgCl_2$, 1 mM ethylenediaminetetraacetic acid (EDTA), 1 mM ethylene glycolbis(betaaminoethyl ether)-N,N,N′,N′-tetraacetic acid (EGTA), 1 mM benzamidine, 1 mM ε-aminocapronic acid, 1 mM phenylmethanesulphonyl fluoride (PMSF) and 0.5 mM dithiothreitol (DTT). PMSF and DTT were prepared fresh and added just prior to extraction.

2.8.2 RuBisCO/3-PGA Cyclic Enzyme-Linked Assay for Determining Maximum and *in vivo* RuBisCO Activity

After extraction, RuBisCO activity was determined indirectly by measuring the conversion of RuBP to the product 3-PGA using the modification method of (Sulpice, Tschoep *et al.* 2007). Experiments were conducted using a PerkinElmer Lambda 800 UV/vis spectrophometer connected to a PC and controlled by UV WinLab software. *In vivo* activity (that in the attached leaf) was determined directly from samples, while maximum activity was estimated after incubation of the leaf extract for 15 min at 25 °C with 100 mM Tricine/KOH pH 8.0, 20 mM $MgCl_2$, 2 mM EDTA and 10 mM $NaHCO_3$. Two microliters of leaf extract (approximately 40 µg FW) was added to the RuBisCO rate assay mix containing 100 mM Tricine/KOH pH 8.0, 20 mM $MgCl_2$, 2 mM EDTA, 10 mM $NaHCO_3$, and 0 (blank) or 1.5 mM RuBP (maximal activity). The final volume was 20 µL. RuBP was added to the RuBisCO rate assay mix less than 5 min before starting the reaction, in order to limit its degradation. The reaction was stopped after 30s by adding 20 µL 80% (v/v) ethanol. After 5 min incubation at 25^0C, the mixture was diluted by adding 50 µl of distilled water. A 96 µL aliquot of 3-PGA Cyclic Enzyme-Linked Assay mix was prepared; final concentrations (in 190 µl of total reaction volume) were 3 $u.mL^{-1}$ phosphoglycerate kinase, 2 $u.mL^{-1}$ NAD-dependent GAP-DH, 0.3 $u.mL^{-1}$ triose-P isomerase, 2 $u.mL^{-1}$ glycerol-3-P dehydrogenase, 1.3 mM ATP, 0.2 mM NADH, 1 mM $MgCl_2$ and 63 mM Tricine/KOH pH 8.0. Two µl of 20 mM NADH was added to get approximately 1.2-1.6 AU at 340 nm. The reaction was initiated by adding the RuBisCO rate assay mix (90 µl total volume) to the 3-PGA Cyclic Enzyme-Linked Assay mix. Once all the 3-PGA was converted to G3P, the cycling reaction was run by adding 5 $u.mL^{-1}$ glycerol-3-P oxidase and the steady state rate was measured after stabilizing for at least 10 minutes. Once steady state NADH oxidation was reached, 0.05 nmol/assay of 3-PGA was added and the new steady state rate determined. A second addition (0.20 nmol/assay 3-PGA) was added subsequently to the reaction and the new steady state rate determined. The amount of 3-PGA was then calculated from the x intercept of the slope of the rate plotted against 3-PGA additions (mAU/min *vs* 3-PGA additions).

2.8.3 Optimization of RuBisCO/3-PGA Cyclic Enzyme-Linked Assay

The rate of RuBisCO activity was determined in a two-step process. First, the RuBisCO rate assay converted RuBP and CO_2 into 3-PGA in 30 seconds. The second step was 3-PGA Cyclic Enzyme-Linked Assay, where the amount of 3-PGA produced in the first step was estimated using a cycling enzyme reaction. Further experiments were conducted to confirm that RuBisCO activity measured by this method reflects the amount of 3-PGA produced in the first step.

2.8.3.1 Calibration Curve for 3-PGA Cyclic Enzyme-Linked Assay

An aliquot of 186 µL of 3-PGA Cyclic Enzyme-Linked Assay mix was prepared as described in section 2.8.2. Two microliters of 20 mM NADH were added to get approximately 1.6 AU at 340 nm. The reaction was initiated by adding 2µl of (0.0, 0.05, 0.10, 0.15 or 0.20 nmol /assay 3-PGA) to the mixture. Once all of the 3-PGA was converted to G3P, the cycling reaction was run by adding 5 $u.mL^{-1}$ glycerol-3-P oxidase and the rate was measured after stabilizing for at least 10 minutes.

2.8.3.2 Substrate Saturation Curve for RuBisCO

Different D-ribulose-1,5-bisphosphate (RuBP) concentrations (0, 10, 40, 80 or 150 µM) were added to the RuBisCO rate assay mix containing two microliters of leaf extract (approximately 40 µg FW), 100 mM Tricine/KOH pH 8.0, 20 mM $MgCl_2$, 2 mM EDTA and 10 mM NaHCO3; the final volume was 20 µL. The reaction was run and the amount of 3-PGA synthesized was then measured using 3-PGA Cyclic Enzyme-Linked Assay as described in section 2.8.2. Data were analyzed using Lineweaver-Burke plots to calculate V_{max} and K_m.

2.8.3.3 Validity of RuBisCO Rate Assay

Barley leaves were incubated for 3 hours at 25.0, 38.0 and 40.0°C (±0.2°C) as described in section 2.2. Samples were collected and extracted as described in section 2.8.1. Two microliters of leaf extracts (approximately 40 µg FW) from stressed and non-stressed barley leaves were incubated with RuBisCO rate assay mix containing 100 mM Tricine/KOH pH 8.0, 20 mM $MgCl_2$, 2 mM EDTA, 10 mM $NaHCO_3$ and 0 (Blank) or 1.5

mM of RuBP for 30s. The amount of 3-PGA synthesized was then measured using the 3-PGA Cyclic Enzyme-Linked Assay described in section 2.8.2.

2.8.4 Effects of Extraction Buffer on RuBisCO Activity

2.8.4.1 Mg^{2+} Concentration

Barley leaves were dark adapted for 3 hours at 25.0°C (±0.2°C) before samples were taken, while light adapted barley leaves were allowed to attain steady state $\mathbf{A_{sat}}$ (20 min) under saturating light (580 µmoles. $m^{-2}.s^{-1}$) and ambient CO_2 levels (380 µmoles CO_2 $.mol^{-1}$ air) prior to sampling, as described in section 2.8.1. Dark adapted leaves (approximately 20 mg ± 0.0001g) were extracted in 1 ml of extraction buffers presented in Section, 2.8.1 except of using different concentrations of $MgCl_2$ (0, 2.5, 5, 8, 10 and 15 mM). Samples from light adapted leaves were extracted in the same buffer containing 0 or 10 mM $MgCl_2$. The *in vivo* activity of RuBisCO was then measured using the RuBisCO/3-PGA Cyclic Enzyme-Linked Assay described in 2.8.2.

2.8.4.2 Mg^{2+} and DTT Additions

Barley leaves were dark adapted for 17 hours at 25.0°C (±0.2°C) before samples were taken, while light adapted barley leaves were incubated for 3 hours at 25.0 and 38.0°C (±0.2°C) as described in section2.2. Samples were collected and extracted in 1 ml of buffer as described in section 2.8.1 except for the $MgCl_2$ or DTT concentrations (0 or 10 mM $MgCl_2$ and 0 or 0.5 mM DTT). The *in vivo* activity of RuBisCO was then measured using the RuBisCO/3-PGA Cyclic Enzyme-Linked Assay described in 2.8.2.

2.9 The Activity of Ribose 5 Phosphate Isomerase (Ri5PI) and Phosphoribulokinase (PRK)

2.9.1 Ri5PI, PRK/3-PGA Cyclic Enzyme Linked Assay

Activities of endogenous Ri5PI and PRK were estimated using the RuBisCO/3-PGA Cyclic Enzyme-Linked Assay described in section 2.8.2 with some modifications. Barley leaves were incubated for 3 hours at 25.0, 36.0, 38.0 and 40.0°C (±0.2°C) as described in section 2.2. Samples were prepared and extracted as described in 2.8.1. Two microliters of leaf extracts (approximately 40 µg FW) were incubated with Ri5PI and PRK rate step assay mix containing 5 mM Ri5P, 1 mM ATP, 2.5 mM $MgCl_2$, 100 mM Tricine/KOH pH 8 and 2 mM EDTA (12 µl total volume) for a range of end time points (0, 30, 60, 120, 300, 600 and 900 seconds) at 30 °C before stopping the reaction by rapidly heating in a thermal cycler to 80°C for 5 minutes (from 30 to 80°C within 10 seconds). The mixture was then diluted 14 fold with d H_2O and a 12 µl aliquot from the diluted mixture was added to reaction mixtures containing 50µg/ml purified wheat RuBisCO, 20 mM $MgCl_2$ and 10 mM $NaHCO_3$ (20 µl final volume) and incubated at 30°C for 5 min to convert all of the RuBP to 3-PGA. The reaction was stopped by adding 20 µL 80% (v/v) ethanol. After 5 min incubation at 25^0C, the mixture was diluted by adding 50 µl of distilled water. The amount of 3-PGA synthesized was then measured using 3-PGA Cyclic Enzyme-Linked Assay as described in section 2.8.2. The combined activity for both enzymes was calculated from the initial slope of their activity (µmol 3-PGA. g^{-1} FW) *versus* time (seconds) curves.

Purified wheat RuBisCO was obtained from Prof Martin Parry, Rothamsted Research, UK, as freeze-dried powder and stored at 4°C. Wheat RuBisCO was prepared as recommended (Keys and Parry 1990a). The dried powder was dissolved in a buffer containing 10 mM $NaHCO_3$, 20 mM $MgCl_2$ and 50 mM HEPES at pH 8, and heated at 40°C for 40 min for activation. The enzyme was then stored in liquid nitrogen until required.

2.9.2 Optimization of Ri5PI, PRK/3-PGA Cyclic Enzyme Linked Assay

The assay was developed to consist of 3 steps. The first one is the conversion of Ri5P to RuBP by incubation with saturating amounts of Ri5P and leaf extracts for a range of end time points. The reaction was then stopped by rapidly increasing the temperature to 80°C. The second step then was the conversion of all of newly synthesized RuBP to 3-PGA using an excess of purified activated wheat RuBisCO and excess CO_2. The last step involved the

determination of the total amount of 3-PGA produced from step 2 using the 3-PGA Cyclic Enzyme-Linked Assay as described in Section 2.8.2.

2.9.2.1 Ri5P-Substrate Saturation Curve

Different Ri5P concentrations (0, 0.05, 0.1, 0.8, 2.5, 5.0 or 10 mM) were added to the Ri5PI and PRK rate step assay mix containing two microliters of leaf extracts (approximately 40 µg FW) and the reaction was run as described in section 2.9.1. Data were analyzed using Lineweaver-Burke plots to calculate apparent V_{max} and K_m.

2.9.2.2 ATP-Substrate Saturation Curve

Different ATP concentrations (0, 10, 50, 70, or 100 µM) were added to the Ri5PI and PRK rate step assay mix containing two microliters of leaf extracts (approximately 40 µg FW) and the reaction was run as described in section 2.9.1. Data were analyzed using Lineweaver-Burke plots to calculate apparent V_{max} and K_m.

2.9.2.3 Temperature Inactivation of Ri5P to RuBP Conversion

Extracts from barley leaves were heated to 80°C for 5 min and then a two microliters aliquot were added to a reaction mixture contain 5 mM Ri5P, 1 mM ATP, 2.5 mM $MgCl_2$, 100 mM Tricine/KOH pH 8, 2 mM EDTA, 50µg/ml purified wheat RuBisCO, 20mM $MgCl_2$ and 10 mM $NaHCO_3$ (20 µl final volume). Parallel experiments were conducted at the same time on leaf extract that had been heated to 25°C for 5 min and added to the reaction mixture (5 mM Ri5P, 2.5 mM $MgCl_2$, 100 mM Tricine/KOH pH 8, 2 mM EDTA, 50µg/ml purified wheat RuBisCO, 20mM $MgCl_2$ and 10 mM $NaHCO_3$ and 0 or 1 mM ATP). The reaction mixture was then incubated at 30°C for 5 min to generate 3-PGA and stopped by adding 20 µL 80% (v/v) ethanol. After 5 min incubation at 25^0C, the mixture was diluted by adding 50 µl of distilled water. The amount of 3-PGA synthesized was then measured using the 3-PGA Cyclic Enzyme-Linked Assay described in Section 2.8.2.

2.9.2.4 Stability of RuBP

The stability of RuBP in the reaction mixture was tested by heating 100 pmol of RuBP to either 25°C or 80°C in thin walled PCR tubes using a thermal cycler for 5 min (from 30 to 80°C within 10 seconds). RuBP was then incubated for 5 min at 30°C with 50µg/ml purified wheat RuBisCO, 10 mM $NaHCO_3$ and 20mM $MgCl_2$ (20 µl final volume) to

generate 3-PGA before the reaction was stopped by adding 20 µL 80% (v/v) ethanol. After 5 min incubation at 25^0C, the mixture was diluted by adding 50 µl of distilled water. The amount of 3-PGA synthesized was then measured using the 3-PGA Cyclic Enzyme-Linked Assay described in Section 2.8.2.

2.9.2.5 RuBP and Ri5P Incubation at 80°C

The stability of RuBP and Ri5P was tested by heating 100 pmol of RuBP and Ri5P in thin walled PCR tubes using a thermal cycler at 80°C (from 30 to 80°C within 10 seconds) for 5 min before adding directly to the 3-PGA Cyclic Enzyme-Linked Assay mix prepared as described in section 2.8.2. The amount of 3-PGA synthesized was then measured using the 3-PGA Cyclic Enzyme-Linked Assay described in Section 2.8.2.

2.9.2.6 Determination of the Upper Limit of RuBP Concentration to Ensure Full Conversion to 3-PGA

Different amounts of 3-PGA (0, 0.05 0.25 0.45 0.65 0.85 1.05 and 3.05 nmol/assay) were added directly to the 3-PGA Cyclic Enzyme-Linked Assay mix prepared as described in section 2.8.2. Once 3-PGA is converted to G3P, the cycling reaction was run by adding 5 $u.mL^{-1}$ glycerol-3-P oxidase and the steady state rate measured (at least 10 minutes). These rates were plotted *versus* the amount of 3-PGA added to the assay and the linear part of the curve determined. The Ri5PI and PRK rate step was then adjusted by diluting with water to ensure the RuBP synthesized in step one never generated enough 3-PGA in step 2 to exceed the linear part of the 3-PGA curve.

2.9.2.7 The Time Required for Full Conversion of RuBP to 3-PGA

Different amounts of RuBP (0, 100, 200, 500, and 1000 pmol/assay) were incubated with 50µg/ml purified wheat RuBisCO, 10 mM $NaHCO_3$ and 20 mM $MgCl_2$ (20 µl final volume) at 30°C for (0, 1, 2, 5, 10 or 15 minutes). The reaction was stopped by adding 20 µL 80% (v/v) ethanol. After 5 min incubation at 25^0C, the mixture was diluted by adding 50 µl of distilled water. The amount of 3-PGA synthesized was then measured using the 3-PGA Cyclic Enzyme-Linked Assay described in section 2.8.2. For further confirmation, the same experiment was conducted by incubation of different amounts of RuBP (0, 100, 200, 500, or 1000 pmol/assay) for only 5 minutes. The amount of 3-PGA synthesized was then measured using the 3-PGA Cyclic Enzyme-Linked Assay described in Section 2.8.2.

2.10 ATP Measurements

2.10.1 Luciferin–Luciferase Bioluminescence Assay

ATP levels in barley leaves were estimated using the luciferin-luciferase bioluminescence assay (Molecular Probes ATP Determination Kit, A22066, Invitrogen, Ltd, UK) according to the manufacturer's instructions. With this protocol, 10 mL of Luciferase assay mixture was prepared containing 0.5 mM D-luciferin, 1.25 μg/mL firefly luciferase, 25mM Tricine buffer, pH 7.8, 5mM $MgSO_4$, 100μM EDTA and 1mM DTT. The solution was kept protected from light and stored at 2-6 °C for no more than 7 days. ATP levels were assayed in 96 flat bottomed well black microplates using a Luminoskan Ascent Microplate Luminometer connected to a PC and controlled by Ascent Software Version 2.6. The reaction was started by adding 100μl of luciferase assay mixture to 10μl of leaf sample or distilled water and allowed to run for 10 minutes. Standard curves of luminescence ATP were generated by adding ATP (0, 0.5, 1, 5, 10, 15, or 25 pmol of ATP). Standard curves generated with different batches of the ATP Determination Kit or with luciferase assay mixture stored at 2-6 °C during 7 days had different slopes, but each was linear; therefore, a new standard curve was generated for each run.

2.10.2 Sample Analysis

Precise timing of the measurement of luminescence after starting the reaction is critical because the rapid decay of light emission over minutes or even seconds (Kimmich, Randles *et al.* 1975) can lead to significant errors. To minimize these errors, the luciferase assay mixture was added at the same time to eight wells containing equal amounts of samples using an 8 channels multi pipette and a clock was started (zero time). Reagents were then added sequentially in columns and the times of additions were recorded (usually 1-10 seconds for each column). The assay (luminescence *versus* time) was then run for 10 minutes. Data were analyzed by plotting the logarithm of the luminescence signal *versus* time (seconds), which is reported to be a straight line (Addanki, Sotos *et al.* 1966). The real time luminescence signal was then determined by extrapolating the line backward to zero time (Figure 2-5). The amount of ATP in the samples was calculated from standard curves generated as described in Section 2.10.1.

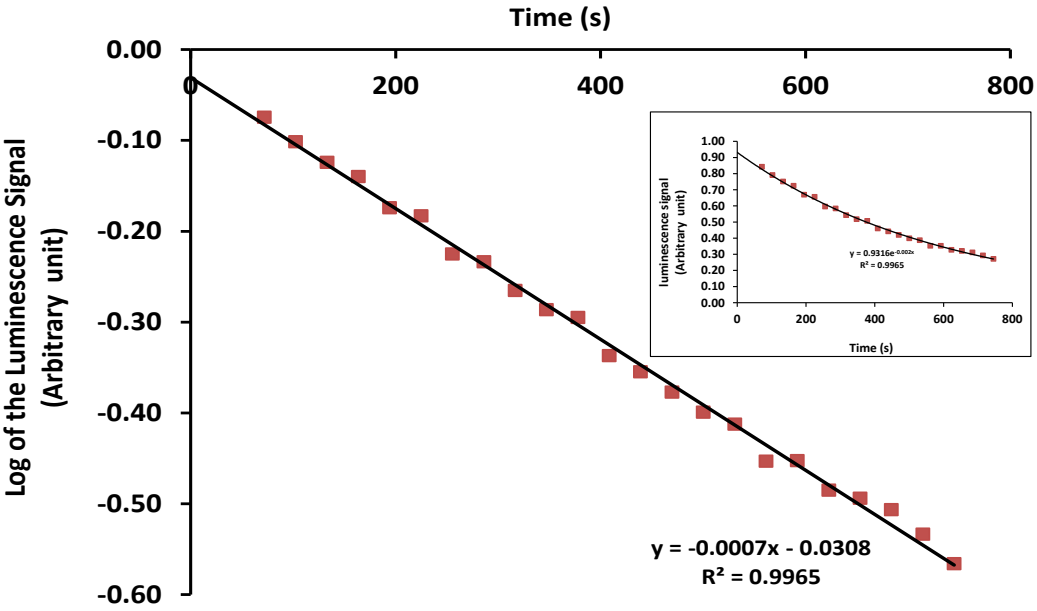

Figure 2-5: Plots of the Logarithm of the Luminescence Signal *versus* Time.

Data were collected as described in section 2.10.2 and analyzed by plotting the logarithm of the luminescence signal *versus* time (seconds). The luminescence at time zero was estimated by extrapolation. The amount of ATP in the samples was then calculated from standard curves generated using a series of known ATP concentrations. In all cases, this method generated linear fits to the log signal *vs* time plots with R^2 values of **>** 0.995. Insert shows the raw data of the luminescence signal.

2.10.3 Extraction and Stability of ATP

ATP was extracted from barley leaves into boiling water as a simple and reliable one-step procedure according to the method of (Yang, Ho *et al.* 2002). To check the stability of ATP extracted by this method, leaf tissue photosynthesizing under saturating light (580 µmoles. $m^{-2}.s^{-1}$) and ambient CO_2 levels (380 µmoles CO_2 $.mol^{-1}$ air) at 25°C using the system described in section 2.8.1, was rapidly frozen in liquid nitrogen, ground to a fine powder < 4°C in a pre-cooled mortar and pestle and then approximately 20 mg (± 0.0001g) of ground leaf powder was placed in pre-cooled and pre-weighed 1 ml Eppendorf tube. The tubes containing ground leaf sample were re-weighted and the volume of distilled water was adjusted to produce 50 fold (w/v) dilutions; samples were then stored at -80°C. When required, samples were removed from the freezer and rapidly 1 ml of water pre-heated to 90°C or 20°C was added and incubated at the same temperature (90°C or 20°C) for 3 min before centrifugation to remove cell debris (12,000g, 5 min at 4°C). The resulting supernatants were then decanted and stored on ice (for 0, 10, 30, 40 and 90 minutes) before determining ATP levels using the luciferin–luciferase bioluminescence assay described in Section 2.10.1and data were analysed as described in Section 2.10.2

2.10.4 Estimation of Chloroplasts ATP

Light-generated ATP in the chloroplast was estimated as light-minus-dark levels in whole leaves. To check if this is an appropriate estimate for chloroplast ATP, attached barley leaves were incubated in the dark for 3 hours at 25.0°C as described in section 2.2 and then exposed to saturated light (560 µmol m^{-2}. s^{-1}) and ambient CO_2 levels (380 µmoles CO_2 $.mol^{-1}$ air) for 3 or 20 minutes using the system described in section 2.8.1. For temperature effects on the pools of chloroplast ATP experment, attached leaves of healthy barley plants were first incubated in the dark for 3 hours on a thermal block set at 25.0, 36.0, 38.0 or 40.0°C (± 0.2°C; see section 2.2). After this period leaves were incubated for a further 20 minutes in air at 25°C either in the dark or light at 560 µmol m^{-2} s^{-1}, using the system described in section 2.8.1. Tissue was harvested and extracted as described in section 2.10.3 and ATP was determined using the luciferin–luciferase bioluminescence assay described in Section 2.10.1 and data were analysed as described in Section 2.10.2.

2.11 Statistical Analysis

Statistical analysis was performed using a General Linear Model ANOVA routine in MINITAB (ver.16). For statistical comparison between different lines, data were on occasion normalized as percentage change from controls. Tukey's Minimum Significant Difference (MSD) was used for comparison across treatments and/or lines. The effects of heat stress on the inhibition and recovery of whole leaf parameters of barley (C3) and maize (C4) leaf photosynthesis were analysed over time (0, 3 and 120 hours) and treated as random factors. ANOVA and grouping comparison along with Figures for residual plots are presented in Appendix. Where appropriate, values were log transformations to convert data sets into a normal distribution.

3 Chapter 3: Comparison of Thermal Inactivation of Whole Leaf Photosynthesis in Tropical and Temperate C3 and C4 Cereals and the Thermotolerant C3 Plant *Y. filimentosa*

It is evident from the literature that the growth of crops is highly affected by heat stress. Over the past decade, a great deal of basic research effort has been focused on the effects of heat stress on specific mechanisms in plants, for example photosynthesis, respiration ETR, *etc*. Unfortunately, there has been little effort to integrate the effects of high temperatures on these processes into whole-plant responses to thermal stress, but there is a consensus that reproduction and photosynthesis are particularly sensitive (Berry and Bjorkman 1980).

Although the effects of high temperatures can be demonstrated on all of these processes, it is unclear why exposure to low and high temperature suppresses plant growth and why some plants appear to be more thermotolerant than others. For example, C4 plants (including maize) have higher temperature optima for photosynthesis and growth than C3 plants (Bird, Cornelius *et al.* 1977) and thus, are better adapted to warmer climates (Kim, Gitz *et al.* 2007). Also, it is still unclear if there is a primary site of injury (and what that would be) or if there is a general suppression of many processes at some critical threshold temperature.

Therefore, it is essential to assess further the effects of high leaf temperatures on plant processes that are known to be heat sensitive. In this chapter results of experiments are reported where C3 and C4 plants from temperate and sub-tropical cereal lines were used in a comparative study to identify the primary site of injury, and to establish whether there is sufficient genetic diversity to be exploited for developing heat tolerant crops.

3.1 Light Saturated CO_2 Assimilation Rates (A_{sat})

Temperature responses of the Light Saturated CO_2 Assimilation Rates at 380 µmol CO_2 mol^{-1}air (**A_{sat}**) were measured in C3 and C4 plant species from contrasting environments. Two Barley lines (C3, Optic and Local) and two Maize lines (C4, Sundance and Katumani) that are routinely grown in temperate and arid sub-tropical regions, respectively, were used. For comparison, **A_{sat}** was also measured in the obligate C3 plant *Y. filimentosa* that is adapted to hot arid habitats. To assess the effects of increasing leaf temperature on the photosynthetic competence of barley (C3), maize (C4) and the thermotolerant C3 plant *Y. filimentosa*, fully expanded leaves were sealed in the leaf chamber of an Infra-Red Gas Analyzer (IRGA). **A_{sat}** was recorded after exposure to a range of temperatures from 25.0^{0}C to 45.0^{0}C (± 0.2^{0}C; for full experimental details see Section 2.3.1).

Figure 3-1 shows that **A_{sat}** declined with increasing T_{leaf} in both C3 and C4 crop plants regardless of their origins (temperate or sub- tropical). When T_{leaf} exceeds 36.0°C (±0.2°C) for 3 hours, **A_{sat}** is significantly ($P< 0.05$) and irreversibly suppressed by >85% in all lines. The exception is the succulent obligate C3 agave *Y. filimentosa*; here, **A_{sat}** retained approximately 50% of its initial activity when T_{leaf} was increased to 45°C for 3 hours, but full recovery occurred within 3 days (see Figure 3-6). Compared with all other lines, the *Y. filimentosa* responded differently to increasing leaf temperature (*cf* 38, 40 and 45°C for 3 hours; $P< 0.05$). No significant differences were observed between the barley lines (Optic and Local) or between the Maize lines (Sundance and Katumani) at any leaf temperature. However, Barley and Maize lines differ in their temperature response only at 36 C; maize >100%, barley <100%.

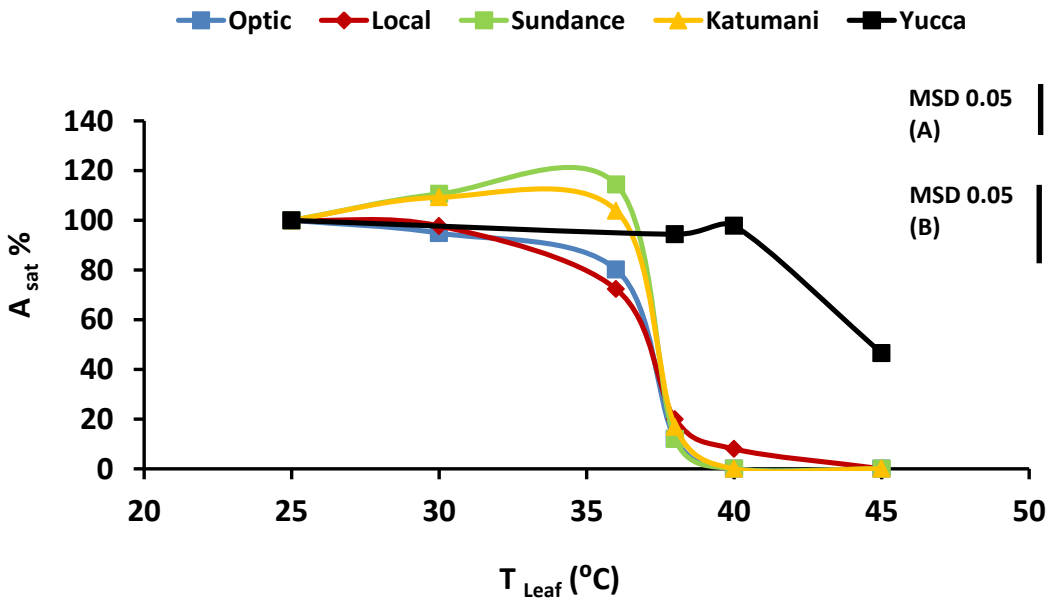

Figure 3-1: The Effect of Increasing Leaf Temperatures on Light Saturated CO_2 Assimilation Rates (A_{sat}) of Barley and Maize Lines and *Y. filimentosa*.

Heat stress was imposed by clamping the attached leaf to a temperature controlled thermal block in the dark at 25.0, 30.0, 36.0, 38.0, 40.0 or 45.0°C (±0.2°C) for three hours. **A_{sat}** was then measured with IRGAs at ambient CO_2 levels (380 µmol CO_2 mol^{-1}air), Saturating light (487 µmol photons. m^{-2}. s^{-1} for barley; 870 µmol photons. m^{-2}. s^{-1} for maize and *Y. filimentosa* and, Tleaf 25.0°C. The values represent the Average and Standard Errors of 3 replicates. ANOVA tests were performed using a General Linear Model and data were normalized as percentage change from control (25°C) which was equivalent to 19.66 (±0.66) µmol . m^{-2}. s^{-1} for Optic, 13.7 (±0.91) µmol . m^{-2}. s^{-1} for Local, 24.76 (±1.12) µmol . m^{-2}. s^{-1} for Sundance and 23.11 (±1.04) µmol . m^{-2}. s^{-1} for Katumani. Tables for ANOVA and group comparisons along with the residual plots are presented in the Appendix (Figure A 3-1a & b). The vertical lines indicate Tukey's Minimum Significant Difference (MSD) at P= 0.05. Treatment means that differ by more than the MSD are significantly different at P= 0.05 level. MSD (A) indicates significant differences across temperatures (within C3 and C4 lines); MSD (B) indicates significant differences across temperatures (within C3, C4 lines and *Y. filimentosa*).

3.2 Effect of Heat Stress on Inhibition and Recovery of Photosynthesis Whole Leaf Parameters of Barley (C3) and Maize (C4)

For C3 and C4 plants, Light Saturated CO_2 Assimilation Rates (**A_{sat}**) were inhibited as temperature exceeded 36.0°C (Figure 3-1)**.** Further experiments were undertaken to investigate the effects of 3 hour heat stress at 38°C and subsequent recovery period on the key parameters of photosynthesis. This included Light Saturated CO_2 Assimilation Rates (**A_{sat}**), carboxylation efficiency **(ΦCO_2)**, transpiration (**E**) and stomatal conductance (**gs**), PSII photochemistry **(ΦPSII**; *i.e.* F_v/F_m), and whole chain photosynthetic electron transport rates (ETR).

3.2.1 Gas Exchange Measurements

3.2.1.1 Light Saturated CO_2 Assimilation Rates (A_{sat}) and Carboxylation Efficiency (ΦCO_2)

The efficiency of the C3 cycle can be estimated from plots of CO_2 assimilation rates and external (**C_a**) and internal (**C_i**) CO_2 concentrations (**A/C_a** and **A/C_i** plots; see Material and Methods, Section 2.3.1). From these plots the parameters **A_{sat}** (Light Saturated CO_2 Assimilation) and the carboxylation coefficient (the efficiency of CO_2 fixation, **ΦCO_2**) can be estimated.

Figure 3-2a presents the results from **A/C_a** measurements on fully expanded leaves of the temperate and sub-tropical lines of barley (Local, Optic) and maize (Sundance, Katamani). In these experiments, measurements were made on the same piece of attached leaf immediately before, immediately after, and five days after raising T_{leaf} to 38.0 (± 0.2 ^{0}C) for 3 hours using a modified thermal cycler (see Material and Methods, Section 2.2 and 2.3.1). From the **A/C_a** curves (CO_2 Assimilation *versus* external CO_2 concentration) **A_{sat}** was estimated at **C_a** 380 µmol CO_2 .mol^{-1} air, and from the corresponding **A/C_i** curves (assimilation *versus* internal CO_2 concentration) the carboxylation coefficient (**ΦCO_2**) was estimated from the initial linear slopes. In all temperate and sub-tropical lines, increasing T_{leaf} to 38.0 (± 0.2 ^{0}C) for 3 hours severely impaired **A_{sat}** to approximately 10 to 20 % of their initial rates. A similar decline was observed in **ΦCO_2** of temperate and sub-tropical lines of barley (Local, Optic). However, the **ΦCO_2** of maize lines declines to 50% of their initial rates. To investigate this observation further, measurements of **A/C_a** responses were monitored on the same piece of attached leaf for up to 5 days post-heat stress to assess the

recovery of photosynthetic competence. There was some evidence of $\mathbf{A_{sat}}$ recovery after 5 days of stress (approximately 20 to 30% of their lost capacity) in all lines; however, it was not significant and there was no evidence that any line recovered better than other lines. No significant recovery of $\mathbf{\Phi CO_2}$ was observed in any of the lines (Figure 3-2a & b).

Figure 3-2: Effects of Three Hours Heat Stress (T_{leaf} 38ºC) and Subsequent Recovery Period on Barley and Maize Photosynthesis.

Top panel **(a):** light saturated CO_2 assimilation rates ($\mathbf{A_{sat}}$); bottom panel **(b):** carboxylation efficiency (ΦCO_2). Parameters were measured with IRGAs and extracted from CO_2 response curves (see Materials and Methods Section 2.3.1) at T_{leaf} 25.0^{0}C (± 0.2^{0}C) and saturating light levels (487µmol .m^{-2} .s^{-1} PAR for barley and 870 µmol photons. m^{-2}. s^{-1} PAR for maize), immediately before, immediately after, and then 5 days after subjecting a marked region of an attached leaf to heat stress. Heat stress was imposed by increasing T_{leaf} to 38.0^{0}C (± 0.2^{0}C) for three hours using a modified thermal cycler (see Materials and Methods Section 2.2). The values represent the Average and Standard Errors of 3 replicates. ANOVA tests were performed using a General Linear Model and data were normalized as percentage change from control which for $\mathbf{A_{sat}}$ measurements are equivalent to 19.66 (±0.66) µmol . m^{-2}. s^{-1} for Optic, 13.7 (±0.91) µmol . m^{-2}. s^{-1} for Local, 24.76 (±1.12) µmol . m^{-2}. s^{-1} for Sundance and 23.11 (±1.04) µmol . m^{-2}. s^{-1} for Katumani; and for ΦCO_2 measurements are equivalent to 0.088 (±0.005) µmol . m^{-2}. s^{-1} for Optic, 0.067 (±0.004) µmol . m^{-2}. s^{-1} for Local, 0.137 (±0.007) µmol . m^{-2}. s^{-1} for Sundance and 0.157 (±0.016) µmol . m^{-2}. s^{-1} for Katumani. The vertical lines indicate Tukey's Minimum Significant Difference (MSD) at P= 0.05 level. Treatment means that differ by more than the MSD are significantly different at P= 0.05. Tables for ANOVA and group comparisons along with residual plots are presented in the Appendix (Figure A 3-2 & 3-3).

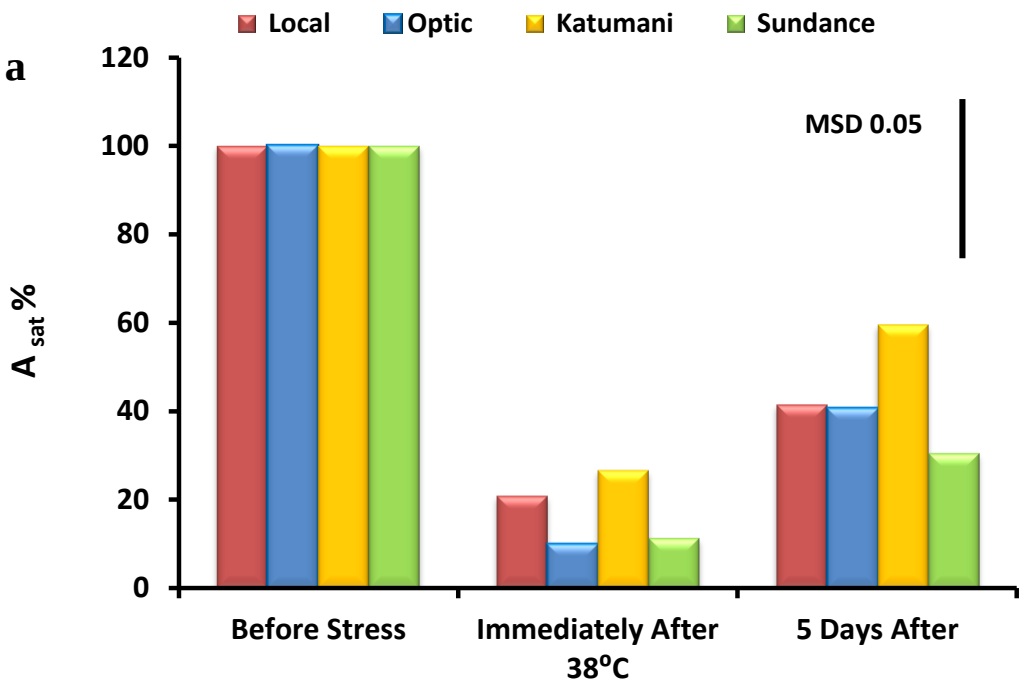
a
Local
Optic
Katumani
Sundance
120
100
80
60
40
20
0
A sat %
MSD 0.05
Before Stress
Immediately After 38°C
5 Days After

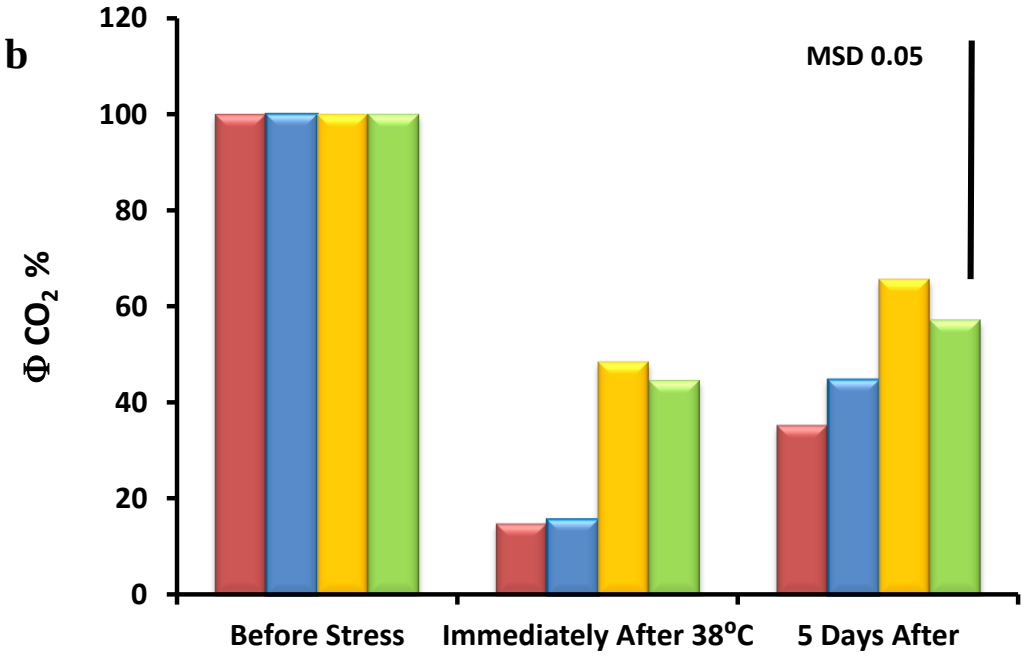
b
120
100
80
60
40
20
0
Φ CO2 %
MSD 0.05
Before Stress
Immediately After 38°C
5 Days After

3.2.1.2 Transpiration (E) and Stomatal Conductance (g_s)

To confirm that the suppression in $\mathbf{A_{sat}}$ arising from a 3 hour heat stress period at 38.0°C was not attributable to stomatal function, parallel measurements of **E** and $\mathbf{g_s}$ were also made on the plants used in the experiments described in Section 2.3.1. The data shown in Figure 3-3a & b were collected from CO_2 response curves (see Material and Methods Section 2.3.1) and revealed that $\mathbf{g_s}$ declined to 30% immediately after heat stress in temperate and sub- tropical maize lines and was not affected by heat stress in the barley line. However, transpiration rates (**E**) remained approximately 70% of the initial rate when T_{leaf} was increased to 38.0°C for 3 hours in all lines, confirming the fact that the substantive suppression in $\mathbf{A_{sat}}$ and $\mathbf{\Phi CO_2}$ could not be attributed to the stomatal closure arising from heat stress events (Figure 3-2 and Figure 3-3a & b; $P<0.05$). No significant recovery of $\mathbf{g_s}$ and **E** was observed in any of the lines.

Figure 3-3: Effects of Three Hours Heat Stress and Subsequent Recovery Period on Stomatal Conductance and Transpiration Rates of Barley and Maize Leaves.

Top panel **(a):** Stomatal Conductance ($\mathbf{g_s}$); bottom panel **(b):** Transpiration (E). Stomatal conductance and transpiration rates were measured at T_{leaf} 25.0ºC (± 0.2 ºC) and saturating light levels (560 µmol .m^{-2} .s^{-1} PAR for barley and 1000 µmol photons. m^{-2}. s^{-1} PAR for maize) immediately before, immediately after, and 5 days after subjecting an attached leaf to heat stress. Heat stress was imposed by increasing T_{leaf} to 38.0ºC (± 0.2 ºC) for three hours using a modified thermal cycler (see Materials and Methods Section 2.2). The values represent the Average and Standard Errors of 3 replicates. ANOVA tests were performed using a General Linear Model and data were normalized as a percentage change from control which for $\mathbf{g_s}$ measurements are equivalent to 0.33 (±0.01) mol. m^{-2}. s^{-1} for Optic, 0.33 (±0.02) mol. m^{-2}. s^{-1} for Local, 0.33 (±0.03) mol. m^{-2}. s^{-1} for Sundance and 0.33 (±0.05) for Katumani; and for E measurements are equivalent to 4.91 (±0.29) m mol. m^{-2}. s^{-1} for Optic, 4.68 (±0.19) m mol. m^{-2}. s^{-1} for Local, 4.51 (±0.21) m mol. m^{-2}. s^{-1} for Sundance and 4.05 (±0.21)) m mol. m^{-2}. s^{-1} for Katumani. The vertical lines indicate Tukey's Minimum Significant Difference (MSD) at P= 0.05 level. Treatment means that differ by more than the MSD are significantly different at P= 0.05. Tables for ANOVA and group comparisons along with residual plots are presented in the Appendix (Figure A 3-4 & 3-5).

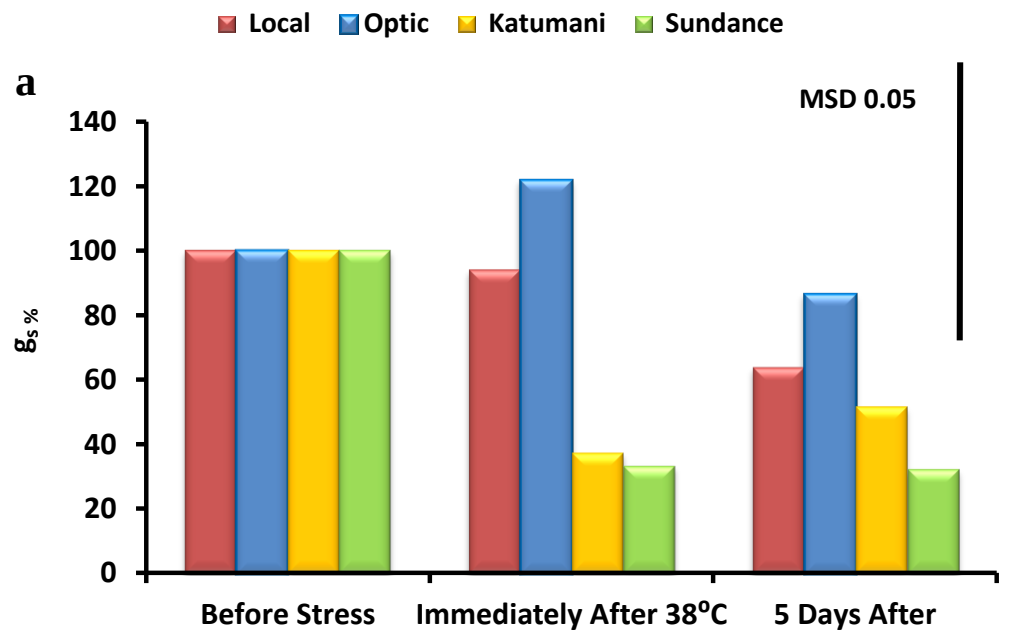
Local
Optic
Katumani
Sundance
a
MSD 0.05
140
120
100
80
60
40
20
0
g_s %
Before Stress
Immediately After 38°C
5 Days After

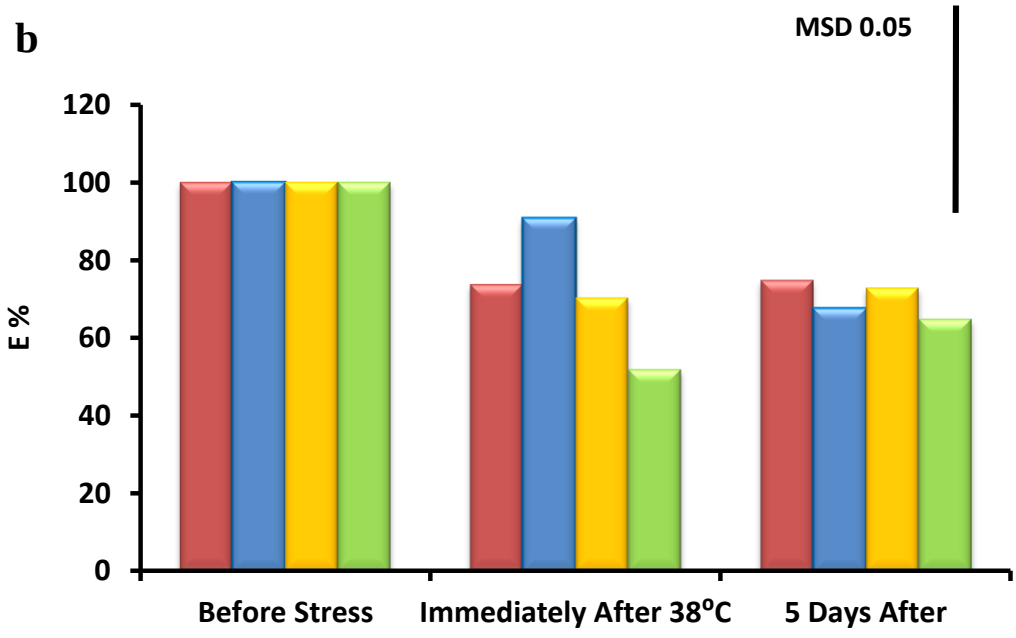
b
MSD 0.05
120
100
80
60
40
20
0
E %
Before Stress
Immediately After 38°C
5 Days After

3.2.2 Fluorescence Measurements

In Figure 3-2 and Figure 3-3 , it was shown that $\mathbf{A_{sat}}$ and $\mathbf{\Phi CO_2}$ were suppressed after 3 hours exposure to T_{leaf} of > 36 ºC, and this was not attributable to changes in the **E** or $\mathbf{g_s}$ of leaves. To investigate whether the suppression in $\mathbf{A_{sat}}$ and $\mathbf{\Phi CO_2}$ could be attributable to primary photochemical events or photosynthetic electron transport, pulse modulated chlorophyll fluorescence techniques were used (Baker 2008).

3.2.2.1 Maximum Quantum Efficiency (F_v/F_m)

The effects of 3 hour heat stress events on PSII photochemistry were assessed using saturating light pulses and modulated fluorescence techniques. Maximum Quantum Efficiency of PSII (**ΦPSII**; *i.e.* $\boldsymbol{F_v/F_m}$ of fully dark adapted leaves), remained approximately 70% of its initial activity after raising T_{leaf} to 38.0 ºC in all lines and this minor decrease was not significantly different after 5 days of stress. No major differences between the lines were observed (Figure 3-4).

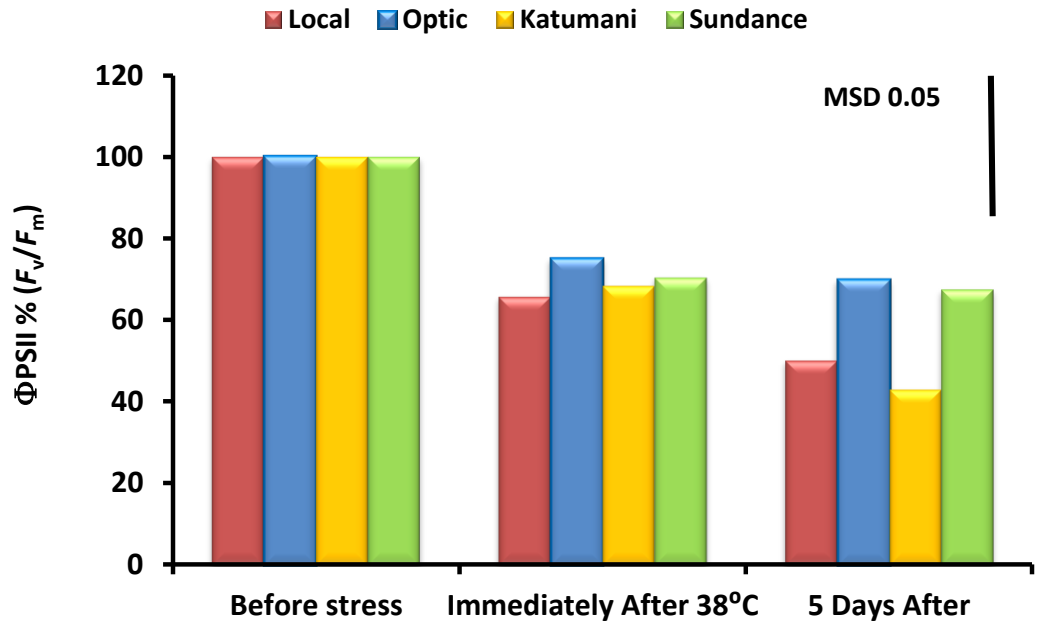

Figure 3-4: Effects of Three Hours Heat Stress and Subsequent Recovery on the Maximum Quantum Efficiency of PSII of Barley and Maize Leaves.

The Maximum Quantum Efficiency **ΦPSII** of dark adapted leaves was measured by pulse amplitude modulated fluorescence (see Materials and Methods, Section 2.4.1) at T_{leaf} 25.0°C (± 0.2°C) immediately before, immediately after, and then 5 days after subjecting a marked region of an attached leaf to heat stress. Heat stress was imposed by increasing T_{leaf} to 38.0ºC (± 0.2ºC) for three hours using a modified thermal cycler (see Materials & Methods Section 2.2). The values represent the Average and Standard Errors of 3 replicates. ANOVA tests were performed using a General Linear Model and data were normalized as a percentage change from control which are equivalent to 0.787 (±0.009) for Optic, 0.787 (±0.004) for Local, 0.740 (±0.009) for Sundance and 0.774 (±0.006) for Katumani. The vertical lines indicate Tukey's Minimum Significant Difference (MSD) at P= 0.05 level. Treatment means that differ by more than the MSD are significantly different at P= 0.05. Tables for ANOVA and group comparisons along with residual plots are presented in the Appendix (Figure A 3-6).

3.2.2.2 *In Vivo* Electron Transport Rates

To observe the thermal stress effects on photosynthetic electron transport rates (ETR) data were collected using a WALZ MINI-PAM fluorimeter fitted with a 2030-B Leaf Clip and an external actinic light (560 µmol m^{-2} .s^{-1} for barley and 800 µmol photons. m^{-2}. s^{-1} PAR for maize) delivered by a 200W quartz halogen bulb. The data shown in Figure 3-5 indicate that increasing T_{leaf} severely impaired steady state ETR in all lines to approximately 10-20% of their pre-stressed values. ETR appears to show no significant recovery after five days in any of the lines (Figure 3-5; $P<0.05$). In addition, no major differences were observed between lines in response to heat stress.

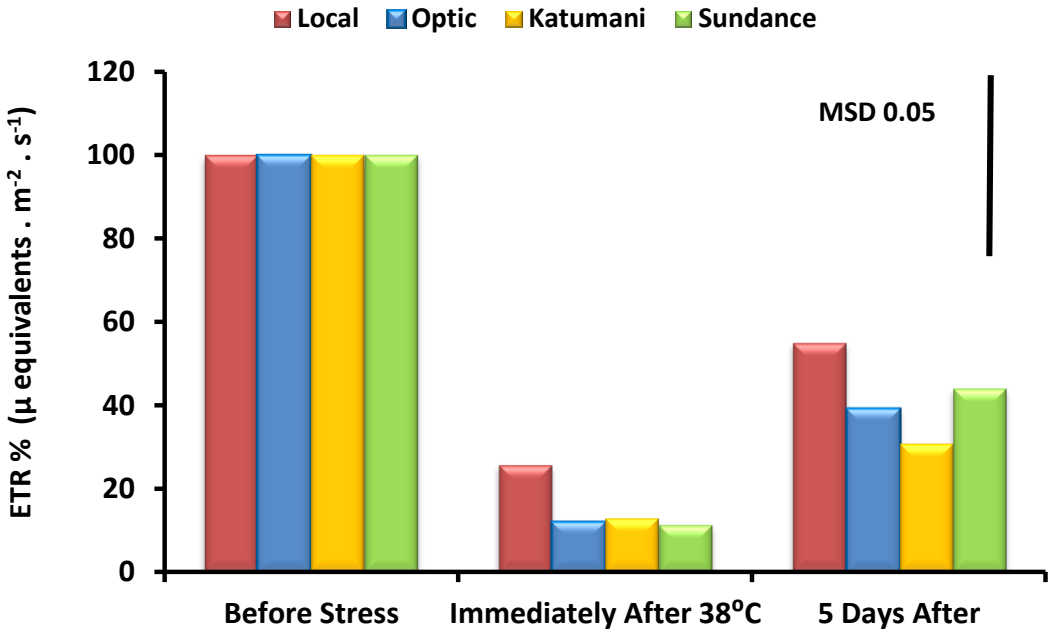

Figure 3-5 : Effects of Three Hours Heat Stress and Subsequent Recovery Period on Barley and Maize *in vivo* Photosynthetic Electron Transport Rates.

Steady state *in vivo* electron transport rates of fully dark adapted barley and maize leaves were collected by pulse amplitude modulated fluorescence (see Materials and Methods, Section 2.4.1) at T_{leaf} 25.0 ºC (± 0.2 ºC) immediately before, immediately after, and then 5 days after subjecting a marked region of an attached leaf to heat stress. Heat stress was imposed by increasing T_{leaf} to 38.0 °C (± 0.2 °C) for three hours using a modified thermal cycler (see Materials and Methods, Section 2.2). The values represent the Average and Standard Errors of 3 replicates. ANOVA tests were performed using a General Linear Model and data were normalized as a percentage change from control which are equivalent to 117.8 (±7.1) for Optic, 79.7 (±3.1) for Local, 127.5 (±14.1) for Sundance and 147.2 (±13.0) for Katumani. The vertical lines indicate Tukey's Minimum Significant Difference (MSD) at P= 0.05. Treatment means that differ by more than the MSD are significantly different at the P= 0.05 level. Tables for ANOVA and group comparisons along with residual plots are presented in the Appendix (Figure A 3-7).

3.3 Characterization of Thermotolerance in *Y. filimentosa*

The range of thermotolerance in the angiosperms is very broad. It has long been known that Agaves, such as *Y. filimentosa*, have the ability to cope with extremely high temperatures (Nobel and Smith 1983). Understanding the mechanism that leads to heat tolerance in plants may be critical for engineering crop plants that can tolerate heat stress and produce economic yield under heat-stress conditions. In order to determine how these plants respond to high leaf temperatures, the effects of increasing *Y. filimentosa* leaf temperature and the following recovery on the key parameters of photosynthesis were examined.

3.3.1 Light Saturated CO_2 Assimilation Rates (A_{sat})

$\mathbf{A_{sat}}$ activity was suppressed markedly immediately after increasing leaf temperature to 38.0, 40.0 and 45.0°C for 3 hours. However, a rapid full recovery was observed after 1 hour exposure to 38.0 and 40.0°C, but full recovery at extreme high temperature (45.0°C) required up to 3 days (Figure 3-6).

3.3.2 Transpiration (E) and Stomatal Conductance (g_s)

At 38 and 40°C treatment, stomata in *Y. filimentosa* were closed for 20 minutes immediately after exposure which presumably resulted in the observed marked suppressions of $\mathbf{A_{sat}}$ activity (98%, see Figure 3-6 and Figure 3-7). Within one hour, however, stomata re-opened. For leaves exposed to 38.0^0C, full recovery was observed after one hour but at higher temperatures, $\mathbf{g_s}$ increased to beyond their pre-stress values ($P < 0.05$). In contrast, stomata were open immediately after stress at 45.0°C. A similar pattern was observed for transpiration rate (Figure 3-7b). The results indicate that the marked decline in $\mathbf{A_{sat}}$ activity of (approximately 50%) observed by increasing leaf temperatures to 45°C was not attributable to stomatal limitation for CO_2 uptake (Figure 3-6 and Figure 3-7). Further, it suggests that unlike the cereal crops studied, *Y. filimentosa* closes its stomata when exposed to moderate heat stress (< 45.0°C), but open at temperatures between 40.0 and 45.0°C.

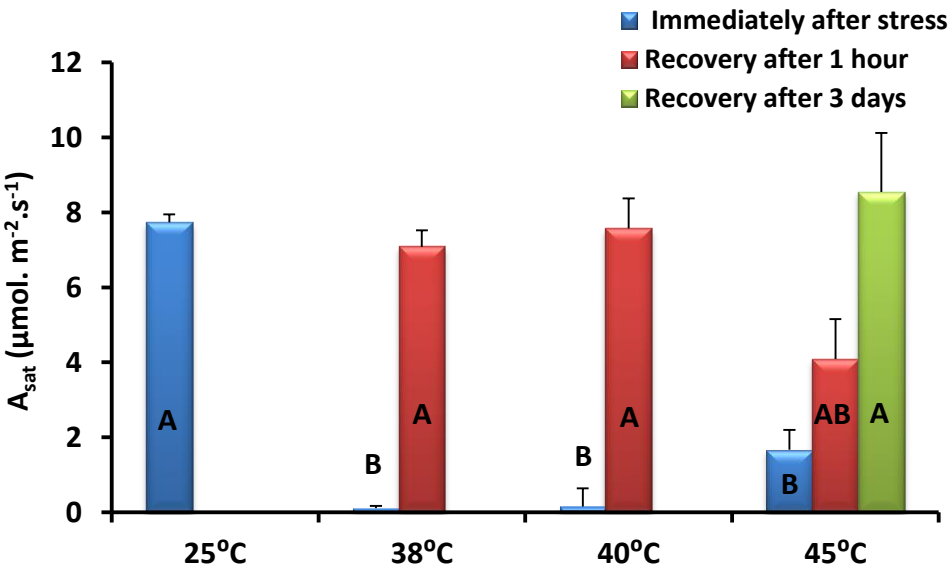

Figure 3-6 : The Effect of Increasing Leaf Temperatures and Subsequent Recovery Period on Light Saturated CO_2 Assimilation Rates (A_{sat}) of *Y. filimentosa*.

Heat stress was imposed by clamping an attached leaf to a temperature controlled thermal block at 25.0, 38.0, 40.0 and 45.0°C (±0.2°C) for three hours. $\mathbf{A_{sat}}$ was then measured at ambient CO_2 levels (380 µmol CO_2. mol^{-1}), high light (1000 µmol photons. m^{-2} s^{-1}), and T_{leaf} 25°C immediately, after 1 hour and then 3 days after subjecting a marked region of an attached leaf to heat stress (see Materials and Methods, Section 2.4.1). The values represent the Average and Standard Errors of 3 replicates. ANOVA tests were performed using a General Linear Model. Different letter codes indicate Tukey's significant differences at $P<0.05$ at each HS treatment compared with control. Tables for ANOVA and grouping comparison along with Figures for residual plots are presented in the Appendix (Figure A 3-8a, b&c).

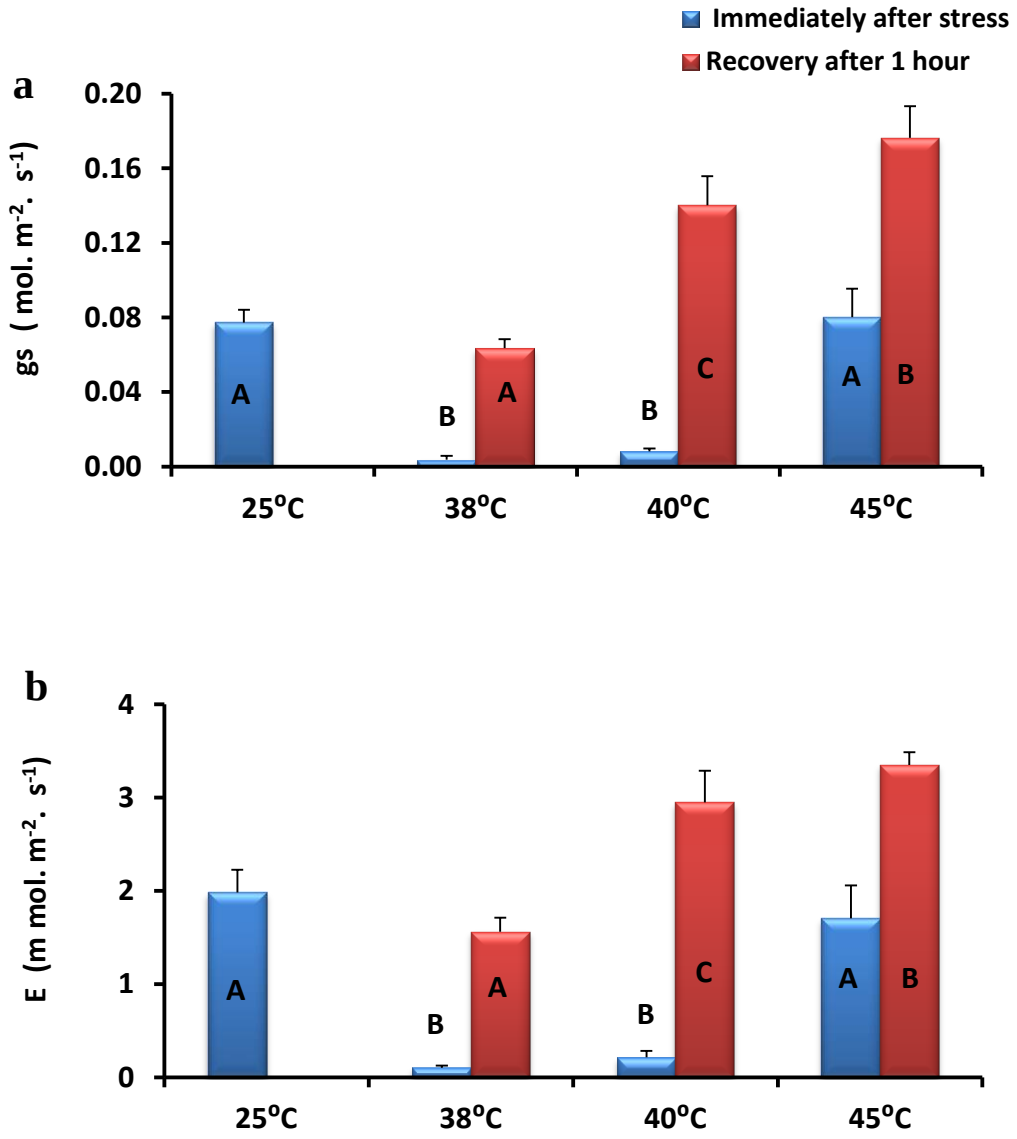

Figure 3-7 : Effect of Increasing Leaf Temperatures and Subsequent Recovery Period on Stomatal Conductance (g_s) and Transpiration Rate (E) of Attached *Y. filimentosa* Leaves.

Top panel **(a):** stomatal conductance ($\mathbf{g_s}$); bottom panel **(b):** transpiration (**E**). $\mathbf{g_s}$ and **E** were measured along with $\mathbf{A_{sat}}$ as described in Materials and Methods, Section 2.3.1, at T_{leaf} 25.0ºC (± 0.2 ºC) and saturating light levels (1000 µmol photons. m^{-2}. s^{-1} PAR) immediately before, immediately after, and 1 hour after subjecting a fully expanded attached leaf to heat stress. Heat stress was imposed by increasing T_{leaf} to 25.0, 38.0, 40.0 or 45.0°C (±0.2°C) for three hours using a modified thermal cycler (see Materials and Methods, Section 2.2). The values represent the Average and Standard Errors of 3 replicates. ANOVA tests were performed using a General Linear Model. Different letters codes indicate Tukey's significant differences at $P<0.05$ at each HS treatment compared with control. Tables for ANOVA and group comparisons along with residual plots are presented in the Appendix (Figure A 3-9a to A 3-10c).

3.3.3 Maximum Quantum Efficiency (F_v/F_m) and Steady State *in vivo* Photosynthetic Electron Transport Rate (ETR)

The Maximum Quantum Efficiency of photosystem II (F_v/F_m) was relatively insensitive to high leaf temperatures. Raising T_{leaf} to a range of high temperatures produced a significant ($P<0.05$) but relatively modest (approximately 30%) suppression at very high leaf temperature (45°C) (Figure 3-8a). In contrast, heat stress did lead to decreases in ETR but this inhibition was marginal until leaf temperature was very high (45°C). As leaf temperature was increased to 45°C, ETR decreased significantly below 20% relative to the 25°C control. However, leaves exposed to extreme temperature (45°C) fully recovered within 3 days (Figure 3-8b).

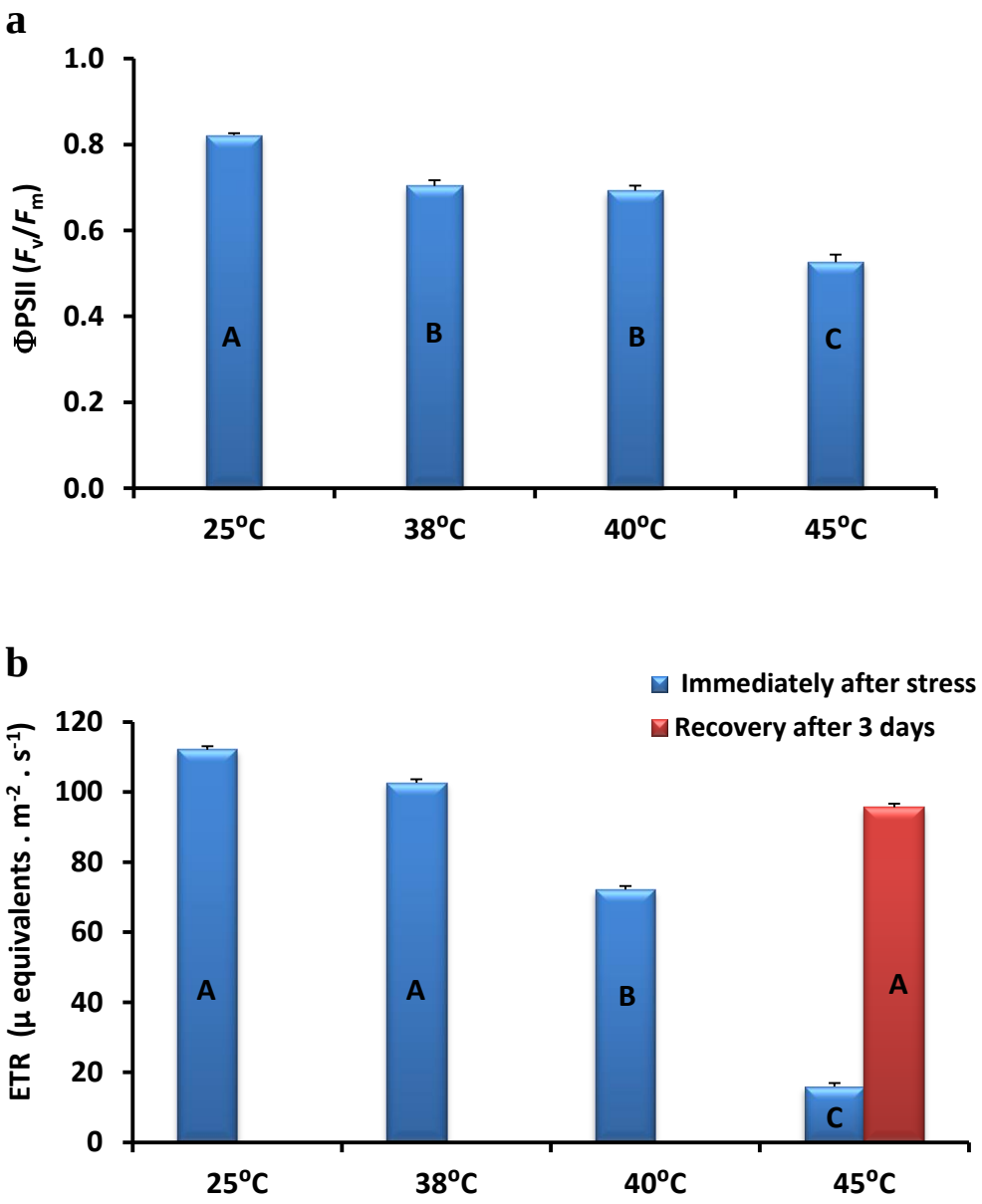

Figure 3-8 : Effects of Increasing Leaf Temperatures and Subsequent Recovery Period on the Maximum Quantum Efficiency (Φ PSII) and *in vivo* Electron Transport Rate of *Y. filimentosa* Leaves.

Top panel **(a):** maximum quantum efficiency (ΦPSII) bottom panel **(b):** electron transport rate ETR: ΦPSII and electron transport rates of fully dark adapted leaves were estimated using pulse amplitude modulated fluorescence (see Materials and Methods, Section 2.4.1) at T_{leaf} 25.0 ºC (± 0.2ºC) immediately before, immediately after, and then 3 days after subjecting a marked region of an attached leaf to heat stress. Heat stress was imposed by increasing T_{leaf} to 38.0, 40.0 or 45.0 °C (± 0.2 °C) for three hours using a modified thermal cycler (see Materials and Methods, Section 2.2). The values represent the Average and Standard Errors of 5 replicates. ANOVA tests were performed using a General Linear Model. Different letters codes indicate Tukey's significant differences at $P<0.05$ at each HS treatment compared with control. Tables for ANOVA and group comparisons along with residual plots are presented in the Appendix (Figure A 3-11 to A 3-12b).

3.4 Discussion

The inherent ability of plants to cope with heat stress is reported to differ between species *e.g.,* temperate and tropical species (Cunningham and Read 2002), and even among ecotypes of the same species (Bjorkman, Mooney *et al.* 1975). Understanding the mechanisms of temperature responses of photosynthesis from species with different thermotolerance is of immense importance for identifying rate limiting targets for enhancing leaf photosynthesis. Therefore, in this study, temperature responses of the Light Saturated CO_2 Assimilation rates at 380 µmol CO_2 mol^{-1}air ($\mathbf{A_{sat}}$) were measured in plant species from contrasting thermal environments: two Barley (C3, Optic and Local) and two Maize (C4, Sundance and Katumani) lines that are routinely grown in temperate and arid sub-tropical regions, respectively. In addition to *Y. filimentosa*, an obligate C3 plant adapted to hot arid habitats was also studied.

Gas exchange measurements on C4 plants presented in this study showed maize lines were tolerant of relatively modest leaf temperatures with inhibition not observed until leaf temperature exceeded 36°C similar to published data (Berry and Bjorkman 1980; Crafts-Brandner and Salvucci 2002). Data presented in this chapter show a significant inhibition also occurred in barley leaves at temperatures higher than 36°C. However, at high leaf temperature, 38, 40 and 45°C, $\mathbf{A_{sat}}$ was suppressed dramatically by >85% in all lines regardless of their origins (temperate or sub- tropical). A decline in CO_2 assimilation rates in crop plants at high leaf temperature has been reported by many (Crafts-Brandner and Salvucci 2002; Sinsawat, Leipner *et al.* 2004). Although C4 plants have a higher temperature optimum than C3 plants (Berry and Bjorkman 1980), the general temperature response of $\mathbf{A_{sat}}$ in maize lines was similar to the response of barley lines. This similarity suggests that for both photosynthesis types, the thermal site of damage might be identical. Compared with both C3 and C4 plants, *Y. filimentosa* responded differently to increasing leaf temperatures with no inhibition observed until leaf temperature exceeded 40°C. However, even when T_{leaf} was increased to 45°C for 3 hours, $\mathbf{A_{sat}}$ in *Y. filimentosa* plants was still 50% of its initial activity immediately after heat stress; full recovery occurred within 3 days (Figure 3-6). It can be concluded that there were no major differences in responses of photosynthesis to increasing leaf temperature between barley and maize from temperate and tropical lines while *Y. filimentosa* showed greater ability to maintain high photosynthesis after heat stress.

Further experiments were conducted to evaluate if the lines differed with respect to their recovery from heat stress. Across all lines, CO_2 assimilation rates were severely suppressed (> 85%) immediately after exposure to 38.0°C for 3 hours. Heat stressed plants failed to recover fully after 5 days in all lines (Figure 3-2). This suggests heat induced irreversible damage for both temperate and arid sub-tropical lines which was not due to stomatal closure, as evidenced by maintenance of relatively high values of $\mathbf{g_s}$ and transpiration rates (Figure 3-3).

Measurements of chlorophyll fluorescence have shown that in both C3 and C4 lines, the maximum quantum efficiency of PSII (**ΦPSII**) was suppressed only by 30% immediately after increasing leaf temperature to 38°C for 3 hours. At this leaf temperature, there was a marked inhibition in $\mathbf{A_{sat}}$ (> 85%) in all lines; therefore, it is unlikely that inhibition of **ΦPSII** made the main contribution to the inhibition of $\mathbf{A_{sat}}$ as reported previously (Havaux 1993). Measurement of *in vivo* photosynthetic electron transport rate (ETR) showed the rate declined after heat stress to the same extent as $\mathbf{A_{sat}}$. This inhibition could be due to the direct effect of heat stress on the components of the electron transport chain. Alternatively, because ETR decreased to the same extent as $\mathbf{A_{sat}}$, it is perhaps more likely that the rate of ETR is correlated with CO_2 assimilation rates as linear ETR requires a coordinated turnover of the C3 cycle. Consequently, any suppression in the efficiency of the C3 cycle would feedback and result in a decrease in ETR. Therefore, the direct effect of heat stress on ETR should be determined when ETR is uncoupled from CO_2 by adding an electron acceptor like methyl viologen (see chapter 4, section4.2).

The gas-exchange responses of *Y. filimentosa* to a range of leaf temperatures were examined. Although *Y. filimentosa* is an obligate C3 plant, the results contrasted with the patterns observed for C3 and C4 crops and showed a marked suppression of $\mathbf{A_{sat}}$ immediately after heat stress which, unlike the other lines, recovered quickly within one hour of release from temperature stress. This response observed in *Y. filimentosa* is consistent with the suppressions of **E** and $\mathbf{g_s}$ and correlated with the rapid recovery of $\mathbf{A_{sat}}$ with changes in stomatal conductance. It is likely that directly after heat stress at 38.0 and 40.0 °C, stomata close to avoid water loss, thereby restricting photosynthesis. Under field conditions, midday closure of stomata has been observed in many species to avoid water loss (Quick, Chaves *et al.* 1992). However, within one hour of recovery, stomata opened for transpirational cooling which was accompanied by a full recovery of $\mathbf{A_{sat}}$. In contrast to this pattern, above 40.0°C, the rate of stomatal conductance was considerably higher and is most probably driven by the plant's need for evaporative cooling to maintain a lower leaf temperature. These observations suggested a different response of stomatal regulation to

temperature in *Y. filimentosa*. It can be assumed that $\mathbf{g_s}$ suppresses $\mathbf{A_{sat}}$, at leaf temperatures of 36°- 40°C by closing to avoid dehydration, but when leaf temperature exceeds 40.0°C, stomata open to maintain lower leaf temperature and prevent thermal damage.

Chlorophyll fluorescence measurements on *Y. filimentosa* showed that Maximum Quantum Efficiency of photosystem II ($\boldsymbol{F_v/F_m}$) was relatively stable in response to increasing leaf temperature up to 45°C. This observation is consistent with findings reported by(Huxman, Hamerlynck *et al.* 1998) where ($\boldsymbol{F_v/F_m}$) was not sensitive to high temperature (up to 53°C) in three species of *Y. filimentosa*. A similar pattern was observed for ETR with no inhibition observed until leaf temperature increased to 45°C. At this leaf temperature, the suppression in $\mathbf{A_{sat}}$ immediately after and 1 hour after heat stress did not appear to be due to stomatal limitation as $\mathbf{g_s}$ values were the same as controls. In addition, after 1 hour of recovery, $\mathbf{g_s}$ and transpiration rates increased significantly compared with controls. It is more likely that inhibition of $\mathbf{A_{sat}}$ at 45°C, is due to the direct effect of heat stress on the components of the electron transport chain or the activity of C3 cycle enzymes.

Table 3-1: Summery of the Effects of Three Hours Heat Stress at 38ºC and Subsequent Recovery on light saturated CO_2 assimilation rates (A_{sat}), carboxylation efficiency (ΦCO_2), Stomatal Conductance (g_s), Transpiration (E), Maximum Quantum Efficiency of PSII (ΦPSII; F_v/F_m) and *in vivo* Electron Transport Rates.

	A_{sat} µmol . m^{-2}. s^{-1} ± SE	ΦCO_2 µmol . m^{-2}. s^{-1} ± SE	g_s mol. m^{-2}. s^{-1} ± SE	E mmol. m^{-2}. s^{-1} ± SE	ΦPSII (F_v/F_m) ± SE	*in vivo* ETR µ equivalents . m^{-2} . s^{-1}± SE
Local- control	13.7 ±0.91	0.067 ±0.004	0.33 ±0.02	4.68 ±0.19	0.787 ±0.004	79.7 ±3.1
38 ºC	2.8 ± 0.90	0.010 ±0.003	0.32 ±0.15	3.50 ±0.78	0.517 ±0.042	21.3 ±10.3
Recovery	5.7 ± 2.11	0.024 ±0.011	0.21 ±0.0	3.51 ±0.56	0.395 ±0.146	45.4 ±23.1
Optic-control	19.66 ± 0.66	0.088 ±0.005	0.33 ±0.01	4.91 ±0.29	0.787 ±0.01	117.8 ±7.1
38 ºC	1.94 ± 0.46	0.013 ±0.003	0.39 ±0.03	4.41 ±0.37	0.589 ±0.12	14.2 ±3.9
Recovery	7.89 ± 2.55	0.038 ±0.011	0.27 ±0.12	3.18 ±0.77	0.548 ±0.07	45.9 ±2.2
Sundance-control	24.8 ±1.12	0.137 ±0.007	0.33 ±0.03	4.51 ±0.21	0.740 ±0.01	127.5 ±14.1
38 ºC	2.9 ±0.40	0.061 ±0.008	0.13 ±0.03	2.64 ±0.33	0.519 ±0.02	20.7 ±6.5
Recovery	7.5 ±1.34	0.078 ±0.016	0.12 ±0.01	2.49 ±0.09	0.478 ±0.03	57.6 ±6.7
Katumani-control	23.11 ±1.04	0.157 ±0.02	0.33 ±0.05	4.05 ±0.21	0.774 ±0.01	147.2 ±13.0
38 ºC	6.25 ±1.33	0.080 ±0.03	0.13 ±0.05	2.84 ±0.48	0.530 ±0.02	18.4 ±8.4
Recovery	13.83 ±2.01	0.104 ±0.03	0.17 ±0.06	2.92 ±0.53	0.333 ±0.02	44.4 ±3.0

4 Chapter 4: Further Studies on the Thermal Sensitivity of Barley: Photosynthesis Rates

In section 3.2.1 and 0, it was shown that A_{sat} and ΦCO_2 were suppressed by 3 hour exposure to T_{leaf} of > 36.0ºC, and this was not attributable to changes in g_s or ΦPSII. However, it is still not clear which photosynthetic processes are affected. For example, a decline in the steady state rates of A_{sat} and ΦCO_2 could arise from thermal injury of the light harvesting capacity of a leaf, primary photochemical events in the reaction centers of PSI and PSII, steady state photosynthetic electron transport rates (ETR), the capacity of the light reactions to generate ATP and NADPH, the kinetic properties of enzymes of the C3 cycle, or the concentration of CO_2 in the chloroplast (the site of RuBisCO; see Figure 4-1.

The C3 cycle is initiated by the enzyme RuBisCO that catalyzes the carboxylation of the CO_2 acceptor molecule RuBP to form 3-PGA. The resulting 3-PGA is converted to glyceraldehyde phosphate and dihydroxyacetone phosphate; the reaction requires the consumption of ATP and NADPH. The regeneration phase of the cycle involves a series of reactions that convert triose phosphates into RuBP (Figure 4-4). Generally, under saturating light condition, the limitations of CO_2 assimilation rate are partitioned between the activity of RuBisCO and the capacity for RuBP generation according to the widely used model of CO_2 uptake (Farquhar, von Caemmerer *et al.* 1980). It has been suggested for some time that a large proportion of the limitation to carbon assimilation by the C3 cycle after heat stress is due to the thermal lability of RuBisCO Activase (Crafts-Brandner and Salvucci 2000; Salvucci and Crafts-Brandner 2004a; Kim and Portis 2005). Phosphoribulokinase (PRK) catalyzes the synthesis of RuBP the substrate for CO_2 fixation and, similar to RuBisCO Activase, PRK is a nuclear-encoded chloroplast stromal protein that requires ATP for activity. It was found that in tobacco, RuBisCO Activase was extremely sensitive to thermal denaturation while RuBisCO and PRK were much more thermally stable up to 48°C (Salvucci, Osteryoung *et al.* 2001).

Metabolic control analysis, however, was used to explore the possibility that enzymes other than RuBisCO may also have a role in determining rates of carbon flux through the C3 cycle. The limitation of the C3 cycle at optimum temperature was explored directly through the use of transgenic plants which were deficient in key enzymes of the pathway (Stitt and Schulze 1994; Raines 2003). It was reported that reductions in the activities of enzymes catalyzing highly regulated, effectively irreversible reactions, for example, glyceraldehyde-3-phosphate dehydrogenase (GAPDH), fructose 1,6-bisphosphatase (FBPase), and phosphoribulokinase (PRK), had little impact on carbon assimilation

(Raines 2003; Stitt, Lunn *et al.* 2010). In contrast, small reductions (<35%) in the enzyme sedoheptulose-1,7-bisphosphatase (SBPase) resulted in a significant decrease in CO_2 fixation and growth, identifying this enzyme as a major control point in the C3 cycle (Harrison, Olcer *et al.* 2001; Olcer, Lloyd *et al.* 2001). It was observed in chilled tomato leaves a decrease in the activity of SBPase and FBPase enzymes suggesting that the activates of these two enzymes are the primary restriction on photosynthesis (Sassenrath, Ort *et al.* 1990). To our knowledge however, none of the antisense lines have been used to study the response of the C3 cycle control coefficients to temperature, although it is conceivable they could have significant control over the response given their ability to affect CO_2 assimilation rate at the thermal optimum. In addition, this approach has demonstrated in model species and need to be tested in crop plants. Further experiments, were conducted to assess the effect of 3 hours of heat stress on several key sites in the C3 cycle to identify the primary site of thermal damage; the results are presented in this chapter.

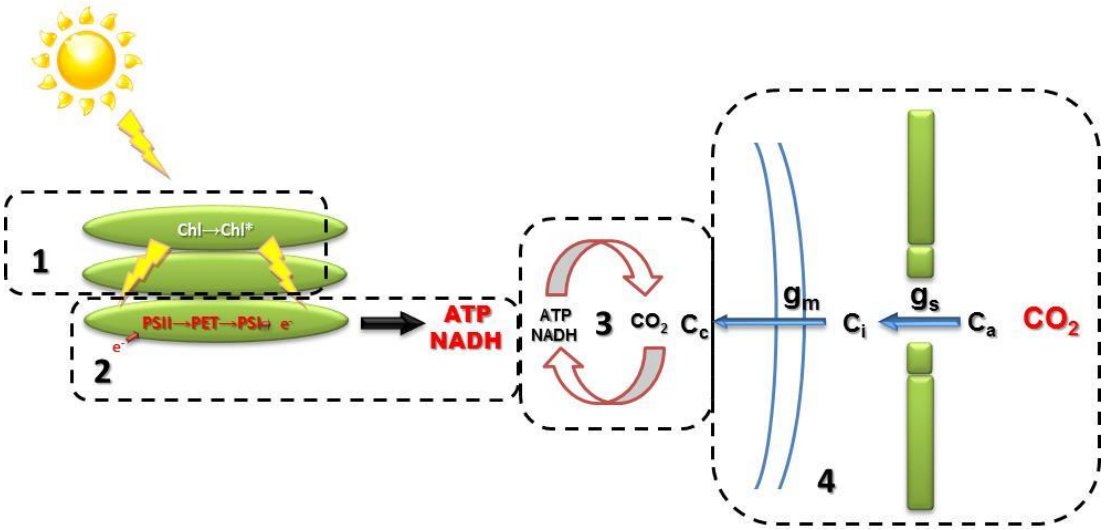

Figure 4-1: Schematic Diagram Showing the Potential Target Sites for Thermal Injury of CO_2 Assimilation in C3 Plants.

Assimilation rates can be affected by changes in the efficiency of one or more processes that contribute to leaf photosynthesis. **1**, light capture and exciton transfer to PSI and PSII reaction centres (RCI and RCII): **2**, Photochemistry in RCI and RCII, photosynthetic electron transport rates (ETR), the generation of ATP (by chemiosmosis) and NADPH (via electron transfer from ferridoxin to $NADP^+$ reductase): **3**, the kinetic properties of the enzymes of the C3 cycle: **4**, the combined conductance controlling the delivery of CO_2 from air to the chloroplast stroma *i.e.* stomatal ($\mathbf{g_s}$) and mesophyll ($\mathbf{g_m}$) conductance.

4.1 Light Harvesting Capacity

To examine whether the dramatic suppression in CO_2 assimilation rates was attributable to the efficiency of the light harvesting processes, leaf absorbance and chlorophyll fluorescence excitation spectra were measured immediately before and after heat stress of leaves from barley *cv*. local.

4.1.1 Leaf Absorbance

Measurements before (T_{leaf} 25.0ºC) and after 3 hours of thermal stress (T_{leaf} 38.0ºC) indicated no major changes in leaf absorbance measured using a Perkin Elmer λ800 spectrophotometer fitted with a Lab-sphere PELA-1020 Integrated Sphere (2 nm slit widths; Figure 4-2a).

4.1.2 Chlorophyll Fluorescence Excitation Spectra

The efficiency of light capture and exciton energy transferred from the Chl*b*-containing peripheral Light Harvesting Complexes (LHCs) to the Chl*a* containing PSII core units can be assessed from room temperature Chl*a* excitation spectra. Fluorescence emission (at 680 nm) emanates from Chl*a* in the core PSII units which are excited directly through Chl*a* absorption (from 420-445 nm), or through Chl*b* absorption in the peripheral LHCs (from 460-490 nm) and energy transfer to Chl*a* in the PSII core (Baker 2008). The Chl*a* fluorescence emission excited directly through Chl*a* (440 nm) and through Chl*b* (480 nm), therefore, providing an estimate of the efficiency of light absorption and energy transfer from the peripheral Chl*a* / Chl*b*-containing LHCs to the Chl*a*-containing PSII units. These spectra indicate that excitation of PSII core complexes through Chl*a* and Chl*b* is similar before and after heat stress (Figure 4-2b), implying the observed decline in $\mathbf{A_{sat}}$ is not attributable to a decrease in the rate of energization of the PSII reaction centres due to decreased energy transfer between the LHCs.

Figure 4-2: Normalized Absorbance and Fluorescence Excitation Spectra Before and After Heat Stress in Single Leaves of Barley *cv.* Local.

Top Panel (**a**): normalized absorbance spectra; bottom panel (**b**): normalized Chl*a* fluorescence excitation spectra. Leaf absorbance was measured before (25.0 ºC) and after a 3 hour heat stress (38.0 ºC) period using a Perkin Elmer λ800 spectrophotometer fitted with a Labsphere PELA-1020 Integrated Sphere (2 nm slit widths). The efficiency of light absorption and exciton delivery to PSII reaction centres was assessed from Chl*a* excitation spectra measured at room temperature using a Perkin Elmer LS55 fluorimeter fitted with a fibre optic attachment (excitation 350-600 nm with 5 nm slit widths; emission, 680 nm 10 nm slit widths; for full details, see Materials and Methods, Section 2.5). The arrows indicate the peaks in PSII Chl*a* emission that arise from direct excitation into Chl*a* and Chl*b* (peripheral LHCs complexes).

a

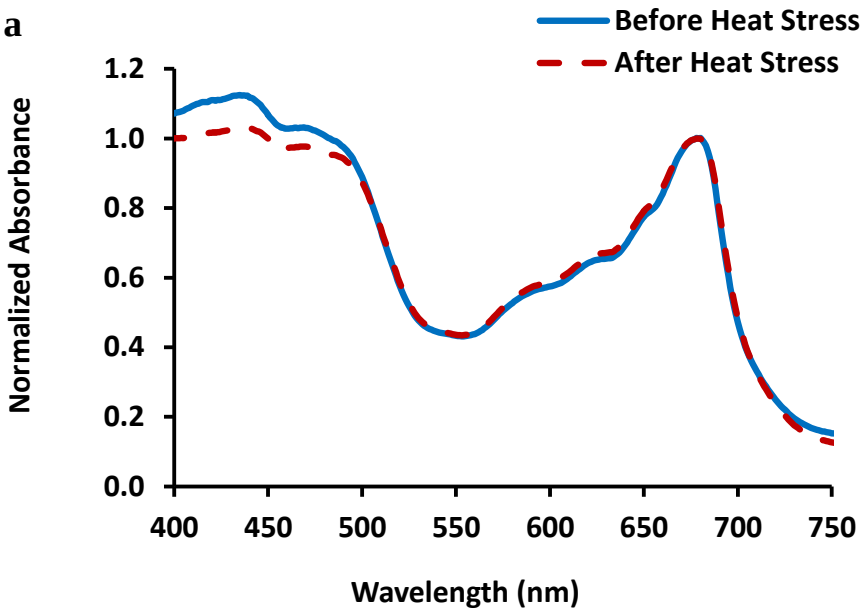
Before Heat Stress
After Heat Stress
Normalized Absorbance
1.2
1.0
0.8
0.6
0.4
0.2
0.0
400
450
500
550
600
650
700
750
Wavelength (nm)

b

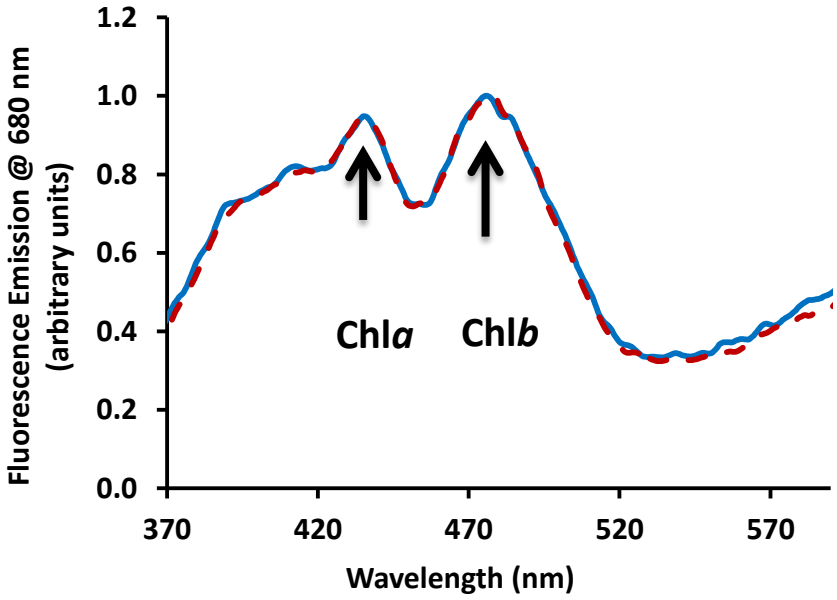
Fluorescence Emission @ 680 nm
(arbitrary units)
1.2
1.0
0.8
0.6
0.4
0.2
0.0
Chl*a*
Chl*b*
370
420
470
520
570
Wavelength (nm)

4.2 *In vitro* Electron Transport Rate (ETR)

Measurements on the response of electron transport capacity to increasing leaf temperature are complex. As shown in section 3.2.2.2, *in vivo* ETR, not surprisingly, was suppressed after heat stress at 38.0^{0}C to a similar extent as $\mathbf{A_{sat}}$. *In vivo,* linear ETR requires a coordinated turnover of the C3 cycle and thus the rate of ETR is correlated with CO_2 assimilation rates. *In vitro* ETR was measured, therefore, to determine whether the suppression in *in vivo* ETR is attributable to a direct effect on the components of the electron transport chain or to thermal damage of downstream mechanisms such as the maintenance of sufficient levels of chloroplast ATP and NADPH, enzyme activity of the C3 cycle, *etc*.

Figure 4-3 shows the effects of increasing leaf temperature on the whole chain photosynthetic electron transport rates (H_2O to methyl viologen) of thylakoid membranes measured *in vitro* isolated form heat stressed barley leaves. This assay measures the light-saturated rate of electron transport from water through PSII and PSI to an excess of the artificial electron acceptor methyl viologen. Electron transport rates (ETR) declined with increasing T_{leaf} but still retained approximately 40% of its control activity even after exposure of leaves to 40.0^{0}C for 3 hours.

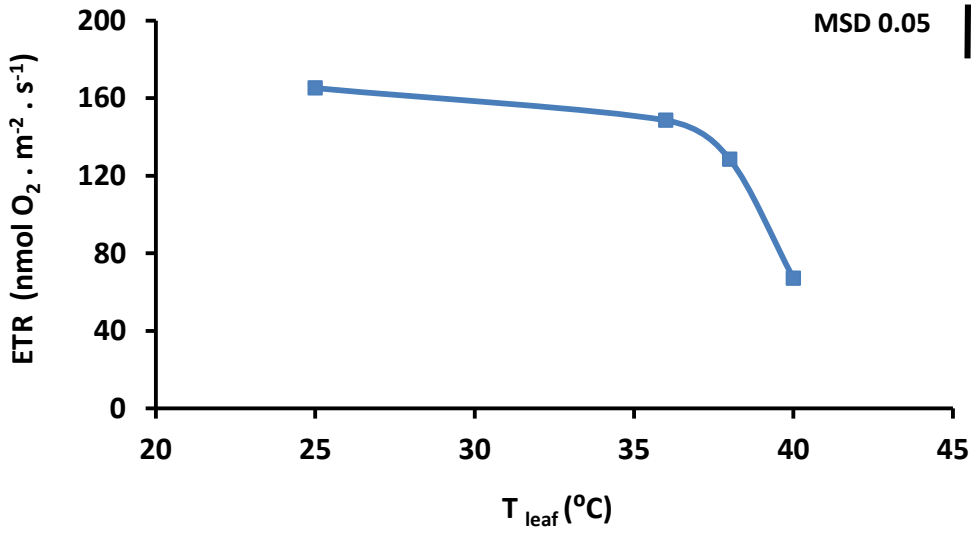

Figure 4-3: Effect of Increasing Leaf Temperatures on Photosynthetic Electron Transport Rates in Isolated Thylakoid Membranes from Barley *cv.* Local Leaves.

Leaves were heat treated as described in section 2.2. Thylakoid membranes were rapidly prepared and whole chain electron transport rates (ETR; H_2O to methyl viologen) measured at 25.0^0C with an oxygen electrode (see Materials and Methods, Section2.6). The values presented are the difference in ETR in saturating light (560 µmol m^{-2} s^{-1} PAR) before and after the addition of DCMU (Diuron;3-(3,4-dichlorophenyl)-1,1-di-methylurea) as an electron transport inhibitor. The values represent the Average and Standard Errors of 5 replicates. ANOVA tests were performed using a General Linear Model. The vertical lines indicate Tukey's Minimum significant difference (MSD) at P= 0.05 level. Treatment means that differ by more than the MSD are significantly different at P= 0.05. Tables for ANOVA and group comparisons along with residual plots are presented in the Appendix (Figure A 4-1).

4.3 Metabolite Profiling of C3 Cycle Enzymes

Metabolite profiles of C3 cycle intermediates before and immediately after heat stress were obtained during previous studies in our laboratory (Shahwani 2011) and were carried out by Dr. Stéphanie Arrivault at the Max Planck Institute of Molecular Plant Physiology, Germany. Samples used for profiling metabolite pools were collected as described previously (see Material and Methods Section 2.8.1). Metabolites of C3 cycle were isolated and quantified using 2D liquid chromatography (LC) linked to triple mass spectrometry (MS/MS/MS, for more details see Material and Methods, Section 2.7 and Arrivault, Guenther *et al.* 2009). The results of these studies suggested carbon flow between Ri5P and 3-PGA is compromised after heat stress as the metabolite pools after CO_2 fixation by RuBisCO (3-PGA, DHAP and S7P) were depleted while those that feed into RuBisCO (X5P/Ru5P, and Ri5P) were unaffected (Table 4-1and Figure 4-4).

Table 4-1: Metabolites Pools in the Leaves of Local and Optic Barley Lines Before and Immediately after Heat Stress of 40.0 ±0.2 ºC for 3 hours (Shahwani 2011).

Amount (nmol .g^{-1} F Wt), * (µmol .g^{-1} F Wt)

Metabolite	Local Control	Local Stressed	Optic Control	Optic Stressed
Aconitate	34.2 ± 4.6	35.1± 5.6	28.8 ± 5.4	18.8 ± 5.4
ADP	**0.9 ± 0.5**	**4.3*± 1.1**	**2.8 ± 1.1**	**8.5*± 1.5**
AMP	**3.1 ± 0.4**	**6.4*± 3.2**	**7.4 ± 2.8**	**6.1 ± 2.1**
ADPG	**2.6 ± 0.5**	**0.4*± 0.2**	**1.5 ± 0.2**	**0.3*± 0.2**
Amino acids*	**8.1 ± 0.3**	**19.6*± 1.1**	**10.9 ± 1.1**	**19.9*± 2.9**
Aspartate	**0.4 ± 0.01**	**1.5*± 0.1**	**0.8 ± 0.1**	**1.7*± 0.4**
Citrate*	4.3 ± 0.9	5.8 ± 0.9	8.6 ± 0.2	7.2 ± 1.3
DHAP	**21.2 ± 2.6**	**5.5*± 1.3**	**29.9 ± 2.8**	**13.9*± 4.9**
F6P	**173.2 ±18.7**	**34.9*± 6.3**	**202.2 ± 10.8**	**77.4*± 30.6**
Fructose*	**1.7 ± 0.6**	**0.8*± 0.1**	**1.8 ± 0.3**	**1.5*± 0.4**
Fummarate*	165.5 ±23.1	124.8 ± 13.5	155.0 ± 10.1	181.3 ± 28.3
G1P	**33.9 ± 2.6**	**17.9*± 3.0**	**36.0 ± 1.5**	**40.6*± 8.8**
G6P	**143 ±11.0**	**45.5*± 9.2**	**149.6 ± 6.9**	**72.8*± 18.7**
Glucose*	**2.7 ± 0.8**	**1.1*± 0.1**	1.6 ± 0.3	1.6 ± 0.4
Glutamate*	4± 0.4	3.5 ± 0.3	4.7 ± 0.2	3.6 ± 0.3
Glycerate*	**1.2 ±0.2**	**0.1*± 0.01**	**1.4 ± 0.3**	**0.4*± 0.02**
Isocitrate*	2.3 ± 0.3	1.5 ± 0.1	1.9 ± 0.2	1.9 ± 0.2
Malate*	36.0 ± 6.4	23.0 ± 2.8	32.2 ± 3.5	39.7 ± 5.9
NAD	**11.1 ± 1.6**	**23.0*± 1.3**	**9.8 ± 1.6**	**25.7*± 3.7**
NADP	**0.9 ± 0.2**	**1.9*± 0.3**	**1.1 ± 0.3**	**1.4 ± 0.2**
2-OG	**207.6 ±34.8**	**85.3*± 23.4**	**166.2 ± 27.3**	**68.8*± 30.5**
3 PGA	**294.7 ±33.03**	**37.7*±6.62**	**389.0 ± 28.3**	**64.7*± 12.6**
Ri5P	2.3 ± 0.3	1.4 ± 0.3	2.6 ± 0.2	1.7 ± 0.4
S7P	**98.0* ±16.7**	**13.2*± 4.2**	**145.6*± 10.4**	**35.6*± 23.4**
Succinate	**101.8 ±14.7**	**344.7*± 58.3**	**133.3 ± 10.8**	**235.3*± 40.4**
Sucrose*	**14.5 ± 4.2**	**8.6*± 1.1**	15.6 ± 1.3	16.3 ± 1.7
Starch*	**1.4 ± 0.4**	**0.3*± 0.1**	**3.7 ± 1.2**	**6.1*± 1.4**
UDPG	24.4 ± 1.9	24.9 ± 3.1	24.8 ± 0.6	32.1 ± 4.1
X5P+Ru5P	198.4 ±25.6	118.1 ± 34.7	316.1 ± 33.9	255.6 ± 53.9

Metabolites were measured by 2D Liquid Chromatography-triple Mass Spectrometry (2D-LC/MS), except fructose, glucose, sucrose, and starch, which were measured by enzymatic assay. Values in cells filled with ▭ and asterisked show a significant decrease after heat stress and values in cells filled with ▭ and asterisked show a significant increase after heat stress. The presented values are the Averages and Standard Errors of 5 replicates. ANOVA tests were performed using General Linear Model (Shahwani 2011).

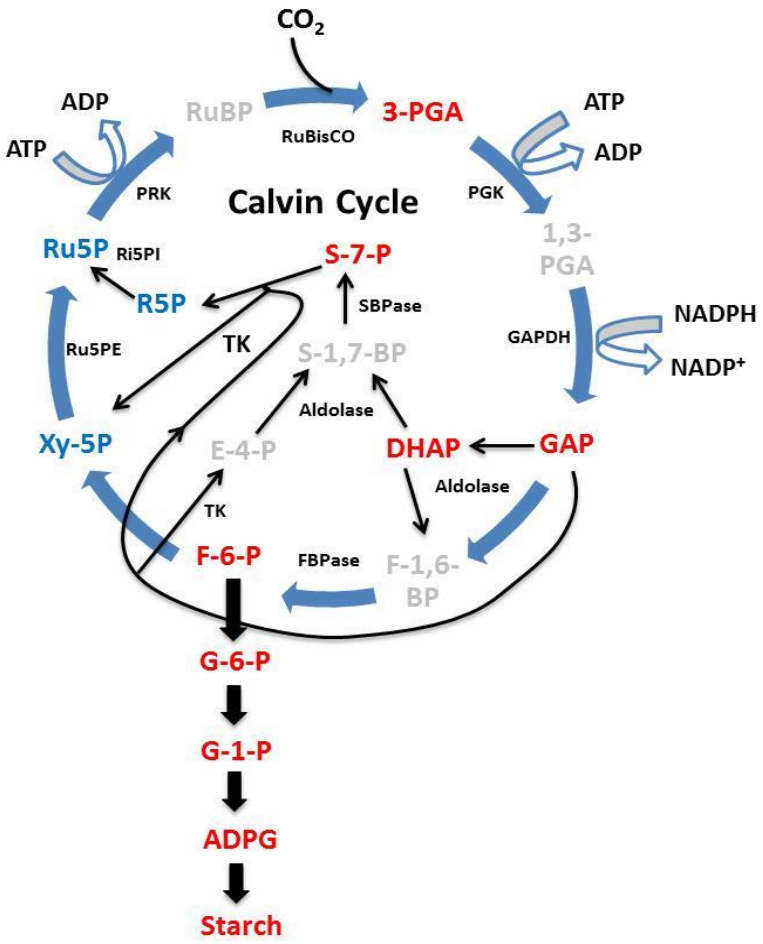

Figure 4-4: Changes in Barley Leaf Metabolite Pools after Heat Stress.

Metabolites were measured by (2D-LC/MS^3), except fructose, glucose, sucrose, and starch, which were measured by enzymatic essay. Differences between the values observed before and after heat stress are shown as significantly decreased, red; no significant change, blue; metabolites not measured, gray. The initial carboxylation stage is catalyzed by RuBisCO to fixes CO_2 into the acceptor molecule RuBP and forming 3-PGA. The reductive phase of the cycle follows with two reactions catalyzed by 3-phosphoglycerate **(PGK)** and glyceraldehyde 3-phosphate dehydrogenase **(GAPDH),** producing glyceraldehyde 3-phosphate **(GAP)** using ATP and NADPH. Glyceraldehyde 3-phosphate is used in the regenerative phase to generate RuBP in reaction catalyzed by aldolase and either Fructose-1,6-bisphosphate phosphatase **(FBPase)** or Sedoheptulose-1,7-bisphosphate phosphatase **(SBPase),** producing Fructose-1,6-bisphosphate phosphate **(F-6-P)** and Sedoheptulose-1,7-bisphosphate phosphate **(S-7-P),** which is subsequently utilized in reactions catalyzed by transketolase (TK), Ribose 5- Phosphate Isomerase **(Ri5PI)** and Ribulose-5-P epimerase producing ribulose-5-phosphate **(Ru5P).** The final step converts Ru5P to RuBP, catalyzed by Phosphoribulokinase **(PRK).**

4.4 Evaluation and Development of Robust, High Throughput Enzyme Linked Assays of C3 Cycle Componnts

The principle of cycling assay method described in Section 2.8.2 is to determine the level of 3-PGA, the product of RuBisCO activity (Gibon, Vigeolas *et al.* 2002). The advantages of using the enzyme-linked assay over other methods are the high sensitivity and production of no radioactive waste. The following section describes the optimisation and validation for measuring the activity of three C3 cycle enzymes, RuBisCO, Ri5P Isomerase (Ri5PI), and Phosphoribulokinase (PRK).

4.4.1 RuBisCO/3-PGA Cyclic Enzyme-Linked Assay

RuBisCO is often the rate-limiting step in carbon assimilation in C3 and C4 plants (Stitt, Quick *et al.* 1991; Stitt and Schulze 1994; Sage 2002). Measurement of RuBisCO activity is very important for many physiological studies. Generally, the activity for RuBisCO is determined by two standard methods, one is based on the incorporation of $^{14}CO_2$ into acid-stable compounds and another uses an enzyme-linked assay where NADH oxidation is monitored during the conversion of 3-PGA to glyceraldehyde 3-phosphate (GAP). NADH oxidation can be followed spectrophotometrically; however, it is time consuming, expensive and relatively insensitive (Lilley and Walker 1974).

RuBisCO activity (conversion of RuBP and CO_2 into 3-PGA) must be measured in short term assays that are completed in less than a minute. This is necessary because of the 'fall-over' of activity as a result of binding inhibitory sugar phosphates, and because RuBP decays in aqueous solutions to form degradation products that inhibit RuBisCO (Kane, Wilkin *et al.* 1998). The rate of RuBisCO activity, therefore, was determined based on the cycling assay method of Sulpice, Tschoep *et al.* (2007). This method is reported to be sensitive, cheap and rapid. Leaf extracts were incubated with a saturating amount of RuBP and CO_2 for 30 seconds before terminating the reaction by the addition of an excess of ethanol; this is the RuBisCO rate step. Traditionally, the product 3-PGA is then converted to dihydroxyacetone-phosphate (DAP) by adding the enzymes PGK, GAP-DH and TPI, ATP and NADH and determining the rates of NADH oxidation (see Figure 4-5). The problem with this traditional assay is that in order to keep costs down, the change in absorbance is very small (typically < 0.01 AU) resulting in large errors. Sulpice, Tschoep *et al*. (2007), have proposed a cycling method (Figure 4-5) where DAP is converted to

glycerol 3-phosphate (G3P) by G3P dehydrogenase (G3PDH) at the expense of NADH, and G3P is then converted back to DAP by G3P oxidase (G3POX). This cycling step effectively amplifies the signal so that absorption changes of 0.2 AU or more are monitored. This method effectively produces a rate of continual NADH oxidation that is dependent only on the amount of DAP (3-PGA) present and the activities of G3POX and G3PDH present. With fixed amounts of the two cycling enzymes, the measured NADH oxidation rate is, therfore, dependent upon the initial amount of DAP (*i.e.* 3-PGA; see Figure 4-5).

In vivo (initial) RuBisCO activity is determined directly in flash-frozen extracts and full maximum activity after a 15 min pre-incubation in the presence of 10 mM HCO^-_3 and 20 mM Mg^{2+} to convert the non-carbamylated RuBisCO into the carbamylated form. The ratio between the initial and total activities provides a measure of the *in vivo* activation state of RuBisCO just prior to flash freezing.

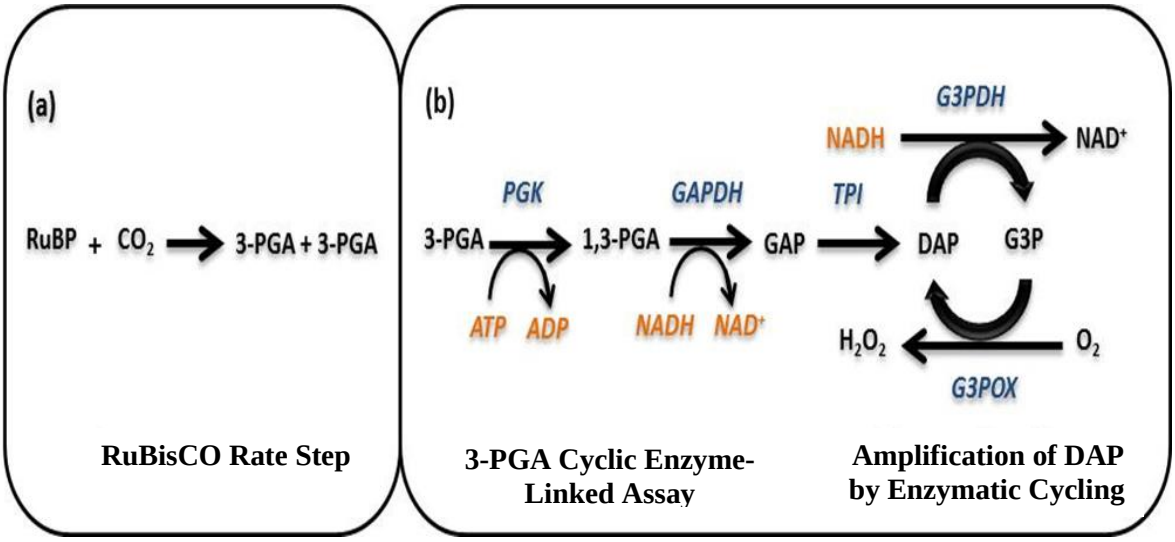

Figure 4-5: Principle of RuBisCO/3-PGA Cyclic Enzyme Linked Assay.

(a) RuBisCO Rate Assay; conversion of RuBP and CO_2 to 3-PGA (30s). **(b)** 3-PGA Cyclic Enzyme Linked Assay, based on the glycerol 3-phosphate cycling assay. **RuBP**, D-ribulose-1,5-bisphosphate; **3-PGA**, 3-phosphoglycerate; **PGK**, phosphoglycerokinase; **GAP**, glyceraldehyde 3-phosphate; **DAP**, dihydroxyacetone-phosphate; **1,3-PGA**, 1,3-bisphophoglycerate; **G3P**, glycerol 3-phosphate; GAPDH, glyceraldehyde 3-phosphate dehydrogenase; **TPI**, triose-P isomerase; **G3PDH**, G3P dehydrogenase; **G3POX**, G3P oxidase.

4.4.1.1 3-PGA Cyclic Enzyme-Linked Assay

It is important first to confirm that the RuBisCO activity measured by this method reflects the amount of 3-PGA converted to G3P. In this step, the cycling enzyme G3POX was not added to the assay. A known amount of 3-PGA was added to the 3-PGA Cyclic Enzyme-Linked Assay mixture containing PGK, GAPDH, TPI, ATP, NADH, $MgCl_2$ and Tricine/KOH PH 8.0. If all of the 3-PGA is converted to G3P, a step decrease in the absorbance at 340 nm as a result of NADH oxidation can be predicted using the Molar extinction coefficient for NADH (6220 AU $M^{-1}.cm^{-1}$). For example, 0.5 nmol of 3-PGA will give changes of 0.052 AU (volume of 120 µl). Further additions were made and the decrease was measured. The rapid decrease in the absorbance was found to be consistent with 3-PGA additions, once dilution factors were taken into account. These findings demonstrated a stable background without the cycling enzyme.

To initiate the cycling, G3POX was then added to the assay. The steady state rate of NADH oxidation was measured when it was stable typically after 10 minutes. However, it proved necessary to check the rate was not an artefact. This was achieved by adding all enzymes and cycling enzymes in the absence of ATP for example. No rate was detected confirming the observed rate was dependent on conversion of 3PGA to DAP in the assay.

To ensure the cyclic enzyme-linked assay was linearly dependent upon 3-PGA concentration, the steady state rate of NADH oxidation was measured with increasing amount of 3-PGA added to the 3-PGA Cyclic Enzyme-Linked Assay. Figure 4-6a shows that in a plant extract-free system, the rate of NADH oxidation was linearly dependent upon the amount of 3-PGA present. Addition of known amounts og 3-PGA to plant samples containing 3-PGA can be used to ensure all of the synthesized 3-PGA is converted to DAP (rate increase) and the assay enzymes (Figure 4-5) are not limiting. Another way to check full 3-PGA conversion is by adding more of these enzymes. If all enzymes and cofactors are added in excess, the rate of the cycle should depend linearly on the the amount of 3-PGA present.

It was important to establish that the rate of NADH oxidation in a cyclic assay was dependent on the amount of 3-PGA present and that the plant extract did not interfere with the assay. To achieve this, plant extract was used in a RuBisCO rate step assay to generate 3-PGA and this was then used in the 3-PGA Cyclic Enzyme-Linked Assay. Once steady state NADH oxidation was achieved, a known amount of 3-PGA (0.05 nmol) was then added. This should be rapidly converted to DAP and the new steady state rate determined. Subsequently, a second known amount of 3-PGA was added (0.20 nmol; Figure 4-6b). The

amount of 3-PGA in the sample before the known additions can then be calculated from the intercept of the slope with the x-axis. In most cases (~90%) these additions of known amounts of 3-PGA produced a linear response indicating the presence of the plant extract did not interfere with the NADH-linked cyclic assay, but this was not always the case. For this reason, in all subsequent assays, after determining the rate of 3-PGA synthesized by RuBisCO, additions of known amounts of 3-PGA were made to ensure a linear relationship.

Figure 4-6: Calibration of Linear Response of 3-PGA Concentration and a 3-PGA Cyclic Enzyme-Linked Assay Rate.

Top Panel **(a)**: Rate of NADH oxidation by the 3-PGA Cyclic Enzyme-Linked Assay. For calibration purposes standard curves were constructed using known amounts of 3-PGA, ranging from 0.0 to 0.20 nmol in plant extract-free assays. For each reaction, 3-PGA was added to 3-PGA Cyclic Enzyme-Linked Assay mix as described in the Materials and Methods, Section 2.8.3.1. Once 3-PGA was fully converted to G3P, the cycling reaction was run and the steady state rate was measured (>10 minutes). Bottom panel **(b)**: Response of RuBisCO/3-PGA Cyclic Enzyme-Linked Assay containing leaf extract to known 3-PGA additions. Barley leaf extract containing RuBisCO was used to convert saturating amounts of CO_2 and RuBP to 3-PGA in a 30s incubation period before stopping the reaction with the addition of ethanol. Samples were then frozen until required. After thawing samples were diluted to 44.4% with water and the 3-PGA Cycling Enzyme-Linked Assay was performed. After a steady state rate of NADH oxidation was achieved (> 10 minutes) the rate was determined (0 addition). A known amount of 3-PGA (0.05 nmol) was added and the new rate determined (>10 minutes), before a final addition of 0.20 nmol of 3-PGA was made. The intercept of the line with x-axis gives the fraction of 3-PGA synthesized by RuBisCO which then can be converted to nmol of 3-PGA. g^{-1} Fw. min^{-1} (see Materials and Methods, Section 2.8.2).

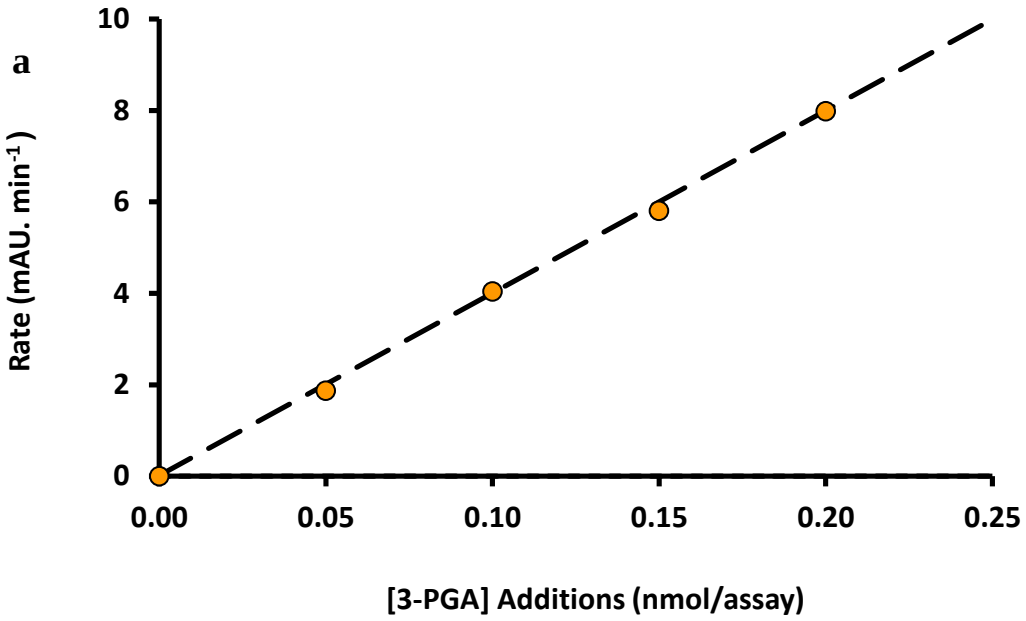
a
Rate (mAU. min-1)
10
8
6
4
2
0
0.00
0.05
0.10
0.15
0.20
0.25
[3-PGA] Additions (nmol/assay)

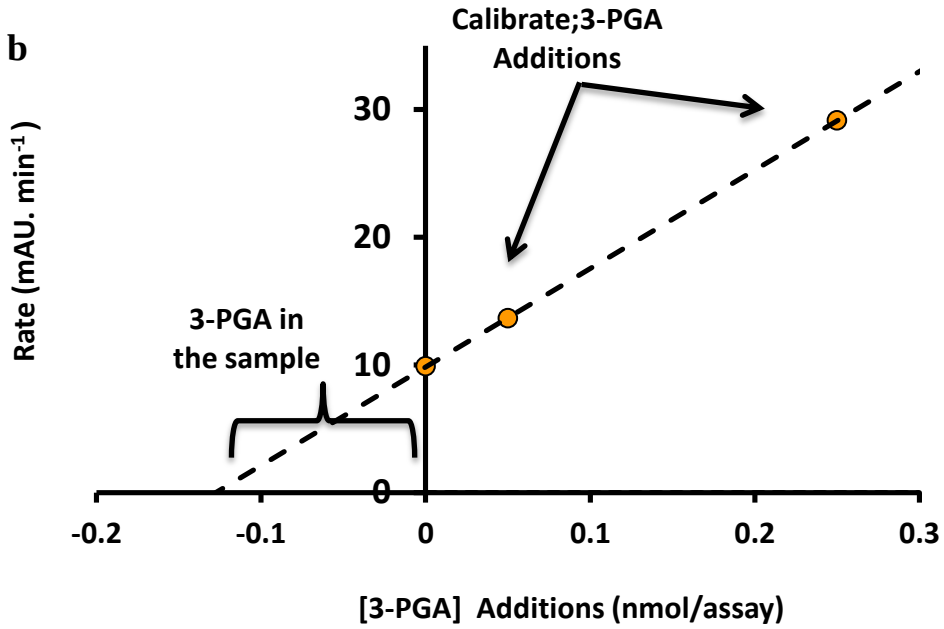
b
Rate (mAU. min-1)
Calibrate;3-PGA Additions
3-PGA in the sample
30
20
10
0
-0.2
-0.1
0
0.1
0.2
0.3
[3-PGA] Additions (nmol/assay)

4.4.1.2 RuBisCO Rate Step

Extracts from control barley leaves were used to optimize this step. The *in vivo* and full activities measured in barley grown in controlled environment growth rooms (09/15 hour Day/Night photoperiod, light intensity 150 µmoles.m^{-2}.s^{-1} 20/18 ^{0}C temperatures) were approximately 6000 and 10000 nmol 3-PGA g^{-1} FW min^{-1}, respectively.

The first step was to optimize the amount of substrate (RuBP) required to saturate D-ribulose-1,5-bisphosphate carboxylase/oxygenase (RuBisCO) in the sample. *In vivo* RuBisCO activity was assayed at different D-ribulose-1,5-bisphosphate (RuBP) concentrations in the presence of saturating CO_2 (10 mM HCO_3^-). Figure 4-7 shows a Michaelis–Menten (substrate-saturation) curve for RuBP in an excess of CO_2 (10 mM $NaHCO_3$). The results are consistent with those reported in the literature with a K_m of below 40 µM RuBP (Yeoh, Badger *et al.* 1981; Sulpice, Tschoep *et al.* 2007). A RuBP concentration of 1.5 mM in the subsequent assay was chosen to ensure RuBisCO was RuBP saturated.

The next step was to confirm the 3-PGA produced after 30s incubation arose only from the conversation of RuBP. Preliminary experiments were conducted on barley leaves incubated in ambient air (380 µmol CO_2 .mol^{-1} air ; 25.0°C and 560 µmol m^{-2} s^{-1} PAR) for 20 minutes and flash frozen in liquid nitrogen. However, to ensure heat stress did not greatly alter the levels of endogenous metabolites, these assays were performed on leaves incubated for 3 hours at 25.0°C, 38.0°C and 40°C (Figure 4-8). The amount of 3-PGA in crude leaf extract (V_{Blank}) produced from endogenous RuBP was approximately similar before and after heat stress. Adding 1.5 mM of RuBP to the reaction (V_{RuBP}) resulted in a significant increase in the product 3-PGA by approximately 900%. This confirmed that the rate of reaction measured the conversion of RuBP to 3-PGA during the 30s period of the of the RuBisCO rate step assay. No rate was detected when RuBP was incubated with H_2O instead of leaf extract for the same fixed time, confirming the conversion of RuBP to 3-PGA is an enzymic process (data not shown).

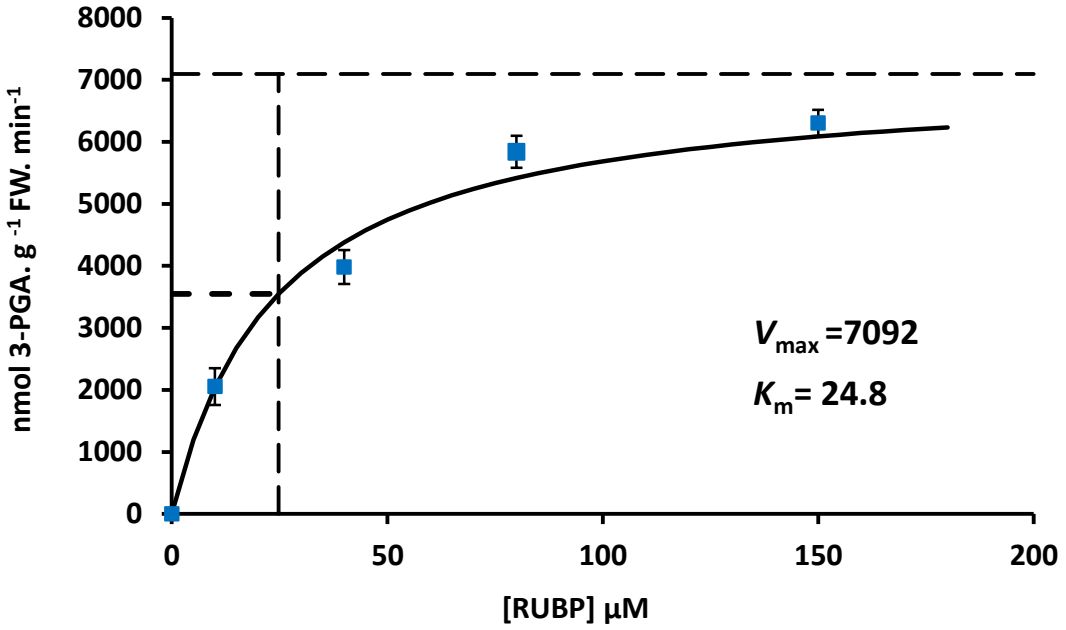

Figure 4-7: Substrate Saturation Curve for D-ribulose-1,5-Bisphosphate Carboxylase/Oxygenase (RuBisCO) in Barley.

In vivo RuBisCO activity was assayed at different D-ribulose-1,5-bisphosphate (RuBP) levels (0, 10, 40, 80 or 150 µM) in the presence of saturating CO_2 (10 mM $NaHCO_3$). The RuBisCO rate step assay was continued for 30s, and RuBisCO was determined without prior activation. V_{max}, and hence K_m, were determined from Lineweaver-Burke plot (see Materials and Methods, Section 2.8.3.2). The presented values are the Averages and Standard Errors of 3 replicates.

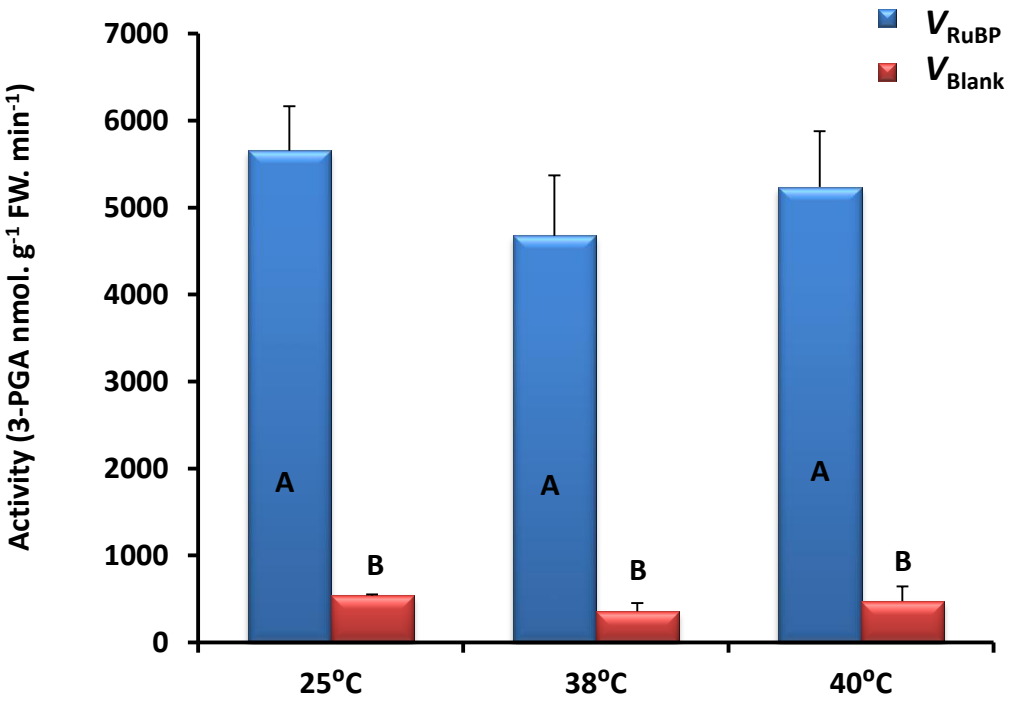

Figure 4-8: Comparison of 3-PGA Production in 30s of RuBisCO Rate Step Assay in Presence and Absence of the Substrate RuBP in Stressed and Non Stressed Barley Leaves.

Leaf extracts from stressed and non-stressed barley leaves were incubated with 1.5 mM of RuBP (V_{RuBP}) or without RuBP (V_{Blank}) for 30s before stopping the reaction with ethanol (see Materials and Methods, Section, 2.8.3.3). Then the amount of 3-PGA synthesized was determined via 3-PGA Cyclic Enzyme-Linked Assay by monitoring the steady state rate of NADH oxidation (for at least 10 minutes). Heat stress was imposed by increasing T_{leaf} to 25.0, 38.0 and 40.0 ºC (± 0.2ºC) for three hours using a modified thermal cycler. ANOVA tests were performed using a General Linear Model. Different letter codes indicate Tukey's significant differences at $P<0.05$. Tables for ANOVA and group comparisons along with residual plots are presented in the Appendix (Figure A 4-2). Different plants were used for each temperature treatment, and presented values are the Averages and Standard Errors of 5 replicates.

4.4.2 Ri5PI, PRK/3-PGA Cyclic Enzyme Linked Assay

There are several reports in the literature for determining the *in vitro* activities of Ri5PI (Wood 1970) and PRK (Hurwitz, Weissbach *et al.* 1956; Gardemann, Stitt *et al.* 1983), but the substrate (*e.g.* Ru5P) and the enzyme (*e.g.* PRK) are no longer commercially available. For this reason the effect of heat stress on the activities of endogenous Ri5PI and PRK had to be estimated in a coupled two-step assay where the rate of RuBP synthesis was monitored over a range of end time points after adding Ri5P as the substrate (Ri5P→ Ru5P→ RuBP). The amount of RuBP was then subsequently estimated by converting all of the RuBP generated to 3-PGA using the 3-PGA Cyclic Enzyme-Linked Assay described in Materials and Methods, Section 2.8.2. This allowed the rate of Ri5P converted to RuBP to be estimated. In practice, therefore, the assay consisted of 3 steps. The first one is the conversion of Ri5P to RuBP (Ri5PI and PRK rate step assay) by incubation with saturating amounts of Ri5P and leaf extracts for a range of end time points in the presence of an excess of ATP at 30°C. Aliquots were removed at the appropriate times and placed in thin walled PCR tubes in a thermal cycler at 80°C (from 30 to 80°C within 10 seconds) to stop the reaction. The second step was the conversion of all of the newly synthesized RuBP to 3-PGA using purified activated wheat RuBisCO and an excess of CO_2. The last step involved the determination of the amount of 3-PGA produced using the 3-PGA Cyclic Enzyme-Linked Assay which was optimized as described in section 2.8.3.

4.4.2.1 Conversion of RuBP to 3-PGA

Estimates of the combined *in vivo* Ri5PI and PRK activities required the conversion of synthesized RuBP to 3-PGA which can then be determined by the 3-PGA Cyclic Enzyme-Linked Assay. It was important to optimize this step to ensure full conversion of RuBP to 3-PGA; this includes consideration of both the amount of RuBP generated and the time required for full conversion to 3-PGA. The saturating amount of purified wheat RuBisCO (50µg/ml) was used in this step as suggested in the literature (Keys and Parry 1990b). The amount of RuBP generated in the first step (Ri5PI and PRK rate step assay) was optimized so that it was detectable but not so excessive that not all of it could be converted to 3-PGA within a few minutes (step-2), and to ensure the 3-PGA generated was within the linear range of the 3-PGA of the Cyclic Enzyme-Linked Assay. Different amounts of 3-PGA were used to assess the upper and lower limits for reliable estimation of 3-PGA concentration. 3-PGA (0, 0.05 0.25 0.45 0.65 0.85 1.05 or 3.05 nmol/assay) was added directly to the 3-PGA Cyclic Enzyme-Linked Assay mixture (see Materials and Methods,

Section2.9.2.6) and the rates were determined. Figure 4-9 shows that the reliable range for 3-PGA concentration using this assay was between 0.25 and 1 nmol/assay. Therefore, the first step (Ri5PI and PRK rate step assay) was adjusted by diluting with water to generate RuBP in the range of 100 to 500 pmol /assay (200 to 1000 pmol 3-PGA).

After optimizing for the appropriate amount of 3-PGA, it was essential to check the time required to fully convert RuBP to 3-PGA. For this, a time course experiment (0, 1, 2, 5, 10 and 15 minutes) was set up where different amounts of RuBP were incubated with purified wheat RuBisCO and HCO^-_3. The results clearly indicated that increasing the amount of RuBP led to an increase in the amount of 3-PGA produced and this reaction required approximately 5 minutes to fully complete (Figure 4-10a). For further confirmation, 5 replicates of different amounts of RuBP (0, 100, 200, 500 or 1000 pmol) were incubated for 5 minutes at 30°C with purified wheat RuBisCO before the reaction was stopped with an excess of ethanol. The amount of 3-PGA produced was measured as described previously. The linear relationship between the amounts of RuBP added and the amount of 3-PGA produced after 5 minutes incubation provides further evidence that the incubation time (5 min) and the amount of RuBP (100 to 500 pmol /assay) determined for the second step reaction ensures 100% conversion (Figure 4-10b).

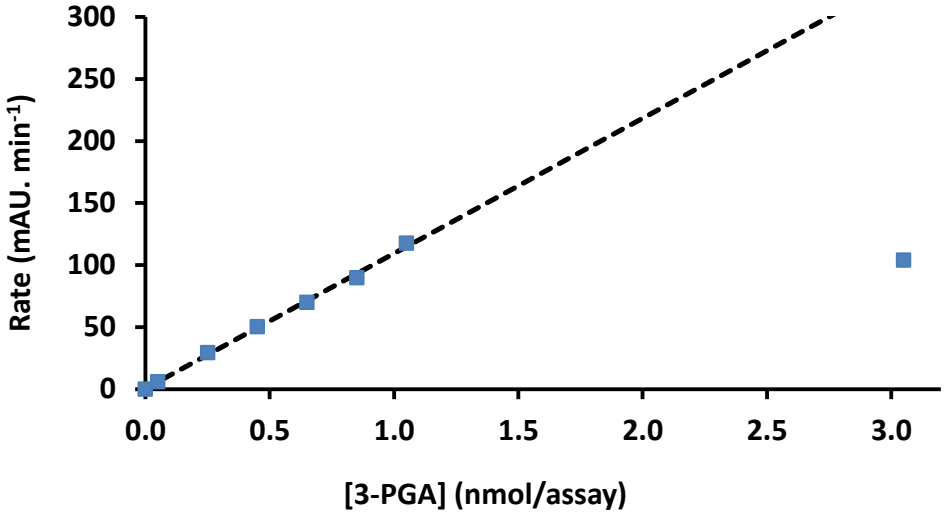

Figure 4-9: Determination of the Concentration Range for a Linear Response of 3-PGA to 3-PGA Cyclic Enzyme-Linked Assay.

Different amounts of 3-PGA (0, 0.05 0.25 0.45 0.65 0.85 1.05 or 3.05 nmol/assay) were added directly to the 3-PGA Cyclic Enzyme-Linked Assay mixture (see Materials and Methods, Section 2.9.2.6). For each addition of 3-PGA, the rate of NADPH oxidation was determined using the 3-PGA Cyclic Enzyme-Linked Assay. The response is linear up to 1 nmol/assay; higher concentration (3 nmol/assay) results in a more complex relationship.

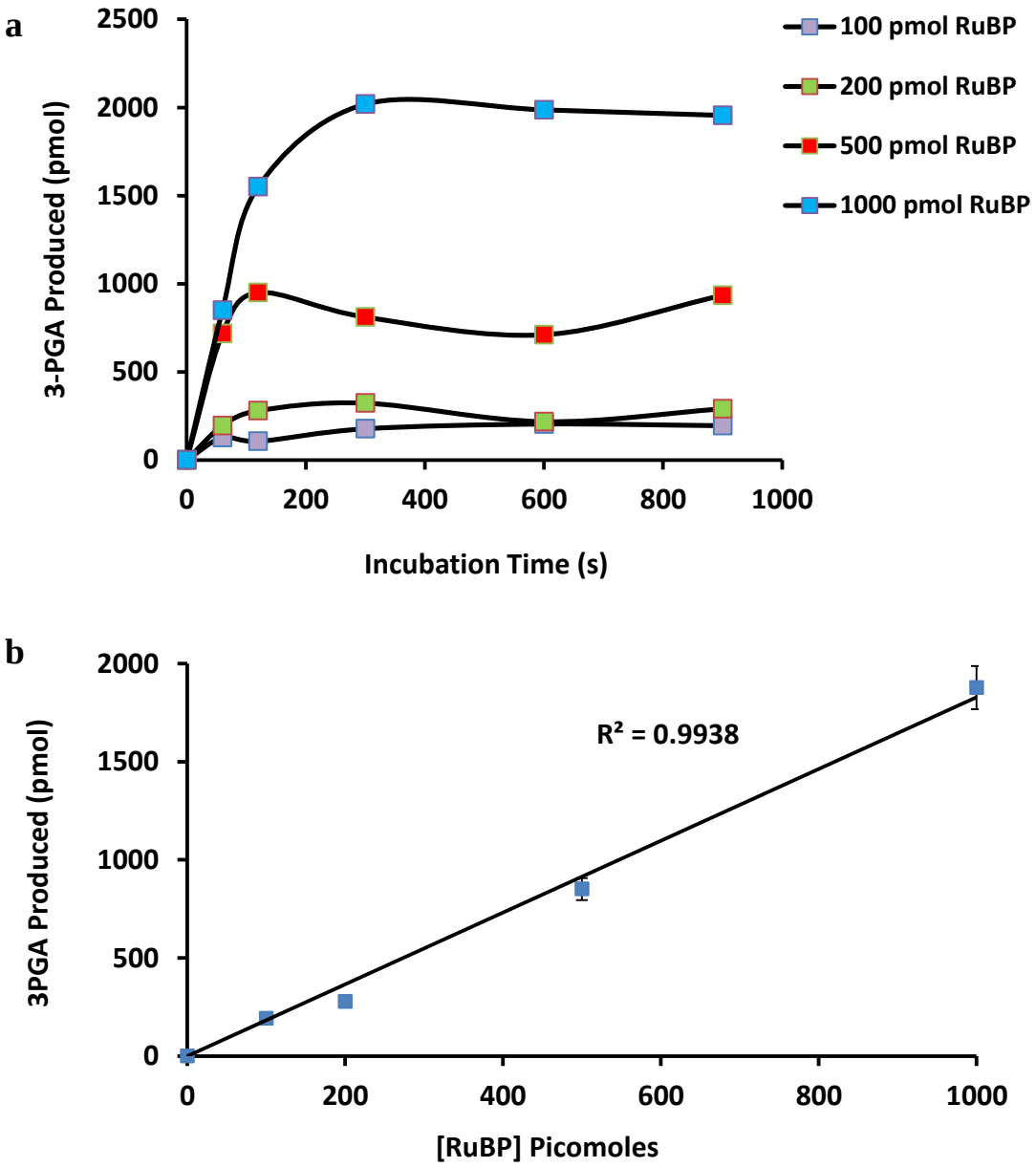

Figure 4-10: Time Course for Conversion of RuBP to 3-PGA.

(a) Determination of the time required for complete RuBP conversion to 3-PGA. Different amounts of RuBP (0, 100, 200, 500, or 1000 pmol/assay) were incubated with purified wheat RuBisCO and 10 mM $NaHCO_3$ (for 0, 1, 2, 5, 10 and 15 minutes); synthesised 3-PGA was then measured using the 3-PGA Cyclic Enzyme-Linked Assay as described in Material and Methods Section, 2.9.2.7. **(b)** 3-PGA produced plotted *versus* RuBP added after incubation for 5 minutes. The presented values are the Averages and Standard Errors of 5 replicates.

4.4.2.2 Ri5PI and PRK Rate Step Assay

Barley leaf extracts were used to generate RuBP from Ri5P using endogenous Ri5PI, PRK and an exogenous excess of ATP at a range of end time points. To ensure that the amount of exogenous Ri5P was not limiting, fixed amounts of leaf extracts from control plants (approximately 40 µg FW) were incubated with different Ri5P levels in the presence of saturating ATP (1mM). Figure 4-11 shows a Michaelis–Menten (substrate-saturation) curve for Ri5P with an excess of ATP. The result shows that the apparent k_m' is 50 µM for the conversion of Ri5P to RuBP. It has been reported that the K_m of Ri5PI for Ri5P is 1.6 mM (Rutner 1970) and the K_m of PRK for Ru5P is in the range of 25 to 70 µM (Gardemann, Stitt *et al.* 1982). However, as mentioned before, because K_m cannot be determined for each enzyme independently, it is important to recognise that K_m is an 'apparent' value (K_m') for both enzymes (Ri5PI and PRK). Therefore, the K_m' obtained for both enzymes (50 µM) is a function of their respective V_{max} and K_m values.. It was decided a Ri5P concentration of 5 mM should be used in subsequent assays to ensure the endogenous enzymes in the samples were saturated with substrate.

The amount of ATP required to saturate the conversion of Ri5P to RuBP was also checked. Figure 4-12 shows a Michaelis–Menten (substrate-saturation) curve for ATP in the presence of 5 mM Ri5P. It has been reported that the K_m of ATP for Ru5P is 35-69 µM (Leegood 1990); the results show, however, the estimated K_m for ATP was 3.8 µM, therefore, it was decided a 1mM concentration of ATP should be used.

To stop the conversion of Ri5P to RuBP, as mentioned previously, aliquots were removed at the appropriate times and placed in thin walled PCR tubes in a thermal cycler at 80°C (from 30 to 80°C within 10 seconds); the reaction was incubated at 80°C for 5 minutes as this high temperature caused the enzymes to denature and lose their activity. However, it is important to check first that 80°C is sufficient to completely stop the reaction and ensure the stability of the RuBP produced. Therefore, leaf extracts were heated to 80°C for 5 min and then added to reaction mixtures containing Ri5P, ATP and 50µg/ml purified wheat RuBisCO and incubated at 30°C for 5 min to generate 3-PGA. 3-PGA was then determined using 3-PGA Cyclic Enzyme-Linked Assay as described in Materials and Methods, Section 2.8.2. It is clear from Figure 4-13 that incubating leaf extract at 80°C for 5 min resulted in a significant suppression in RuBP synthesis due to thermal inactivation of the activities of endogenous Ri5PI and/or PRK. For further evidence that this suppression was produced only by high temperature, parallel experiments were conducted at the same time using identical mixtures containing leaf extracts heated to 25°C for 5 min with or without

1mM ATP (Figure 4-13). Clearly, the results confirmed the reaction for producing RuBP is ATP dependent and increasing sample temperature to 80°C for 5 minutes severely impaired Ri5P conversion to RuBP.

Also, the stability of the product RuBP at 80°C was checked by heating 100 pmol of RuBP either to 25°C or 80°C for 5 minutes. The amount of RuBP remaining was then assessed by conversion to 3-PGA using 10 mM $NaHCO_3$ and purified wheat RuBisCO. The results show clearly a full recovery (200 pmol) of metabolite at both temperatures (Figure 4-14). Taken together these results confirm that rapidly heating samples to 80°C prevents further metabolic and thermal conversion of Ri5P to RuBP.

Another important check is to establish whether the heating step affects the stability of both the substrate Ri5P and the product RuBP as any breakdown product could interfere with the assay. Therefore, 100 pmol of Ri5P and RuBP was heated to 80°C for 5 min, cooled and then added directly to a reaction to determine 3-PGA using the 3-PGA Cyclic Enzymes-Linked Assay. For comparison, distilled water was heated to the same temperature and added to the reaction. There was no evidence that 5 min incubation at 80°C affected the stability of Ri5P or RuBP or produce any interference with the assay (Figure 4-15).

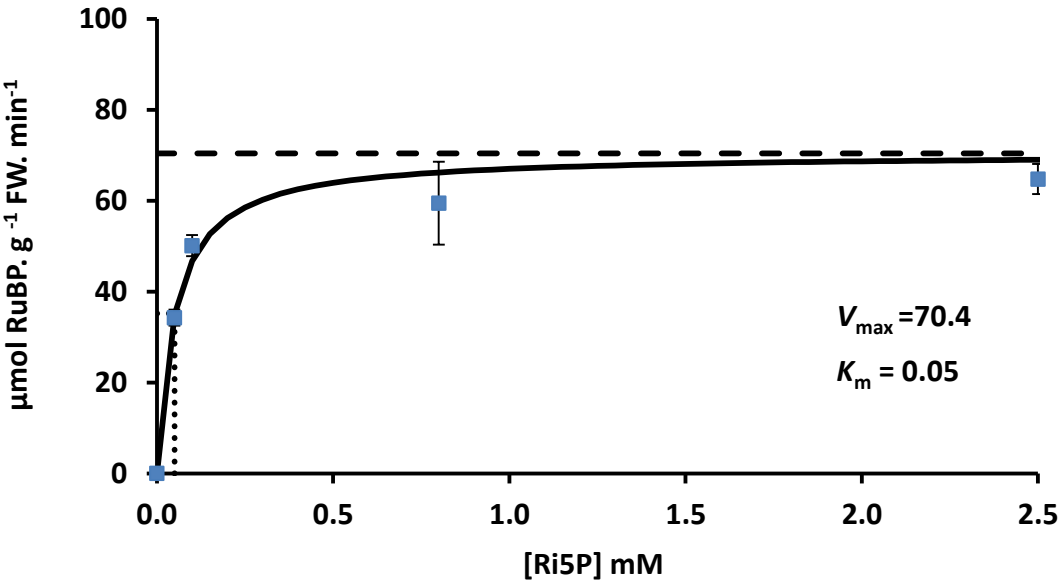

Figure 4-11: Ri5P-Substrate Saturation Curve for Ri5P Conversion to RuBP in Barley Leaf Extracts.

In vivo combined activities of Ri5PI and PRK were assayed at different Ri5P levels (0, 0.05, 0.1, 0.8, 2.5, 5.0 or 10 mM) in the presence of 1 mM ATP. The reaction was incubated for 1 minute at 30°C and then stopped by rapidly heating the mixture to 80°C for 5 minutes. Purified wheat RuBisCO was then added to the reaction with 10 mM $NaHCO_3$ and incubated for 5 minutes at 30°C to convert all of the newly synthesized RuBP to 3-PGA before adding ethanol to terminate the reaction. The amount of 3-PGA produced was then determined using the 3-PGA Cyclic Enzyme-Linked Assay (see Materials and Methods Section 2.9.2.1). V_{max}, and hence K_m, were determined from the Lineweaver-Burke plot. The presented values are the Averages and Standard Errors of 3 biological replicates.

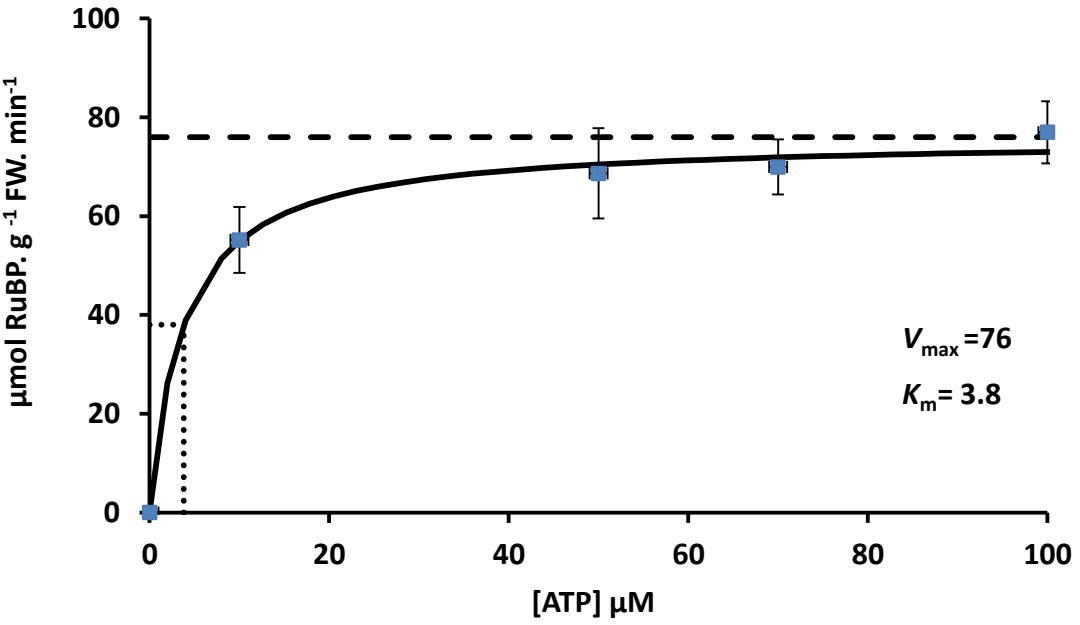

Figure 4-12: ATP-Substrate Saturation Curve for Ri5P Conversion to RuBP in Barley Leaf Extracts.

In vivo combined activities of Ri5PI and PRK were assayed at different ATP levels (0, 10, 50, 70, or 100 µM) in the presence of saturating Ri5P (5 mM). The reaction was incubated for 1 minute at 30°C and then stopped by rapidly heating to 80°C for 5 minutes. Purified wheat RuBisCO was then added to the reaction with 10 mM $NaHCO_3$ and incubated at 30 °C for 5 minutes before adding ethanol to terminate the reaction. 3-PGA was subsequently determined using the 3-PGA Cyclic Enzyme-Linked Assay (see Materials and Methods Section 2.9.2.2). V_{max}, and hence K_m, were determined from the Lineweaver-Burke plot. The presented values are the Averages and Standard Errors of 3 biological replicates.

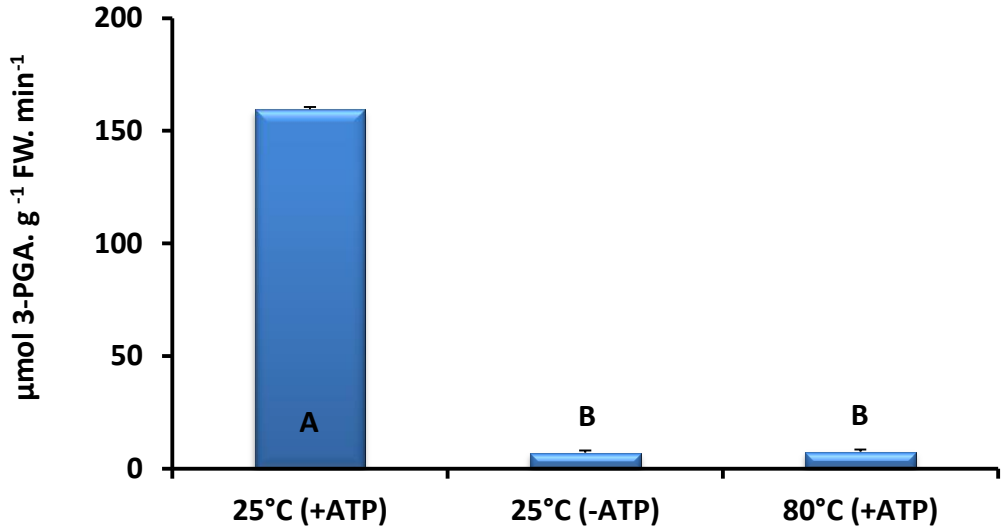

Figure 4-13: Effect of Leaf Extract Temperature and ATP Concentration on the Conversion of Ri5P to RuBP.

Extracts from barley leaves were heated to 80°C for 5 min and then added to the reaction mixture (containing Ri5P, ATP and purified wheat RuBisCO). A parallel experiments were conducted using leaf extracts that has been heated to 25°C for 5 min and added to the reaction mixture containing ATP (25°C +ATP) or not (25°C -ATP). The reaction mixture was then incubated at 30°C for 5 min to generate 3-PGA which was then determined using the 3-PGA Cyclic Enzyme-Linked Assay (see Material and Methods, Section, 2.9.2.3. ANOVA tests were performed using a General Linear Model. Different letter codes indicate Tukey's significant differences at $P<0.05$. Tables for ANOVA and group comparisons along with residual plots are presented in the Appendix (Figure A 4-3). Different plants were used for each temperature treatment, and presented values are the Averages and Standard Errors of 3 replicates.

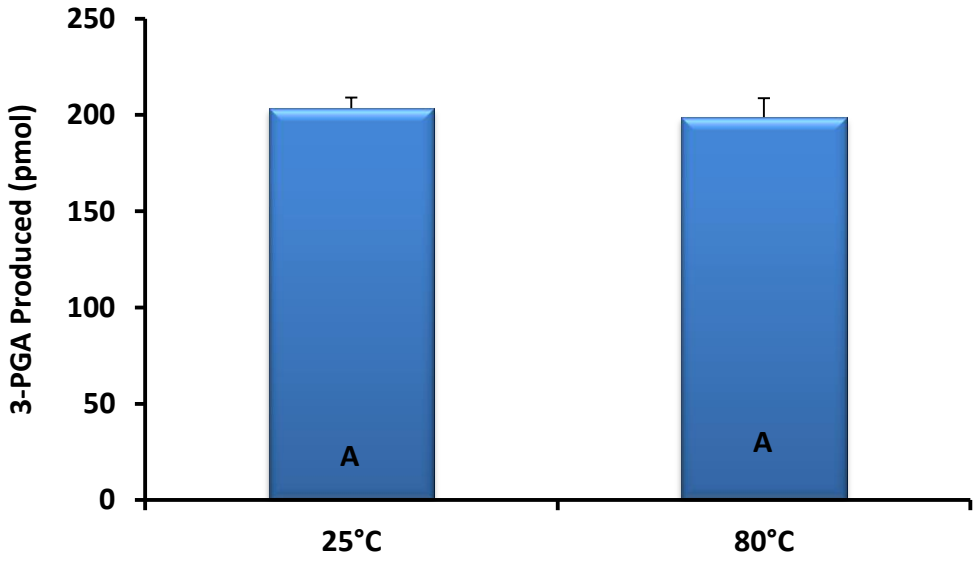

Figure 4-14: Stability of RuBP at 80°C.

The stability of RuBP was tested by heating 100 pmol of RuBP to either 25°C or 80°C for 5 min before incubation for 5 min at 30°C with purified wheat RuBisCO and 10mM $NaHCO_3$ to generate 3-PGA which was subsequently determined using the 3-PGA Cyclic Enzyme-Linked Assay (see Material and Methods, Section, 2.9.2.4). ANOVA tests were performed using a General Linear Model. Different letter codes indicate Tukey's significant differences at $P<0.05$. Tables for ANOVA and group comparisons along with Figures for residual plots are presented in the Appendix (Figure A 4-4). Different plants were used for each temperature treatment, and presented values are the Averages and Standard Errors of 2 replicates.

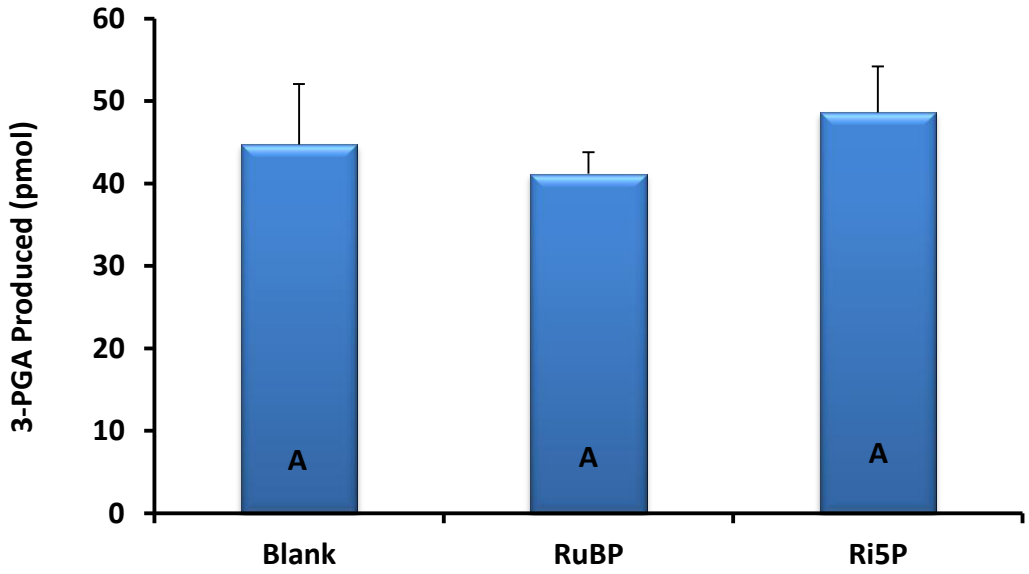

Figure 4-15: Effect of Incubation of RuBP and Ri5P at 80°C.

The stability of RuBP and Ri5P was tested by heating 100 pmol of RuBP and Ri5P to 80°C for 5 min before adding them directly to the third step which involved the determination of the amount of 3-PGA using the 3-PGA Cyclic Enzyme-Linked Assay (see Material and Methods, Section 2.9.2.5). ANOVA tests were performed using a General Linear Model. Different letter codes indicate Tukey's significant differences at $P<0.05$. Tables for ANOVA and grouping information along with Figures for residual plots are presented in the Appendix (Figure A 4-5). Different plants were used for each temperature treatment, and presented values are the Averages and Standard Errors of 3 replicates (blanks were typically 40 pmol of 3-PGA/sample).

4.5 RuBisCO Activity

Based on the finding of LC-MS and enzymic analysis of leaf metabolite levels, it can be concluded that a thermally induced blockage is probably in the region of the carboxylation phase by impairment of RuBisCO, RuBisCO Activase, or processes close to the carboxylation step. This finding is consistent with a considerable body of evidence suggesting the inhibition of photosynthesis by heat stress is attributed to declines in activation state of RuBisCO (Law and Crafts-Brandner 1999; Crafts-Brandner and Salvucci 2000; Yamori, Noguchi *et al.* 2008). To confirm this possibility, direct measurements were made on the activity of RuBisCO isolated from control and heat stress barley leaves by rapidly freezing attached light saturated leaves photosynthesizing under steady state condition. The samples were subsequently measured for *in vivo* (initial) and total RuBisCO activities using enzyme-linked assays (Marital and Methods, Section 2.8.1 and 2.8.2).

From Figure 4-16a, it is clear that *in vivo* RuBisCO activity was not significantly affected until T_{leaf} increased above 40.0°C, and resulted in a significant decrease of approximately 50% when compared with non-stressed barley leaves at 25.0°C. The *in vivo* activity of RuBisCO reflects the activity present in the intact leaf and so it is concluded that a T_{leaf} of 42.0°C reduces endogenous RuBisCO activity to approximately half of that in non-stressed leaves. A decline in endogenous *in vivo* RuBisCO activity may result from a failure of RuBisCO Activase to maintain RuBisCO in an active state, or from a thermal destruction of the RuBisCO complexes themselves. To investigate this possibility further, flash-frozen samples were thawed on ice and incubated with 10 mM $NaHCO_3$ and 20 mM $MgCl_2$, a method that is routinely used to fully activate RuBisCO without the requirement for RuBisCO Activase (Keys and Parry 1990b; Crafts-Brandner and Salvucci 2000; Sulpice, Tschoep *et al.* 2007). Figure 4-16b shows there were no differences in the activation state of RuBisCO (the ratio between the *in vivo* and total activities) from control and heat stressed leaves and it is concluded that the 50% decrease in *in vivo* RuBisCO activity observed at 42°C arises from a loss of the enzyme from the endogenous pool.

When *in vivo* (endogenous) RuBisCO activity is plotted with the corresponding CO_2 assimilation rate ($\mathbf{A_{sat}}$) estimated by measuring *in vivo* ETR for the same leaf just prior to flash freezing, it is clear, $\mathbf{A_{sat}}$ was impaired severely (85%) while *in vivo* RuBisCO activity still had >80% of its activity up to T_{leaf} of 40.0°C and still maintained 50% activity at 42.0°C (Figure 4-17).

Figure 4-16: Effect of Increasing Leaf Temperature on the *in vivo*, Total and Activation State Activity of RuBisCO in Barley Leaves.

Control and heat-stressed leaves were allowed to attain steady-state $\mathbf{A_{sat}}$ (20 min) under saturating light (560 µmol $.m^{-2}.s^{-1}$ PAR) and ambient CO_2 levels (380 µmol CO_2 mol^{-1}air), at 25.0°C, before flash-freezing in liquid nitrogen, and samples extracted (see Materials and Methods Section, 2.8.1). The activity of RuBisCO was then determined using a two-step assay: step 1, a carboxylation step whereby RuBP and CO_2 are converted to 3-PGA during a 30s incubation: step 2, determination of the amount of 3-PGA produced using a Cyclic Enzyme-Linked Assay (see Materials and Methods, Section 2.8.2). Top Panel **(a)** *in vivo* Activity of RuBisCO was measured directly in fresh extracts. Middle Panel **(b)** Total activity of RuBisCO which measured by performing stopped RuBisCO assays after a 15 min pre-incubation period of the extract in the presence of 10 mM $NaHCO_3$ and 20 mM Mg^{2+}. Bottom Panel **(c)** the ratio between the *in vivo* and total activities provides a measure of the activation state of RuBisCO. Heat stress was imposed by increasing T_{leaf} to desired temperature (± 0.2°C) for three hours using a modified thermal cycler. The values represent the Average and Standard Errors of 5 replicates. ANOVA tests were performed using a General Linear Model. Different letter codes indicate Tukey's significant differences at $P<0.05$. Tables for ANOVA and group comparisons along with Figures for residual plots are presented in the Appendix (Figure A 4-6a,b & 4-7).

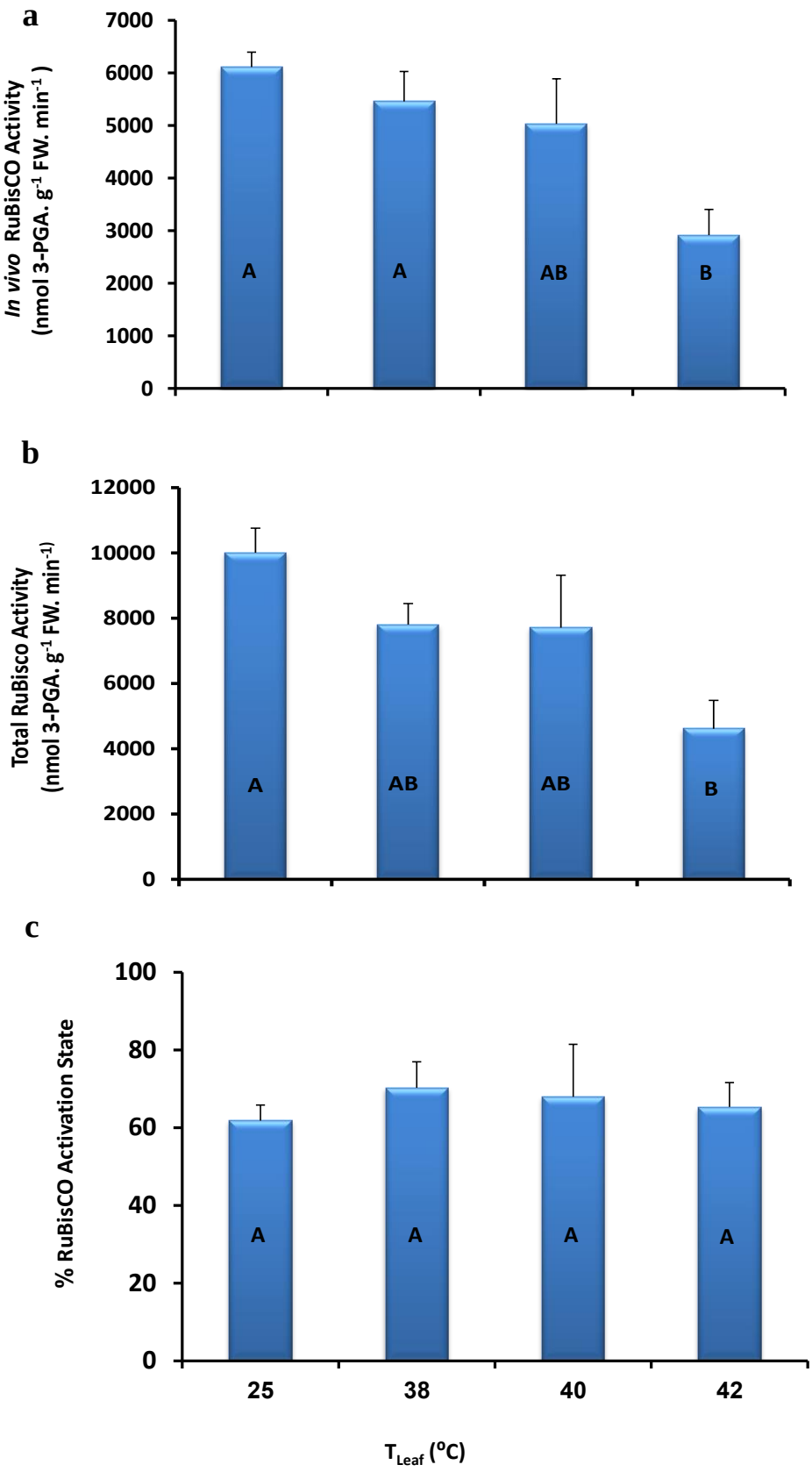
a
In vivo RuBisCO Activity
(nmol 3-PGA. g-1 FW. min-1)
7000
6000
5000
4000
3000
2000
1000
0
A
A
AB
B
b
Total RuBisco Activity
(nmol 3-PGA. g-1 FW. min-1)
12000
10000
8000
6000
4000
2000
0
A
AB
AB
B
c
% RuBisCO Activation State
100
80
60
40
20
0
A
A
A
A
25
38
40
42
TLeaf (°C)

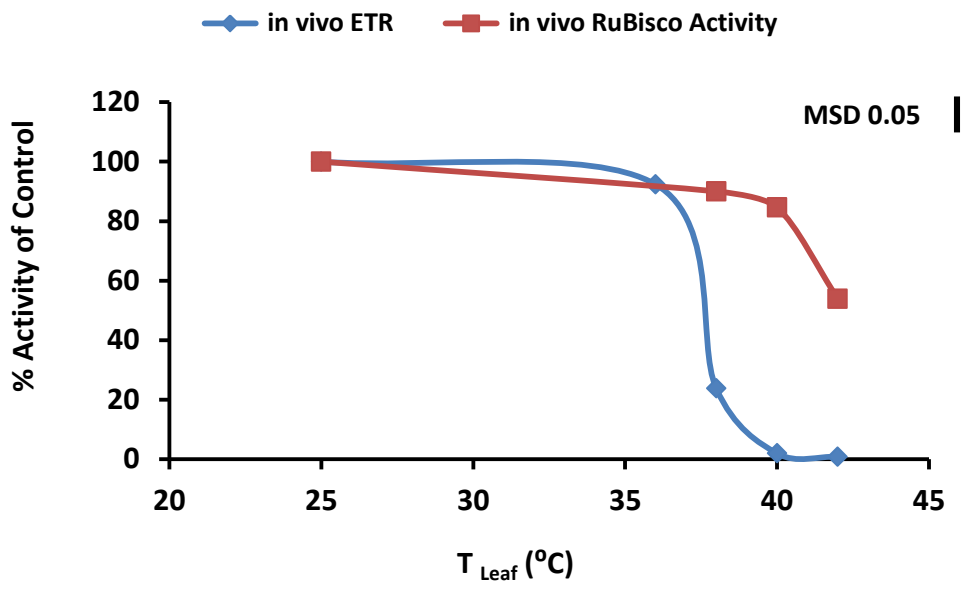

Figure 4-17: Comparison of Temperature Response for *in vivo* RuBisCO Activity and Corresponding *in vivo* ETR Rate in Barley Leaves.

In vivo RuBisCO Activity was measured as described in Materials and Methods, Section 2.8.2, while *in vivo* ETR was estimated using modulated chlorophyll fluorescence techniques form the same leaf. Immediately following heat treatment (3 hours in the dark), attached barley leaves were exposed to ambient air at 25.0°C and irradiated with 560 µmol m^{-2} s^{-1} PAR and *in vivo* ETR monitored by PAM fluorimeter (see Materials and Methods, Section 2.4.1). After a 20 minute period, leaves were rapidly flash-frozen in liquid nitrogen and samples collected and stored. Subsequently, the *in vivo* activity of RuBisCO was determined. Values are normalized on the *in vivo* activity (100%) of controls which are equivalent to 5655.1 (±508.9) for RuBisCO and 108.8 (±2.4) for ETR. The values represent the Average and Standard Errors of 5 replicates. ANOVA tests were performed using a General Linear Model. The vertical lines indicate Tukey's Minimum Significant Difference (MSD) at P= 0.05 level. Treatment means that differ by more than the MSD are significantly different at P= 0.05. Tables for ANOVA and group comparisons along with Figures for residual plots are presented in the Appendix (Figure A 4-8).

4.5.1 Effects of Mg^{2+} and DTT Additions to the Extraction Buffer on RuBisCO Activity

Primary experiments conducted to ensure the *in vivo* RuBisCO activities presented in Figure 4-16 were not anomalous. Samples were extracted from control barley leaves that were dark adapted for a minimum of 3 hours. Under these conditions, RuBisCO should be < 20% active (Vu, Allen *et al.* 1984) and the *in vivo* RuBisCO assay should reflect this. However, when isolated from dark adapted leaves in standard buffer (50 mM HEPES/ KOH pH 7.5, 10 mM $MgCl_2$, 1 mM EDTA, 1 mM EGTA and 0.5 mM DTT), *in vivo* RuBisCO rate was approximately 6000 nmol 3-PGA g^{-1}FW. min^{-1}, which is similar to the rate from light adapted leaves. Similar results were obtained from the isolation of RuBisCO from dark adapted tobacco leaves (data not shown).

It has been suggested that RuBisCO in the chloroplast can be activated by light-induced changes in stromal pH and Mg^{2+} (Lorimer and Miziorko 1980), redox state and RuBisCO Activase (Portis 1992). The standard RuBisCO extraction buffer, therefore, has been designed to isolate RuBisCO in its native activation state in the leaf. However, this was not the case with RuBisCO isolated from dark adapted barley and tobacco leaves in this study as using the standard extraction buffer the activity was much higher than expected. To confirm this observation, RuBisCO activity was measured from dark adapted barley leaves in a range of buffers containing increasing Mg^{2+} concentrations. Figure 4-18 compares these results with those of light adapted leaves. Clearly, low concentration of Mg^{+2} in the extraction buffer resulted in low *in vivo* RuBisCO activities from dark adapted leaves but increasing Mg^{+2} concentration to 8.0 mM produced a progressive activation. In contrast, low and high Mg^{+2} concentrations had no effect on RuBisCO activity extracted from light adapted leaves leading to the isolation of partially activated RuBisCO.

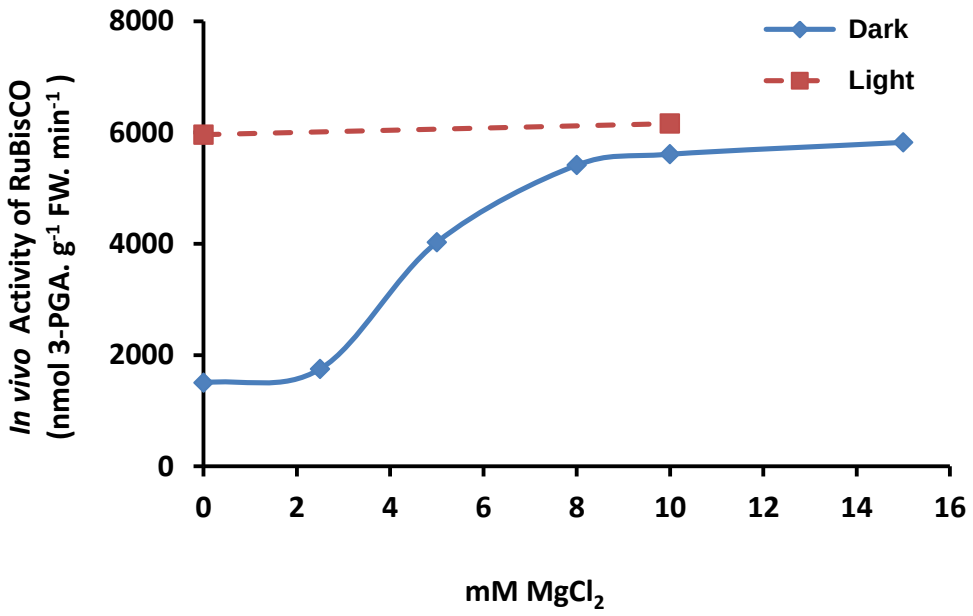

Figure 4-18: Effects of Mg^{2+} Concentration in the Extraction Buffer on Estimates of the *in vivo* RuBisCO Activity of Dark and Light Adapted Barley Leaves.

Non-stressed barley leaves were dark adapted for 3 hours before samples were taken and non-stressed light adapted barley leaves were allowed to attain steady-state $\mathbf{A_{sat}}$ (20 min) under saturating light and ambient CO_2 levels prior to sampling. Samples were extracted from dark adapted leaves in extraction buffers presented in Section, 2.8.1 except of using different concentrations of $MgCl_2$ (0, 2.5, 5, 8, 10 and 15 mM). Light adapted leaves were extracted in the same buffer containing 0 or 10 mM $MgCl_2$. *in vivo* activity of RuBisCO was then measured using a 2-step Cyclic Enzyme-Linked Assay (see Materials & Methods, Section 2.8.4.1).

Further experiments were conducted to compare the effect of the isolation buffer on the *in vivo* activity of RuBisCO in the dark and light of control and heat stressed leaves (Figure 4-19a & b). The results from Figure 4-19a clearly show that an absence of Mg^{+2} from the extraction buffer resulted in low estimates of *in vivo* RuBisCO activity from dark treated leaves at 22°C. Inclusion of 10 mM Mg^{2+} in the extraction buffer, however, resulted in significant RuBisCO activation (approximately 6000 nmol 3-PGA g^{-1}FW. min^{-1}) which confirmed the results obtained from preliminary experiments presented in Figure 4-18.

In contrast, the presence of DTT in the extraction buffer had no major effect on the measured *in vivo* rate of RuBisCO activity from dark adapted leaves (Figure 4-19b). Inclusion of Mg^{2+} and DTT in the extraction buffer had no significant effect on *in vivo* RuBisCO activity of control light adapted leaves. Similar results were obtained from heat stressed leaves extracted after incubation in the light for 20 minutes. It is clear that despite raising T_{leaf} to 38.0°C (± 0.2°C) for 3 hours, a subsequent 20 minute illumination period results in a partial activation of RuBisCO regardless of the Mg^{2+} and DTT content of the extraction buffer (Figure 4-19a & b).

Figure 4-19: Effects of Mg^{2+} and DTT Addition to the RuBisCO Extraction Buffer on Estimates of in *vivo* RuBisCO Activity in Barley Leaves.

Samples were extracted from dark and light adapted control and heat stressed leaves. Non-stressed barley leaves were dark adapted for 17 hours before samples were taken. Non-stressed and heat stressed (38.0 ^{0}C (± 0.2°C) for 3 hours) light adapted leaves were allowed to attain steady-state $\mathbf{A_{sat}}$ (20 min) under saturating light and ambient CO_2 levels prior to sampling. Top Panel **(a)**: leaves were extracted in buffer presented in Materials and Methods, Section, 2.8.1 except for the $MgCl_2$ concentrations (± 10 mM $MgCl_2$) as indicated. Bottom Panel **(b)**: leaves were extracted in buffer presented in Materials and Methods, Section, 2.8.1 except for the DTT concentrations (± 0.5 mM DTT) as indicated. The *in vivo* activity of RuBisCO was measured in a 2-step NADH Cyclic Enzyme-Linked Assay (see Materials & Methods, Section, 2.8.4.2). ANOVA tests were performed using a General Linear Model. Different letter codes indicate Tukey's significant differences at $P<0.05$ level. Tables for ANOVA and group comparisons along with Figures for residual plots are presented in the Appendix (Figure A 4-9 and 4-10). Different plants were used for each temperature treatment, and presented values are the Averages and Standard Errors of 3 replicates.

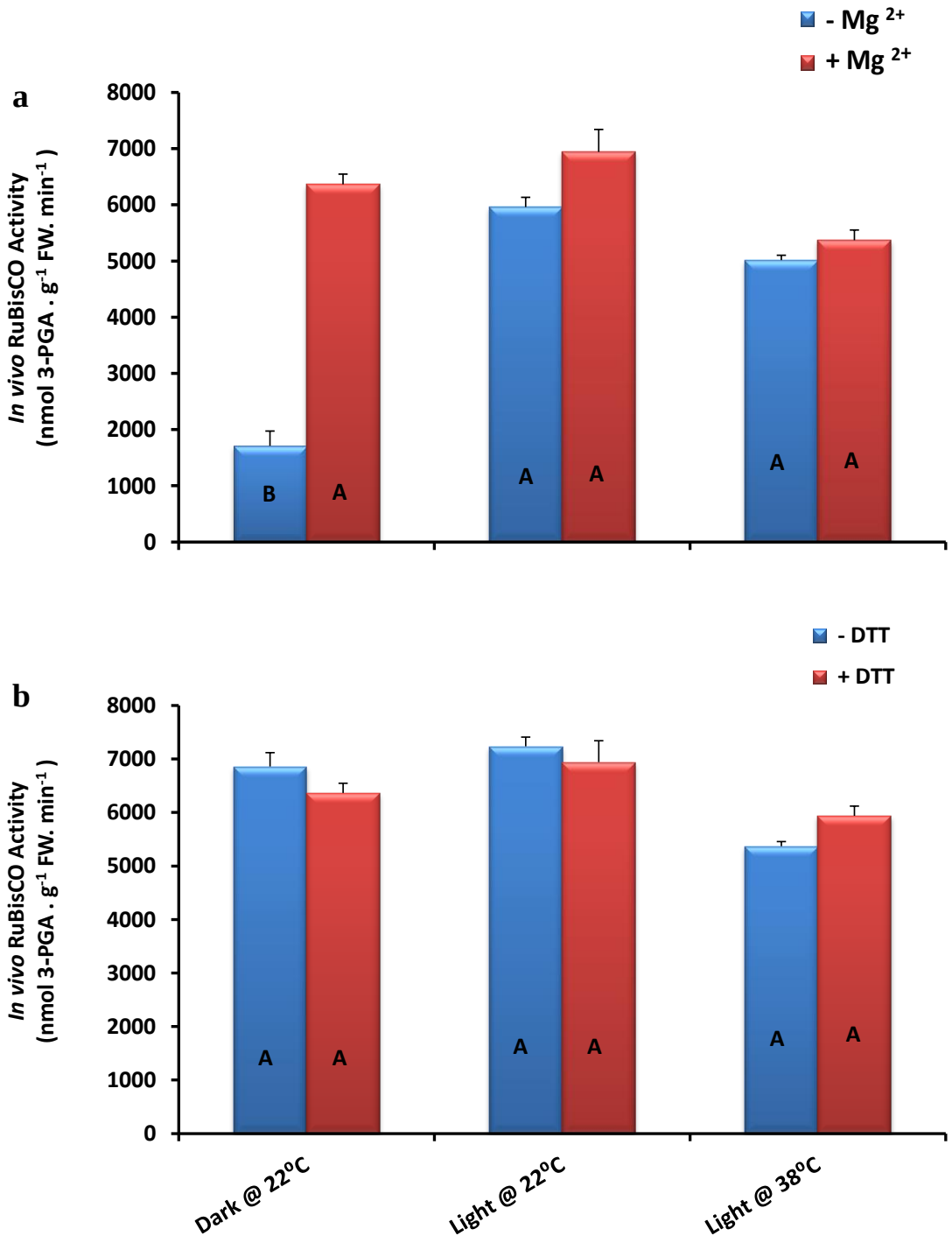
a
- Mg 2+
+ Mg 2+
In vivo RuBisCO Activity
(nmol 3-PGA . g-1 FW. min-1)
8000
7000
6000
5000
4000
3000
2000
1000
0
B
A
A
A
A
A
b
- DTT
+ DTT
In vivo RuBisCO Activity
(nmol 3-PGA . g-1 FW. min-1)
8000
7000
6000
5000
4000
3000
2000
1000
0
A
A
A
A
A
A
Dark @ 22°C
Light @ 22°C
Light @ 38°C

4.6 Carbon Flow between Ri5P and 3-PGA

The results from the metabolomics profiling suggested carbon flow through RuBisCO appears to be suppressed by high T_{leaf} and this is consistent with the notion that RuBisCO Activase is the primary site of thermal injury (Law and Crafts-Brandner 1999; Crafts-Brandner and Salvucci 2000; Kim and Portis 2005; Hozain, Salvucci *et al.* 2010). In contrast, *in vitro* enzyme-linked assays on carbon flow from RuBP to 3-PGA suggest that RuBisCO activity is not suppressed in barley leaves by T_{leaf} up to 40^0C and the RuBisCO activation state is >60% that of controls (see Figure 4-16).

The results also suggest that RuBisCO itself is not greatly affected over this range of T_{leaf} as there are only minor differences in the rates of fully activated RuBisCO after heat stress. Taken together, these results suggest the decline in $\mathbf{A_{sat}}$ is attributable to low concentrations of substrate for the RuBisCO-dependent reaction. These include chloroplast CO_2 levels ($\mathbf{C_c}$) and/or RuBP levels. A decline in ($\mathbf{C_c}$) might arise from a decline in mesophyll conductance ($\mathbf{g_m}$). As Ri5P levels were found to be unaffected by heat stress (Table 4-1), the decline in endogenous RuBP levels might arise from impairment of the activities of the enzymes responsible for RuBP synthesis, Ri5P Isomerase (Ri5P to Ru5P), Phosphoribulokinase (PRK; Ru5P to RuBP), or stromal ATP levels (see Figure 4-20).

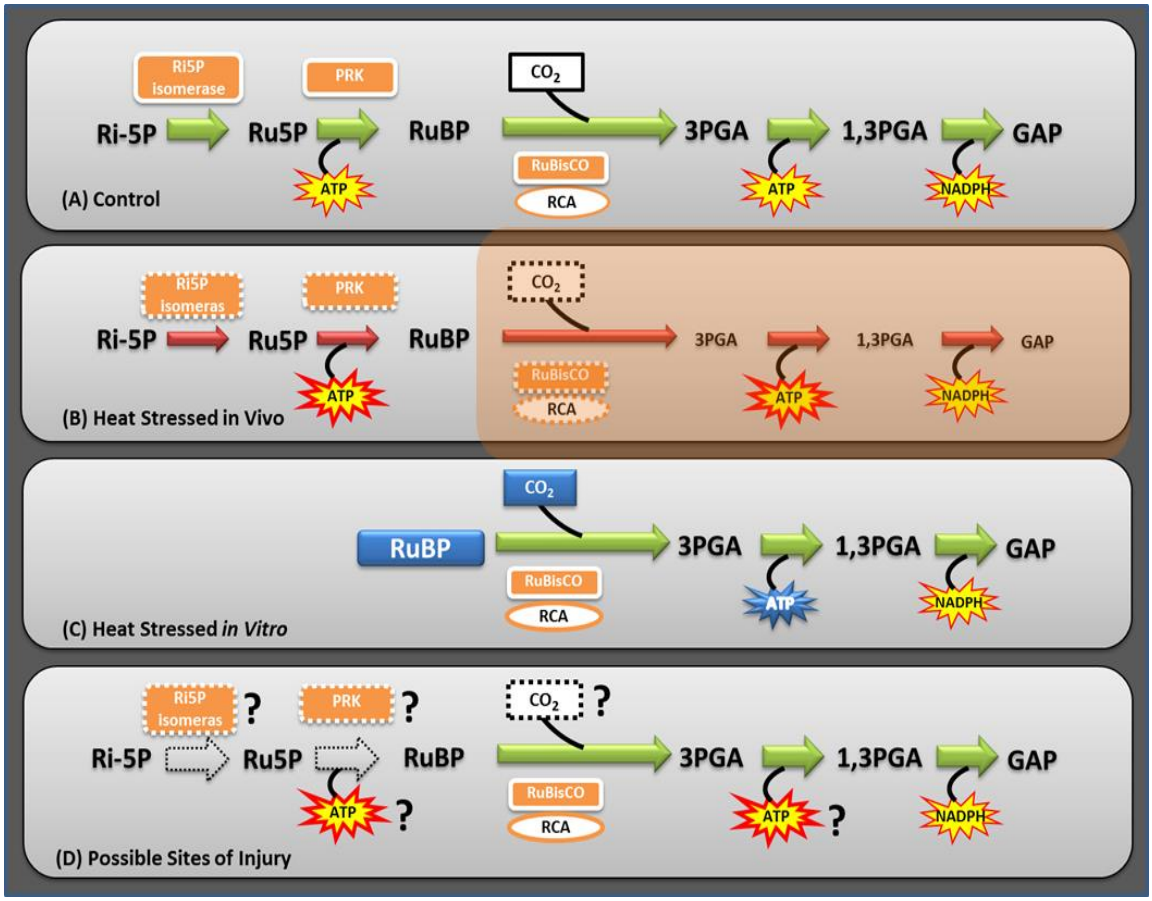

Figure 4-20: Schematic Representation of Carbon Flow between Ri5P and GAP in Control and Heat Stressed Barley Leaves.

(A) Carbon flow between Ribose 5-phosphate (Ri5P) and glyceraldehyde 3-phosphate (GAP) in control Barley leaves at 25^0C. **(B)** Carbon flow is impaired by heat stress (40°C, 3 hours) and the blockage is probably between Ri5P and 3-PGA. **(C)** *In vitro* assays with saturating substrate concentration (CO_2, RuBP, ATP, and NADPH) indicate RuBisCO and RuBisCO Activase are not affected by heat stress. **(D)** Inhibition of $\mathbf{A_{sat}}$ *in vivo* may be attributable to limitation of the substrates for RuBisCO (CO_2 and RuBP); RuBP synthesis is dependent on ATP and the activities of Ri5P isomerase and phosphoribulokinase (PRK).

4.6.1 The Activities of Ri5P Isomerase (Ri5PI) and Phosphoribulokinase (PRK)

As shown in Figure 4-16, the carbon flow through RuBisCO was not greatly affected by heat stress. These finding suggest the inhibition in $\mathbf{A_{sat}}$ and concomitant changes in metabolite levels might be attributable to the RuBisCO-dependent reaction becoming limited by impaired RuBP synthesis. The levels of Ri5P are normal after stress (see Table 4-1) and so the two metabolic steps that convert Ri5P to RuBP catalysed by the enzymes Ri5P isomerase and PRK and/or the supply of stromal ATP are possible candidates for the observed inhibition. To test these possibilities, the activity of Ri5P isomerase and PRK was estimated in response to a range of T_{leaf}.

Ri5P isomerase (Ri5PI) and phosphoribulokinase (PRK) activities were measured in samples extracted from barley leaves exposed to a range of temperatures using an enzyme-linked assay developed specifically for this purpose (see Section 4.4.2). Ri5PI activity is dependent on the amount of Ri5P which is saturating in the in vitro reaction. However, phosphoribulokinase (PRK) activity is dependent on the concentration of the product of the first reaction (Ru5P) which may not be saturating. For that reason, the reaction from Ri5P to RuBP was run for a range of end time points (0, 30, 60, 120, 300, 600 and 900 seconds) before the reaction was stopped by heating to 80°C, then the amount of RuBP produced was estimated (for full details, see Material and Methods, Section 2.9.1). The combined activity for both enzymes was then calculated from the initial slope of the activity (µmol 3-PGA. g -1 FW) versus time (seconds) curves (see Figure 4-21; insert).

Figure 4-21 presents the effect of increasing leaf temperature on the *in vivo* activity of Ri5PI and PRK. Clearly, the activity of both enzymes in leaves stressed at 38.0°C and 40.0°C declined by only 50% compared with controls. Regardless, even in heat stressed leaves that demonstrated 80% inhibition of ETR just prior to sampling, the rate of RuBP generation from Ri5P appears to be at least 6 times higher than the corresponding maximum rates of RuBisCO activity (35 µmol RuBP. g $^{-1}$ FW. min^{-1} *versus* 6 µmol 3-PGA. g $^{-1}$ FW. min^{-1}). It is concluded that high T_{leaf} does not greatly affect the production of RuBP from Ri5P and is unlikely, therefore, to account for the observed thermal suppression of $\mathbf{A_{sat}}$.

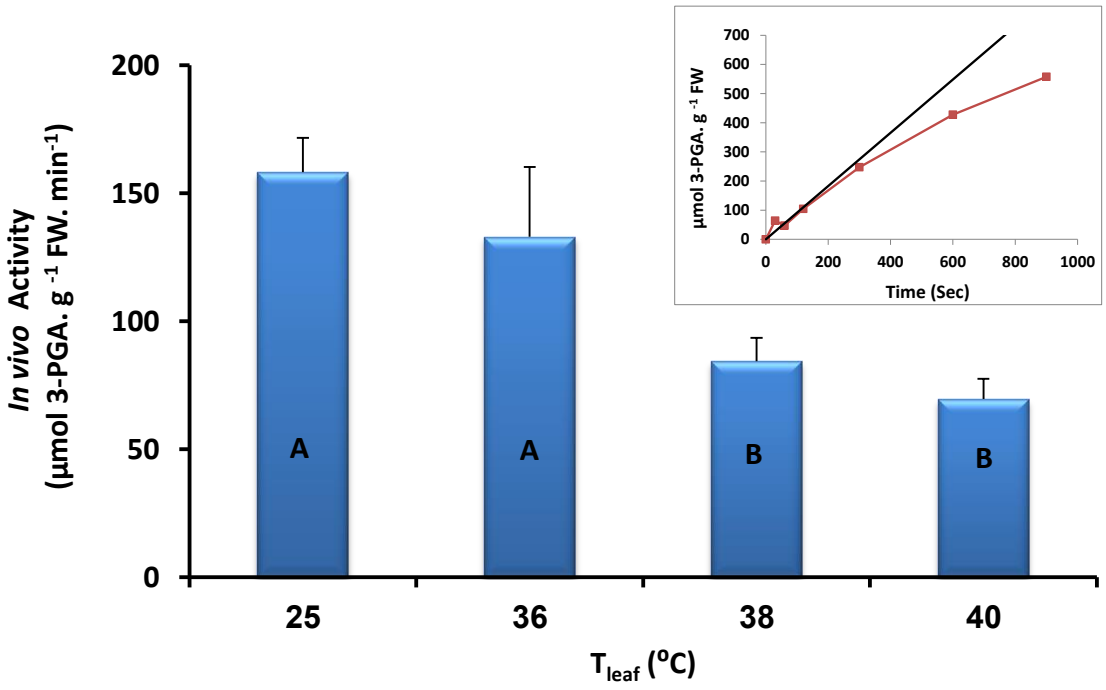

Figure 4-21: Effect of Increasing Barley Leaf Temperature on the Conversion of Ri5P to RuBP.

The combined *in vivo* activity of Ri5PI and PRK were measured on extracts from leaves incubated for 3 hours at different leaf temperatures (25, 36, 38 or 40°C). Heat stress was imposed as described in Material and Methods Section 2.2. Ri5P was added to leaf extract and samples removed at different time points (0, 30, 60, 120, 300, 600 and 900 seconds) and the reaction stopped by rapidly heating to 80°C. Newly synthesized RuBP was then measured (Material and Methods, Section 2.9.1). The combined activity of both enzymes was calculated from the initial slope of their activity (µmol 3-PGA. g $^{-1}$ FW) *versus* time (seconds) curve (Insert). ANOVA tests were performed using a General Linear Model. Different letter codes indicate Tukey's significant differences at $P<0.05$. Tables for ANOVA and group comparisons along with Figures for residual plots are presented in the Appendix (Figure A 4-11). Different plants were used for each temperature treatment, and presented values are the Averages and Standard Errors of 3 replicates.

4.6.2 Mesophyll Conductance (g_m)

The turnover of RuBisCO *in vivo* and corresponding rates of $\mathbf{A_{sat}}$ may also be limited by the diffusion of CO_2 from the intracellular leaf space to the chloroplast stromal (mesophyll conductance, $\mathbf{g_m}$). Attempts were made to estimate g_m in control and heat stressed tissues using both the 'Constant J' and 'Variable J' methods (Loreto, Harley *et al.* 1992). Although reliable estimates for g_m were obtained from control barley leaves using a Constant J' method (approximately 0.12 ± 0.03 mol $.m^{-2}$ $.s^{-1}$), no sensible values were collected from heat stressed leaves. It appears that the model for photosynthesis upon which these two measurements are based breaks down when heat stress is applied making estimates of $\mathbf{g_m}$ impractical.

To test whether g_m is a potential temperature sensitive target that limits photosynthesis, $\mathbf{A_{sat}}$ was measured in control and heat stressed leaves exposed to increasing $\mathbf{C_a}$ to increase carbon flux to the chloroplast. If $\mathbf{g_m}$ was limiting CO_2 diffusion from intercellular spaces to the chloroplast (active sites of RuBisCO), increasing $\mathbf{C_a}$ should produce a corresponding increase in $\mathbf{A_{max}}$. No stimulation of A_{max} was observed in heat stressed leaves when $\mathbf{C_a}$ was increased from 400 to 1000 μmol CO_2. mol^{-1} air (Figure 4-22).

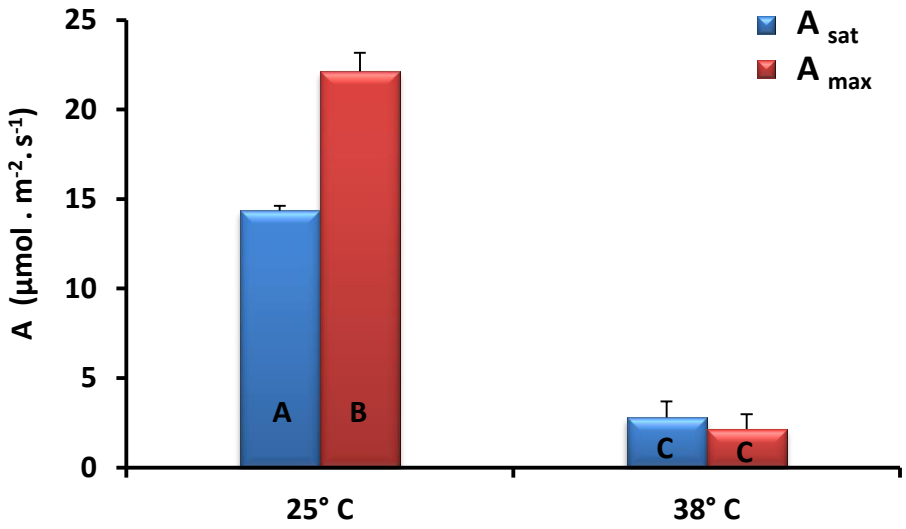

Figure 4-22: Effect of Increasing CO_2 Concentration on Assimilation Rate in Control and Heat Stressed Barley Leaves.

Assimilation rate (A) was measured at 25.0 °C and saturating irradiance (560 µmol. m^{-2} s^{-1} PAR) and ambient air (400 µmol CO_2. mol^{-1} air ($\mathbf{A_{sat}}$) or CO_2 enriched air (1000 µmol CO_2. mol^{-1} air ($\mathbf{A_{max}}$), with IRGA before and after leaves were heat stressed for 3 hours at 38. 0°C (see Material and Methods, Section 2.3.2). ANOVA tests were performed using a General Linear Model. Different letter codes indicate Tukey's significant differences at $P<0.05$. Tables for ANOVA and group comparisons along with Figures for residual plots are presented in the Appendix (Figure A 4-12). Different plants were used for each temperature treatment, and presented values are the Averages and Standard Errors of 3 replicates.

4.7 Discussion

Although at high leaf temperatures (> 36°C) neither stomatal conductance ($\mathbf{g_s}$) nor damage to PSII was a limiting factor for photosynthesis immediately after heat stress (Chapter 3, Section 3.2), it is unclear what processes were the principal limitations on photosynthesis. To identify the possible sites responsible for the irreversible inhibition in $\mathbf{A_{sat}}$, four potential target processes that control the rate of CO_2 assimilation were examined: (1), capture of excitation energy by the Light Harvesting Complexes (LHCs) and energy transfer to PSI and PSII reaction centers (RCI and RCII: (2) primary photochemistry, photosynthetic electron transport rates (*in vitro* ETR), and the production of ATP: (3), the kinetic properties of the enzymes of the C3 cycle: (4) the diffusion of CO_2 from the intracellular leaf space to the chloroplast controlled by mesophyll conductance ($\mathbf{g_m}$).

Leaf absorbance and PSII exaction spectra clearly showed that transfer of the exaction energy to the reaction centers was not affected by heat stress (Figure 4-2), and therefore was not limiting $\mathbf{A_{sat}}$ after heat stress.

In vivo measurement of ETR showed a significant decline after heat stress similar to the decline in the CO_2 saturated photosynthetic rate (see Chapter 3, Section 3.2.2.2). Generally, there is agreement that CO_2 assimilation and *in vivo* ETR are correlated well (Baker 2008). It is important however, to realize that no conclusion can be drawn on the direct effects of heat stress on the electron transport chain measured by modulated fluorescence because the linear ETR is coupled to the C3 cycle. It is suggested therefore, that direct effects of heat stress on the ETR should be obtained when ETR is uncoupled from CO_2 assimilation by adding an electron acceptor like methyl viologen (Bugg, Whitmarsh *et al.* 1980).

Comparison between the results of ETR measurements *in vivo* and *in vitro* showed the responses to high temperature were different. After increasing leaf temperature to 38.0 ºC for 3 hours, *in vivo* ETR was less than 20% of control while ETR measured *in vitro* showed rates of >80% (see Chapter 3, Section 0 and Chapter 4, Section 4.2). Thus, it is possible that CO_2 assimilation may not necessarily be limited by the direct effect of thermal stress on ETR. Therefore, it can be assumed that limitations were imposed beyond the electron transport chain possibly by the activities of some C3 enzymes (Price, Evans *et al.* 1995; Muschak, Willmitzer *et al.* 1999; Paul, Driscoll *et al.* 2000).

This conclusion is supported by the direct measurements of metabolite levels completed by previous work in our laboratory which showed that metabolite levels after RuBisCO (3-PGA, triose phosphate and S7P) were depleted while those that feed into RuBisCO

(X5P/Ri5P, and Ru5P) were unaffected (Shahwani 2011). Although important metabolites like RuBP and GAP are not detected directly by mass spectrometry, it can be concluded that carbon flow between Ri5P and 3-PGA is compromised after heat stress, possibly by impairment of the activity of RuBisCO, RuBisCO Activase, or by processes close to the carboxylation step (stromal ATP levels and/or chloroplast CO_2 levels (C_c)). Published measurements of metabolites are consistent with this hypothesis, suggesting RuBP levels increase and 3-PGA decrease when photosynthesis is inhibited by heat stress and this has been attributable to a decrease in activation state of RuBisCO (Weis 1981; Crafts-Brandner and Salvucci 2002).

Measurements of RuBisCO activity and estimates of the corresponding CO_2 assimilation rate ($\mathbf{A_{sat}}$ from *in vivo* ETR for the same leaves) showed that even at high leaf temperature (42.0°C), where CO_2 assimilation is completely abolished, the endogenous activity of RuBisCO from illuminated leaves is still approximately 50% that of control leaves. In addition, increasing leaf temperature had no effect on RuBisCO activation state. Taken together all these observation provide no evidence to support the contention that the observed inhibition in photosynthesis with increasing leaf temperature is attributable to an inactivation of RuBisCO Activase and subsequently RuBisCO (Law and Crafts-Brandner 1999; Crafts-Brandner and Salvucci 2000; Kim and Portis 2005).

It was important to ensure the estimates of *in vivo* RuBisCO activities presented (in *eg.* Figure 4-16) were not anomalous due to enzyme activation during the isolation procedure. Unpredictably, *in vivo* RuBisCO rates of dark adapted leaves were high and showed approximately a 60% activation state, similar to the activity from illuminated leaves. Low levels of RuBisCO activity, however, can be observed from dark adapted barley leaves when Mg^{2+} is omitted from the extraction buffer. These observations suggest the Mg^{2+} present in standard isolation buffer that has been routinely used for two decades (Milos, Bloom *et al.* 1985; Loza-Tavera, Martínez-Barajas *et al.* 1990) partially activates dark adapted barley RuBisCO and does not, therefore, faithfully reflect *in vivo* activity of RuBisCO. In contrast, raising T_{leaf} to either 22.0 or 38.0°C (± 0.2°C) for 3 hours in the dark and a subsequent 20 minute illumination period, results in a partial activation of RuBisCO regardless of the Mg^{2+} and DTT content of the extraction buffer. Another interesting finding from this study is that RuBisCO Activase might not be required to activate RuBisCO in barley leaves as stromal Mg^{2+} levels may be sufficiently high to activate RuBisCO to approximately 60% of control leaves in the light at 22°C and after heat stress at 38.0°C. RuBisCO Activase could, however, be required at low leaf temperatures. Taking all these observations together, it is clear that although heat stressed leaves show 85%

inhibition in CO_2 assimilation, the endogenous activity of RuBisCO from illuminated leaves is still approximately 60% that of control leaves, which is not due to activation during the isolation procedure, and therefore the decline in $\mathbf{A_{sat}}$ cannot be attributed to a corresponding decline in the endogenous activity of RuBisCO by an inhibition of RuBisCO Activase.

This finding is in stark contrast to the conclusions in the literature where RuBisCO Activase activity has been shown to be temperature sensitive and implicated in the thermal inactivation of photosynthesis (Law and Crafts-Brandner 1999; Crafts-Brandner and Salvucci 2000). Conversely, the result presented in this chapter supports the view that photosynthesis becomes limited by the effect of heat stress on the process related to regeneration of RuBP rather than by RuBisCO deactivation (Schrader, Wise *et al.* 2004; Wise, Olson *et al.* 2004; Cen and Sage 2005; Kubien and Sage 2008).

In this study, the activity of Ri5P isomerase (Ri5PI) and phosphoribulokinase (PRK) enzymes were relatively unaffected by heat stress at 38.0°C and 40.0°C, with only 50% inhibition compared with controls. However, even at the highest temperature (40°C), the rate of carbon flow from Ri5P to 3-PGA through Ri5PI and PRK was six fold greater than the carbon flow from RuBP to 3-PGA through fully activated RuBisCO. It has been reported that PRK was considerably more stable to thermal denaturation up to 48°C compared with RuBisCO Activase (Salvucci, Osteryoung *et al.* 2001). Therefore the inhibition in $\mathbf{A_{sat}}$ cannot be attributable to the RuBP synthesis becoming limited by impairment of the activity of Ri5PI and/or PRK.

The diffusion of CO_2 from the intracellular leaf space to the chloroplast stroma (mesophyll conductance $\mathbf{g_m}$) was estimated using both the 'Constant J' and 'Variable J' methods (Loreto, Harley *et al.* 1992). Although reliable estimates for $\mathbf{g_m}$ were obtained from control barley leaves using the Constant J' method, estimates of $\mathbf{g_m}$ after heat stress were impracticable as the model for photosynthesis upon which these two measurements are based breaks down when heat stress is applied. To overcome this difficulty, limitation by $\mathbf{g_m}$ was estimated by increasing CO_2 concentration in the air ($\mathbf{C_a}$) which should produce an increase in CO_2 flux to the chloroplast and a corresponding increase in $\mathbf{A_{sat}}$ if $\mathbf{g_m}$ was limiting CO_2 diffusion at high temperature. The inhibition of $\mathbf{A_{sat}}$ after heat stress was not reversed by increasing $\mathbf{C_a}$, which is an indicator that $\mathbf{A_{sat}}$ was not limited by low mesophyll conductance after heat stress.

5 Chapter 5: Investigation into the Effects of High Leaf Temperature on ATP Production in Barley Leaves

Previous results presented in Chapter 4, Section 4.6, suggested that the decline in photosynthesis rate after heat stress might be attributable to limitation in the conversion of Ri5P to RuBP, an ATP-dependent process. The thylakoid membrane has been suggested as the primary site of injury at high temperatures (Schrader, Wise *et al.* 2004). High leaf temperature can cause thylakoid membranes to become leaky and impair the ability to form a transthylakoid proton gradient for the generation of ATP by chemiosmosis (Bukhov, Wiese *et al.* 1999a) which is essential in providing ATP for RuBP regeneration. In this section, the effect of high leaf temperatures on the chloroplast ATP content was estimated using a luciferin-luciferase assay to establish whether chloroplast ATP content correlates with the thermal decline in $\mathbf{A_{sat}}$. In addition, Modulated Chlorophyll Fluorescence techniques were used to probe the capacity of the thylakoid membrane to develop a proton motive force (pmf) before and after heat stress (Baker 2008).

5.1 Estimates of Chloroplast ATP Pools

In the chloroplasts of leaf cells, the flow of electrons through electron carriers in the thylakoid membrane causes the generation of NADPH and a proton gradient (ΔpH) which drives the synthesis of ATP by the ATP synthase complex. The C3 cycle uses ATP and NADPH to synthesize RuBP, which reacts with CO_2 in a reaction catalysed by RuBisCO. Also, ATP is consumed by RuBisCO Activase in a reaction required to free tightly bound inhibitors (RuBP itself and sugar phosphatase inhibitors such as 2-Carboxyarabinitol 1-Phosphate (Robinson and Portis jr 1988) from the RuBisCO catalytic site.

The chloroplast ATP synthase is a multi-subunit enzyme complex associated with the thylakoid membrane and consists of two major components: a membrane-embedded CF_0 part and a peripheral CF_1 part. The CF_0 part consists of three different subunits: a single subunit **a**, two subunits of **b** and several subunits **c** (10–15 mer) and acts as H^+ channel (Stock, Leslie *et al.* 1999; Mitome, Suzuki *et al.* 2004). The hydrophilic CF_1 part consists of five different subunits with the stoichiometry α_3, β_3, γ, δ and ε (Yoshida, Sone *et al.* 1979; Hisabori, Sunamura *et al.* 2013). The rotational catalysis model for synthesis of ATP has been proposed by (Gresser, Myers *et al.* 1982), in which relative rotational movement of α_3 and β_3 core against the γ subunit occurs during catalytic reaction. The chloroplast

ATP synthase is regulated by pH gradient and the supply of ADP. The turnover of CF_1 is inhibited when the pH gradient decreases below a certain level and the disulfide bond located on the γ subunit is reduced by thioredoxin (Mills and Mitchell 1982).

Measurments of ATP levels in heat stressed leaves vary considrably between studies. *In vivo* measurements of chloroplasts ATP in spinach and tobacco showd that chloroplast ATP levels do not decrease under moderate heat stress (Weis 1981; Wang, Duan *et al.* 2006). In contrast, ATP levels in cotton were significantly decreased in response to increasing leaf temperature (Loka and Oosterhuis 2010). In fact, few studies have considered the role of the chloroplast ATP synthase as a limiting factor for photosynthetic capacity in response to heat stress due to the widely held belief that ATP levels are maintend by stimulation of cyclic electron transport around PSI (Bukhov, Wiese *et al.* 1999a). Therefore, The effect of high leaf temperatures on the chloroplast ATP content was estimated using a luciferin-luciferase assay to establish whether chloroplast ATP content correlates with the thermal decline in $\mathbf{A_{sat}}$. Further experiments were first conducted to optimize the luciferin-luciferase assay before using it for ATP measurements.

5.1.1 Extraction of Foliar ATP

To provide reliable estimates of tissue ATP levels in illuminated leaves, it is essential that endogenous phosphatases are rapidly denatured and these processes should not interfere with the luciferin–luciferase assay. Two extraction methods are commonly used for measuring tissue ATP, the perchloric acid method and the Tris–borate/heat method. Yang, Ho *et al.* (2002), found both of these methods interfered with the luciferin–luciferase reaction resulting in low ATP bioluminescence. Alternatively, they reported that extraction into hot water was a simple and reliable one-step procedure that provided reliable results. Figure 5-1a shows that ATP extracted from illuminated barley leaves into water at 90°C resulted in a stabilization of ATP for at least 90 min; whereas, omission of this high temperature step resulted in a rapid loss of ATP presumably through the action of endogenous phosphatases. The amounts of ATP in the samples were calculated from standard curves generated using a series of known ATP concentrations ranging from 0 to 25 pmol (0-230 nM). For each experiment, fresh standard curves were generated. The bioluminescence was found to increase linearly with ATP concentration (Figure 5-1b).

Figure 5-1: Stability of ATP in Barley Leaf Extracts and ATP Calibration Curve.

Top panel **(a)**: Leaf tissue photosynthesizing under saturating light and ambient CO_2 levels at 25°C was rapidly frozen in liquid nitrogen, ground to a fine powder, accurately weighed to approximately 20 mg, and then stored at -80°C. When required, samples were removed from the freezer and rapidly placed in 1 ml of water pre-heated to 90°C or 20°C for 3 min before centrifugation to remove cell debris (12,000g, 5 min at 4°C). The resulting supernatants were then decanted and stored on ice for the indicated incubation times before determining ATP levels using the luciferin–luciferase bioluminescence assay (see Materials and Methods, Section 2.10.3). Values are the Averages and Standard Errors of 4 replicates. Bottom panel **(b)**: Standard curve for ATP was generated by adding a series of ATP concentrations ranging from 0 to 25 picomoles added to a reaction containing 1.25 µg/mL of firefly luciferase, 50 µM D-luciferin and 1 mM DTT in 1X Reaction Buffer (100 µl total volume). Luminescence was measured immediately for 10 min using a luminometer (arbitrary units) as described in Materials and Methods, Section 2.10.2.

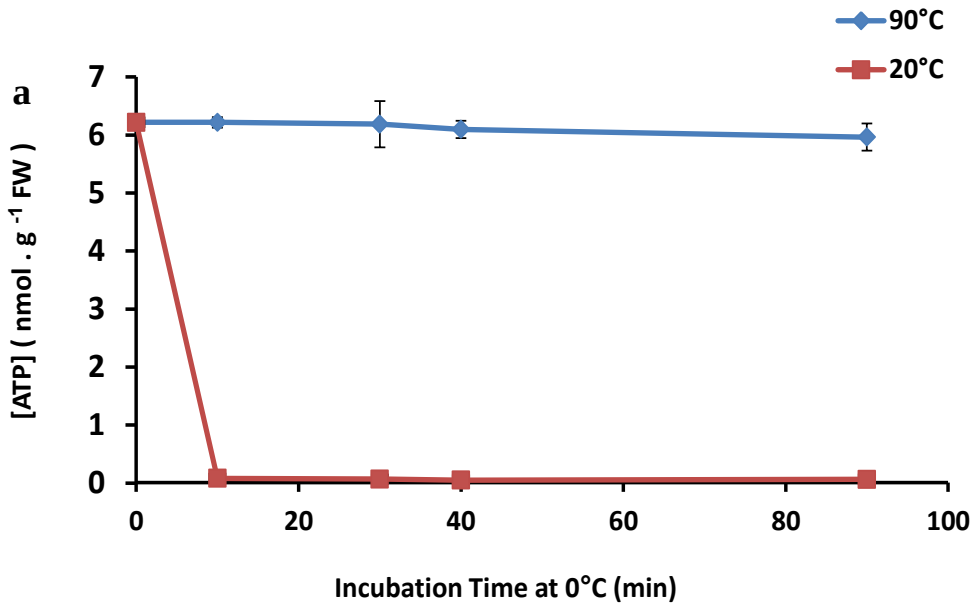
a
90°C
20°C
[ATP] (nmol . g -1 FW)
0
1
2
3
4
5
6
7
0
20
40
60
80
100
Incubation Time at 0°C (min)

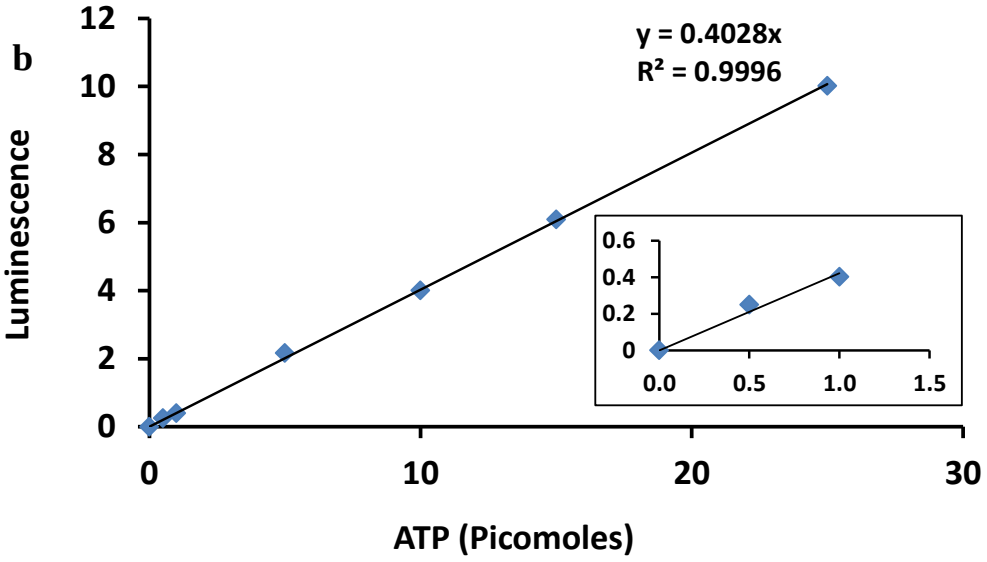
b
y = 0.4028x
R² = 0.9996
Luminescence
0
2
4
6
8
10
12
0
10
20
30
ATP (Picomoles)
0
0.2
0.4
0.6
0.0
0.5
1.0
1.5

5.1.2 Estimation of Chloroplast ATP Levels

ATP levels can be estimated using different methods. The synthesis of ATP can be quantified *in vitro* by monitoring pH change due to ATP formation with a sensitive pH electrode or appropriate pH-sensitive dyes (Mitsuo, Takeru *et al.* 1962; Mills, Hipkins *et al.* 1986). Also, measuring the relaxation kinetics of the electrochromic shift (ECS) is a spectroscopic technique that can be used to estimate the rate of ATP synthesis *in vivo* (Zhang and Sharkey 2009). Alternatively, ATP synthesis *in vitro* can be determined by measuring the incorporation of radiolabeled P_i into ATP (Hangarter and Good 1982; Flores and Ort 1984). A limitation to these methods is that it measures all of the ATP present in the sample, so any ATP present prior to the initiation of the ATP-synthesizing reaction will also be included in the final measurements. In addition, after heat stress, not all thylakoid preparations are capable of performing photophosphorylation. Therefore, ATP content in intact barley leaves was estimated by the amount of light emitted from the luciferin–luciferase assay and calibrated using known amounts of ATP. Although this assay has an advantage in that it does not use radionuclides and is more sensitive than most other methodologies, it is also measures the total ATP present in the sample. To overcome this limitation, chloroplast ATP was estimated as Light-minus-Dark levels (Wang, Duan *et al.* 2006) from whole leaves after 20 minutes incubation in 560 µmol m^{-2} s^{-1} PAR or in the dark (Figure 5-2). The results indicated that whole leaf ATP levels are over three times greater in light *versus* dark adapted leaves and that this increase is observed within 3 minutes of illumination. The difference between leaf ATP levels in the light and dark, therefore, can be used as an estimate of the light-generated ATP in the chloroplasts of intact leaves.

5.1.3 Temperature Effects on the Concentrations of Chloroplast ATP

Levels of Light-generated ATP in the chloroplast were greatly affected when leaf temperatures exceeded 36.0°C. Both high leaf temperatures (38.0 and 40.0°C) caused a significant decline in leaf ATP levels (>75%) when compared with control temperature. This reduction correlated well with the corresponding photosynthetic electron transport rates measured by modulated fluorescence from the same leaves just prior to ATP extraction (Figure 5-3 a & b).

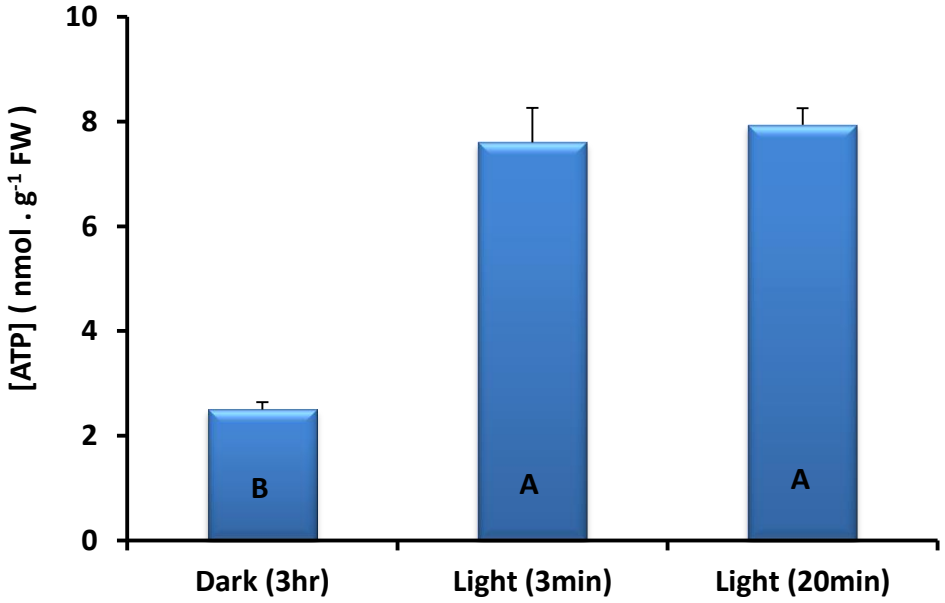

Figure 5-2: ATP Levels in Non-Stressed Barley Leaves in the Light and Dark.

Light-generated ATP in the chloroplast was estimated as light-minus-dark levels in whole leaves after the indicated times. Attached leaves were incubated in the dark for 3hr at 25.0C° and then exposed to light (560 µmol m^{-2}. s^{-1}) for 3 or 20 minutes. Tissue was harvested by rapid freezing in liquid nitrogen and ATP extracted into hot water and measured using the luciferin-luciferase bioluminescence assay (see Material and Methods Section 2.10.4). ANOVA tests were performed using a General Linear Model. Different letter codes indicate Tukey's significant differences at $P<0.05$. Tables for ANOVA and group comparisons along with Figures for residual plots are presented in the Appendix (Figure A 5-1). Different plants were used for each temperature treatment, and presented values are the Averages and Standard Errors of 3 replicates.

Figure 5-3: Effect of Increasing Leaf Temperature on (a) Light-generated ATP in the Chloroplast, (b) Corresponding ETR Rate in Barley Leaves.

(a) Attached leaves of healthy barley (*cv.* local) plants were first incubated in the dark for 3hr on a thermal block set at 25.0, 36.0, 38.0 or 40.0°C (± 0.2°C). After this period leaves were incubated for a further 20 minutes in air at 25°C either in the dark or in 560 µmol m^{-2} s^{-1} PAR. Leaf tissue was then rapidly extracted in liquid nitrogen and ATP levels determined using the luciferin-luciferase bioluminescence assay (see Material and Methods Section 2.10.4). Light-generated ATP in the chloroplast was estimated as Light-Dark values, for n=4 independent biological replicates at each temperature (4 light, 4 dark). **(b)** ETR was measured using modulated fluorescence from the same leaves just prior to flash-freezing for ATP measurements. ANOVA tests were performed using a General Linear Model. Different letter codes indicate Tukey's significant differences at $P<0.05$. Tables for ANOVA and group comparisons along with Figures for residual plots are presented in the Appendix (Figure A 5-2 & 5-3). Different plants were used for each temperature treatment, and presented values are the Averages and Standard Errors of 4 replicates.

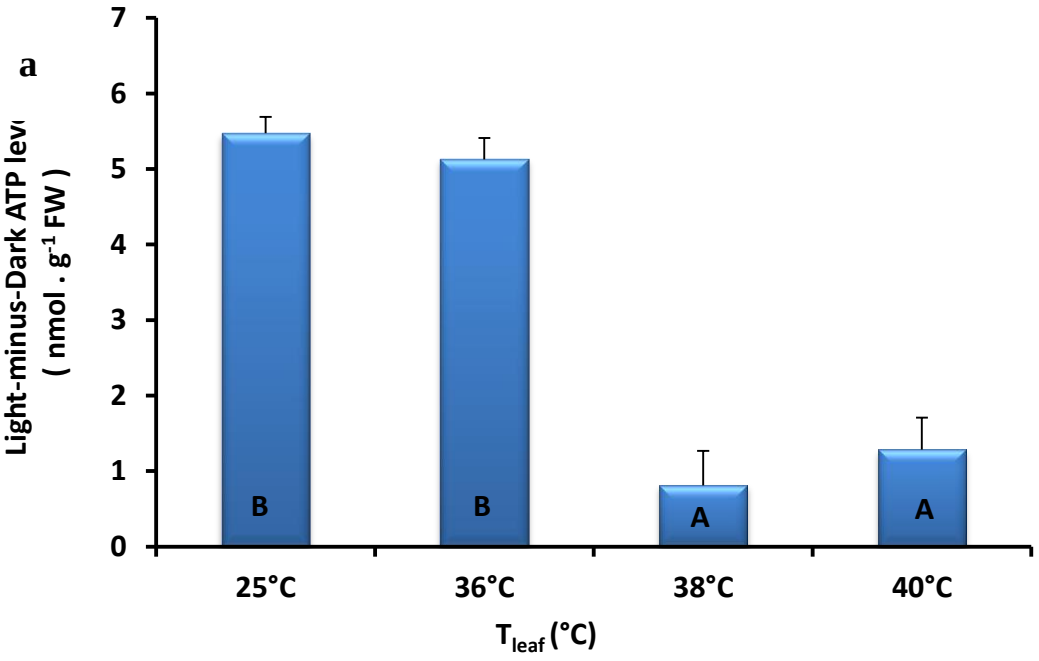
a
Light-minus-Dark ATP lev
(nmol . g-1 FW)
7
6
5
4
3
2
1
0
B
B
A
A
25°C
36°C
38°C
40°C
Tleaf (°C)

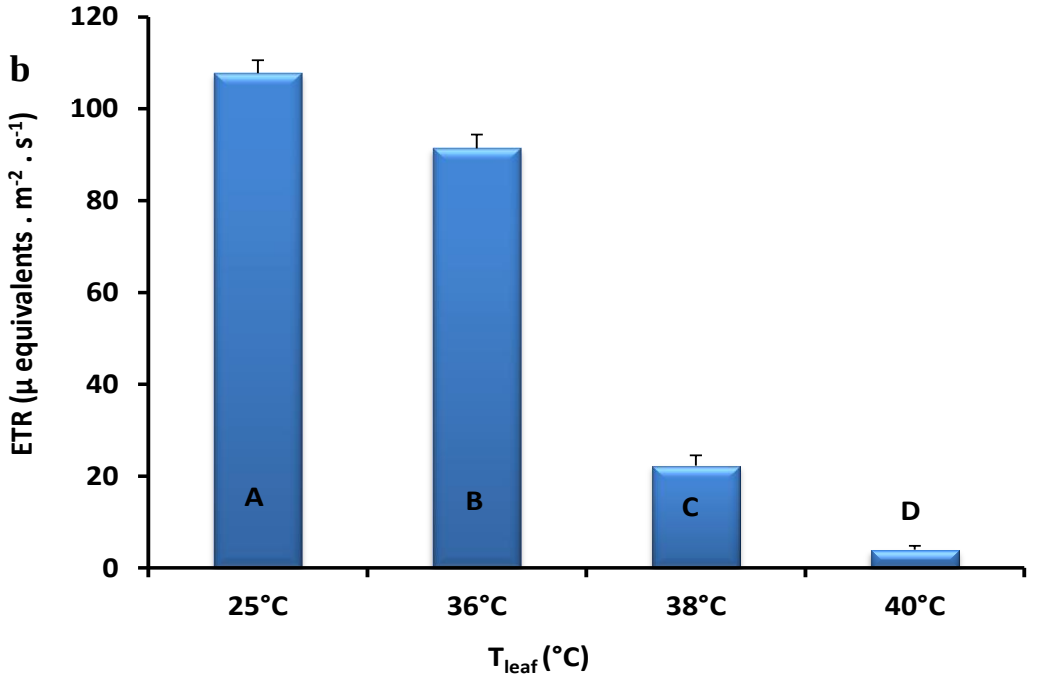
b
ETR (µ equivalents . m-2 . s-1)
120
100
80
60
40
20
0
A
B
C
D
25°C
36°C
38°C
40°C
Tleaf (°C)

5.2 The Thermal Stability of Thylakoid Membrane

5.2.1 The Kinetics of NPQ Fluorescence Dark Relaxation

Non-photochemical quenching (**NPQ**) is considered to be an important protective mechanism that prevents damage to the photosynthetic apparatus in higher plants (Ralph, Wilhelm *et al.* 2010). **NPQ** has been analyzed by monitoring its relaxation in the dark, by applying saturating pulses of light. At least three kinetically distinct phases of **NPQ** light-to-dark recovery are observed, which have previously been identified (Horton and Hague 1988; Quick and Stitt 1989; Walters and Horton 1991; Baker 2008). The fast phase is due to high-energy state quenching (***qE***), the middle phase which arises from excitation energy redistribution due to a state transition quenching (***qT***), and the slow phase due to photoinhibition quenching (***qI***). However, in the literature it is widely reported that the ΔpH-dependent quenching (***q*E**) is the major component of **NPQ** in non-stressed leaves under moderate-to-saturating light (reviewed in Baker, 2008). Analysis of these phases will provide information about how each of the three components responds to heat stress, particularly (***q*E**).

5.2.1.1 Analysis of NPQ Dark Relaxation

Dark Relaxation of **NPQ** was analysed using theoretical models described previously (Horton and Hague 1988). Attached non-stressed barley leaves were light adapted (560 µmol m^{-2} s^{-1} PAR) for 20 min in air to achieve steady state photosynthesis before the actinic light was switched off. The dark relaxation was recorded for 20 min using saturating pulses of light applied in the dark (at 0, 30, 60, 150, 210, 330, 450, 750, 1050 and 1350 seconds). Figure 5-4 shows a plot of log **NPQ** relaxation against dark relaxation time and three phases can be resolved similar to those expected for components of **NPQ** (fast, middle and slow kinetic phase). The fast phase accounted for 57% of total **NPQ** has a half-time of 90s, consistent with it being the major component of **NPQ** in non-stressed leaves (Baker 2008). The middle component (15% of the total **NPQ**) has a half-time of 713s, and the slow component (28% of the total **NPQ**) had a half-time of 2833s.

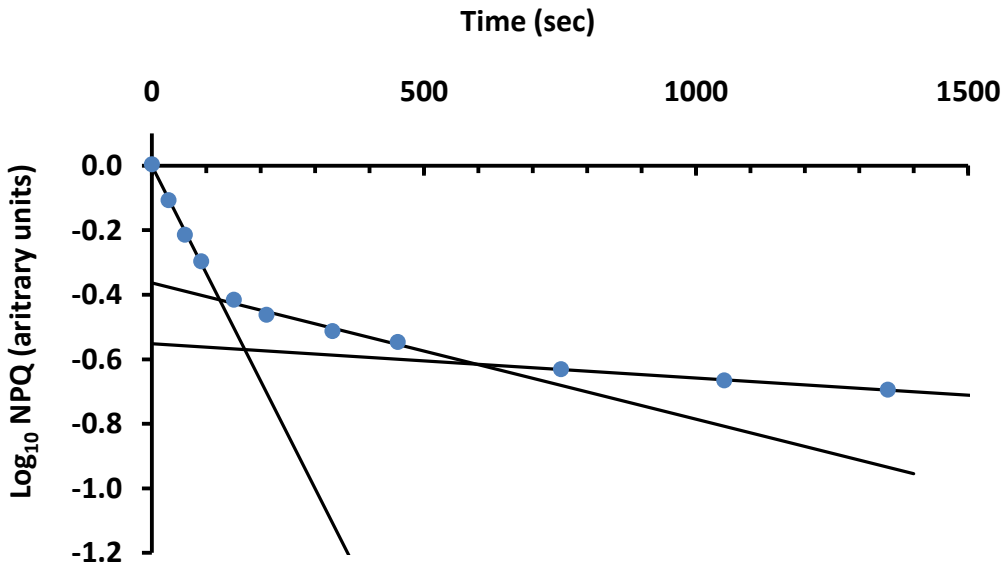

Figure 5-4: Semi-logarithmic Plot of NPQ Dark Relaxation in Barley Leaves.

NPQ dark relaxation of non-stressed barley leaf measured using WALZ PAM fluorimeter. The actinic light was switched off after 20 min and saturating pulses were applied (at 0, 30, 60, 90, 150, 210, 330, 450, 750, 1050 and 1350 seconds); see Material and Methods, Section 2.4.2 for experimental details. Plot of log (**NPQ**) as a function of relaxation time is shown and best linear fit for each kinetic component has been calculated. The plot shows a fast, intermediate and slow kinetic component of **NPQ**.

5.2.1.2 Effect of Pulse Frequency on Analysis of NPQ Dark Relaxation

Although the dark relaxation of **NPQ** using saturating light pulses often resolves 3 distinct phases, it has been suggested that the method incurs artefacts that arise from the pulse train frequency and intensity (Peter Dominy, per.comm; Walters and Horton 1991). To check this possibility, dark relaxation of **NPQ** was reassessed using the same method but different pulse frequencies to those recommended (Horton and Hague 1988; WALZ MINI-PAM Handbook). Two pulse regimes were used, the first one, a standard Induction Curve Program using the MINI-PAM fluorimeter (PAM 2000H Walz, Effeltrich, Germany) with standard saturation pulses applied at 0, 30, 90, 210, 510 and 1110 seconds after switching the actinic light off. Data were analysed by plotting the log (**NPQ**) as a function of relaxation time and the best linear was fit for each of the three kinetic components resolved. Two phases were observed instead of three, a fast phase which accounted for 74% of total **NPQ** and had a half time of 67s and a slow (or middle phase) which accounted for 26% of the total **NPQ** and had a half time of 730 s (Figure 5-5a).

In the second pulse regime, **NPQ** relaxation was analysed after increasing pulse frequency to 0, 30, 60, 90,120, 150, 180, 210, 300, 420, 730, and 1330 seconds (Figure 5-5b). The results showed two phases, a fast phase which accounted for 33% of the total **NPQ** and had a half time of 186s and a slower phase which accounted for 67% of the total **NPQ** with a half time of 1690s. Increasing the pulse frequency applied during the dark recovery might prevent complete relaxation of the **NPQ** phases (compare Figure 5-5a with Figure 5-5b)

Taken together these results indicated that resolving dark relaxation of **NPQ** to three components is highly dependent on the pulse frequency applied during dark recovery and any changes in duration between pulses can have a large effect on the calculated quenching parameters, and provide inaccurate information about the dark recovery.

Figure 5-5: Effect of Pulse Frequency on the Resolution of NPQ Dark Relaxation.

NPQ recovery from a dark adapted non-stressed barley leaf was re-assessed using two pulse regimes. **(a)** Reduce pulse frequency where **NPQ** recovery was measured using the Induction Curve Program (PAM 2000H Walz, Effeltrich, Germany); standard saturation pulses were applied at 0, 30, 90, 210, 510 and 1110 seconds; only the fast and (middle or slow) kinetic components of **NPQ** were resolved. Dotted line presents the missing phase. **(b)** Increase in pulse frequency where **NPQ** recovery was measured by triggering saturation pulses at 0, 30, 60, 90,120, 150, 180, 210, 300, 420, 730, and 1330 seconds; fast, middle or slow kinetic components of **NPQ** were observed. Data were obtained from plots of log (**NPQ**) as a function of relaxation time in the dark after 20 minutes exposure to actinic light (560 µmol m^{-2} s^{-1} PAR) and the best linear was fit for each kinetic component (see Material and Methods, Section 2.4.2 for experimental details).

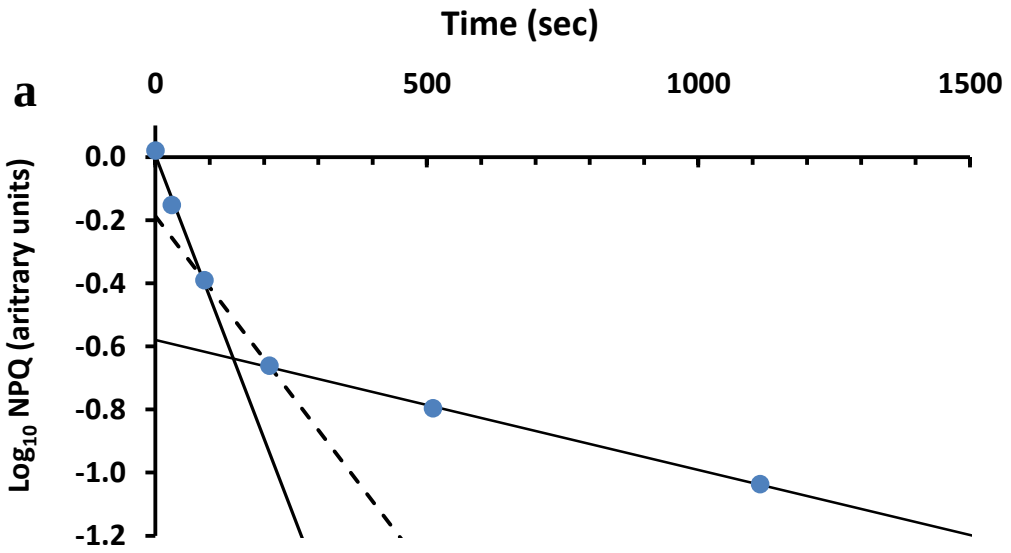
a
Time (sec)
0
500
1000
1500
0.0
-0.2
-0.4
-0.6
-0.8
-1.0
-1.2
Log10 NPQ (aritrary units)

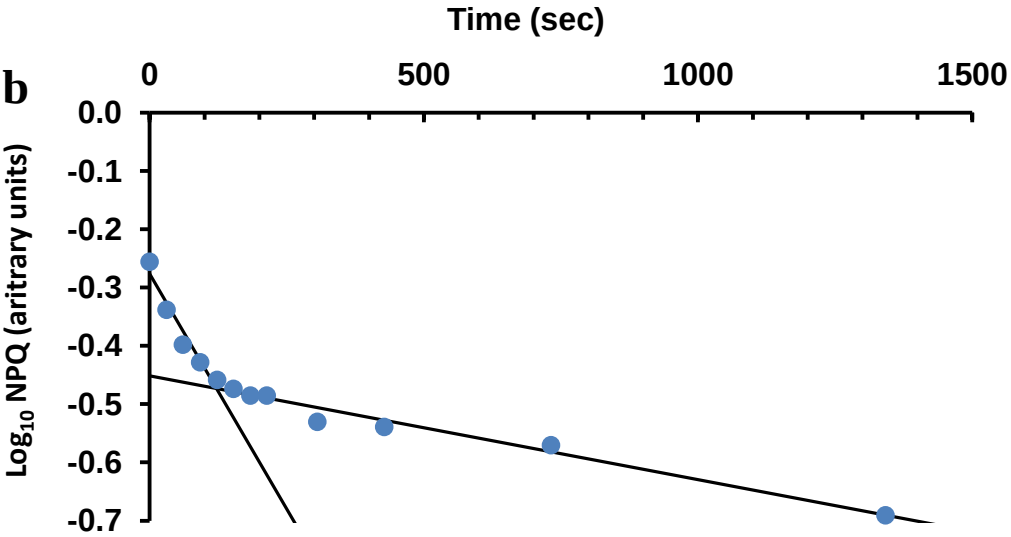
b
Time (sec)
0
500
1000
1500
0.0
-0.1
-0.2
-0.3
-0.4
-0.5
-0.6
-0.7
Log10 NPQ (aritrary units)

5.2.2 Relaxation of Thylakoid Proton Gradient by Post-illumination Fluorescence

It is clear that, at least in barley, the accepted method for estimating the dark relaxation of **NPQ**, a method that has been used widely in plants and alga (Gotoh, Kobayashi *et al.* 2010) can generate two or more phases depending on the frequency of the light pulses and their intensity. The reliability of this method to report anything of biological significance is highly questionable; therefore, its use and application should be met with caution.

Nonetheless, changing in the fluorescence signal is observed when the actinic beam is switched off and fully light adapted leaves are allowed to fully adapt in the dark without the application of saturating pulses. This dark adaption must contain information relating to the light and dark states of thylakoid, and it seems sensible, therefore, to attempt to deconvolute the signals. Further, post-illumination fluorescence has been shown to be sensitive to environmental condition such as temperature (Bosco, Lezhneva *et al.* 2004; Haldimann and Feller 2005; Wang, Duan *et al.* 2006), suggesting that post-illumination fluorescence has potential for investigating the thermal stability of the thylakoid membrane.

5.2.2.1 Effect of Heat Stress on Relaxation of Thylakoid Proton Gradient

Attempts have been made to resolve the dark relaxation kinetics of NPQ into three constituent phases by plotting the log of fluorescence signal *versus* time. No phases that fit a straight line were observed. Therefore, changes of the Chl*a* fluorescence that occur during a light-to-dark transition were monitored in barley and *Y. filimentosa* leaves immediately after and one day after recovery of subjecting a marked region of an attached leaf to 25.0, 38.0 or 40.0°C (±0.2°C) for 3 hours in the dark (Figure 5-6 & Figure 5-7). In unstressed barley and *Y. filimentosa* leaves, at the end of the light period, the actinic light source was switched off and, as expected, the modulated (dark) fluorescence signal decreased rapidly corresponding to the initial F'_0, the minimal level of fluorescence in the light. The signal then increased over a period of minutes in a multiphasic fashion before attaining a new $\boldsymbol{F_0}$, the minimal level of fluorescence in the dark. Relaxation half times were obtained by estimating the minimum and maximum values of fluorescence during the recovery and time take for half recovery. Use of the term half time does not imply a first order process.

The average relaxation half time was 45s in the control barley leaves (Table 5-1) which increased markedly to 178 and 180s after leaf exposure to 38.0 and 40.0°C (±0.2°C)

respectively (Figure 5-6 and Table 5-1). However, the relaxation half time in the *Y. filimentosa* leaves was increased slightly from 48s to 96 and 120 s after leaf exposure to 38.0 and 40.0°C (±0.2°C) respectively (Figure 5-7 and Table 5-1). After a recovery of one day at 23°C, the relaxation half time in the heat tolerant *Y. filimentosa* leaves was fully restored to the pre-heat treatment levels at both 38.0 and 40.0°C (±0.2°C) treatments. In contrast, the relaxation half time was still high in barley leaves exposed to 38 and 40°C (Table 5-1).

Non-photochemical fluorescence quenching (**NPQ**) was quite insensitive to increasing leaf temperature in barley leaves. **NPQ** values were typically 1.5 before stress and did not change significantly after increased leaf temperature. **NPQ** values for *Y. filimentosa* increased slightly but were also not significantly different from controls (25°C) immediately after heat stress at either 38 or 40°C. One day later, **NPQ** levels had returned to pre-stress levels (Table 5-1).

Figure 5-6: Chlorophyll Fluorescence Induction and Relaxation Profile of Attached Barley Leaves.

Left hand panel; attached barley leaves were dark adapted for 20 min before the measuring beam was switched on to determine the minimal level of fluorescence in the dark (***F*$_0$**). Maximum fluorescence in the dark (***F*$_m$**) was determined then by providing a 0.4 s saturating pulse of white light (9000 µmol.m^{-2}.s^{-1} PPFD). Actinic light was switched on (arrow up) 560 µmol m^{-2} s^{-1} PAR for 20 min and fluorescence emission from light adapted leaf (***F'***) was recorded; saturated pulses were given every minute to determine the maximum fluorescence in the light (***F'*$_m$**) and **NPQ**. The actinic light was then turned off (arrow down) and the dark induced 'recovery' phase recorded for 20 min. The chlorophyll fluorescence induction profiles were measured directly after exposing the leaf to 25.0, 38.0 or 40.0°C (±0.2°C) for 3 hours using a temperature controlled heating block (see Materials and Methods, Section 2.4.3). Leaves were allowed to recover at 23°C after heat stress for one day to assess recovery. Inset, the dark recovery phase. **Right hand panel;** expanded view of dark recovery phase; note, the final steady state dark F_0 often differs from the initial F_0 level (green dashed line).

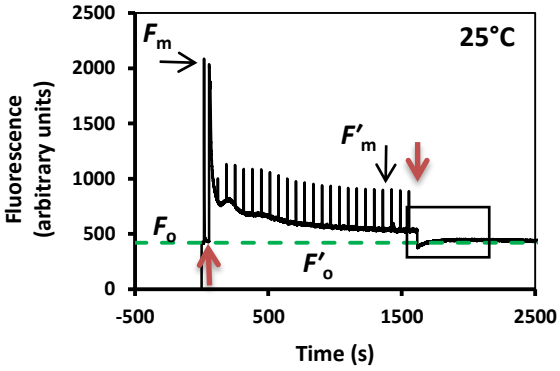
F_m
25°C
F'_m
F_o
F'_o
Fluorescence (arbitrary units)
Time (s)

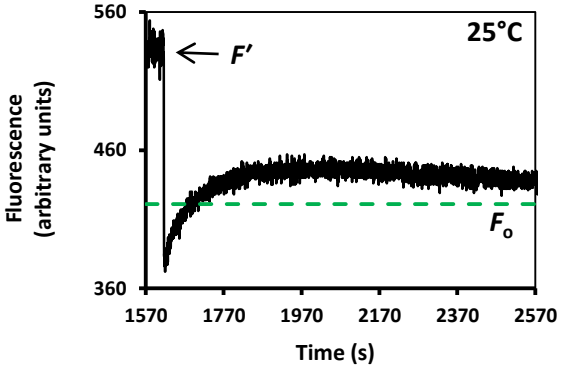
F'
25°C
F_o
Fluorescence (arbitrary units)
Time (s)

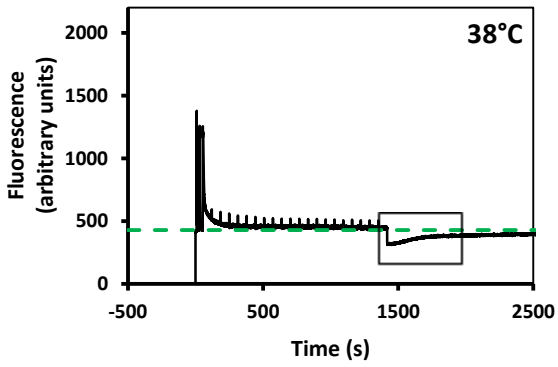
38°C
Fluorescence (arbitrary units)
Time (s)

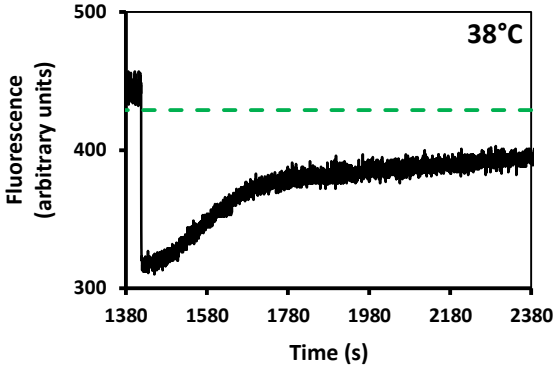
38°C
Fluorescence (arbitrary units)
Time (s)

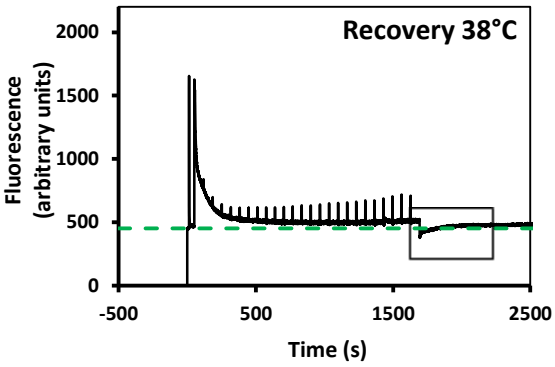
Recovery 38°C
Fluorescence (arbitrary units)
Time (s)

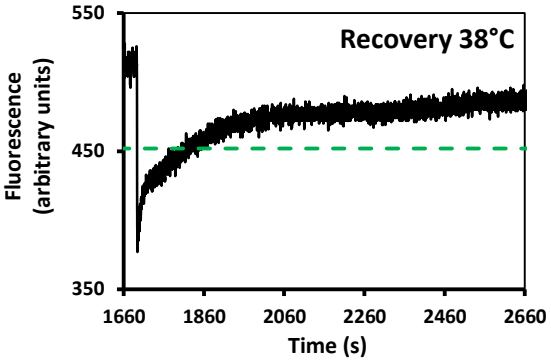
Recovery 38°C
Fluorescence (arbitrary units)
Time (s)

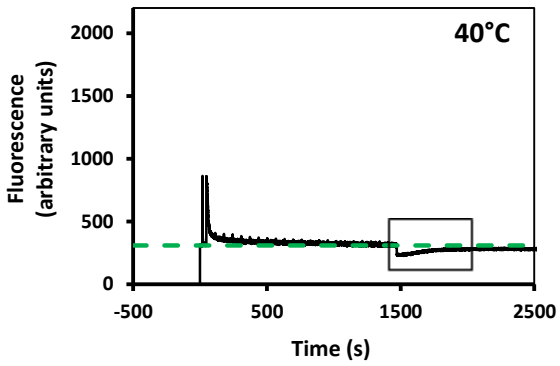
40°C
Fluorescence (arbitrary units)
Time (s)

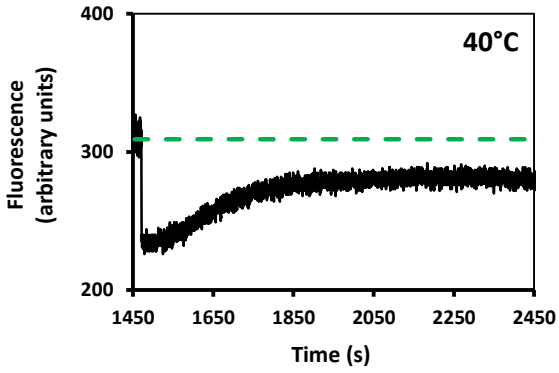
40°C
Fluorescence (arbitrary units)
Time (s)

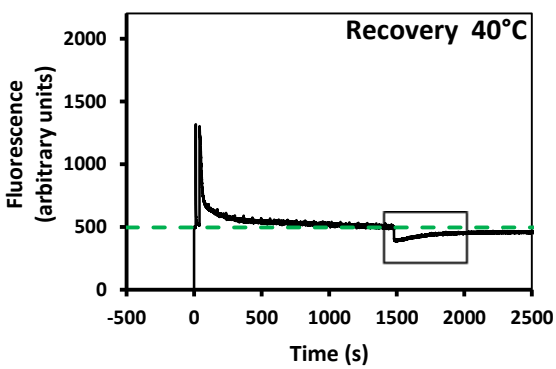
Recovery 40°C
Fluorescence (arbitrary units)
Time (s)

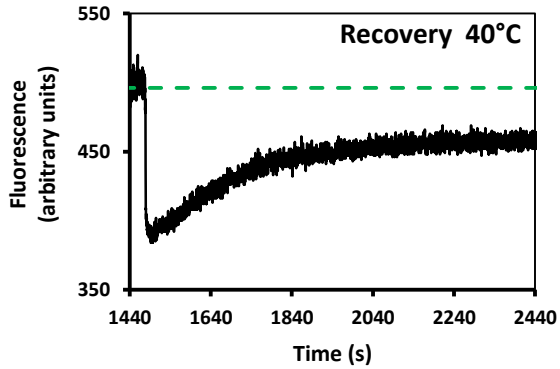
Recovery 40°C
Fluorescence (arbitrary units)
Time (s)

Figure 5-7: Chlorophyll Fluorescence Induction and Relaxation Profile of Attached *Y. filimentosa* Leaves.

Left hand panel; attached *Y. filimentosa* leaves were dark adapted for 20 min before the measuring beam was switched on to determine the minimal level of fluorescence in the dark (***F*$_0$**). Maximum fluorescence in the dark (***F*$_m$**) was determined then by providing a 0.4 s saturating pulse of white light (9000 µmol.m^{-2}.s^{-1} PPFD). The actinic light was then switched on (arrow up) 800 µmol m^{-2} s^{-1} PAR for 20 min and fluorescence emission from light adapted leaves (***F'***) was recorded; saturated pulses were given every minute to determine maximum fluorescence in the light (***F'*$_m$**) and **NPQ**. Actinic light was then turned off (arrow down) and the dark induced 'recovery' phase recorded for 20 min. The chlorophyll fluorescence induction profiles were measured directly after exposing the leaf to 25.0, 38.0 or 40.0°C (±0.2°C) for 3 hours using a temperature controlled heating block (see Materials and Methods, Section 2.4.3). Leaves were allowed to recover at 23°C after heat stress for one day to assess recovery. Inset, the dark recovery phase. **Right hand panel;** expanded view of dark recovery phase; note, the final steady state dark F_0 often differs from the initial F_0 level (green dashed line).

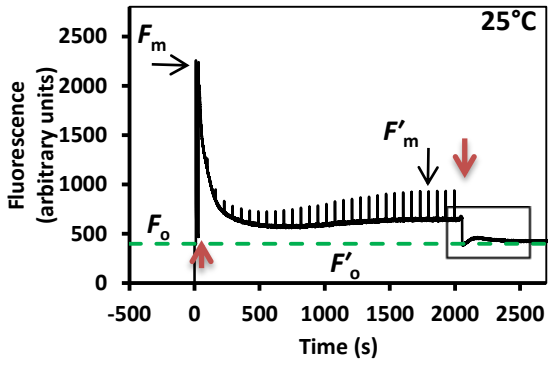
25°C
F_m
F'_m
F_o
F'_o
Fluorescence (arbitrary units)
Time (s)

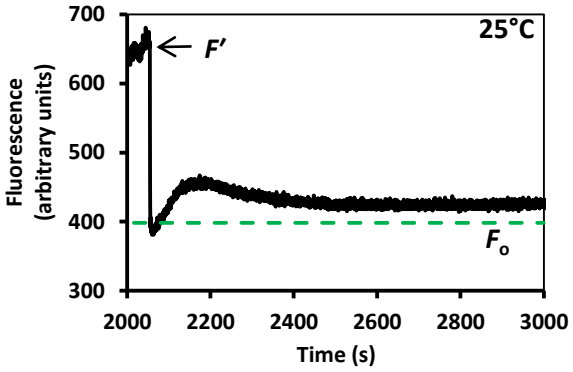
25°C
F'
F_o
Fluorescence (arbitrary units)
Time (s)

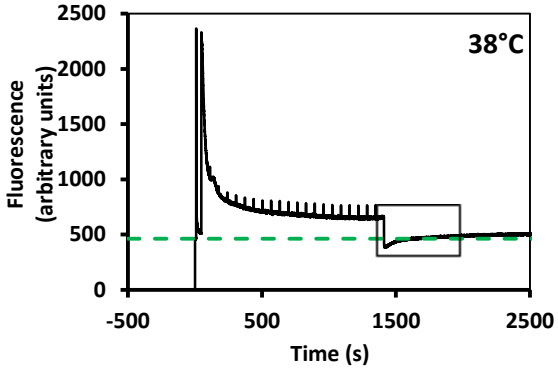
38°C
Fluorescence (arbitrary units)
Time (s)

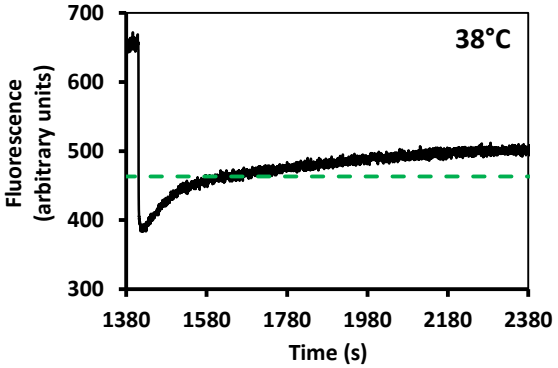
38°C
Fluorescence (arbitrary units)
Time (s)

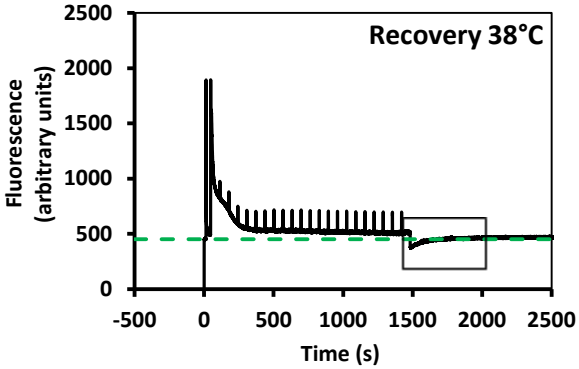
Recovery 38°C
Fluorescence (arbitrary units)
Time (s)

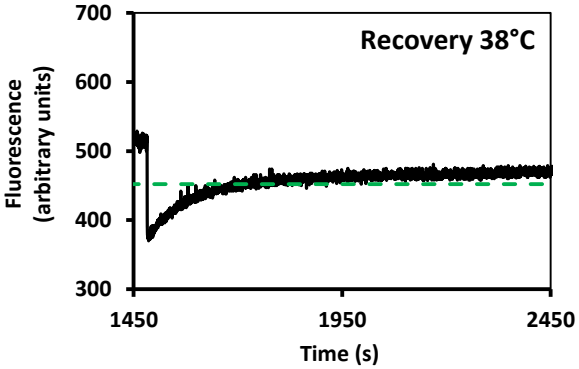
Recovery 38°C
Fluorescence (arbitrary units)
Time (s)

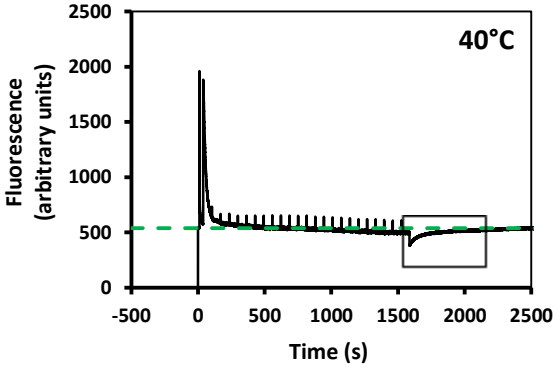
40°C
Fluorescence (arbitrary units)
Time (s)

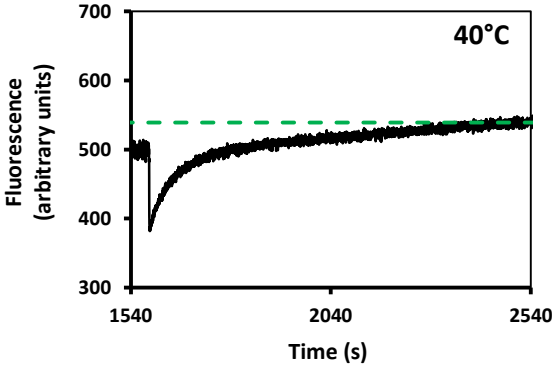
40°C
Fluorescence (arbitrary units)
Time (s)

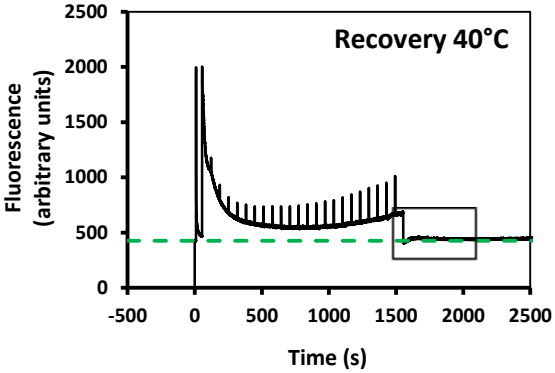
Recovery 40°C
Fluorescence (arbitrary units)
Time (s)

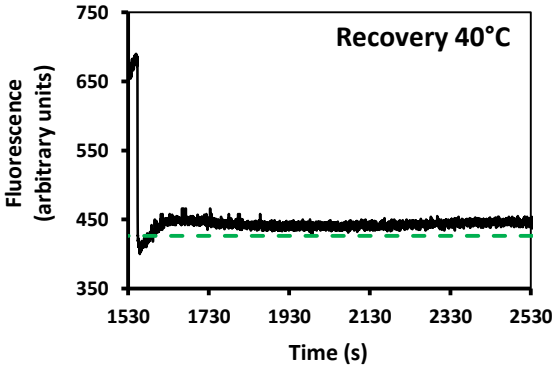
Recovery 40°C
Fluorescence (arbitrary units)
Time (s)

Table 5-1: Effects of Increasing Leaf Temperature on Fluorescence Relaxation Half Time (t½) and NPQ.

Treatment	Relaxation t ½	NPQ
Barley 25°C	**45 ± 2**	**1.5 ± 0.09**
Barley 38°C	***178 ± 20**	**1.5 ± 0.24**
Barley 38°C recovery	**68 ± 7**	**1.4 ± 0.01**
Barley 40°C	***180 ± 12**	**1.7 ± 0.20**
Barley 40°C recovery	***111 ± 41**	**1.6 ± 0.11**
***Y. filimentosa* 25°C**	**48 ± 3**	**1.7 ± 0.21**
***Y. filimentosa* 38°C**	**96 ± 18**	**2.4 ± 0.15**
***Y. filimentosa* 38°C recovery**	**55 ± 17**	**1.8 ± 0.17**
***Y. filimentosa* 40°C**	***120 ± 24**	**2.0 ± 0.06**
***Y. filimentosa* 40°C recovery**	**51 ± 7**	**1.4 ± 0.32**

Attached leaves were dark adapted for 20 min before exposure to the actinic light (560 and 800 µmol m^{-2} s^{-1} PAR for barley and *Y. filimentosa* respectively) for 20 min. Saturated pulses were given every minute to determine **NPQ**. The actinic light was then turned off and the fluorescence signal was recorded for 20 min. Relaxation half time (t½) was estimated by calculating the time required for minimum fluorescence level recorded in the dark to reach a steady state level (see Materials and Methods, Section 2.4.3). Relaxation half time (t½) and **NPQ** was measured in barley and *Y. filimentosa* immediately after and one day after exposing leaves to 25.0, 38.0 and 40.0ºC (± 0.2ºC) for 3 hours in the dark. The presented values are the Averages and Standard Errors of 4 replicates. ANOVA tests were performed using a General Linear Model. Valuse marked with asterix were significantly different at $P<0.05$. Tables for ANOVA and grouping comparison along with Figures for residual plots are presented in the Appendix (Figure A 5-4 to 5-11).

5.3 Discussion

To accurately assess tissue ATP levels, methods for the extraction of ATP had to be developed. ATP content in the chloroplasts of intact leaves was extracted using a hot deionized water (DW) method (Yang, Ho *et al.* 2002). There are several advantages of using this method over other extraction methods. Unlike the two commonly used extraction methods for ATP, (*i.e.*, Tris–borate buffer (pH 9.2) coupled with a heating process (to inactivate ATPase), and perchloric acid followed by neutralization), extraction in hot DW required only one step and thus, was more convenient. The results showed that extraction of ATP into water at 90°C was effective in inhibiting ATPase activity and resulted in a stabilization of extracted ATP levels for at least 90 min. Therefore, extraction of ATP in the hot water is a simple and reliable one-step procedure for subsequent determination of ATP by the luciferin–luciferase assay.

Metabolite profiling obtained from previous work in our laboratory (Shahwani 2011) and carried out by Dr. Stéphanie Arrivault at the Max Planck Institute of Molecular Plant Physiology, Germany, showed a significant increase in ADP levels (80%) in heat stressed barley leaves. Although caution should be applied before these changes in whole leaf ATP levels can be attributed to chloroplast ATP levels, it is a strong indicator that total leaf ATP content decreased to 80% after heat stress compared with non-stressed barley leaves. To elucidate the impact of such limitations, ATP content in the chloroplasts of intact leaves was estimated as Light-minus-Dark levels. The observed low level of ATP in dark adapted (non-stressed) leaves and the subsequent rapid increase in the light (3 min) suggests the difference between leaf ATP levels in the light and dark is largely due to the light-generated ATP in the chloroplast and this can then be used as an estimate of the chloroplast ATP in the intact leaves.

Light-generated ATP in the chloroplasts of plants exposed to higher leaf temperatures showed a significant decline compared to those exposed to optimal temperatures. The significantly lower ATP levels observed with heat stress was in agreement with the observations of others (Loka and Oosterhuis 2010), who reported a reduction in the ATP levels in cotton as a result of high night temperatures. However, the results are in contrast with other reports that suggest ATP levels are not affected by heat stress (Schrader, Wise *et al.* 2004). At any moment, ATP content in the chloroplasts is the balance between production and consumption rates. If ATP is not consumed by the Calvin cycle, then ATP content would be expected to rise. Decreased ATP however, indicates that ATP synthesis may be impaired, possibly by direct effect of heat stress on the ATP synthase although

increased ATP consumption cannot be excluded. It can be concluded that heat stress may inhibit photosynthesis through decreased ATP supply, establishing ATP content as a potentially limiting factor of photosynthesis at high leaf temperatures.

It is clear from Figure 5-5 that analysis of the dark relaxation kinetics of **NPQ** by applying saturated pulses, as described in the WALZ MINI-PAM user manual, is an inappropriate method. The results show how small changes in methodology can have a large effect on the number of phases observed and the calculated quenching parameters. By altering the pulse frequency, **NPQ** can be resolved into two or three phases and this is clearly unsatisfactory. The reason for the absence of one phase was due to standard procedures used in the Induction Curve Program of the MINI-PAM which is dependent on the assumption that the fast phase (***q*E**) occurs with a half-time of 10-30s and the middle (***q*T**) phase with a t½ of 60-180s whilst the slow phase (***q*I**) has a t½ of 300-900s. Although the photoinhibitory processes (***q*I**) can be characterised due to its slow relaxation time, *q*T (the middle phase) can be confounded with qI and qE causing unreliable measurement due to overlap with time. The repetitive pulses applied during dark recovery might also affect the relaxation of **NPQ**, by preventing a complete relaxation of **NPQ** and providing inaccurate information about dark recovery. These finding suggested that resolving dark relaxations of **NPQ** into three components as originally proposed by Walters and Horton (1991) is an inaccurate method and probably reflects artefact.

Monitoring the changes of the chlorophyll fluorescence signal during a light-dark transition (Post-illumination Fluorescence) following heat stress has been employed to assess the energization of the thylakoid membrane and thus, to estimate its thermal stability (Bosco, Lezhneva *et al.* 2004; Haldimann and Feller 2005). This assumption is consistent with the finding that the kinetics of fluorescence relaxation is temperature sensitive (Bosco, Lezhneva *et al.* 2004). These workers observed that at a low temperature (0 °C) where the thylakoid membrane is less leaky to protons, fluorescence relaxation was severely slowed down while increasing the temperature to 35°C accelerated the relaxation process. Therefore, this technique was used to analyze the fluorescence relaxation kinetics of the thylakoid membrane after heat stress.

In barley, heat stress severely slowed down the fluorescence relaxation resulting in a considerable increase in half life time (about 4 fold) which was not recovered. This might be explained by the significant proton accumulation indicating that ATP synthase activity is suppressed in barley leaves after heat stress (*i.e.*, chloroplast ATP was reduced to >75% of control levels after exposure to 38.0°C). This finding is in agreement with the observed decrease of linear electron rates (see section 5.1.3). Further evidence supporting this view

has been reported by (Rott, Martins *et al.* 2011) who showed the average relaxation half-time was increased by 2.5 fold in antisense lines of tobacco where ATP synthase activity was reduced to <50% of wild-type levels by antisense directed depletion of the nuclear encoded γ-subunit (AtpC). This was measured by the fast dark relaxation kinetics of the maximum electrochromic absorption shift (ECS) at 515nm which represents a measure of the light-induced proton motive force (pmf) across the thylakoid membrane.

It is well established that the development of a full pmf across the thylakoid membrane occurs within 3-5 minutes of illumination and that **NPQ** follows a similar time course. It is tempting, therefore, to conclude that **NPQ** reflects the development of the transthylakoid pmf as postulated in the literature (Horton and Hague 1988; Baker 2008). In barley leaves, **NPQ** was not different after heat stress. This observation suggested that the proton gradient is maintained under heat stress and is sufficient to provide ATP for RuBP regeneration. A similar conclusion on the thermal stability of the transthylakoid pH gradient under heat stress has been reported (Crafts-Brandner and Salvucci 2002; Salvucci and Crafts-Brandner 2004b).

The magnitude of the pmf in the light is dependent upon the electron transport rate which generates the proton gradient, and the rate by which it is dissipated (leakage and ATP synthesis and subsequent consumption). If the early phase of dark relaxation (0-200s) reflects the dissipation of the pmf in the dark, leakiness would be expected to decrease the t½. The opposite is observed, suggesting it does not cause thylakoid membranes to become leaky. A faster dark relaxation (low t½) is observed in control leaves where ATP consumption by a range of active metabolic processes should quickly dissipate the pmf. In contrast, the slower dark relaxation kinetics observed in leaves at 38.0°C and 40.0°C suggest that ATP demand had fallen in these tissues resulting in the maintenance of the pmf. Alternatively, the ATP synthase may have been damaged so that ATP generation was impaired

In *Y. filimentosa*, a heat tolerant plant, increased leaf temperatures to 40.0°C for three hours results in an increased relaxation half life time (doubling) but this fully recovered after one day. In contrast to barley, this might be a protective mechanism rather than ATP synthase activity inhibition. The evidence for this suggestion comes from the response of *Y. filimentosa* leaves to heat stress. Stomata tend to close after heat stress for about 20 minutes which results in a dramatic suppression of CO_2 assimilation. Thus, ATP was not consumed by the Calvin cycle causing increased half-life time for fluorescence relaxation. Furthermore, relaxation half-life time returned to the pre-heat level after one day recovery which correlated well with the full recovery of CO_2 assimilation.

In conclusion, taken together these results suggested that thylakoid membranes of barley leaves were not leaky for protons after heat stress and the proton gradient was available for ATP synthase; but a high rate of photosynthesis was not maintained, possibly because of limitations in the activity of ATP synthase.

6 Chapter 6: General Discussion

The suppression of light-saturated CO_2 assimilation rates (A_{sat}) might arise from thermal damage to the processes involving light capture to CO_2 fixation (Figure 4-1). These sites include: (1) light capture and energy transduction in the photosystem: (2) photosynthetic electron transport rates (*in vitro* ETR) and generation of proton gradient across the thylakoid membrane: (3) the synthesis of ATP and NADPH: (4) the kinetic properties of the C3 cycle enzymes, in particular, RuBisCO Activase: (5) the diffusion of CO_2 from the intracellular leaf space to the chloroplast controlled by mesophyll conductance (**g_m**). The main objective of this study was to assess the effect of heat stress on these potential sites of thermal damage and identify the most sensitive sites.

The Earth's climate is predicted to warm by an average of 1.4 to more than 5° C per century by 2100 as a result of increased greenhouse gases in the atmosphere (IPCC 2001). In addition, there will also be increases in the frequency, duration, and severity of periods with exceptionally high temperatures (*i.e.*, heat waves) (Haldimann and Feller 2004). Thus, in the future, high leaf temperatures will likely reduce plant growth, development, and limit crop yields with estimates of up to a 17 % decrease in yield per 1.0° C increase in average growing season temperature (Lobell and Asner 2003). Enhancing photosynthesis by genetic manipulation is a promising approach to increase crop yields under heat stress (Parry, Reynolds *et al.* 2011; Evans 2013; Parry, Andralojc *et al.* 2013). However, what are the potential targets for enhancing leaf photosynthesis? In fact, there is no single answer, since the limiting step of photosynthesis under high temperature remains unclear. Therefore, the effect of increasing leaf temperature on photosynthesis was re-investigated via comparisons between C3 and C4 crop plants from contrasting thermal environments to establish if there is a genetic basis for thermotolerance, and to identify the potential thermal target limiting photosynthesis as this might provide opportunities for achieving faster improvements in crop production.

In well-hydrated plants, transpirational cooling prevents leaves from experiencing heat stress and leaf temperature (T_{leaf}), may be 10–15 °C lower than ambient temperature (Hasanuzzaman, Nahar *et al.* 2013). Most of the published work on the effect of heat stress on plants has reported experiments where T_{air} not T_{leaf} was controlled (Salvucci and Crafts-Brandner 2004b; Sinsawat, Leipner *et al.* 2004; Haldimann and Feller 2005), and as a result, precise conclusions are difficult to be drawn. Therefore, the experimental approach used in this study to impose heat stress was designed to control leaf temperature very precisely (± 0.2°C; see Martials and Methods, Section 2.2).

Inhibition of CO_2 assimilation rates in crop plants when leaf temperature increased above optimum temperatures has been reported (Crafts-Brandner and Salvucci 2002; Sinsawat, Leipner *et al.* 2004; Wise, Olson *et al.* 2004). The limiting step of photosynthesis causing this inhibition at high temperature was suggested to be different depending on plant species (*e.g.*, heat-sensitive *vs* heat-tolerant) (Yamori, Hikosaka *et al.* 2014). The limiting step controlling the response of the photosynthetic rate remains unclear, but several hypotheses have been proposed. The leading hypotheses for photosynthetic limitation above the photosynthetic optimum temperature are the heat lability of RuBisCO Activase and a limitation in photosynthetic electron transport (Salvucci and Crafts-Brandner 2004a; Wise, Olson *et al.* 2004; Cen and Sage 2005; Kim and Portis 2005; Sharkey 2005; Makino and Sage 2007; Sage and Kubien 2007).

The results presented in this study showed that in both C3 and C4 plants, $\mathbf{A_{sat}}$ was suppressed dramatically by >85% in all lines when leaf temperature increased above 36.0 °C regardless of their origins (temperate or sub-tropical). The irreversible suppression of $\mathbf{A_{sat}}$ at the critical leaf temperature 38.0 °C was not attributable to efficiency of PSII or stomata closure as transpiration rates were maintained. The similarity of C3 and C4 in response to heat stress suggests that the principal limitation process on photosynthesis might be identical for plants demonstrating both types of photosynthesis. In contrast to maize and barley, the thermal stability of photosynthesis in *Y. filimentosa*, an obligate C3 plant, with rising leaf temperature up to 45°C was confirmed by the lack of a temperature effect on the light-saturated CO_2 assimilation rates ($\mathbf{A_{sat}}$) and the maximum quantum efficiency of photosystem II ($\boldsymbol{F_v/F_m}$). Indeed, the high temperature tolerance of *Y. filimentosa* is remarkable as all C3 and C4 species examined in this study were unable to survive at this extreme temperature. It seems that although *Y. filimentosa* performs C3 photosynthesis, the processes that are most affected by heat stress in C3 plants were not sensitive or were protected by unknown endogenous mechanisms.

One of the interesting observations from gas-exchange measurements in *Y. filimentosa* is the rapid response of stomata to high leaf temperatures. In contrast to stomata responses at 38 and 40°C, stomata tend to open during and immediately after stress to the same pre-stress level when leaf temperatures were increased to 45°C, and $\mathbf{g_s}$ was increased further after one hour of recovery. It seems that when leaf temperature increased above 40°C, a signaling mechanism was activated that causes stomatal opening and consequently increasing transpiration rate. In fact, in arid areas, heat stress is often combined with water stress driven by increased evaporative cooling and transpiration as VPD increases (Lobell, Sibley *et al.* 2012). In order for plants to use water efficiently, stomata must balance the

demand for CO_2 uptake with transpirational water loss (Wong, Cowan *et al.* 1979; Lawson, Caemmerer *et al.* 2011). The *Y. filimentosa* plants used in this study however, were well watered which suggests that preventing heat damage is more important than conserving water when leaf temperature exceeds 40°C. It can be concluded that stomatal responses in *Y. filimentosa* are regulated by two different signaling mechanisms. When leaf temperature increased to below a threshold level, stomata tended to close to conserve water but when leaf temperature exceeded this threshold level ($>$ 40°C), stomata opened to prevent heat damage to the leaf. Stomatal regulation by temperature signalling is novel and has not been studied in depth before.

Heat stress has been reported to induce dissociation and aggregation of the Light Harvesting Complexes (Srivastava, Guissé *et al.* 1997; Tang, Wen *et al.* 2007). These changes can be easily detected by changes in chlorophyll fluorescence excitation spectra. No evidence was found to support the possibility that suppression of $\mathbf{A_{sat}}$ induced by increasing leaf temperature to 38.0°C for three hours in barley was attributable to the effect of heat stress on the Light Harvesting Complexes (LHCs) and transduction of excitation energy for electron transport.

Measurements of *in vivo* electron transport capacity as a function of temperature using pulse-modulated fluorescence are often correlated with the capacity of CO_2 assimilation (Baker 2008). Therefore, direct assessment of electron transport capacity *in vitro* was conducted to investigate electron transport limitations at high temperatures. Comparison between the results of ETR measurements *in vivo* and *in vitro* showed that the severe inhibition observed in *in vivo* ETR was not reflected when ETR was uncoupled from the C3 cycle. This indicates that the major limitation for CO_2 assimilation may be located beyond the electron transport chain possibly by the activity of the C3 cycle enzymes (Price, Evans *et al.* 1995; Muschak, Willmitzer *et al.* 1999; Paul, Driscoll *et al.* 2000) or the capacity of the ATPase synthase (Farquhar, Caemmerer *et al.* 1980).

The elegance of the RuBisCO Activase heat lability hypothesis led to its rapid and widespread acceptance, and efforts are now underway to improve heat tolerance of photosynthesis by enhancing the thermal tolerance of Activase (Spreitzer and Salvucci 2002; Wu, Ding *et al.* 2006; Kurek, Chang *et al.* 2007; Parry, Andralojc *et al.* 2013). Our results from metabolite profiling of C3 cycle intermediates in barley immediately after heat stress were initially in agreement with this view, as carbon flow between Ri5P and 3-PGA and through RuBisCO was compromised.

The findings reported in this study however, suggest that the decline in $\mathbf{A_{sat}}$ with increasing temperature cannot always be explained by the heat lability of RuBisCO Activase, at least in barley. Three lines of evidence support this conclusion:

- The first one is the lack of any significant thermal inhibition for *in vivo* RuBisCO activity after heat stressing barley leaves up to 40.0°C, while the corresponding CO_2 assimilation rate ($\mathbf{A_{sat}}$) and *in vivo* ETR for the same leaves was irreversibly suppressed. In addition, no heat treatment had a significant effect on activation state of RuBisCO which is considered as an indirect estimation of RuBisCO Activase activity.

- The second line of evidence is the finding that in barley, RuBisCO Activase may not be required to activate RuBisCO in either control or stressed plants as fully activated RuBisCO from light adapted leaves was extracted using a buffer lacking the activating factors CO_2 and $MgCl_2$. This interesting observation poses a very important question: what are the roles of RuBisCO Activase if it is not implicated in the re-activation of RuBisCO in barley? Recent evidence has shown that RuBisCO more strongly limits photosynthesis below the thermal optimum (Makino and Sage 2007). Further experiments therefore, are needed to assess the role of RuBisCO Activase activity at low temperature in barley plants.

- The third line of evidence comes from the assumption that if RuBisCO activity was the only factor limiting whole leaf photosynthesis following heat stress, then it should be possible to remove that limitation by increasing the supply of substrate CO_2 to the enzyme. The same argument can be used for limitations of mesophyll conductance ($\mathbf{g_m}$). If the limitation is not reversed by high CO_2, then the observed decline in $\mathbf{A_{sat}}$ cannot be attributable to low mesophyll conductance. The results from Figure 4-22 showed that increasing carbon dioxide does not remove or alleviate the inhibition compared with control plants. This finding supports the view that RuBisCO activity and low CO_2 in the chloroplast were not the limiting step and that inhibition lies (at least partially) in other processes related to the regeneration of RuBP.

The composition of standard extraction buffer used for determining *in vivo* RuBisCO activity affects the results obtained. Generally, extraction of RuBisCO from dicots in buffers containing 1 mM EDTA and lacking the activating factors of CO_2 and $MgCl_2$ leads to the isolation of inactive RuBisCO (Carmo-Silva and Salvucci 2011). Conversely, the results from this study found that RuBisCO extracted from light adapted leaves was

unexpectedly nearly fully activated while RuBisCO extracted from dark adapted leaves was inactive. These differences suggest that the high activities of RuBisCO in the light from control and stressed barley leaves were not due to the re-activation during the extraction procedure, but to *in vivo* activation in the light. The most important role for RuBisCO Activase is the removal of the inhibitors (RuBP and CA1P) from the active site of RuBisCO. It is widely accepted that at night, the sugar-phosphate 2-Carboxyarabinitol 1-Phosphate (CAlP) binds to RuBisCO causing inhibition of enzyme activity (Moore and Seemann 1994), and subsequently the inhibitor is removed from RuBisCO in the light by Activase. The results obtained in this study suggested that in the dark, inhibition caused by CAlP or other pentose phosphate sugars might not occur in barley as found in some species (Vu, Allen *et al.* 1984). If sugar phosphate inhibitors do bind to RuBisCO in the dark, they can be removed by including of 5 mM Mg^{2+} in the extraction buffer (not too dissimilar from endogenous levels) which contrasts widely with observations in many species where RuBisCO extracted from dark leaves was not activated even after incubation with saturating CO_2 and Mg^{2+}(Vu, Allen *et al.* 1984). This difference might be an indicator of differences in the regulatory properties of RuBisCO from barley. It is important to take into account the effects of the inclusion of Mg^{2+} in the extraction buffer in studies of RuBisCO activity and its dark/light regulation as it can lead to false conclusions. For example, (Usuda 1985) reported relatively high RuBisCO activity in the dark in maize leaves which was attributable to an unknown mechanism. Obviously, inclusion of high levels of Mg^{2+} in the extraction buffer could have resulted in a re-activation of RuBisCO during isolation. It can be concluded that the standard isolation buffer that has been routinely used for two decades (Milos, Bloom *et al.* 1985; Loza-Tavera, Martínez-Barajas *et al.* 1990) partially activates dark adapted barley RuBisCO and may not, therefore, faithfully reflect *in vivo* activity of RuBisCO.

The possibility that $\mathbf{A_{sat}}$ inhibition is attributable to the RuBP synthesis becoming limited by impairment of the activity of Ri5PI and PRK was excluded because at the highest temperature (40°C), the rate of carbon flow from Ri5P to 3-PGA through Ri5PI and PRK was six fold greater than the highest rates of carbon flow from RuBP to 3-PGA through fully activated RuBisCO. It is reasonable to assume that if high leaf temperature inhibits the C3 cycle by decreasing the activities of Ri5P isomerase and/or phosphoribulokinase (PRK), then RuBP content will decrease but ATP levels will remain high as reported in transgenic tobacco with much reduced phosphoribulokinase activity (Paul, Knight *et al.* 1995); but this was not observed in the heat stressed barley leaves investigated in the present study.

A possible explanation for the difference between the results of RuBisCO activity presented in this study and previous studies where RuBisCO Activase has been implicated as the limiting factor for photosynthesis at high leaf temperature (Law and Crafts-Brandner 1999; Crafts-Brandner and Salvucci 2000; 2002), might be related to the fact that most of these studies have measured RuBisCO activity during heat stress, while in this study the activity of RuBisCO was determined after 20 minutes from removal of stress. Rising leaf temperatures lead to significant changes in photosynthetic metabolism but these changes do not often cause permanent damage as they are fully and rapidly reversible (Sharkey and Zhang 2010). In fact, heat stress causes changes in photosynthesis rates which at first are reversible when the leaf is returned to pre-stress temperature but, with increasing the temperature or duration of the heat stress, the damage may become ultimately irreversible. The changes occurring during heat stress may reflect tolerance mechanisms that cope with stress and not necessarily a cause of thermal damage. Actually this assumption is in agreement with the hypothesis that deactivation of RuBisCO is a protective mechanism rather than a cause of limitation (Sharkey, Badger *et al.* 2001). Therefore, it is essential to separate the response by heat damage from the response to cope with stress. Knowing which of the photosynthetic processes do or do not recover after heat stress when the rate of photosynthesis is irreversibly inhibited will provide insights into which of these processes are the most sensitive to heat stress and could be considered as the rate limiting step. Thus, the approach used in this study was to assess the photosynthetic components after recovery from critical temperatures.

Few studies have focused on the effect of heat stress on the inhibition and recovery of RuBisCO activity and link that with direct measurements of photosynthesis rate. One of these studies (Feller, Crafts-Brandner *et al.* 1998) has shown in both cotton and wheat leaves, the inhibition of RuBisCO activation was fully reversible at temperatures below 40°C, but irreversible above 40°C. Although RuBisCO activation was recovered from heat stress up to 40°C, no measurement was conducted on CO_2 assimilation rate to find if the inhibition and recovery of RuBisCO activation correlated with photosynthesis rates. In fact, they examined the hypothesis that the inhibition of RuBisCO activation induced by heat stress is caused by changes in the structural properties of RuBisCO Activase. Another study, conducted by (Crafts-Brandner and Law 2000), has shown photosynthesis rates and RuBisCO activation in cotton leaves were inhibited after 30 minutes of heat stress at 40.0 and 42.5°C, and both recovered after 30 minutes at 28.0°C. At very high leaf temperatures of 45°C, however, RuBisCO activation recovered to a greater extent than photosynthesis rates (11% and 5% of initial activity respectively). These findings have been interpreted as

RuBisCO activation being the site of photosynthesis inhibition due to close correlation between the inhibition and recovery of RuBisCO activities and photosynthesis rates. Also, at extreme high temperature where photosynthesis is irreversibly inhibited and RuBisCO activation is not, it was suggested that heat stress inhibited photosynthesis as a result of multiple damage to other photosynthetic components. Although these authors showed that RuBisCO activation was recovered after 30 minutes of heat stress at extremely high temperature while photosynthesis was not, they still conclude RuBisCO activation is the site of thermal damage at this high temperature (Crafts-Brandner and Law 2000). Similar results were reported for pea plants treated at 40°C as RuBisCO activation state and photosynthesis rate almost completely fully recovered within 30 min at 25°C (Haldimann and Feller 2005). In contrast to these reports, the results of this study showed clearly that when the photosynthesis rate was severely inhibited after heat stress for 3 hours at 40°C, the activity of RuBisCO was not affected, indicating that the irreversible inhibition of photosynthesis was not caused by a decline in RuBisCO activity. In fact, unlike most previous work (Crafts-Brandner and Law 2000; Haldimann and Feller 2005) where the photosynthesis rate was measured in a set of plants and the activity of RuBisCO in another set, the experimental approach used in this study allowed for measuring photosynthesis rate and activity of RuBisCO from the same leaf, thus providing a more integrated evaluation of the correlation between the inhibition and recovery of RuBisCO activity and photosynthesis rate.

Based on the interaction between the findings from this study and our understanding of the results from the previous cited work (Crafts-Brandner and Law 2000; Crafts-Brandner and Salvucci 2002; Salvucci and Crafts-Brandner 2004a), it can be concluded that RuBisCO activation by RuBisCO Activase might decline during heat stress as a tolerance mechanism but rapidly restore when the stress is removed. However, as mentioned before, RuBisCO Activase may not be required for RuBisCO activation in barley and RuBisCO activity assayed with saturating substrate concentration (CO_2 and RuBP) was not affected by heat stress. It can be concluded that the irreversible inhibition of CO_2 assimilation rate observed after 20 minutes of recovery from heat stress is due to decline in the substrates of RuBisCO not the activity of RuBisCO itself.

In support of this view, (Yamori and von Caemmerer 2009) have argued that although the RuBisCO activation state decreased at high temperature and limited the CO_2 assimilation rate in tobacco, this inhibition was not strongly influenced by RuBisCO Activase content, suggesting that other processes may also modulate RuBisCO activation. The levels of different regulatory metabolites (*e.g.* ATP and NADPH) and ionic concentration in the

stroma (*e.g.* Mg^{2+}) can be changed by photosynthetic electron transport and thylakoid membrane leakiness. Kim and Portis (2006) showed that low concentration of stromal Mg^{2+} caused a reduction in the RuBisCO activation state at high temperature. High temperature was reported to increase leakage of protons across the thylakoid membrane (Bukhov, Wiese *et al.* 1999b; Zhang and Sharkey 2009) leading to lower stromal pH and Mg^{2+} concentration. Therefore, changes in stromal Mg^{2+} concentration could be a possible factor in the reduction of the RuBisCO activation state at high temperature. The effects of high temperature on stromal pH and Mg^{2+} have not been reported and they may be difficult to determine *in planta* (Kim and Portis Jr 2006). The results of this study suggested that in barley leaves, stromal Mg^{2+} levels were sufficiently high even after heat stress as evidenced by extraction of activated RuBisCO from stressed and non-stressed light adapted leaves using a buffer lacking the activating factors CO_2 and $MgCl_2$. This conclusion is further supported by chlorophyll fluorescence measurements which showed that in barley leaves, the thylakoid membrane was not leaky and the proton gradient was maintained under heat stress.

The ATP/ADP ratio in the chloroplast has also been implicated in the regulation of RuBisCO Activase activity (Robinson and Portis Jr 1989; Zhang and Portis 1999; Zhang, Kallis *et al.* 2002). As the electron transport capacity becomes limiting at high leaf temperatures, ATP/ADP ratios in chloroplast decline, causing a down-regulation of Activase activity, and in sequence, a reduction in the RuBisCO activation state (Zhang and Portis 1999; Zhang, Kallis *et al.* 2002; Sage and Kubien 2007). Although this possibility has been demonstrated and may explain the decrease in the CO_2 assimilation rate, most of the studies supported the view that the CO_2 assimilation rate was limited by RuBisCO activity at high leaf temperatures (Crafts-Brandner and Salvucci 2000; 2002; Salvucci and Crafts-Brandner 2004b) and ATP pools were maintained due to the widely held belief that heat stress activates cyclic electron flow providing an additional mechanism to maintain high ATP levels (Weis 1981; Bukhov, Wiese *et al.* 1999b). Based on the results of this study, estimation of ATP content in the chloroplast showed that the level decreased with increasing leaf temperature indicating that heat stress may inhibit ATP synthesis and this subsequently affects the Calvin cycle. If heat stress inhibits Calvin cycle activity, ATP will not be consumed and levels will be expected to increase, as reported in transgenic tobacco with reduced phosphoribulokinase activity (Paul, Knight *et al.* 1995). In contrast, if the capacity for ATP synthesis is limiting, the level of ATP will decrease. Furthermore, high temperatures were reported to increase respiration rates (Reddy, Baker *et al.* 1991; Bednarz and van Iersel 2001) which caused a drain in the leaf ATP pools (Loka and Oosterhuis

2010). However this possibility can be excluded as dark respiration rates in barley were relatively unaffected by heat stress (data not shown). Consistent with this finding, analysis of dark relaxation using modulated fluorescence in stressed barley leaves clearly showed no evidence of thylakoid membrane leakiness, but a significant increase in the relaxation half time (t½) suggests a decrease in proton conductance through the ATP synthase. These observations strongly indicate that the proton gradient was available but did not lead to the maintenance of a high rate of photosynthesis, possibly because of limitations in the activity of the ATP synthase.

If the supply of ATP is the principle limitation for photosynthesis at high temperature, how do heat tolerant plants like *Y. filimentosa*, prevent the thermal inhibition of ATP synthesis? *Y. filimentosa* shows a brief inhibition in the CO_2 assimilation rate due to stomatal closure after heat stress presumably as a protective mechanism. Thus, the synthesis of ATP is regulated to match the activity of the C3 cycle. At 40°C, the slight increase in fluorescence dark relaxation may reflect this protective mechanism as full recovery of $\mathbf{A_{sat}}$ from heat stress correlated well with the dark relaxation. In addition to stomatal regulation by temperature, heat-shock proteins (HSPs) almost certainly play a significant role in preventing high temperature damage to *Y. filimentosa* as reported in some Agaves plants (LujÁN, LledÍAs *et al.* 2009).

Taken together all the findings presented in this study, suggest that low ATP supply for photosynthetic carbon metabolism might be the primary limitation to photosynthesis at high temperature. Insufficient levels of ATP in the chloroplast would decrease the ability of the C3 cycle to generate RuBP by PRK. Carbon flow through RuBisCO would then be compromised due to limitations in RuBP availability. The assays for *in vitro* activity of RuBisCO are conducted with saturating substrate concentrations (CO_2 and RuBP), and thus the *in vivo* suppression of ATP and RuBP supply would not be observed. In fact, at optimum leaf temperatures, it is reported that a reduction in ATP synthesis by shading leads to reduced RuBisCO Activase activity, resulting in a decrease in carbon flux through RuBisCO (Portis Jr 2003). Low ATP levels in the chloroplast caused by shading or heat stress could also inhibit PRK-dependent synthesis of RuBP and thus also reduce carbon flux through RuBisCO.

In conclusion, there is controversy over the thermal site of injury and which process decreases the photosynthetic assimilation of CO_2. The results of this study show that this inhibition was not correlated with activity of RuBisCO but correlated well with the decreased amounts of chloroplast ATP levels. Furthermore, the thermal stability of photosynthesis in heat-tolerant plants like agaves possibly indicates that these plants might

display distinct strategies to cope with heat stress or have unique enzyme properties to support their photosynthetic activity at elevated leaf temperatures. The efforts to enhance photosynthesis in crop plants by genetic manipulation in response to increased temperature and desiccation levels should perhaps focus more on these plants.

6.1 Conclusion

- If T_{leaf} rises to 38^0C or above for three hours, CO_2 assimilation rates are similarly inhibited in C3 and C4 crops regardless of their origin. Three hour periods almost completely and irreversibly suppress $\mathbf{A_{sat}}$.
- Some *Agave* plants such as *Y. filimentosa* can withstand prolonged periods with T_{leaf} up to 45^0C. The mechanisms of thermotolerance are unclear at present.
- Stomatal responses in *Y. filimentosa* is regulated by two different signalling mechanisms, when $T_{leaf} < 40^0$C, stomata closed to conserve water but $T_{leaf} > 40$°C, stomata opened to prevent heat damage.
- Thermal suppression of $\mathbf{A_{sat}}$ in crop plants is not attributable to PSII photochemistry or $\mathbf{g_s}$.
- Comparison between *in vivo* and *in vitro* ETR suggested that the major limitation for CO_2 assimilation may be located downstream of photosynthetic electron transport.
- Metabolite profiling suggests carbon flux between Ri5P and 3-PGA is compromised, but contrary to reports in the literature, it is not attributable to the endogenous activation state of RuBisCO.
- RuBisCO is autoactivated in barely leaves by light, a process that is not heat sensitive, and may not require the action of RuBisCO Activase.
- The extraction buffer routinely used for determining *in vivo* RuBisCO activity partially activates RuBisCO from dark adapted leaves and therefore, affects the results obtained.
- The observed inhibition in $\mathbf{A_{sat}}$ was not caused by the effect of heat stress on the activities of the C3 cycle enzymes Ri5P isomerase and/or PRK or low levels of CO_2 in the chloroplast.
- Low stromal ATP levels are probably the primary limitation for $\mathbf{A_{sat}}$, leading to low RuBP supply and as a result compromise RuBisCO activity.

6.2 Directions for the future

Although low ATP levels in chloroplasts of stressed plants are unlikely to result from increased ATP consumption, this possibility cannot be excluded and needs to be addressed. ATP levels measured in this study in the light and dark are reporting the steady state values resulting from the production and consumption rates. More information about the effect of high leaf temperature on the production and consumption rate can be obtained by monitoring the changes in ATP levels that occur during light-to-dark transitions in control and heat stressed leaves. There are numerous options for monitoring ATP synthesis in chloroplasts using isolated thylakoid membranes, intact chloroplasts, and even whole leaves. One of the direct *in vitro* measurements of ATP that can be used is the incorporation of ^{32}P into ATP which has the advantage of being able to distinguish newly synthesized from total ATP in the sample. Also, ATP synthesis can be measured *in vitro* by monitoring the changes in pH due to ATP using sensitive pH electrode or appropriate pH-sensitive dye, and it may be possible to adapt this method for *in vivo* measurements. In addition, the rate of ATP synthesis in isolated thylakoids, intact chloroplasts and attached leaves can be estimated by the relaxation kinetics of the electrochromic shift (ECS) which also provide indication on thylakoid membrane leakiness.

The remarkable heat tolerance of *Y. filimentosa* might be due to a thermostable ATP synthase complex. The introduction of that version of the enzyme into crops plants will result in transgenic lines with higher photosynthetic rates. To check this possibility, the heat sensitivity of the enzyme will be investigated further. The response of ATP synthase activity to temperature could be determined by incubating the complex isolated from barley and *Y. filimentosa* tissues exposed to a range of temperatures before initiation of the assays. More importantly however, leaf extracts might contain heat shock proteins (HSPs) that play a significant role in protecting the ATP synthase isolated from *Y. filimentosa* from thermal damage. These features are important for assessing the properties of the enzyme. There is evidence from the literature that suggests heat tolerance in Agave plants is correlated with the accumulation of HSPs. Protein profiles in *Y. filimentosa* could be measured using high resolution, two-dimensional electrophoresis to separate proteins from control and heat stressed *Y. filimentosa* leaves, followed by selection and staining of differentially expressed proteins which can subsequently be identified by mass spectrometry. If the heat tolerance of ATP synthase in *Y. filimentosa* correlates with induction of HSPs,

experiments should be conducted to examine if the heat sensitivity of the ATP synthase from barley can be enhanced by expression of these heat shock proteins.

There is some evidence in this study that suggested RuBisCO Activase may not be required to activate RuBisCO in either control or stressed barley plants as fully activated RuBisCO from light adapted leaves was extracted using a buffer lacking the activating factors CO_2 and $MgCl_2$. To test the hypothesis and re-evaluate the roles of RuBisCO Activase in barley, wild type and knockout/knockdown RuBisCO Activase from barley line could be produced and RuBisCO activation state, rates of photosynthesis, and growth over a wide range of temperatures (5-35^{0}C) assessed.

Further experiments need to be conducted in the future to explore the thermotolerance mechanisms in *Y. filimentosa*. One of these mechanisms might be the heat stability of the chloroplast membranes. It has been suggested that increased levels of saturated fatty acids in membrane lipids plays a role in enabling the plant to tolerate elevated temperature. Thylakoid membranes could be isolated from barley and *Y. filimentosa* and their stability examined over a range of temperatures. If the results showed more heat stable thylakoid membranes in in *Y. filimentosa,* then the fatty acid profile could be determined to find if their level increase with increasing leaf temperature. Producing a transgenic barley line with altered fatty acid composition in their photosynthetic membranes may result in increased heat stability of photosynthesis.

7 Appendices

Figure A 3-1a: General Linear Model: A_{sat} *versus* HS Treatment, line

```
Factor        Type   Levels  Values
HS Treatment  fixed       6  25, 30, 36, 38, 40, 45
line          fixed       4  Katumani, Local, optic, Sundance


Analysis of Variance for A sat, using Adjusted SS for Tests

Source              DF    Seq SS    Adj SS   Adj MS       F      P
HS Treatment         5  165406.6  161999.4  32399.9  868.31  0.000
line                 3     788.5     997.2    332.4    8.91  0.000
HS Treatment*line   15    3002.9    3002.9    200.2    5.37  0.000
Error               50    1865.7    1865.7     37.3
Total               73  171063.7


S = 6.10851   R-Sq = 98.91%   R-Sq(adj) = 98.41%

Grouping Information Using Tukey Method and 95.0% Confidence

HS
Treatment  line      N     Mean  Grouping
36         Sundance  3  114.416  A
30         Sundance  3  110.625  A B
30         Katumani  3  109.255  A B
36         Katumani  3  103.888  A B
25         optic     4  100.000  A B
25         Local     3  100.000  A B
25         Katumani  3  100.000  A B
25         Sundance  4  100.000  A B
30         Local     3   97.738  A B C
30         optic     3   94.863    B C
36         optic     3   80.164      C D
36         Local     2   72.307        D
38         Local     3   19.944          E
38         Katumani  3   16.894          E F
38         optic     3   12.140          E F
38         Sundance  4   11.935          E F
40         Local     3    2.660          E F
40         Sundance  3    0.000            F
45         optic     3    0.000            F
45         Sundance  3    0.000            F
40         optic     3    0.000            F
40         Katumani  3    0.000            F
45         Local     3   -0.000            F
45         Katumani  3   -0.000            F

Means that do not share a letter are significantly different.
```

MSD= 17.8

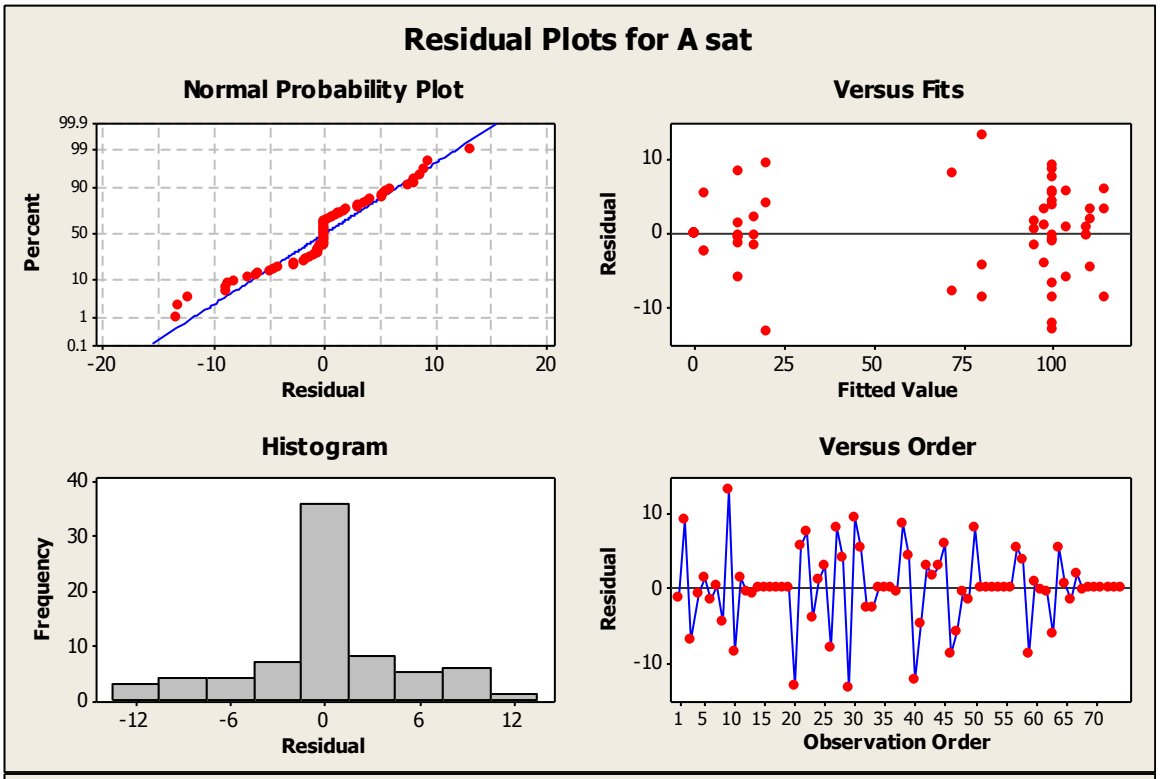
Residual Plots for A sat
Normal Probability Plot
Percent
Residual
Versus Fits
Residual
Fitted Value
Histogram
Frequency
Residual
Versus Order
Residual
Observation Order

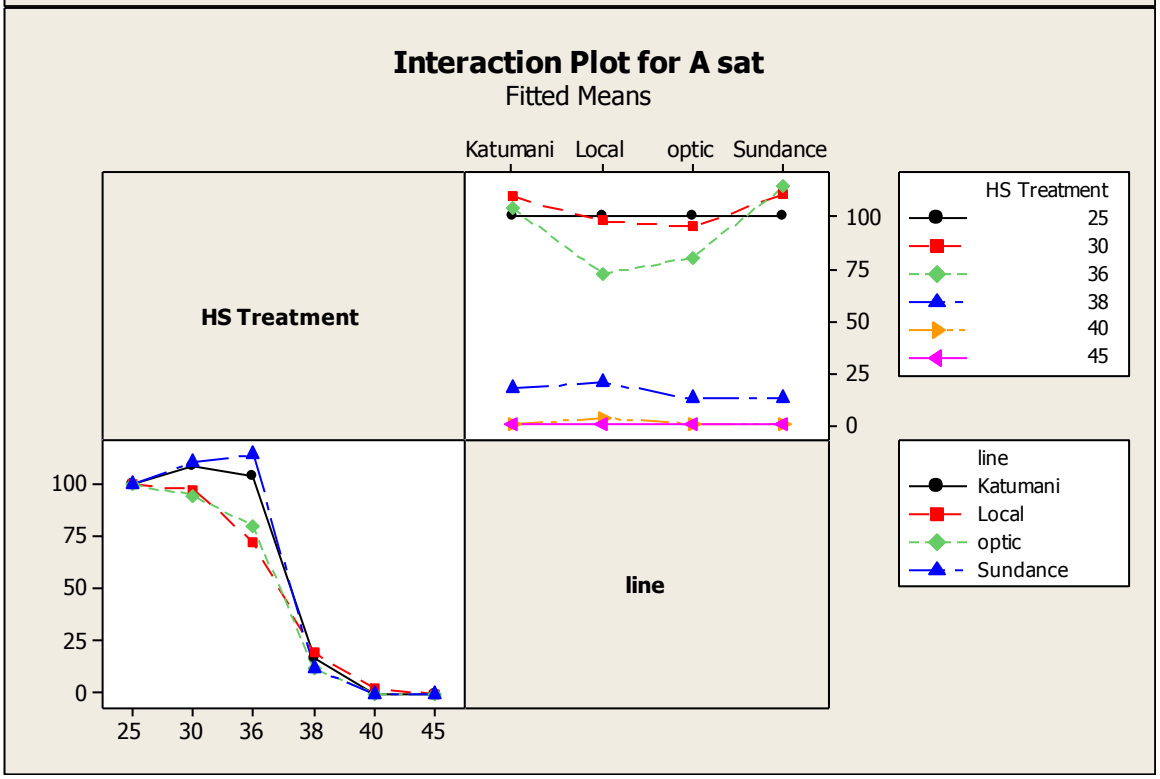
Interaction Plot for A sat
Fitted Means
Katumani
Local
optic
Sundance
HS Treatment
line
HS Treatment
25
30
36
38
40
45
line
Katumani
Local
optic
Sundance

Figure A 3-1b: General Linear Model: A_{sat} all Lines *versus* HS Treatment, all Lines

Factor	Type	Levels	Values
HS Treatment	fixed	4	25, 38, 40, 45
all Lines	fixed	5	Katumani, Local, optic, Sundance, Yucca

Analysis of Variance for A_{sat} all Lines, using Adjusted SS for Tests

Source	DF	Seq SS	Adj SS	Adj MS	F	P
HS Treatment	3	81489.5	81992.0	27330.7	321.17	0.000
all Lines	4	31142.8	31798.2	7949.6	93.42	0.000
HS Treatment*all Lines	12	13516.0	13516.0	1126.3	13.24	0.000
Error	44	3744.2	3744.2	85.1		
Total	63	129892.6				

S = 9.22476 R-Sq = 97.12% R-Sq(adj) = 95.87%

Grouping Information Using Tukey Method and 95.0% Confidence

HS Treatment	all Lines	N	Mean	Grouping
25	Sundance	4	100.000	A
25	optic	4	100.000	A
25	Local	3	100.000	A
25	Katumani	3	100.000	A
25	Yucca	3	100.000	A
40	Yucca	3	97.763	A
38	Yucca	3	94.374	A
45	Yucca	4	46.558	B
38	Local	3	19.944	C
38	Katumani	3	16.894	C
38	optic	3	12.140	C
38	Sundance	4	11.935	C
40	Local	3	2.660	C
45	Katumani	3	0.000	C
40	Katumani	3	0.000	C
40	optic	3	0.000	C
45	Local	3	0.000	C
40	Sundance	3	-0.000	C
45	optic	3	-0.000	C
45	Sundance	3	-0.000	C

Means that do not share a letter are significantly different.

MSD= 26.1

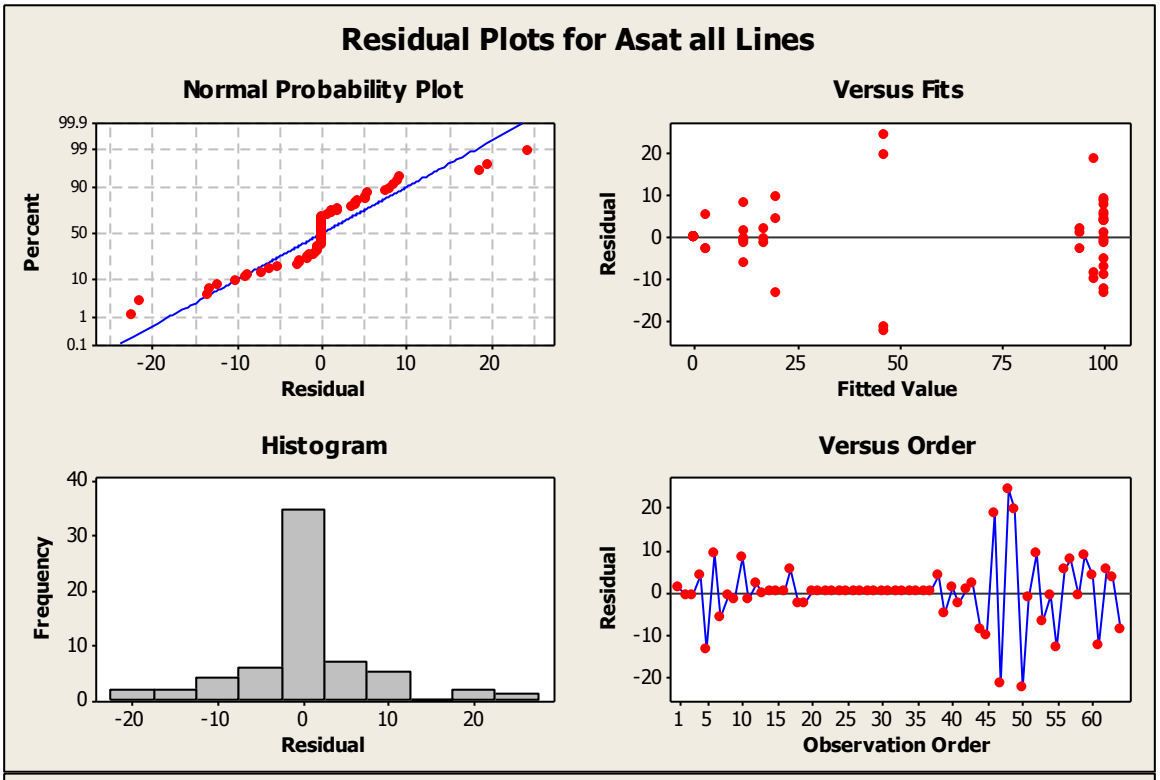
Residual Plots for Asat all Lines
Normal Probability Plot
Percent
Residual
Versus Fits
Residual
Fitted Value
Histogram
Frequency
Residual
Versus Order
Residual
Observation Order

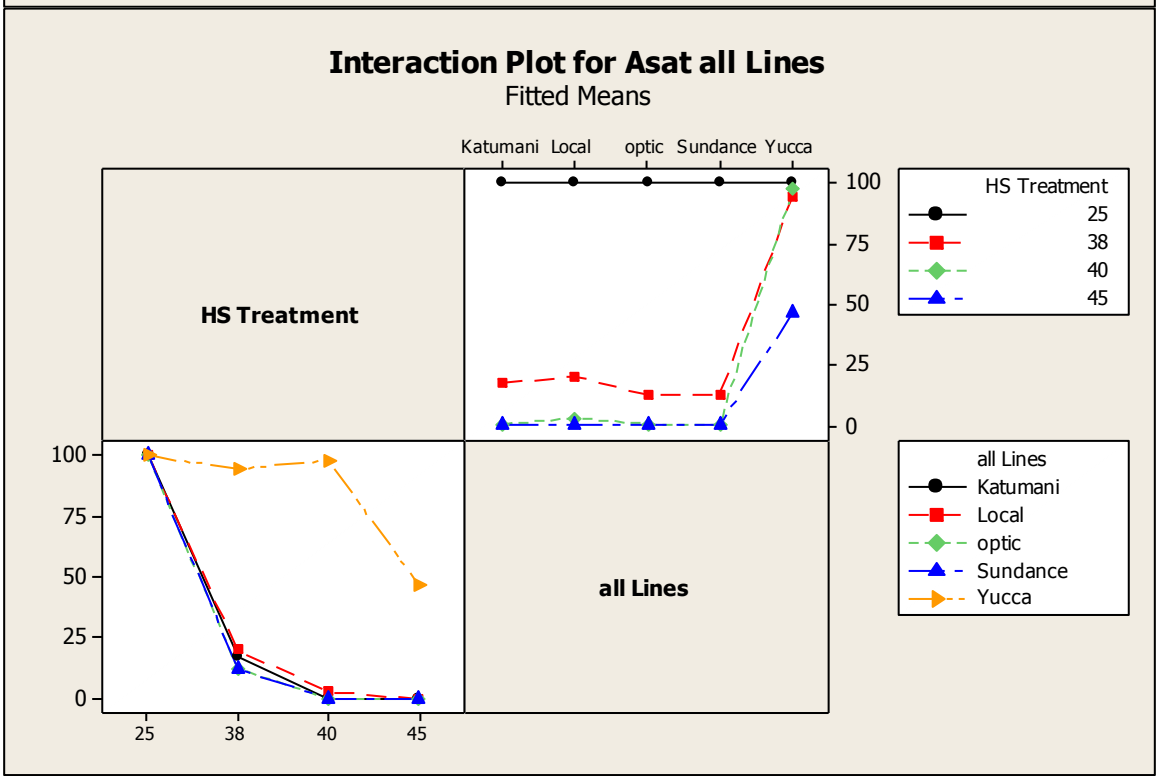
Interaction Plot for Asat all Lines
Fitted Means
Katumani Local optic Sundance Yucca
HS Treatment
HS Treatment
25
38
40
45
all Lines
all Lines
Katumani
Local
optic
Sundance
Yucca

Figure A 3-2: General Linear Model: A_{sat} *versus* HS Treatment, Line, R

Factor	Type	Levels	Values
HS Treatment	fixed	3	0, 3, 120
Line	fixed	4	Katumani, Local, Optic, Sundance
R	random	3	1, 2, 3

Analysis of Variance for A_{sat}, using Adjusted SS for Tests

Source	DF	Seq SS	Adj SS	Adj MS	F	P
HS Treatment	2	43553.2	43553.2	21776.6	108.75	0.000
Line	3	1323.4	1323.4	441.1	2.20	0.116
HS Treatment*Line	6	893.3	893.3	148.9	0.74	0.621
R	2	273.7	273.7	136.9	0.68	0.515
Error	22	4405.3	4405.3	200.2		
Total	35	50448.9				

S = 14.1506 R-Sq = 91.27% R-Sq(adj) = 86.11%

Grouping Information Using Tukey Method and 95.0% Confidence

HS Treatment	Line	N	Mean	Grouping
0	Local	3	100.000	A
0	Sundance	3	100.000	A
0	Optic	3	100.000	A
0	Katumani	3	100.000	A
120	Katumani	3	59.652	A B
120	Local	3	41.598	B C
120	Optic	3	35.761	B C
120	Sundance	3	28.201	B C
3	Katumani	3	26.755	B C
3	Local	3	20.999	B C
3	Sundance	3	11.754	C
3	Optic	3	9.177	C

Means that do not share a letter are significantly different.

MSD= 35.9

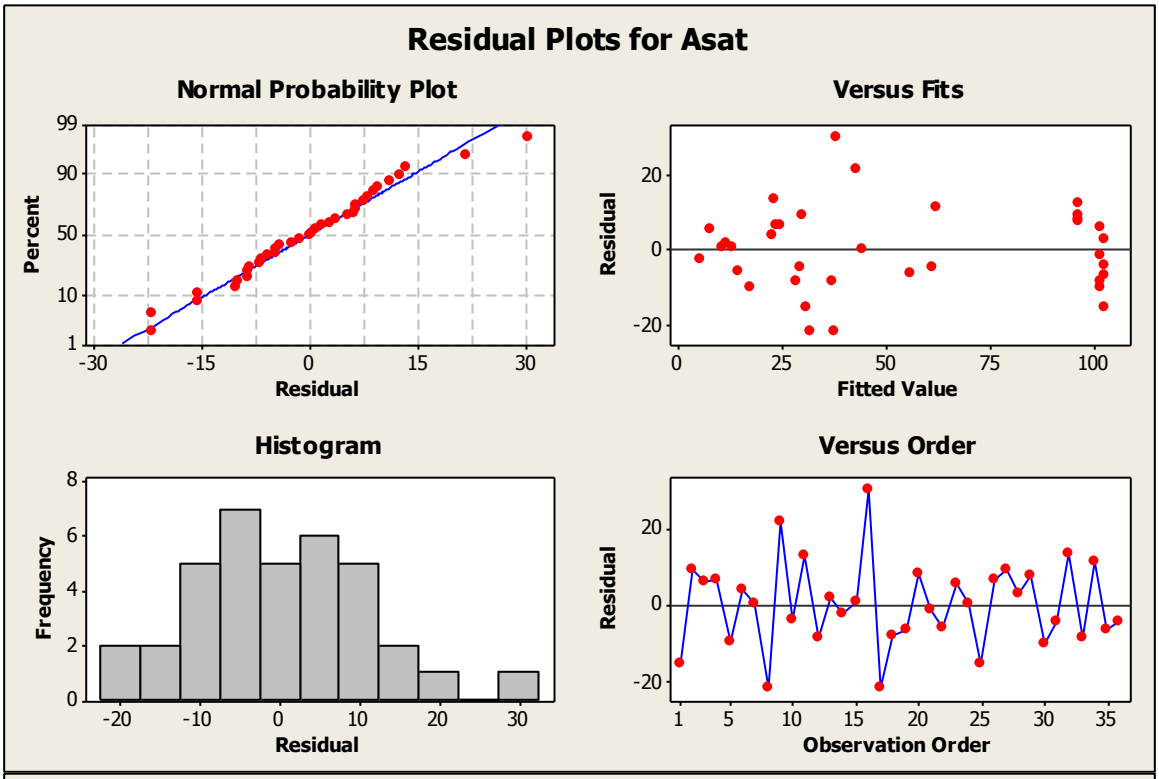
Residual Plots for Asat
Normal Probability Plot
Percent
Residual
Versus Fits
Residual
Fitted Value
Histogram
Frequency
Residual
Versus Order
Residual
Observation Order

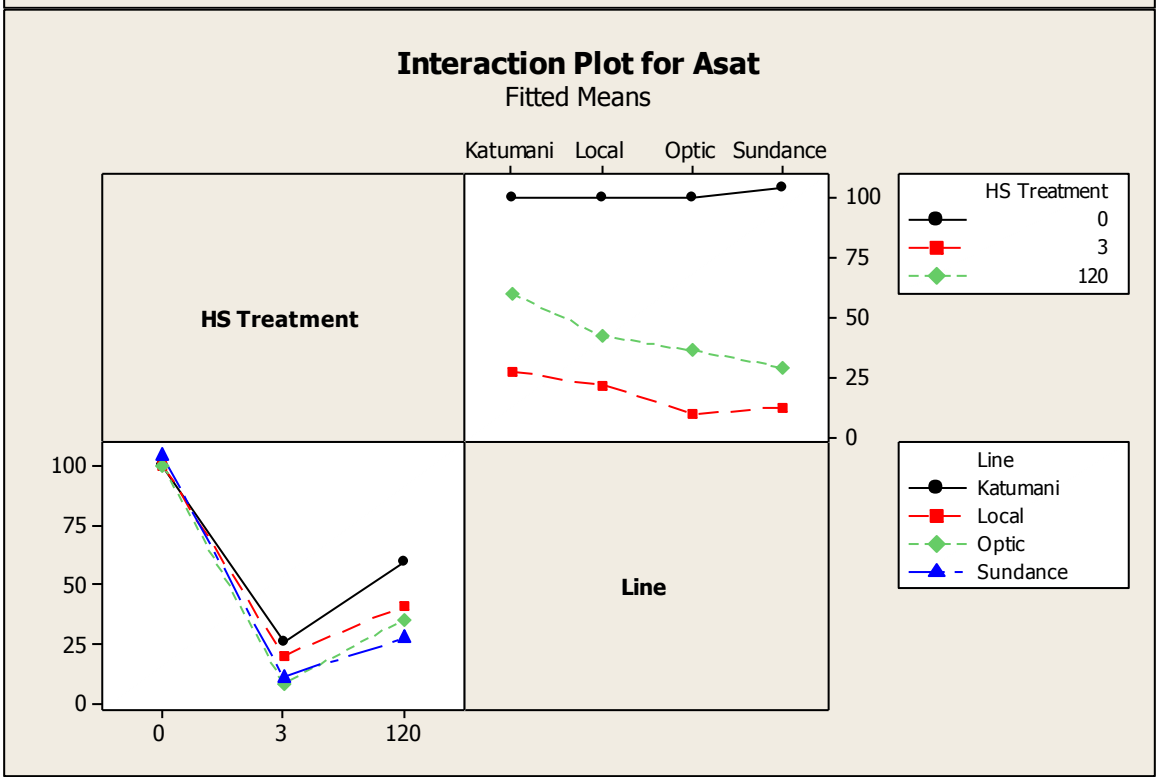
Interaction Plot for Asat
Fitted Means
Katumani
Local
Optic
Sundance
HS Treatment
Line
HS Treatment
0
3
120
Line
Katumani
Local
Optic
Sundance

Figure A 3-3: General Linear Model: Carboxylation Efficiency *versus* HS Treatment, Line, R

Factor	Type	Levels	Values
HS Treatment	fixed	3	0, 3, 120
Line	fixed	4	Katumani, Local, Optic, Sundance
R	random	3	1, 2, 3

Analysis of Variance for Carboxylation Efficiency, using Adjusted SS for Tests

Source	DF	Seq SS	Adj SS	Adj MS	F	P
HS Treatment	2	31162.6	31162.6	15581.3	41.34	0.000
Line	3	3014.7	3014.7	1004.9	2.67	0.073
HS Treatment*Line	6	1729.6	1729.6	288.3	0.76	0.605
R	2	208.0	208.0	104.0	0.28	0.761
Error	22	8291.8	8291.8	376.9		
Total	35	44406.7				

S = 19.4140 R-Sq = 81.33% R-Sq(adj) = 70.29%

Grouping Information Using Tukey Method and 95.0% Confidence

HS Treatment	Line	N	Mean	Grouping
0	Local	3	100.00	A
0	Sundance	3	100.00	A
0	Optic	3	100.00	A
0	Katumani	3	100.00	A
120	Katumani	3	65.78	A B
120	Sundance	3	53.18	A B
3	Katumani	3	48.60	A B
3	Sundance	3	44.26	A B
120	Optic	3	40.05	B
120	Local	3	35.41	B
3	Local	3	14.96	B
3	Optic	3	14.38	B

Means that do not share a letter are significantly different.

MSD= 49.4

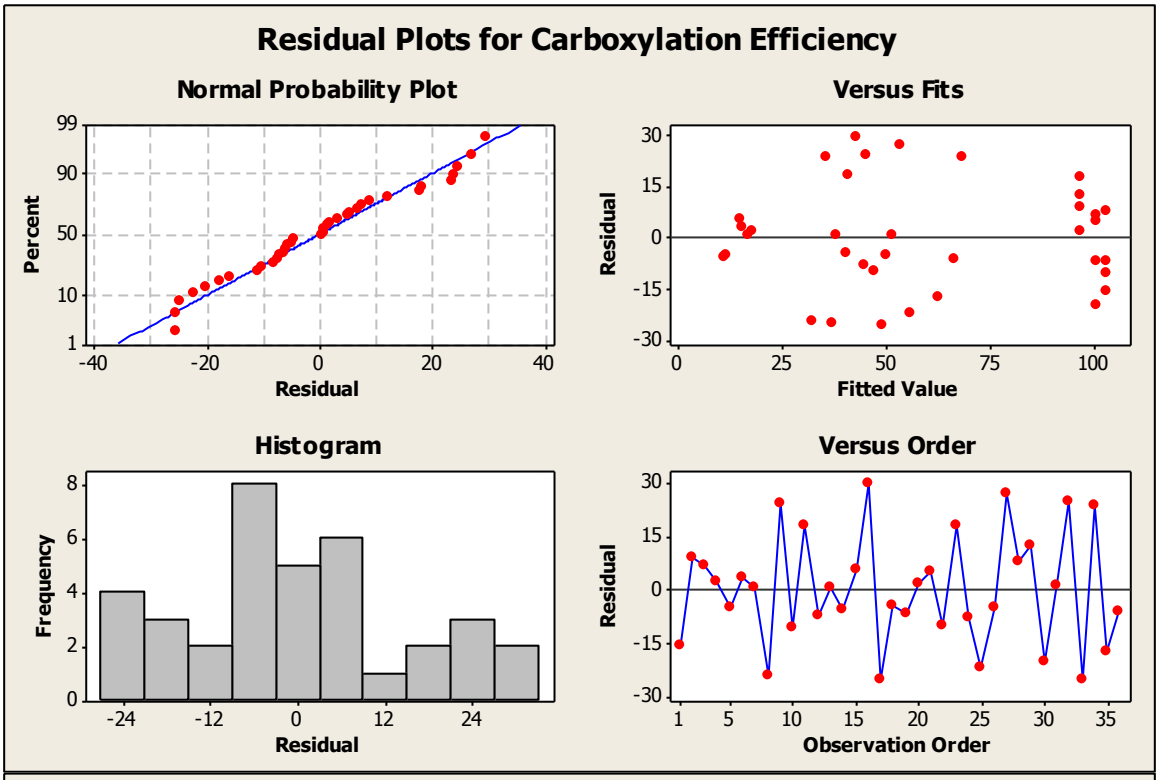
Residual Plots for Carboxylation Efficiency
Normal Probability Plot
Percent
Residual
Versus Fits
Residual
Fitted Value
Histogram
Frequency
Residual
Versus Order
Residual
Observation Order

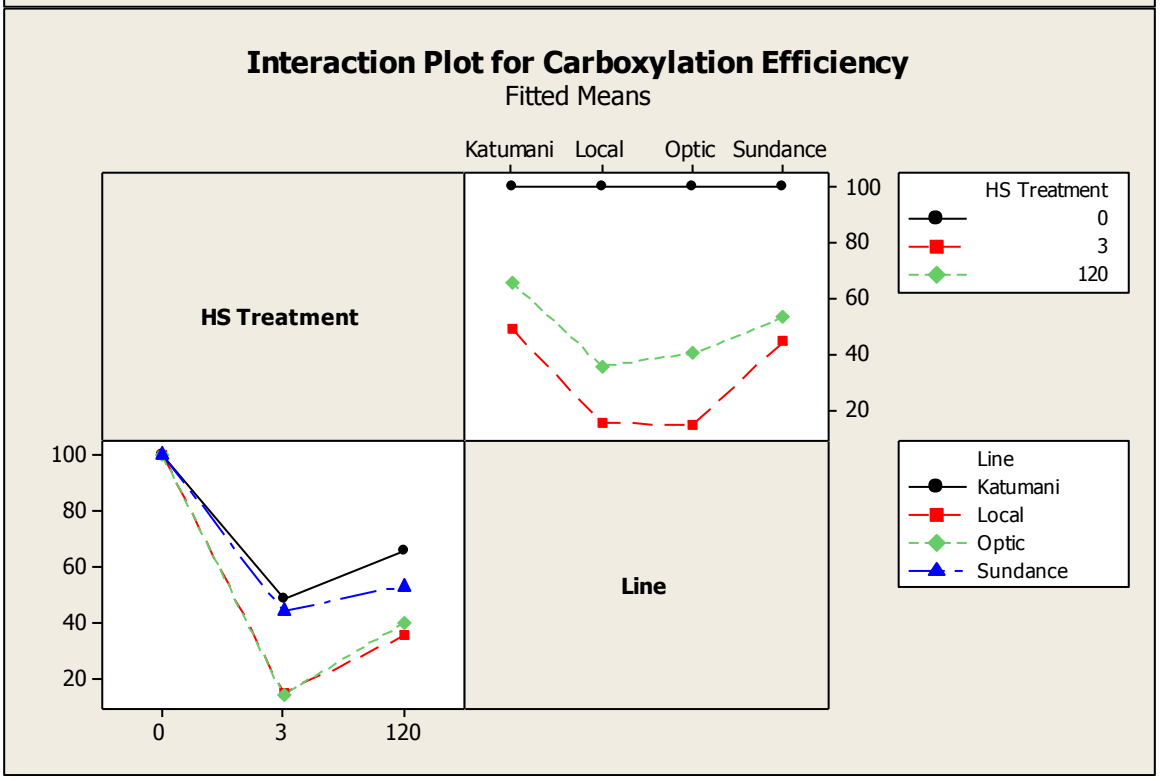
Interaction Plot for Carboxylation Efficiency
Fitted Means
Katumani
Local
Optic
Sundance
HS Treatment
HS Treatment
0
3
120
Line
Line
Katumani
Local
Optic
Sundance

Figure A 3-4: General Linear Model: g_s *versus* HS Treatment, Line, R

Factor	Type	Levels	Values
HS Treatment	fixed	3	0, 3, 120
Line	fixed	4	Katumani, Local, Optic, Sundance
R	random	3	1, 2, 3

Analysis of Variance for g_s, using Adjusted SS for Tests

Source	DF	Seq SS	Adj SS	Adj MS	F	P
HS Treatment	2	10117	10117	5059	4.77	0.019
Line	3	11458	11458	3819	3.60	0.030
HS Treatment*Line	6	8193	8193	1366	1.29	0.303
R	2	3606	3606	1803	1.70	0.206
Error	22	23318	23318	1060		
Total	35	56693				

S = 32.5560 R-Sq = 58.87% R-Sq(adj) = 34.57%

Grouping Information Using Tukey Method and 95.0% Confidence

HS Treatment	Line	N	Mean	Grouping
3	Optic	3	121.78	A
0	Sundance	3	100.00	A
0	Local	3	100.00	A
0	Katumani	3	100.00	A
0	Optic	3	100.00	A
3	Local	3	93.94	A
120	Optic	3	86.53	A
120	Local	3	63.80	A
120	Katumani	3	51.62	A
3	Sundance	3	39.37	A
3	Katumani	3	37.29	A
120	Sundance	3	36.78	A

Means that do not share a letter are significantly different.

MSD= 82.8

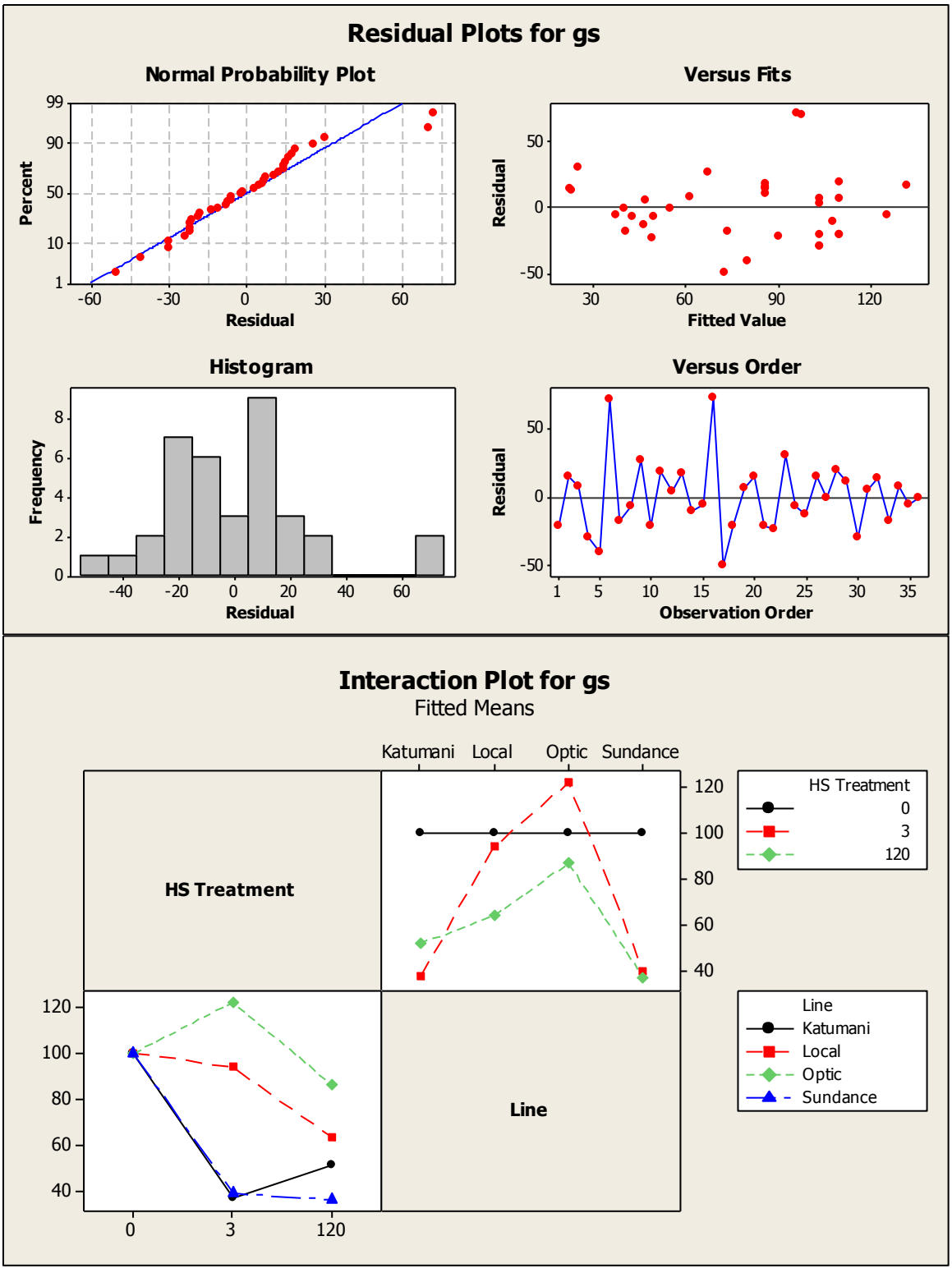
Residual Plots for gs
Normal Probability Plot
Percent
Residual
Versus Fits
Residual
Fitted Value
Histogram
Frequency
Residual
Versus Order
Residual
Observation Order
Interaction Plot for gs
Fitted Means
Katumani
Local
Optic
Sundance
HS Treatment
0
3
120
Line
Katumani
Local
Optic
Sundance

Figure A 3-5: General Linear Model: E *versus* HS Treatment, Line, R

Factor	Type	Levels	Values
HS Treatment	fixed	3	0, 3, 120
Line	fixed	4	Katumani, Local, Optic, Sundance
R	random	3	1, 2, 3

Analysis of Variance for E, using Adjusted SS for Tests

Source	DF	Seq SS	Adj SS	Adj MS	F	P
HS Treatment	2	6852.7	6852.7	3426.3	7.31	0.004
Line	3	424.3	424.3	141.4	0.30	0.824
HS Treatment*Line	6	1041.4	1041.4	173.6	0.37	0.890
R	2	995.7	995.7	497.8	1.06	0.363
Error	22	10317.7	10317.7	469.0		
Total	35	19631.8				

S = 21.6561 R-Sq = 47.44% R-Sq(adj) = 16.39%

Grouping Information Using Tukey Method and 95.0% Confidence

HS Treatment	Line	N	Mean	Grouping
0	Local	3	100.00	A
0	Sundance	3	100.00	A
0	Katumani	3	100.00	A
0	Optic	3	100.00	A
3	Optic	3	86.54	A
120	Local	3	74.84	A
3	Local	3	73.75	A
120	Katumani	3	72.87	A
3	Katumani	3	70.28	A
120	Sundance	3	66.20	A
120	Optic	3	63.92	A
3	Sundance	3	58.24	A

Means that do not share a letter are significantly different.

MSD= 55.1

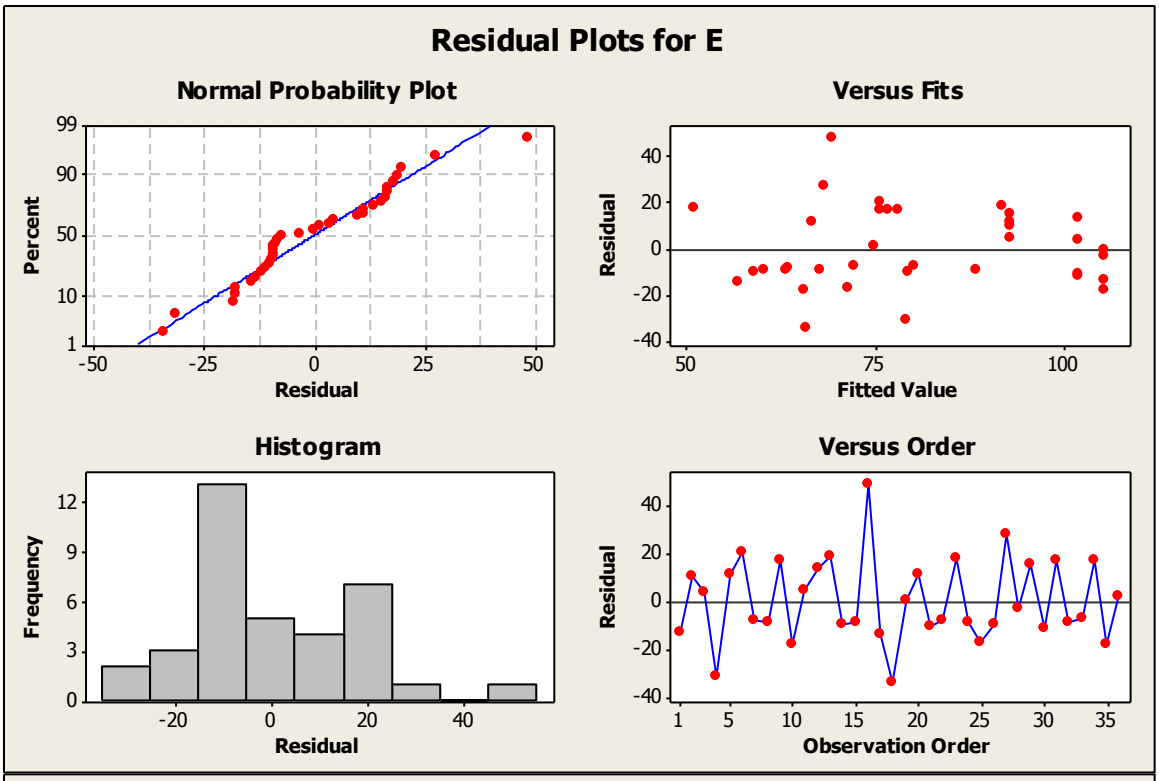
Residual Plots for E
Normal Probability Plot
Percent
Residual
Versus Fits
Residual
Fitted Value
Histogram
Frequency
Residual
Versus Order
Residual
Observation Order

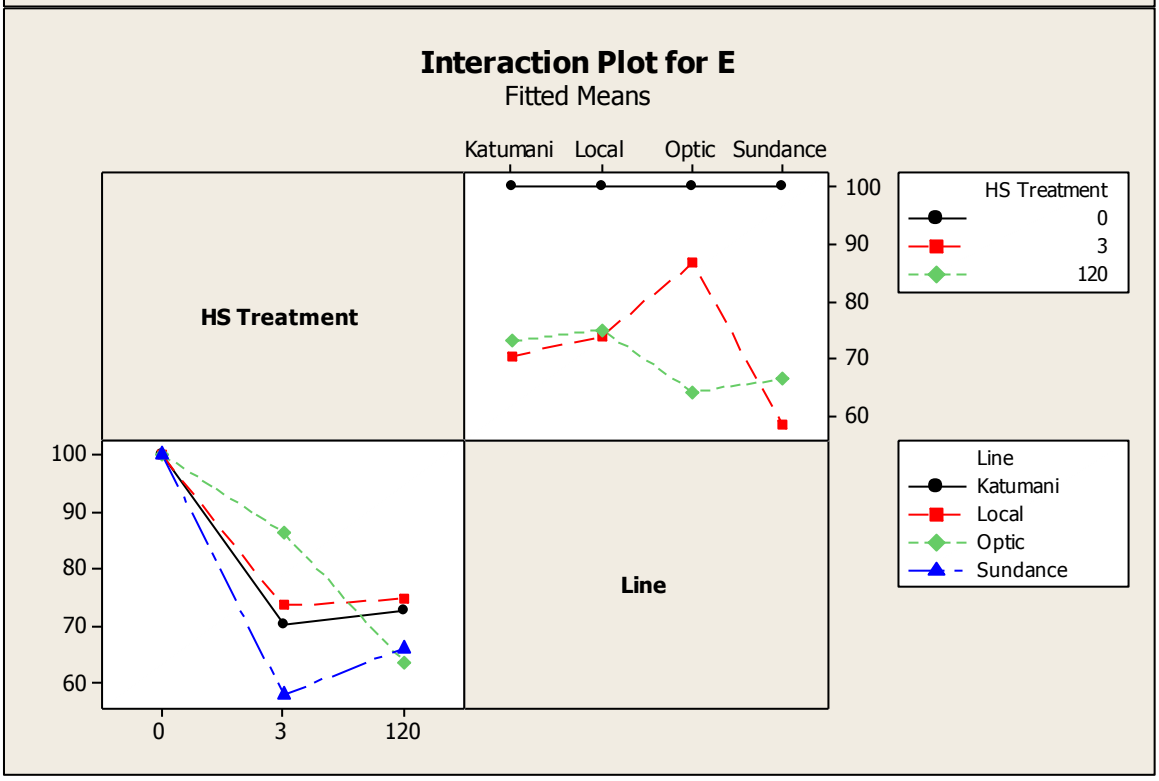
Interaction Plot for E
Fitted Means
Katumani
Local
Optic
Sundance
HS Treatment
HS Treatment
0
3
120
Line
Line
Katumani
Local
Optic
Sundance

Figure A 3-6: General Linear Model: PSII Efficiency *versus* HS Treatment, Line, R

Factor	Type	Levels	Values
HS Treatment	fixed	3	0, 3, 120
Line	fixed	4	Katumani, Local, Optic, Sundance
R	random	3	1, 2, 3

Analysis of Variance for PSII Efficiency, using Adjusted SS for Tests

Source	DF	Seq SS	Adj SS	Adj MS	F	P
HS Treatment	2	11392.3	11392.3	5696.2	27.85	0.000
Line	3	803.2	803.2	267.7	1.31	0.297
HS Treatment*Line	6	884.1	884.1	147.4	0.72	0.637
R	2	20.2	20.2	10.1	0.05	0.952
Error	22	4498.9	4498.9	204.5		
Total	35	17598.7				

S = 14.3003 R-Sq = 74.44% R-Sq(adj) = 59.33%

Grouping Information Using Tukey Method and 95.0% Confidence

HS Treatment	Line	N	Mean	Grouping
0	Katumani	3	100.00	A
0	Sundance	3	100.00	A
0	Local	3	100.00	A
0	Optic	3	100.00	A
3	Optic	3	75.01	A B
3	Sundance	3	70.50	A B
120	Optic	3	69.85	A B
3	Katumani	3	68.46	A B
120	Sundance	3	67.56	A B
3	Local	3	65.74	A B
120	Local	3	50.19	B
120	Katumani	3	43.03	B

Means that do not share a letter are significantly different.

MSD= 36.4

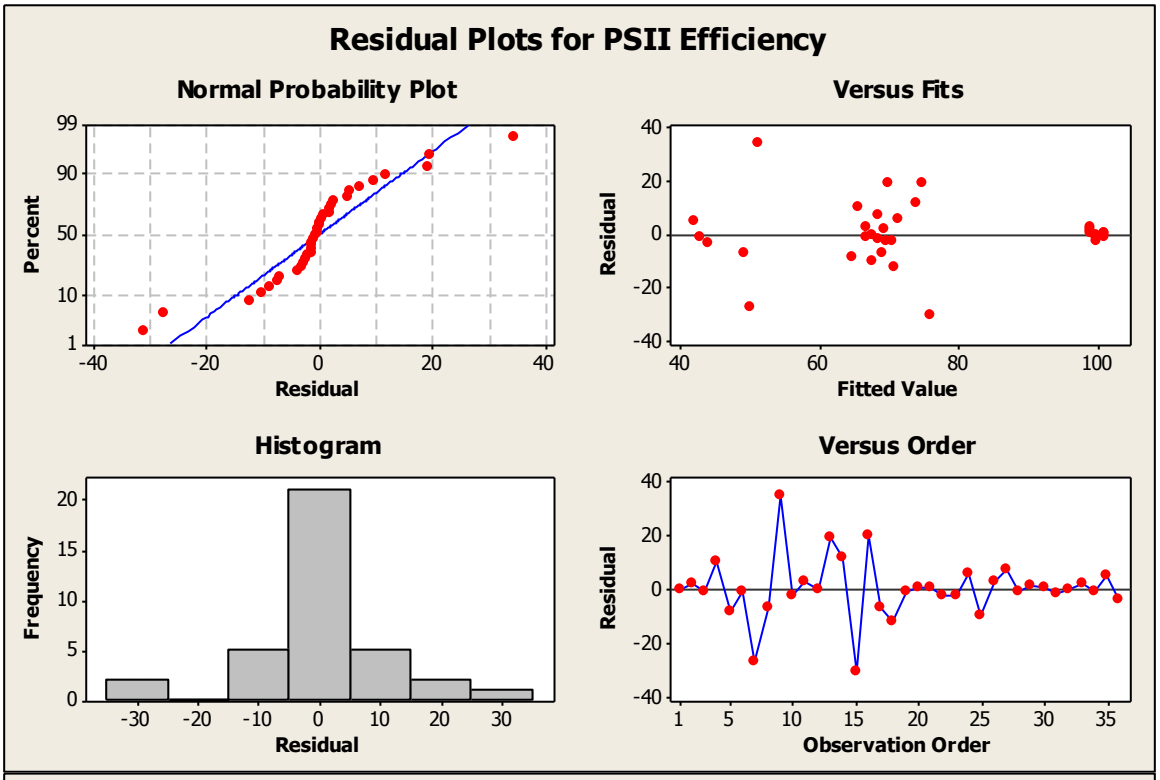
Residual Plots for PSII Efficiency
Normal Probability Plot
Percent
Residual
Versus Fits
Residual
Fitted Value
Histogram
Frequency
Residual
Versus Order
Residual
Observation Order

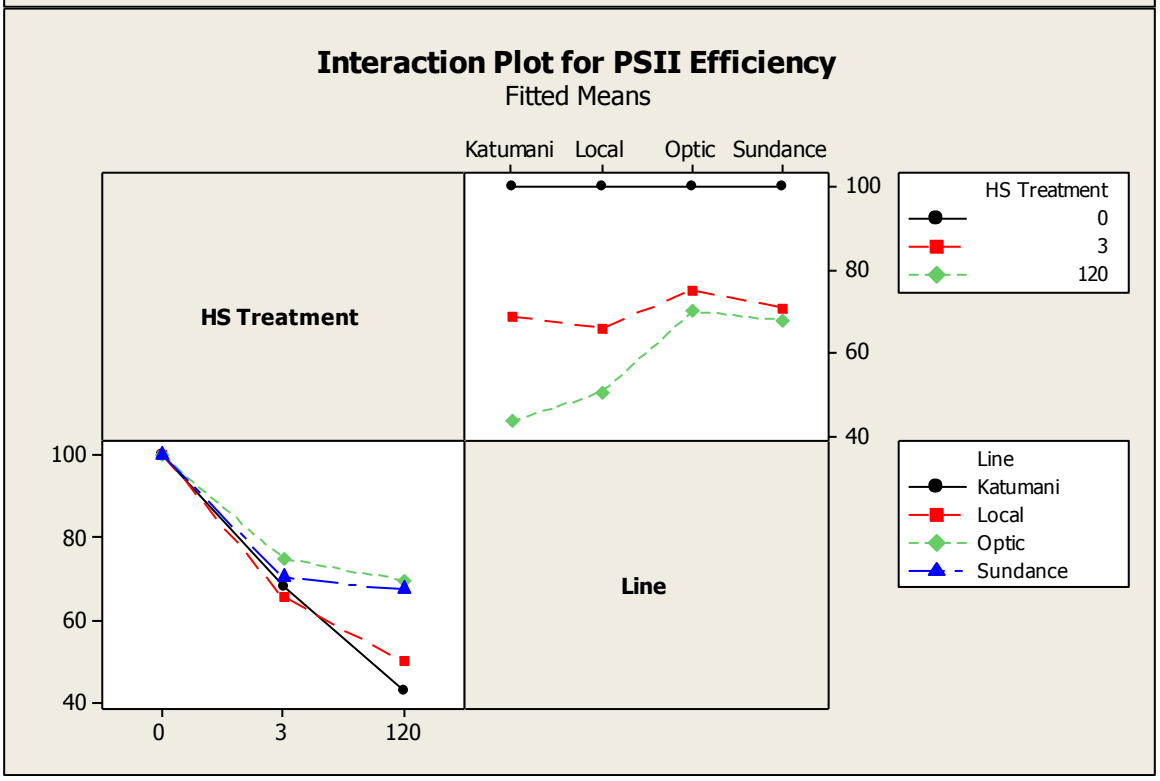
Interaction Plot for PSII Efficiency
Fitted Means
Katumani
Local
Optic
Sundance
HS Treatment
0
3
120
Line
Katumani
Local
Optic
Sundance
HS Treatment
Line

Figure A 3-7: General Linear Model: ETR *versus* HS Treatment, Line, R

Factor	Type	Levels	Values
HS Treatment	fixed	3	0, 3, 120
Line	fixed	4	Katumani, Local, Optic, Sundance
R	random	3	1, 2, 3

Analysis of Variance for ETR, using Adjusted SS for Tests

Source	DF	Seq SS	Adj SS	Adj MS	F	P
HS Treatment	2	44671.2	44671.2	22335.6	76.75	0.000
Line	3	767.1	767.1	255.7	0.88	0.467
HS Treatment*Line	6	563.0	563.0	93.8	0.32	0.918
R	2	894.0	894.0	447.0	1.54	0.237
Error	22	6402.7	6402.7	291.0		
Total	35	53298.0				

S = 17.0596 R-Sq = 87.99% R-Sq(adj) = 80.89%

Grouping Information Using Tukey Method and 95.0% Confidence

HS Treatment	Line	N	Mean	Grouping
0	Katumani	3	100.00	A
0	Sundance	3	100.00	A
0	Optic	3	100.00	A
0	Local	3	100.00	A
120	Local	3	55.00	A B
120	Sundance	3	44.05	B
120	Optic	3	39.23	B
120	Katumani	3	30.92	B
3	Local	3	25.78	B
3	Katumani	3	13.04	B
3	Optic	3	12.13	B
3	Sundance	3	11.41	B

Means that do not share a letter are significantly different.

MSD= 43.4

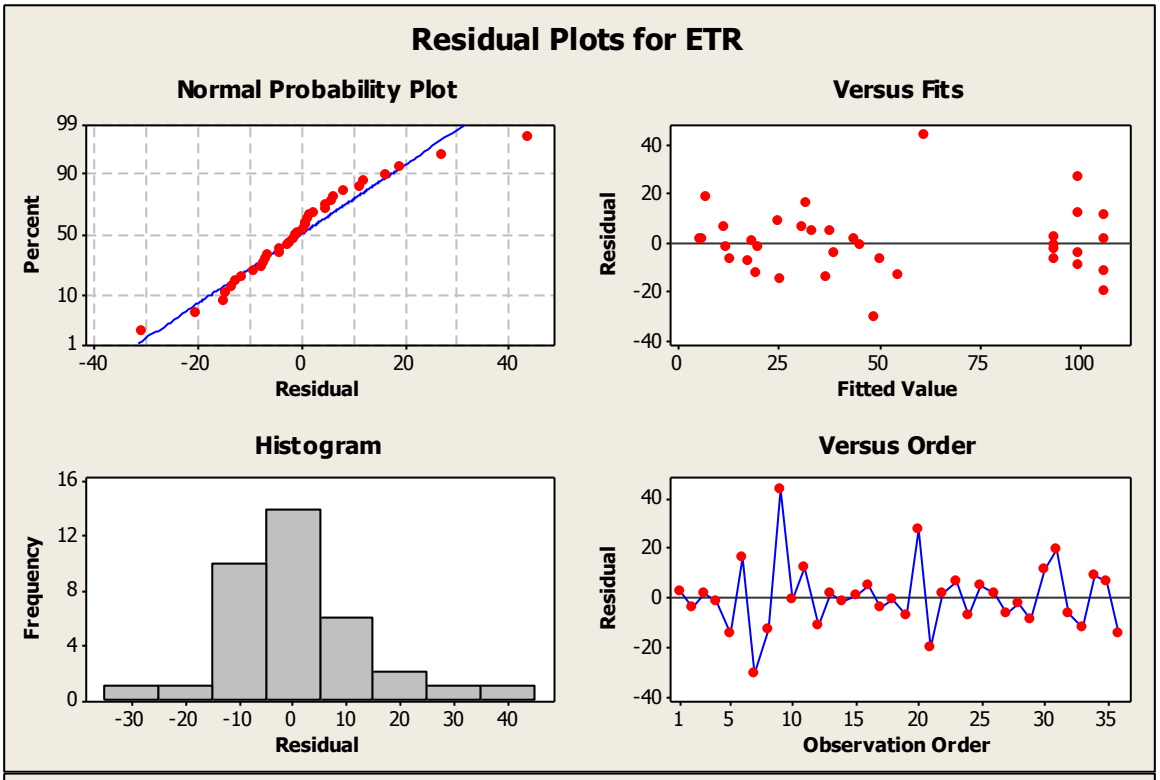
Residual Plots for ETR
Normal Probability Plot
Percent
Residual
Versus Fits
Residual
Fitted Value
Histogram
Frequency
Residual
Versus Order
Residual
Observation Order

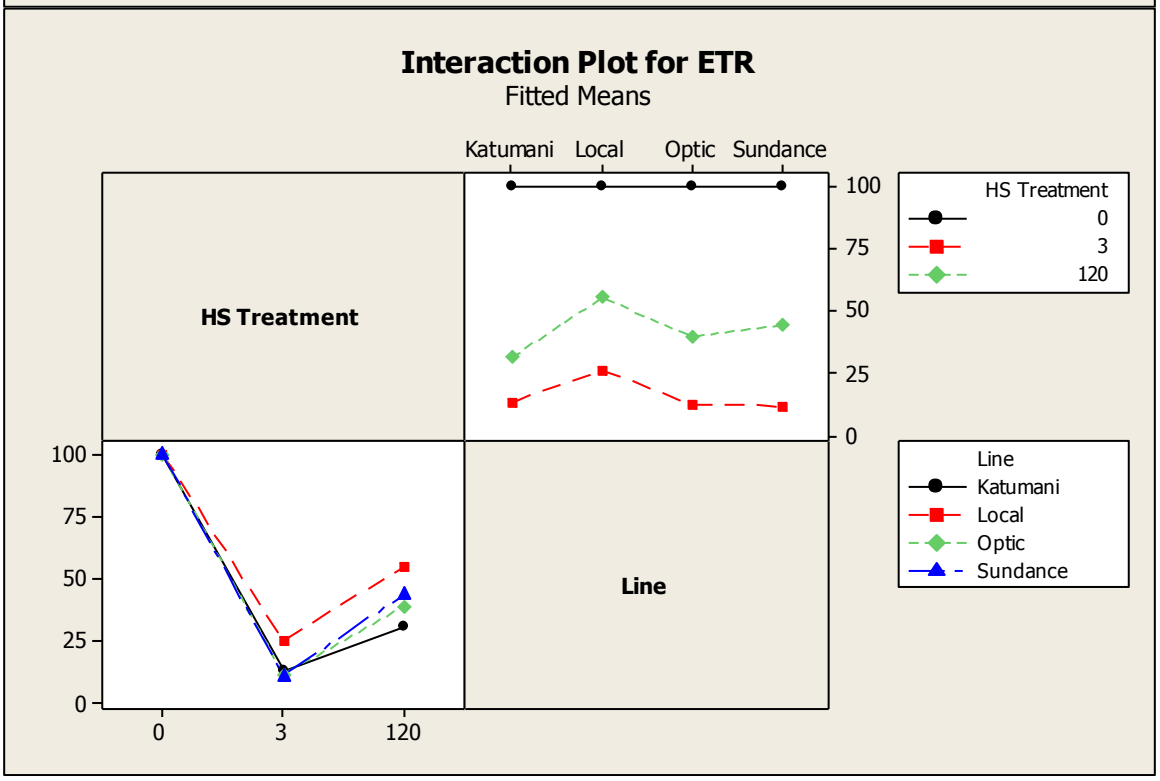
Interaction Plot for ETR
Fitted Means
Katumani
Local
Optic
Sundance
HS Treatment
HS Treatment
0
3
120
Line
Line
Katumani
Local
Optic
Sundance

Figure A 3-8a: General Linear Model: Yucca A_{sat} *versus* HS Treatment @ 38°C

```
Factor         Type   Levels  Values
HS Treatment   fixed       3  After 38, Before stress, Recovery after 1 hr


Analysis of Variance for Asat, using Adjusted SS for Tests

Source         DF   Seq SS   Adj SS  Adj MS       F      P
HS Treatment    2  107.226  107.226  53.613  222.60  0.000
Error           6    1.445    1.445   0.241
Total           8  108.671


S = 0.490759   R-Sq = 98.67%   R-Sq(adj) = 98.23%


Grouping Information Using Tukey Method and 95.0% Confidence

HS Treatment          N    Mean  Grouping
Before stress         3  7.7372  A
Recovery after 1 hr   3  7.0825  A
After 38              3  0.1097    B

Means that do not share a letter are significantly different.
```

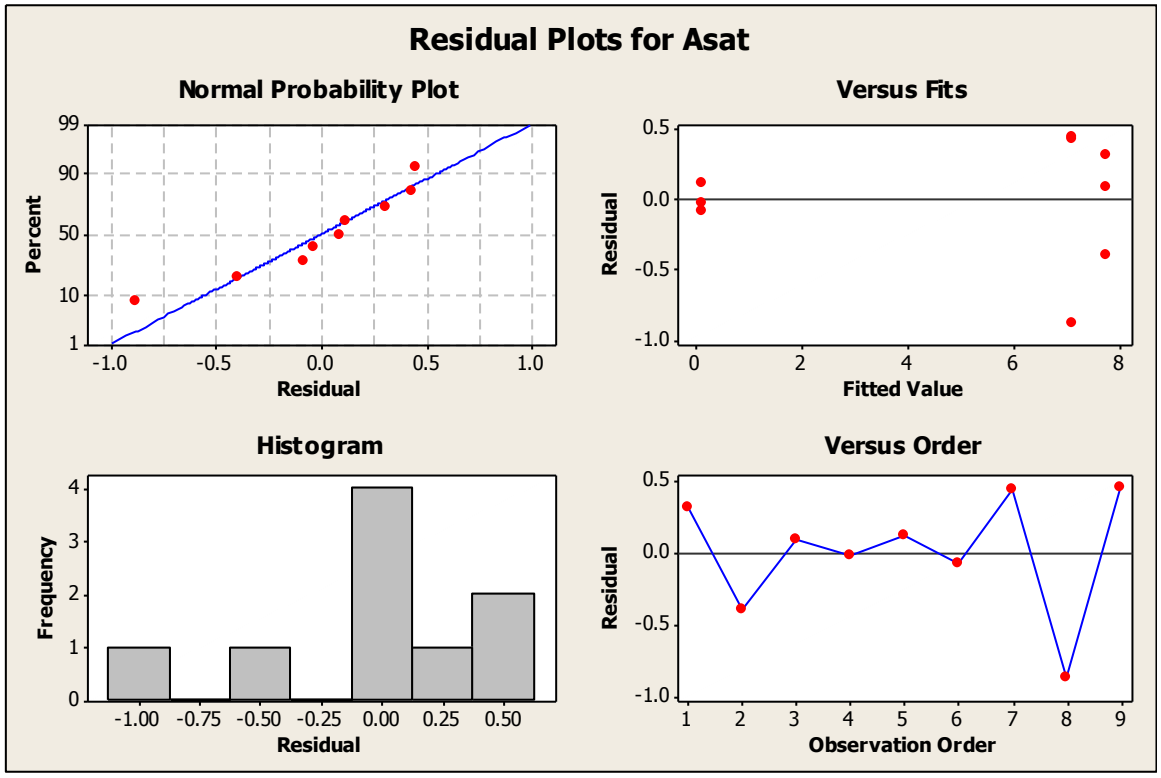

Figure A 3-8b: General Linear Model: Yucca A_{sat} *versus* HS Treatment @ 40°C

```
Factor         Type   Levels  Values
HS Treatment   fixed       3  After 40, Before stress, Recovery after 1 hr


Analysis of Variance for Asat, using Adjusted SS for Tests

Source         DF   Seq SS   Adj SS  Adj MS      F      P
HS Treatment    2  112.734  112.734  56.367  61.27  0.000
Error           6    5.520    5.520   0.920
Total           8  118.253


S = 0.959155   R-Sq = 95.33%   R-Sq(adj) = 93.78%


Grouping Information Using Tukey Method and 95.0% Confidence

HS Treatment          N    Mean  Grouping
Before stress         3  7.7372  A
Recovery after 1 hr   3  7.5739  A
After 40              3  0.1491     B

Means that do not share a letter are significantly different.
```

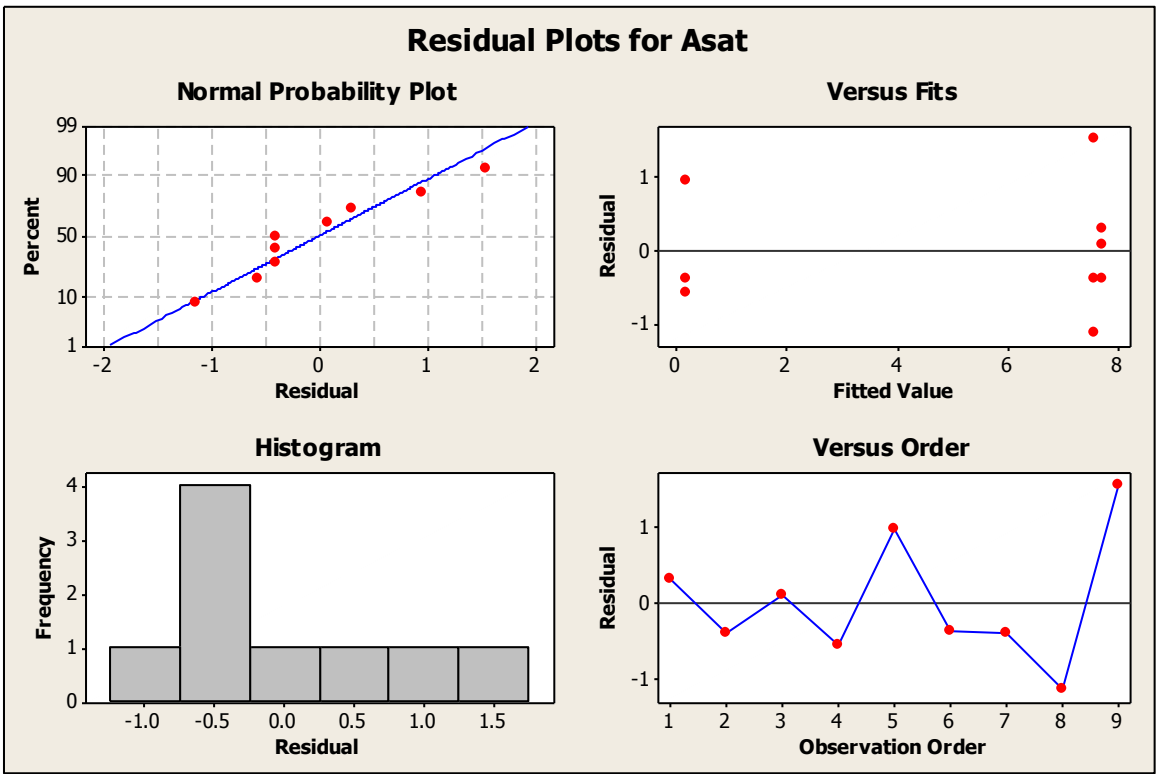

Figure A 3-8c: General Linear Model: Yucca A_{sat} *versus* HS Treatment @ 45°C

```
Factor         Type   Levels  Values
HS Treatment   fixed       4  After 45, Before stress, Recovery after 1 hr,
                              Recovery after 72 hr
```

Analysis of Variance for A_{sat}, using Adjusted SS for Tests

Source	DF	Seq SS	Adj SS	Adj MS	F	P
HS Treatment	3	92.764	92.764	30.921	10.45	0.004
Error	8	23.678	23.678	2.960		
Total	11	116.442				

S = 1.72040 R-Sq = 79.67% R-Sq(adj) = 72.04%

Grouping Information Using Tukey Method and 95.0% Confidence

HS Treatment	N	Mean	Grouping
Recovery after 72 hr	3	8.542	A
Before stress	3	7.737	A
Recovery after 1 hr	3	4.089	A B
After 45	3	1.670	B

Means that do not share a letter are significantly different.

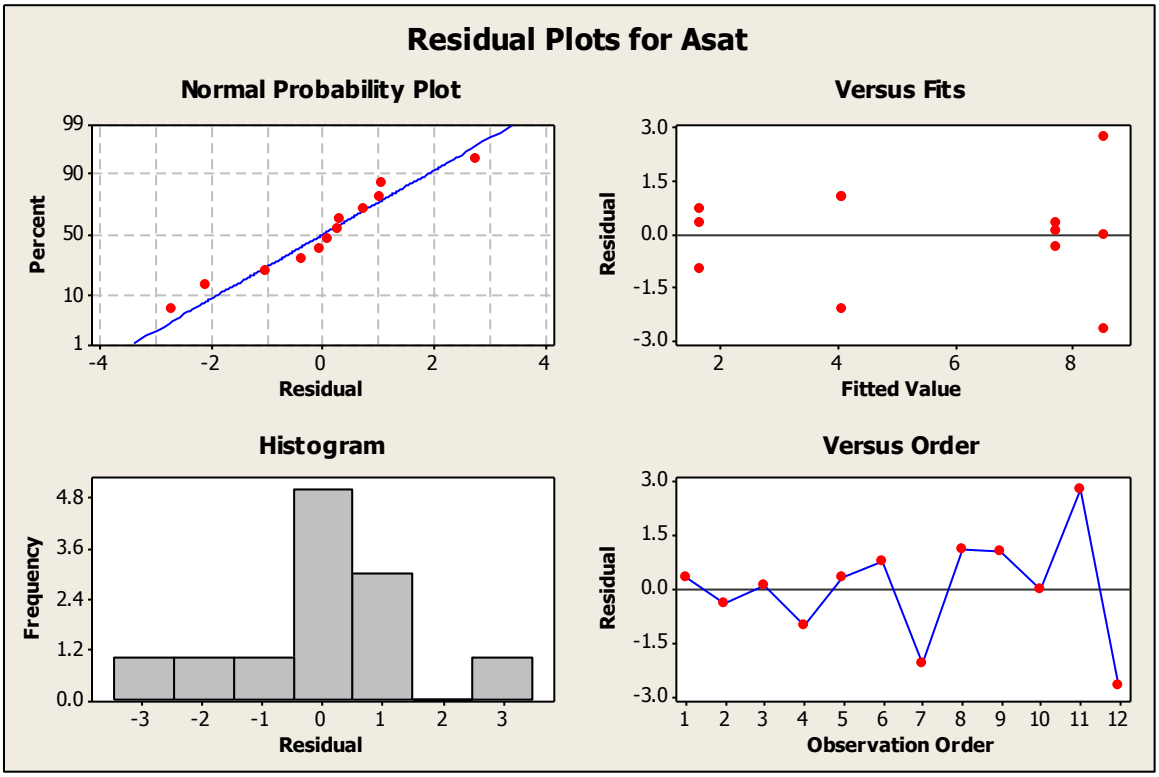

Figure A 3-9a: General Linear Model: Yucca g_s *versus* HS Treatment @ 38°C

```
Factor        Type   Levels  Values
HS Treatment  fixed       3  After 38, Before stress, Recovery after 1 hr


Analysis of Variance for gs, using Adjusted SS for Tests

Source        DF     Seq SS     Adj SS     Adj MS       F      P
HS Treatment   2  0.0091981  0.0091981  0.0045990   62.77  0.000
Error          6  0.0004396  0.0004396  0.0000733
Total          8  0.0096377


S = 0.00855987   R-Sq = 95.44%   R-Sq(adj) = 93.92%


Grouping Information Using Tukey Method and 95.0% Confidence

HS Treatment         N      Mean  Grouping
Before stress        3  0.077333  A
Recovery after 1 hr  3  0.063482  A
After 38             3  0.003661    B

Means that do not share a letter are significantly different.
```

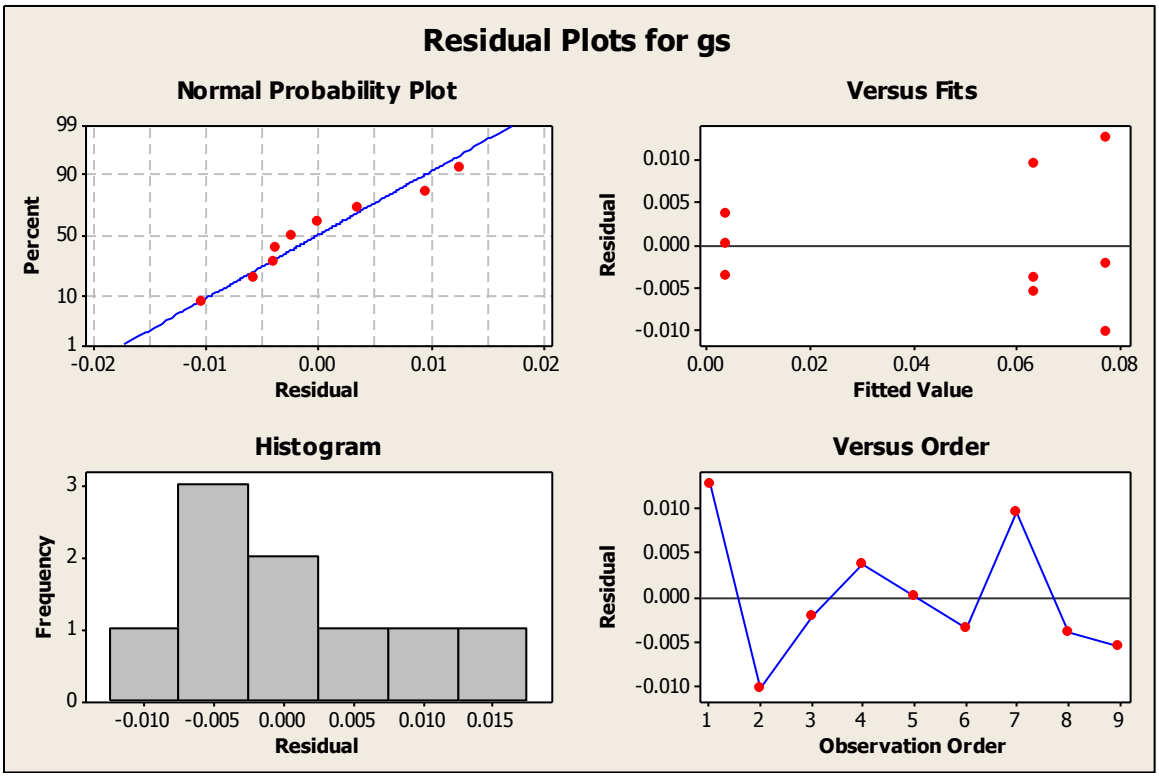

Figure A 3-9b: General Linear Model: Yucca g_s *versus* HS Treatment @ 40°C

```
Factor         Type   Levels  Values
HS Treatment   fixed       3  After 40, Before stress, Recovery after 1 hr


Analysis of Variance for gs, using Adjusted SS for Tests

Source         DF     Seq SS     Adj SS     Adj MS       F      P
HS Treatment    2   0.026137   0.026137   0.013069   44.65  0.000
Error           6   0.001756   0.001756   0.000293
Total           8   0.027894


S = 0.0171088    R-Sq = 93.70%    R-Sq(adj) = 91.60%


Grouping Information Using Tukey Method and 95.0% Confidence

HS Treatment          N      Mean  Grouping
Recovery after 1 hr   3  0.140110  A
Before stress         3  0.077333    B
After 40              3  0.008158      C

Means that do not share a letter are significantly different.
```

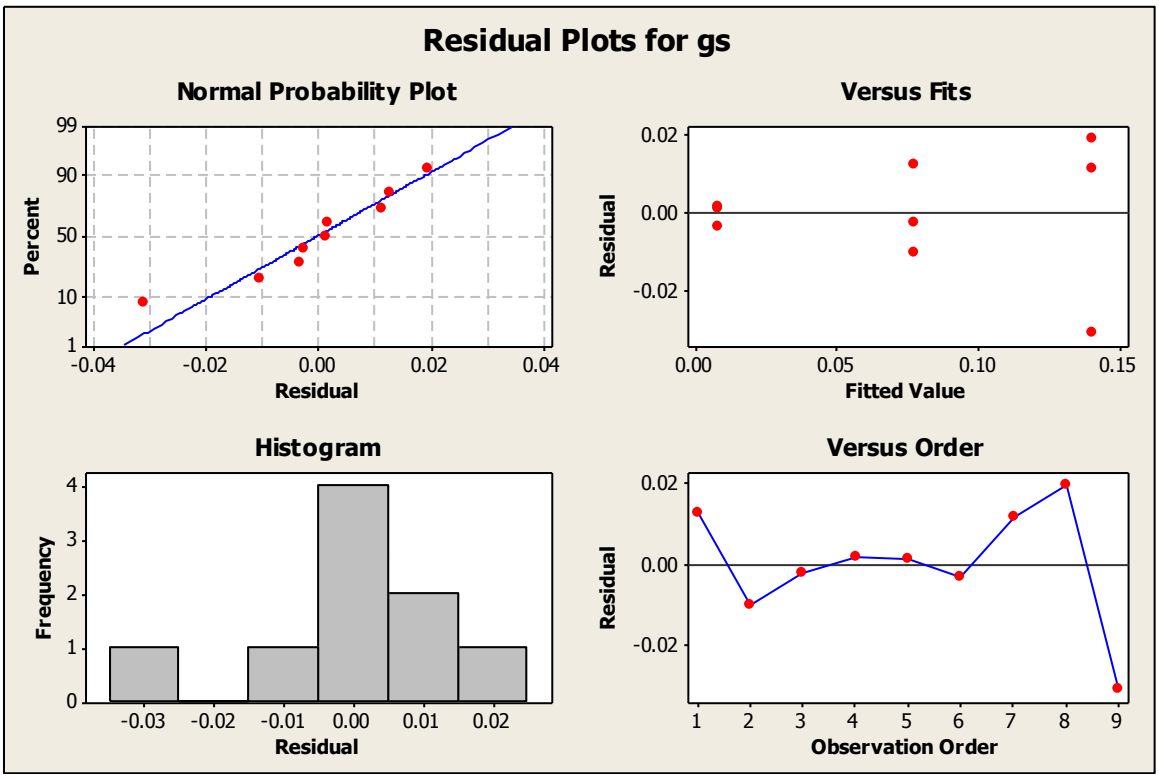

Figure A 3-9c: General Linear Model: Yucca g_s *versus* HS Treatment @ 45°C

```
Factor         Type   Levels  Values
HS Treatment   fixed       3  After 45, Before stress, Recovery after 1 hr


Analysis of Variance for gs, using Adjusted SS for Tests

Source         DF     Seq SS     Adj SS     Adj MS       F      P
HS Treatment    2  0.023676   0.023676  0.011838   15.09  0.001
Error           9  0.007059   0.007059  0.000784
Total          11  0.030736


S = 0.0280066   R-Sq = 77.03%   R-Sq(adj) = 71.93%


Grouping Information Using Tukey Method and 95.0% Confidence

HS Treatment          N     Mean  Grouping
Recovery after 1 hr   4  0.17637  A
Before stress         4  0.08425    B
After 45              4  0.08018    B

Means that do not share a letter are significantly different.
```

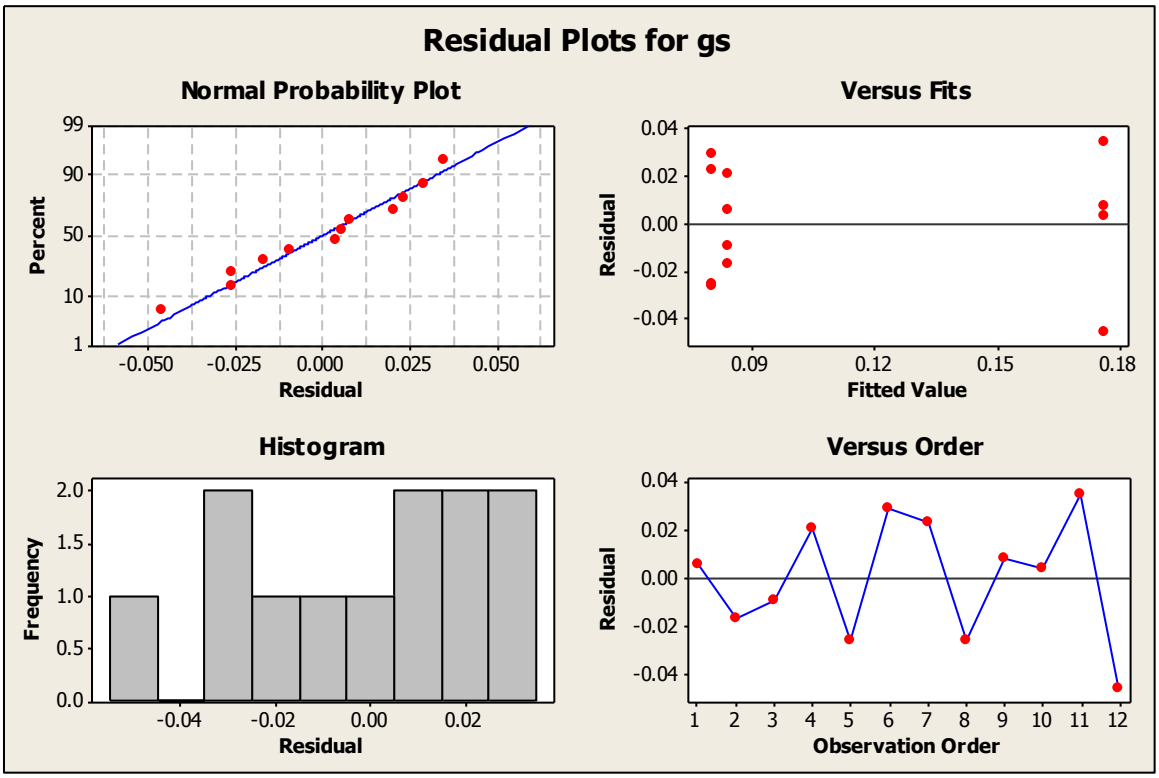

Figure A 3-10a: General Linear Model: Yucca E *versus* HS Treatment @ 38°C

```
Factor          Type   Levels  Values
HS Treatment    fixed       3  After 38, Before stress, Recovery after 1 hr


Analysis of Variance for E, using Adjusted SS for Tests

Source          DF   Seq SS  Adj SS  Adj MS      F      P
HS Treatment     2   9.4341  9.4341  4.7171  28.69  0.000
Error           12   1.9731  1.9731  0.1644
Total           14  11.4073


S = 0.405496   R-Sq = 82.70%   R-Sq(adj) = 79.82%


Grouping Information Using Tukey Method and 95.0% Confidence

HS Treatment          N     Mean  Grouping
Before stress         5   1.9817  A
Recovery after 1 hr   5   1.4694  A
After 38              5   0.1028    B

Means that do not share a letter are significantly different.
```

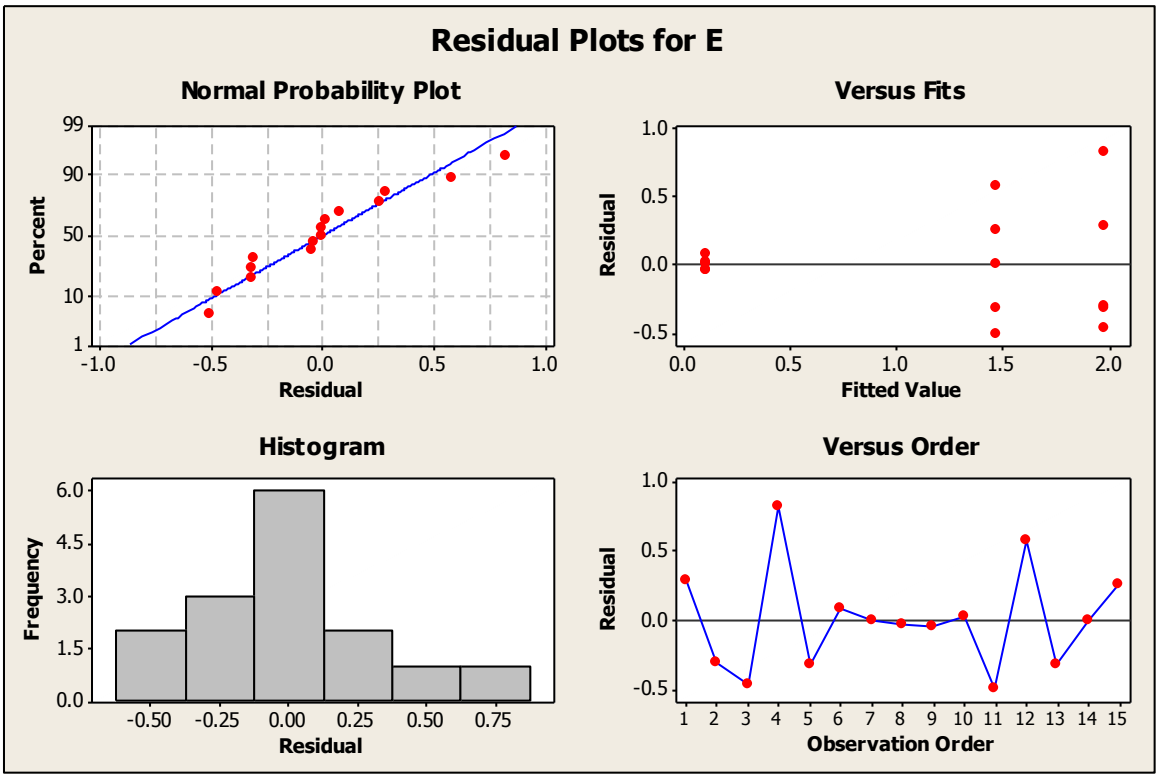

Figure A 3-10b: General Linear Model: Yucca E *versus* HS Treatment @ 40°C

```
Factor          Type   Levels  Values
HS Treatment    fixed       3  After 40, Before stress, Recovery after 1 hr


Analysis of Variance for E, using Adjusted SS for Tests

Source          DF   Seq SS   Adj SS  Adj MS      F      P
HS Treatment     2  11.3158  11.3158  5.6579  32.79  0.001
Error            6   1.0353   1.0353  0.1726
Total            8  12.3511


S = 0.415392   R-Sq = 91.62%   R-Sq(adj) = 88.82%


Grouping Information Using Tukey Method and 95.0% Confidence

HS Treatment          N    Mean  Grouping
Recovery after 1 hr   3  2.9478  A
Before stress         3  1.8130    B
After 40              3  0.2143      C

Means that do not share a letter are significantly different.
```

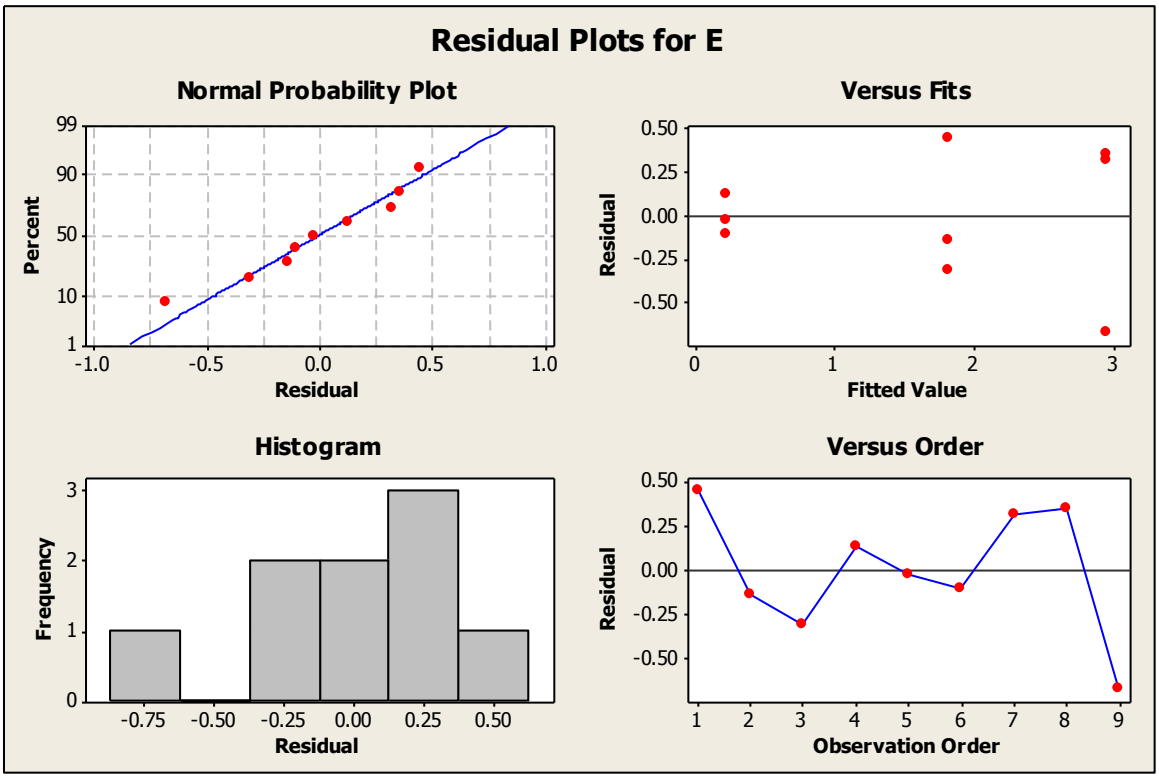

Figure A 3-10c: General Linear Model: Yucca E *versus* HS Treatment @ 45°C

```
Factor         Type   Levels  Values
HS Treatment   fixed       3  After 45, Before stress, Recovery after 1 hr


Analysis of Variance for E, using Adjusted SS for Tests

Source         DF  Seq SS  Adj SS  Adj MS     F      P
HS Treatment    2  5.9905  5.9905  2.9952  9.62  0.006
Error           9  2.8008  2.8008  0.3112
Total          11  8.7913


S = 0.557852   R-Sq = 68.14%   R-Sq(adj) = 61.06%


Grouping Information Using Tukey Method and 95.0% Confidence

HS Treatment          N   Mean  Grouping
Recovery after 1 hr   4  3.350  A
Before stress         4  2.063     B
After 45              4  1.705     B

Means that do not share a letter are significantly different.
```

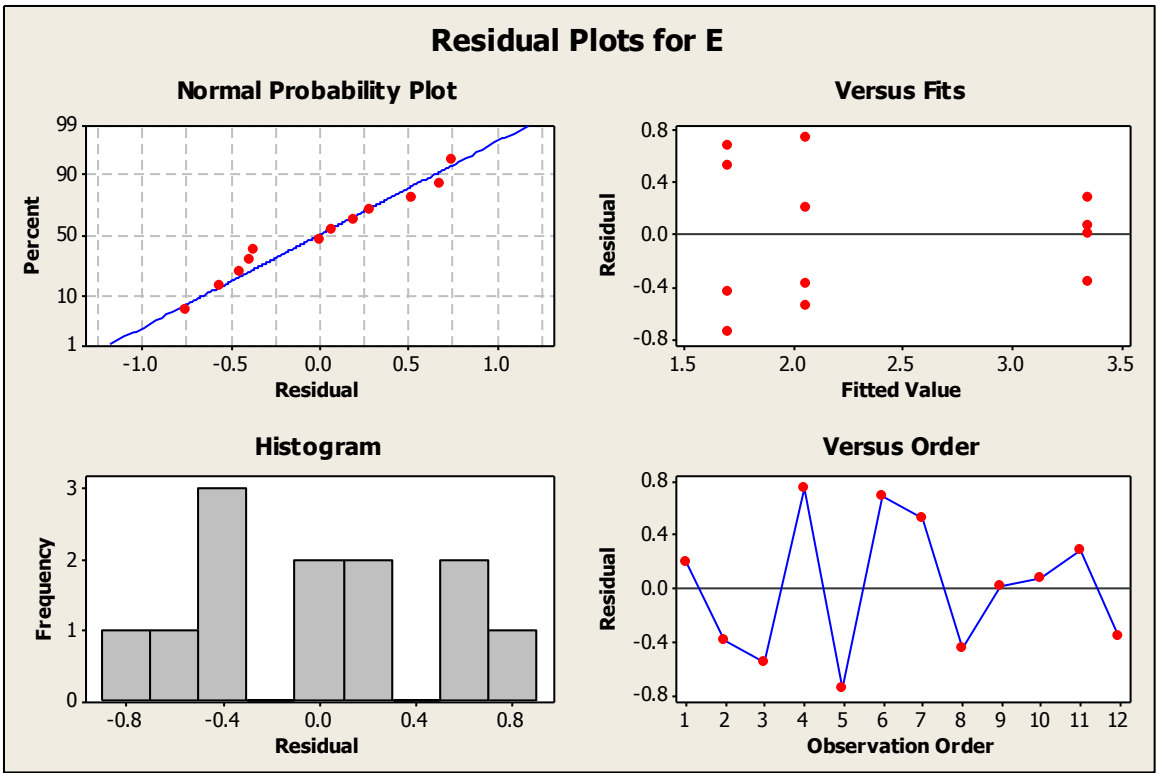

Figure A 3-11: General Linear Model: Yucca PSII Efficiency *versus* HS Treatment

```
Factor         Type   Levels  Values
HS Treatment   fixed       4  25, 38, 40, 45


Analysis of Variance for Yucca PSII Efficiency, using Adjusted SS for Tests

Source         DF     Seq SS     Adj SS     Adj MS      F      P
HS Treatment    3   0.133059   0.133059   0.044353  76.77  0.000
Error          10   0.005777   0.005777   0.000578
Total          13   0.138836


S = 0.0240356   R-Sq = 95.84%   R-Sq(adj) = 94.59%


Grouping Information Using Tukey Method and 95.0% Confidence

HS
Treatment  N     Mean  Grouping
25         3   0.8217  A
38         4   0.7035    B
40         4   0.6928    B
45         3   0.5263      C

Means that do not share a letter are significantly different.
```

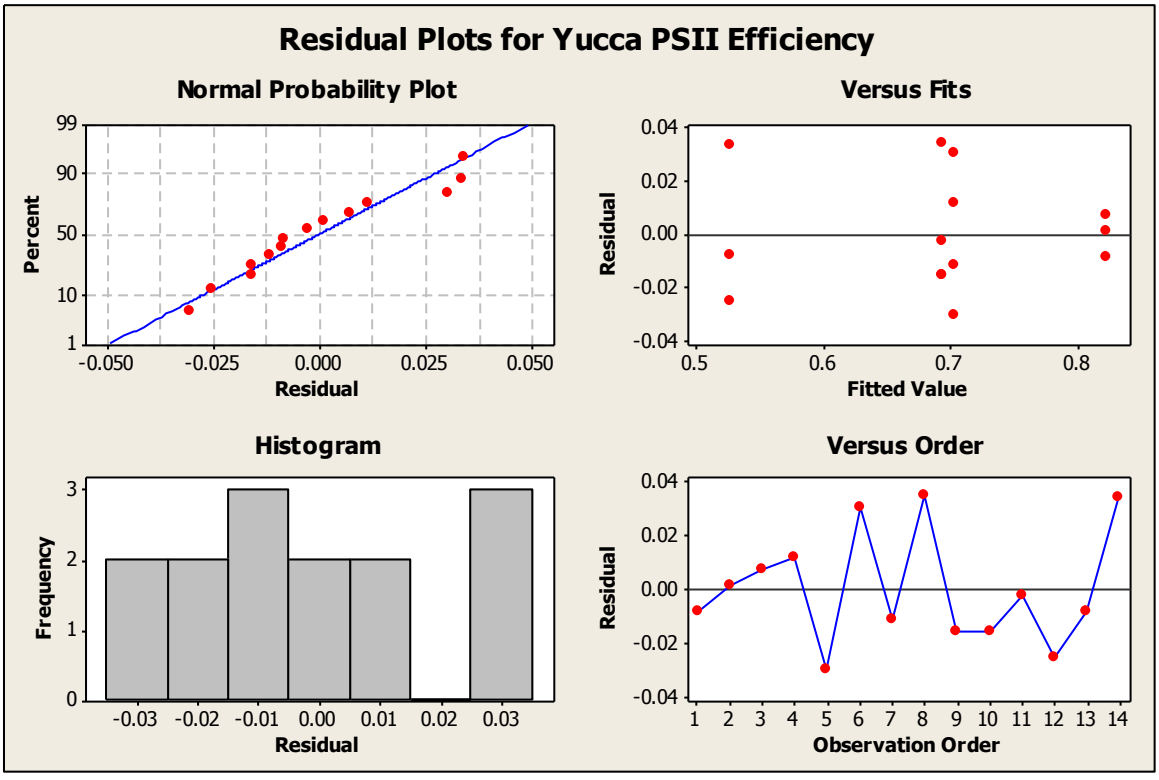

Figure A 3-12a: General Linear Model: Yucca ETR *versus* HS Treatment

```
Factor         Type   Levels  Values
HS Treatment   fixed       4  25, 38, 40, 45


Analysis of Variance for Yucca ETR, using Adjusted SS for Tests

Source         DF  Seq SS  Adj SS  Adj MS      F      P
HS Treatment    3   31526   31526   10509  90.87  0.000
Error          15    1735    1735     116
Total          18   33261


S = 10.7537   R-Sq = 94.78%   R-Sq(adj) = 93.74%


Grouping Information Using Tukey Method and 95.0% Confidence

HS
Treatment  N    Mean  Grouping
25         5  112.05  A
38         5  102.64  A
40         3   72.13     B
45         6   15.98       C

Means that do not share a letter are significantly different.
```

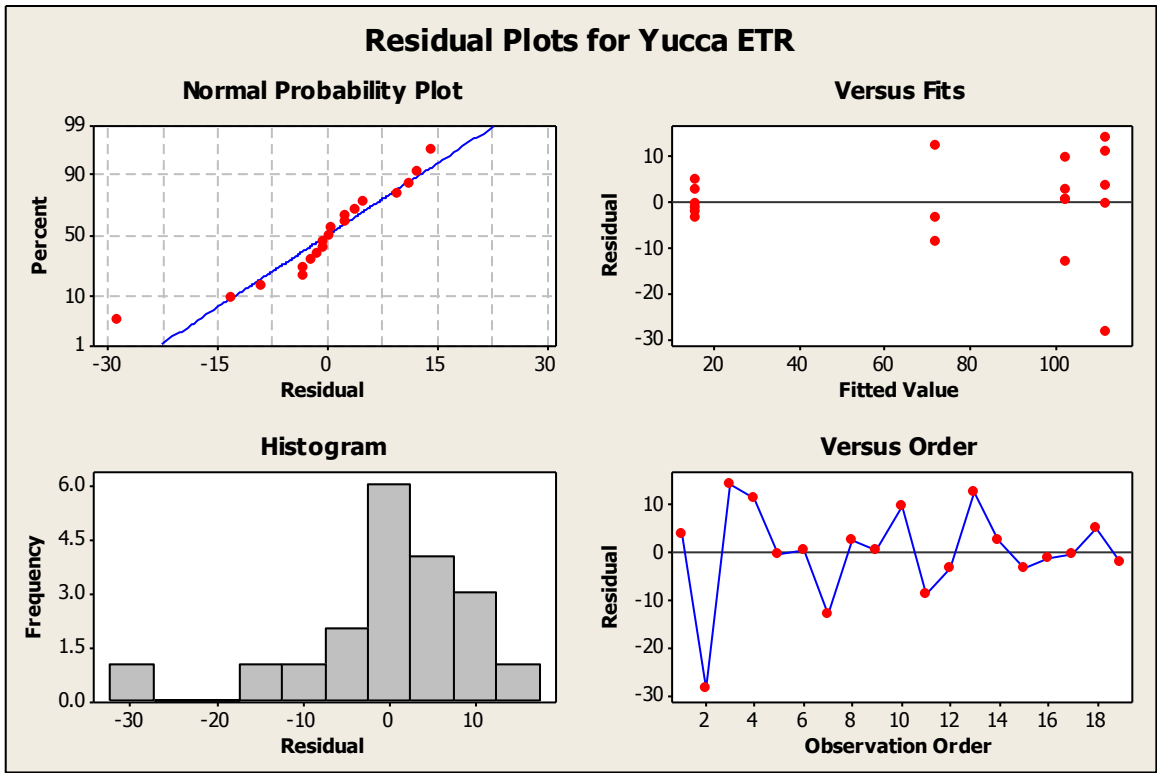

Figure A 3-12b: General Linear Model: Log ETR *versus* HS Treatment @ 45°C

```
Factor        Type   Levels  Values
HS Treatment  fixed       3  0, 3, 72


Analysis of Variance for LOG, using Adjusted SS for Tests

Source        DF   Seq SS   Adj SS   Adj MS       F      P
HS Treatment   2  1.61753  1.61753  0.80876  198.76  0.000
Error          9  0.03662  0.03662  0.00407
Total         11  1.65415


S = 0.0637888   R-Sq = 97.79%   R-Sq(adj) = 97.29%

Grouping Information Using Tukey Method and 95.0% Confidence

HS
Treatment  N   Mean  Grouping
 0         4  2.044  A
72         4  1.980  A
 3         4  1.235     B
```

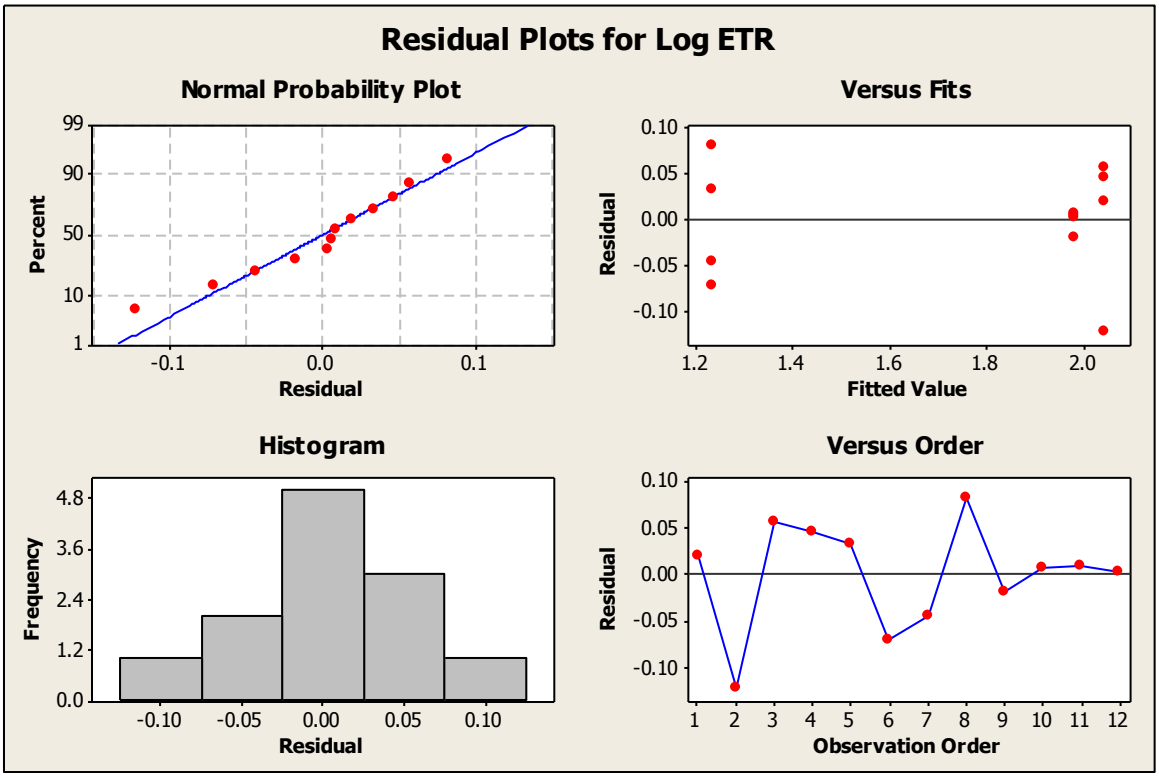

Figure A 4-1: General Linear Model: ETR *in vitro versus* HS Treatment

```
Factor        Type   Levels  Values
HS Treatment  fixed       4  25, 36, 38, 40


Analysis of Variance for ETR in vitro, using Adjusted SS for Tests

Source        DF   Seq SS   Adj SS  Adj MS      F      P
HS Treatment   3  27572.0  27572.0  9190.7  31.33  0.000
Error         16   4693.6   4693.6   293.3
Total         19  32265.6


S = 17.1274   R-Sq = 85.45%   R-Sq(adj) = 82.73%


Grouping Information Using Tukey Method and 95.0% Confidence

HS
Treatment  N    Mean  Grouping
25         5  165.17  A
36         5  148.51  A B
38         5  128.41    B
40         5   67.06      C

Means that do not share a letter are significantly different.
```

MSD= 27.9

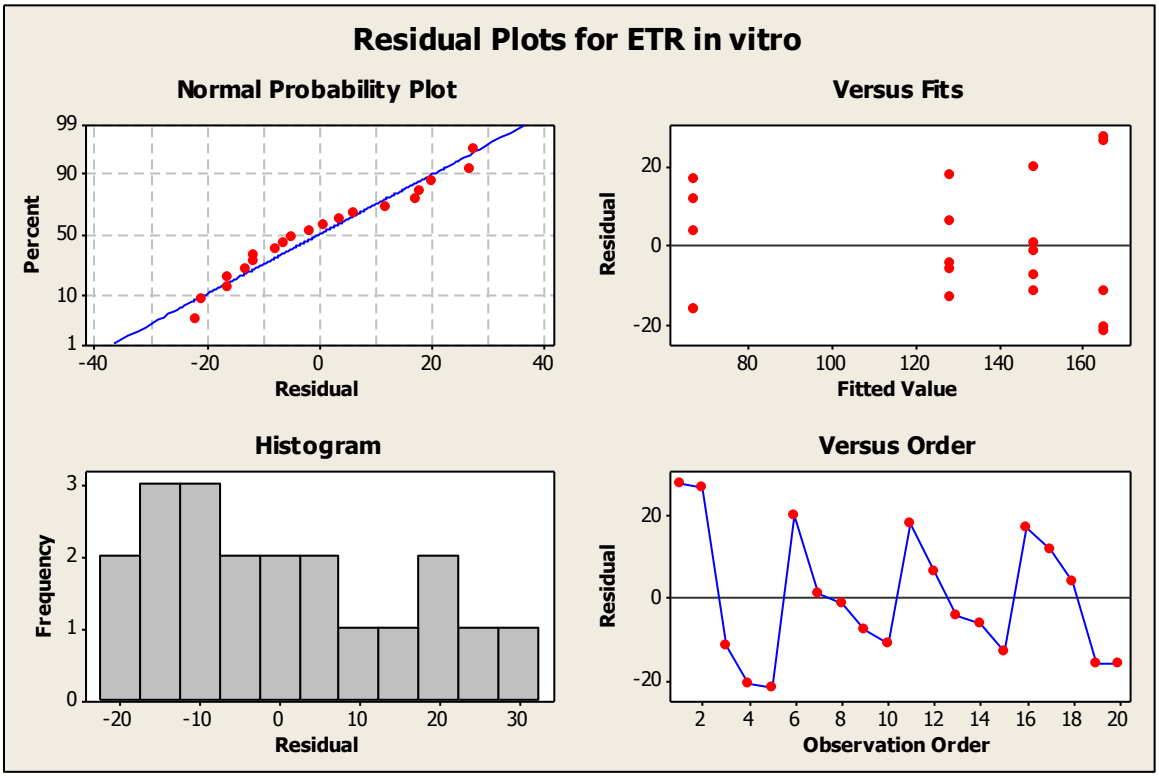

Figure A 4-2: General Linear Model: 3-PGA Production *versus* Substrate, HS Treatment

```
Factor         Type   Levels  Values
Substrate      fixed       2  1(+ RuBP), 2(Blank)
HS Treatment   fixed       3  25, 38, 40


Analysis of Variance for 3-PGA Production, using Adjusted SS for Tests

Source                   DF     Seq SS     Adj SS     Adj MS       F      P
Substrate                 1  122493744  122135759  122135759  103.69  0.000
HS Treatment              2    1870319    1281984     640992    0.54  0.590
Substrate*HS Treatment    2     592619     592619     296310    0.25  0.780
Error                    17   20023831   20023831    1177872
Total                    22  144980513


S = 1085.30   R-Sq = 86.19%   R-Sq(adj) = 82.13%

Grouping Information Using Tukey Method and 95.0% Confidence

            HS
Substrate   Treatment  N    Mean  Grouping
1           25         5  5655.1  A
1           40         4  5235.8  A
1           38         5  4676.2  A
2           25         3   541.1     B
2           40         3   474.3     B
2           38         3   355.7     B

Means that do not share a letter are significantly different.
```

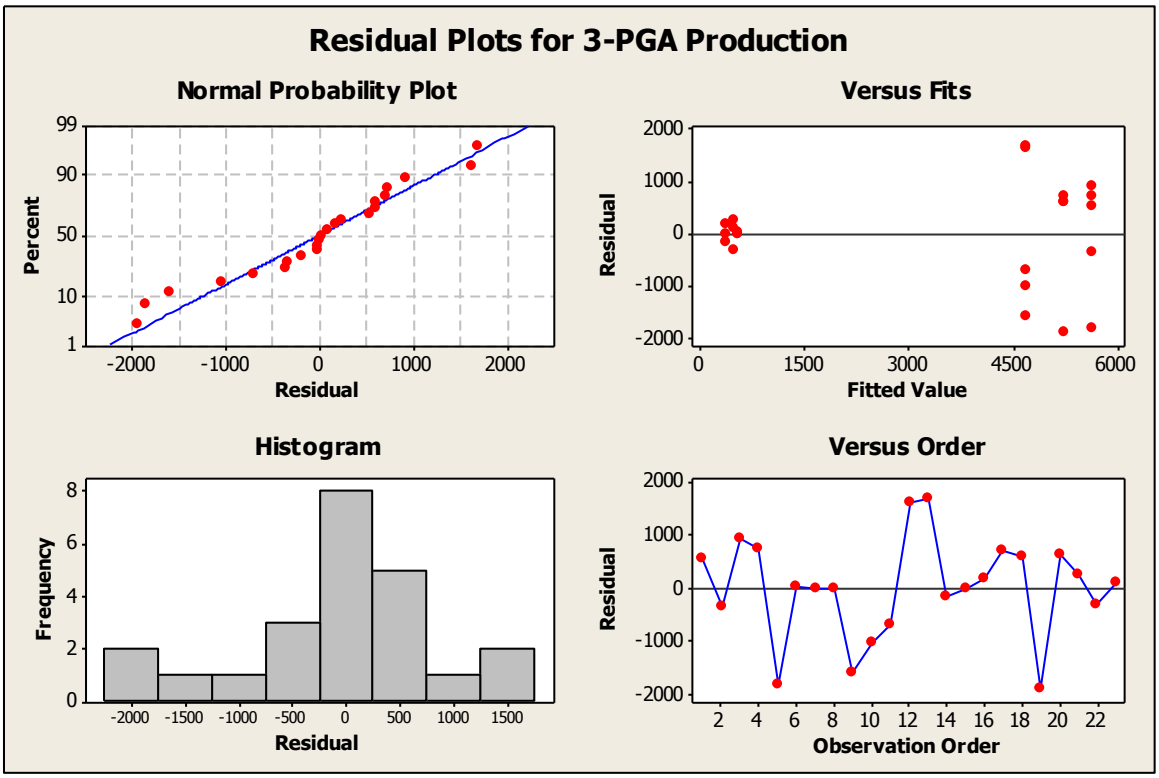

Figure A 4-3: General Linear Model: Activity *versus* Factor

```
Factor  Type   Levels  Values
Factor  fixed       3  1 (25°C+ATP), 2(25°C-ATP), 3(80°C+ATP)


Analysis of Variance for Activity, using Adjusted SS for Tests

Source  DF  Seq SS  Adj SS  Adj MS        F      P
Factor   2   46419   46419   23209  3529.15  0.000
Error    6      39      39       7
Total    8   46458


S = 2.56446   R-Sq = 99.92%   R-Sq(adj) = 99.89%


Grouping Information Using Tukey Method and 95.0% Confidence

Factor  N     Mean  Grouping
1       3  159.593  A
3       3    7.434    B
2       3    7.060    B

Means that do not share a letter are significantly different.
```

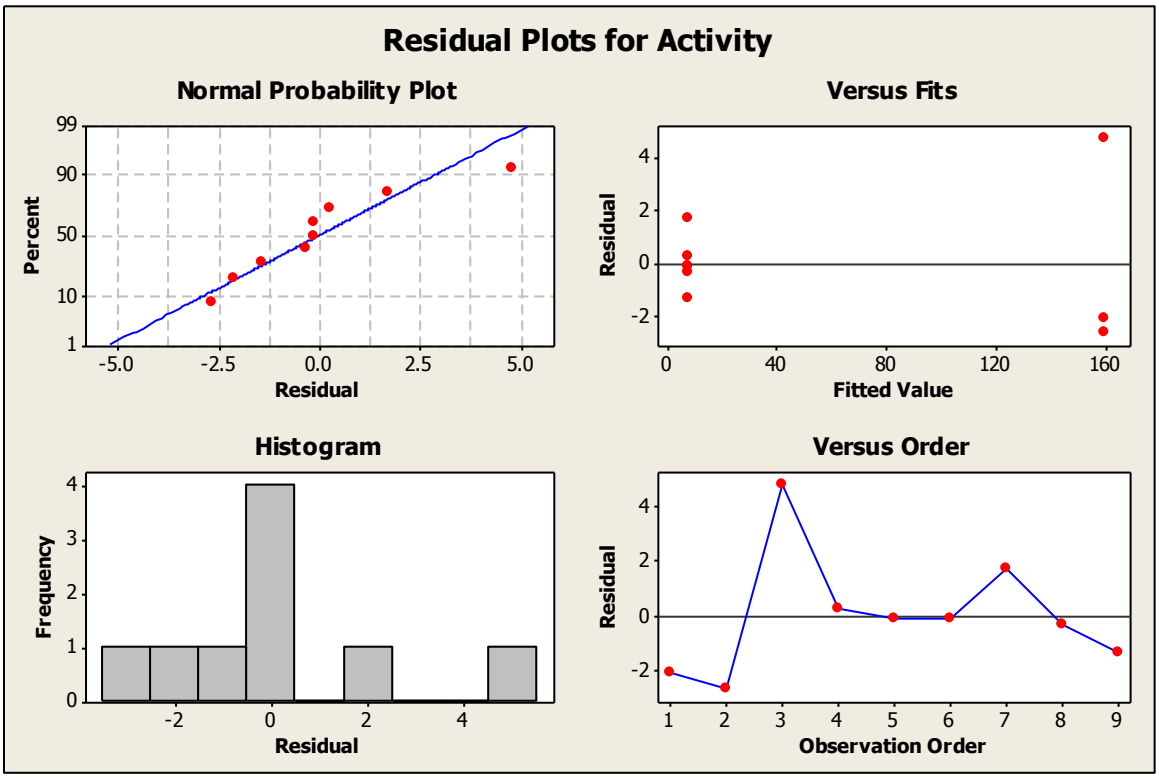

Figure A 4-4: General Linear Model: Activity *versus* Temperature

```
Factor       Type   Levels  Values
Temperature  fixed       2  25, 80


Analysis of Variance for Activity, using Adjusted SS for Tests

Source       DF  Seq SS  Adj SS  Adj MS     F      P
Temperature   1    22.0    22.0    22.0  0.17  0.719
Error         2   256.3   256.3   128.1
Total         3   278.2


S = 11.3194   R-Sq = 7.90%   R-Sq(adj) = 0.00%


Grouping Information Using Tukey Method and 95.0% Confidence

Temperature  N   Mean  Grouping
25           2  203.6  A
80           2  198.9  A

Means that do not share a letter are significantly different.
```

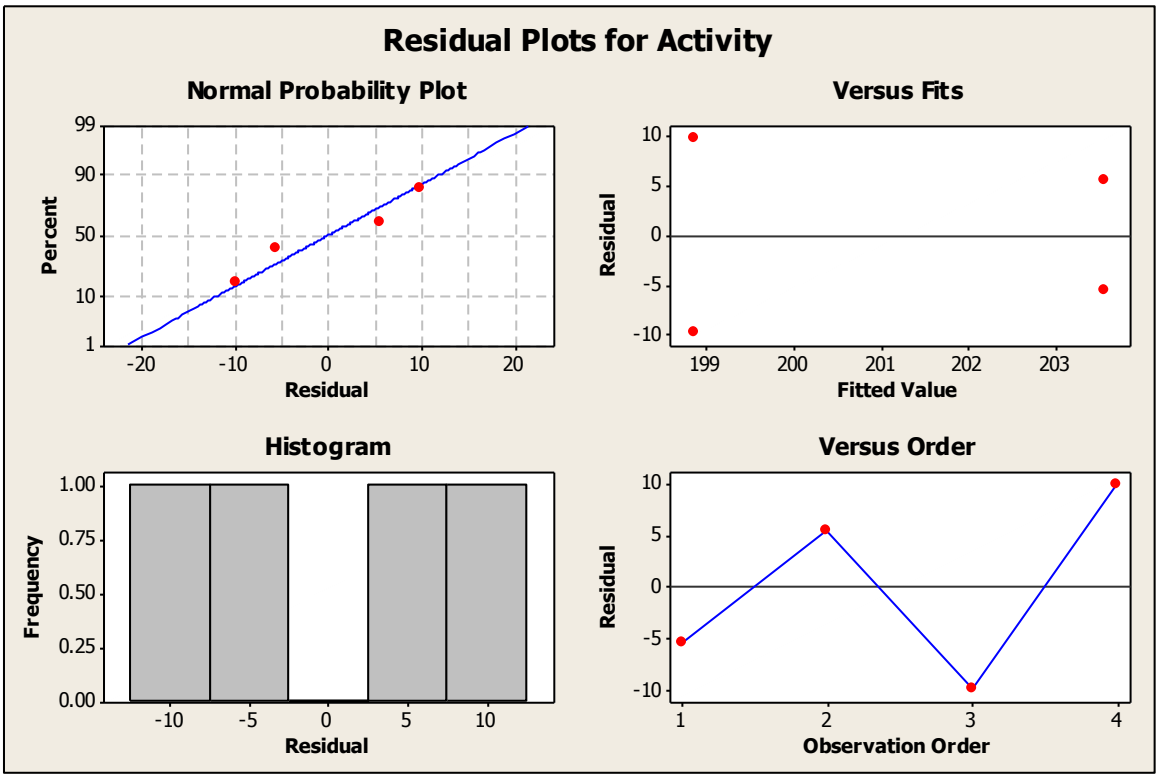

Figure A 4-5: General Linear Model: Activity *versus* Incubation at 80°C

```
Factor                Type   Levels  Values
Incubation at 80°C    fixed       3  blank, Ri5P, RuBP


Analysis of Variance for Activity, using Adjusted SS for Tests

Source                DF  Seq SS  Adj SS  Adj MS     F      P
Incubation at 80°C     2    54.7    54.7    27.4  0.27  0.774
Error                  4   400.8   400.8   100.2
Total                  6   455.5


S = 10.0099   R-Sq = 12.02%   R-Sq(adj) = 0.00%


Grouping Information Using Tukey Method and 95.0% Confidence

Incubation
at 80°C      N   Mean  Grouping
Ri5P         2  48.60  A
blank        3  44.73  A
RuBP         2  41.21  A

Means that do not share a letter are significantly different.
```

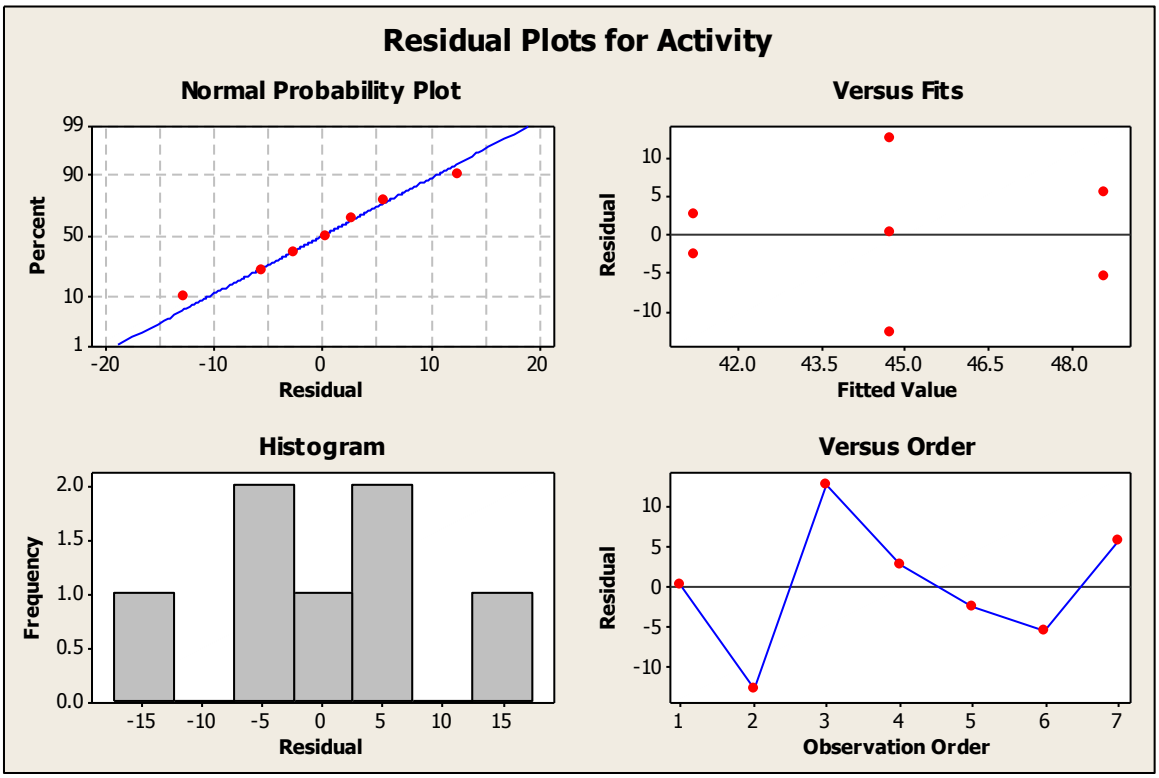

Figure A 4-6a: General Linear Model: *in vivo* RuBisCO Activity *versus* HS Treatment

```
Factor        Type   Levels  Values
HS Treatment  fixed       4  25, 38, 40, 42


Analysis of Variance for In Vivo RuBisCO Activity, using Adjusted SS for Tests

Source        DF    Seq SS    Adj SS   Adj MS     F      P
HS Treatment   3  22916546  22916546  7638849  6.96  0.007
Error         11  12071802  12071802  1097437
Total         14  34988348


Grouping Information Using Tukey Method and 95.0% Confidence

HS
Treatment  N  Mean  Grouping
25         4  6116  A
38         4  5462  A
40         3  5031  A B
42         4  2919    B

Means that do not share a letter are significantly different.
```

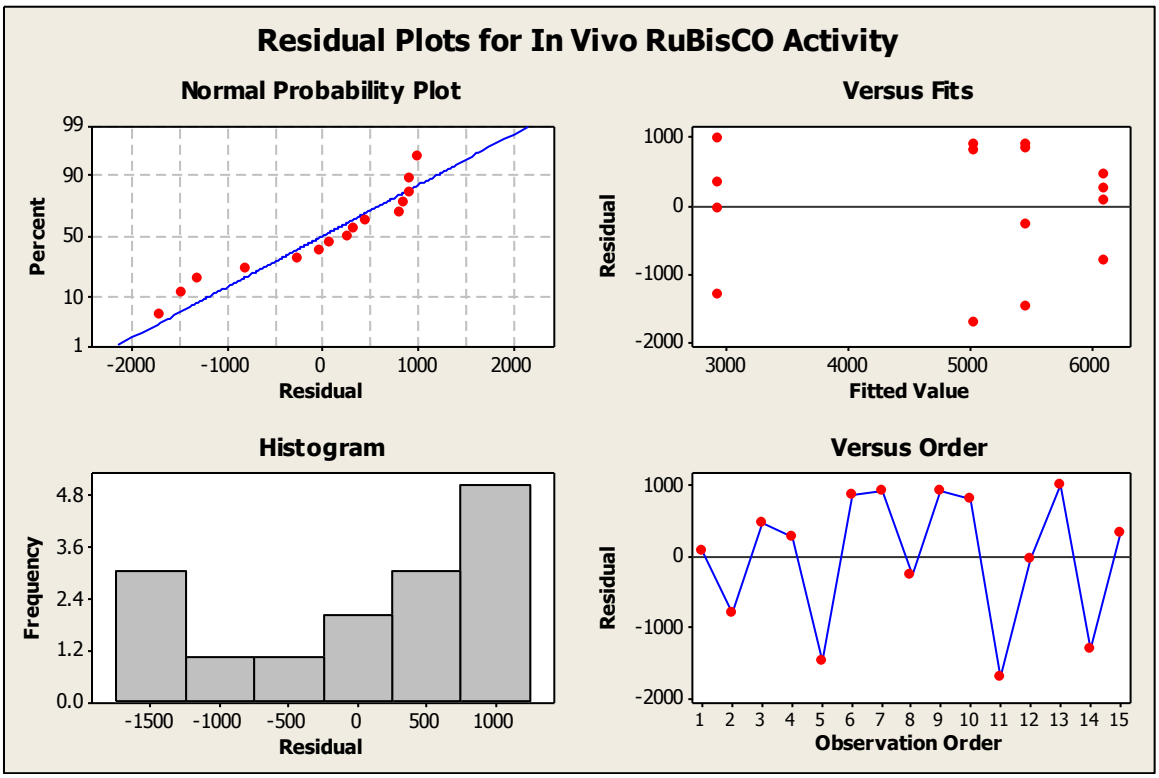

Figure A 4-6b: General Linear Model: Total RuBisCO Activity versus HS Treatment

```
Factor        Type   Levels  Values
HS Treatment  fixed       4  25, 38, 40, 42


Analysis of Variance for Total  RuBisco Activity, using Adjusted SS for Tests

Source        DF    Seq SS    Adj SS    Adj MS     F      P
HS Treatment   3  58978132  58978132  19659377  5.96  0.011
Error         11  36292673  36292673   3299334
Total         14  95270805


S = 1816.41   R-Sq = 61.91%   R-Sq(adj) = 51.52%


Grouping Information Using Tukey Method and 95.0% Confidence

HS
Treatment  N   Mean  Grouping
25         4  10006  A
38         4   7810  A B
40         3   7713  A B
42         4   4613    B

Means that do not share a letter are significantly different.
```

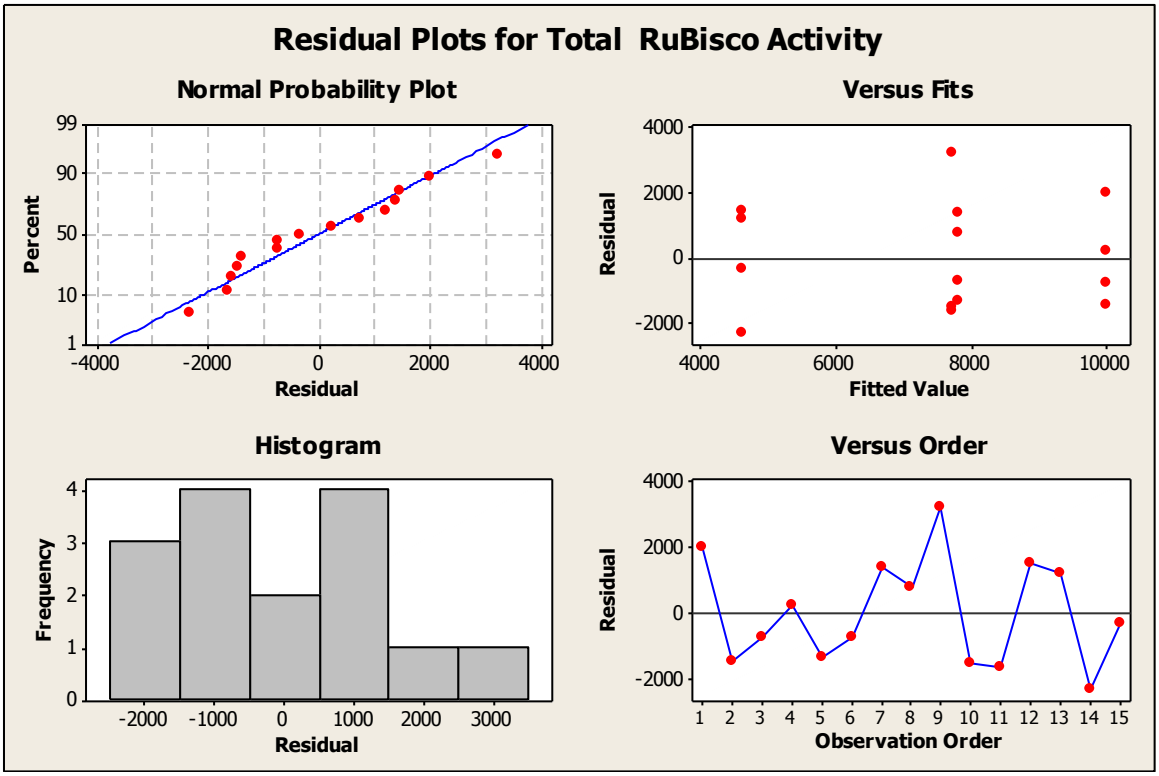

Figure A 4-7: General Linear Model: RuBisCO Activation state *versus* HS Treatment

```
Factor        Type   Levels  Values
HS Treatment  fixed       4  25, 38, 40, 42


Analysis of Variance for RuBisco Activation state, using Adjusted SS for Tests

Source        DF  Seq SS  Adj SS  Adj MS     F      P
HS Treatment   3   155.8   155.8    51.9  0.25  0.859
Error         11  2279.6  2279.6   207.2
Total         14  2435.4


S = 14.3956   R-Sq = 6.40%   R-Sq(adj) = 0.00%


Grouping Information Using Tukey Method and 95.0% Confidence

HS
Treatment  N   Mean  Grouping
38         4  70.29  A
40         3  67.98  A
42         4  65.36  A
25         4  61.82  A

Means that do not share a letter are significantly different.
```

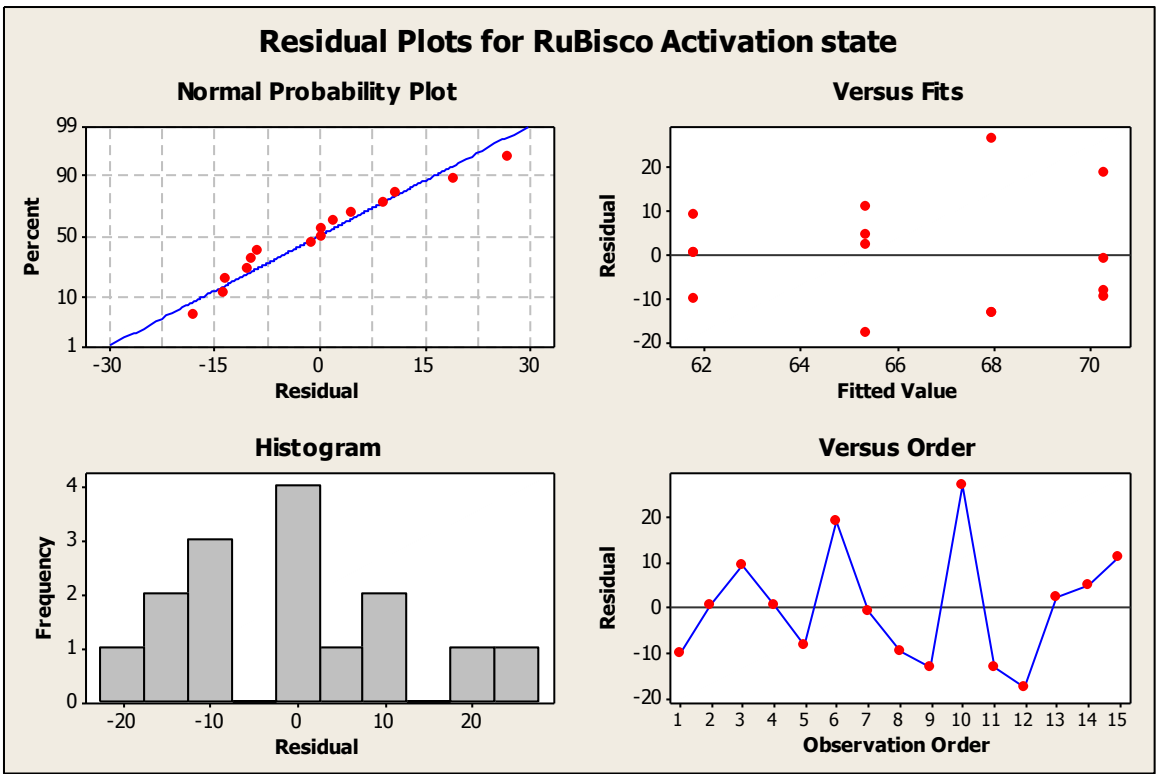

Figure A 4-8: General Linear Model: *in vivo* RuBisCO and ETR *versus*, HS Treatment

Factor	Type	Levels	Values
RuBisCO (1), ETR (2)	fixed	2	1, 2
HS Treatment	fixed	4	25, 38, 40, 42

Analysis of Variance for in vivo RuBisCO and ETR, using Adjusted SS for Tests

Source	DF	Seq SS	Adj SS	Adj MS	F	P
RuBisCO (1), ETR (2)	1	22638.1	24010.6	24010.6	233.84	0.000
HS Treatment	3	28744.0	28744.0	9581.3	93.31	0.000
RuBisCO (1), ETR (2)*HS Treatment	3	9055.2	9055.2	3018.4	29.40	0.000
Error	30	3080.4	3080.4	102.7		
Total	37	63517.7				

S = 10.1331 R-Sq = 95.15% R-Sq(adj) = 94.02%

Grouping Information Using Tukey Method and 95.0% Confidence

RuBisCO (1), ETR (2)	HS Treatment	N	Mean	Grouping
1	25	5	100.000	A
2	25	5	100.000	A
1	38	5	90.002	A
1	40	4	84.662	A
1	42	5	53.948	B
2	38	5	23.775	C
2	40	4	1.984	C D
2	42	5	0.818	D

Means that do not share a letter are significantly different.

MSD= 15.9

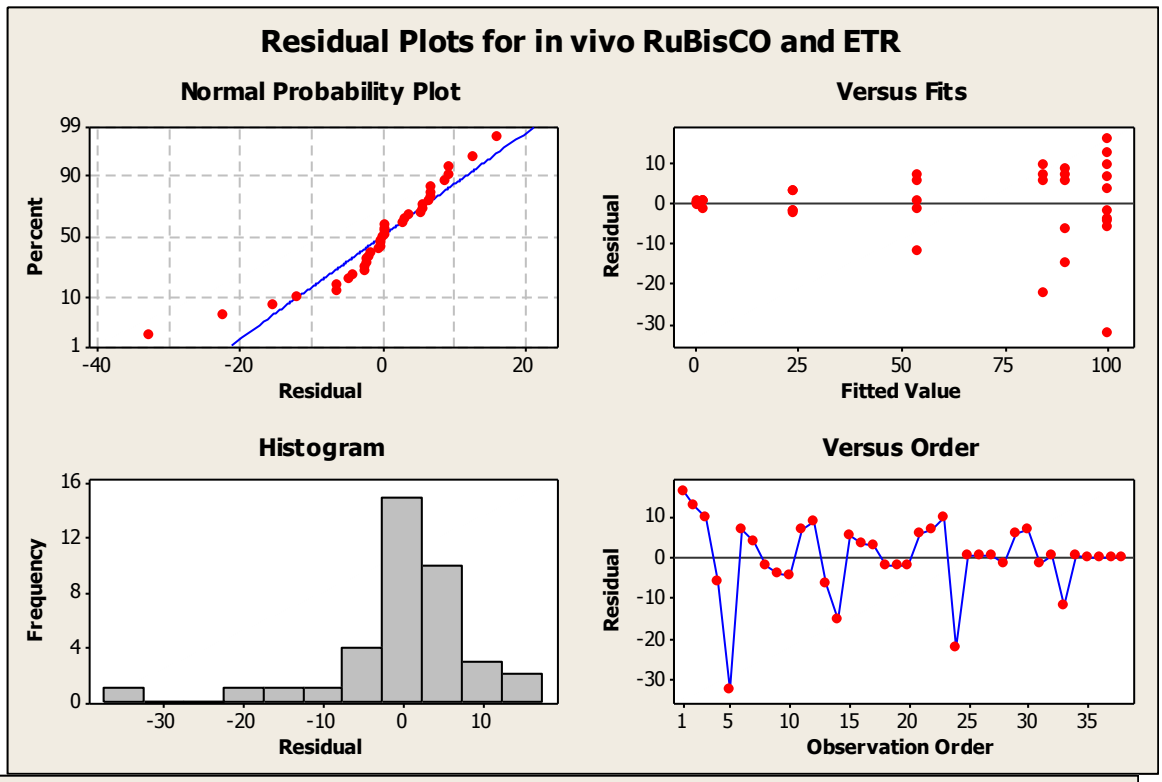
Residual Plots for in vivo RuBisCO and ETR
Normal Probability Plot
Percent
Residual
Versus Fits
Residual
Fitted Value
Histogram
Frequency
Residual
Versus Order
Residual
Observation Order

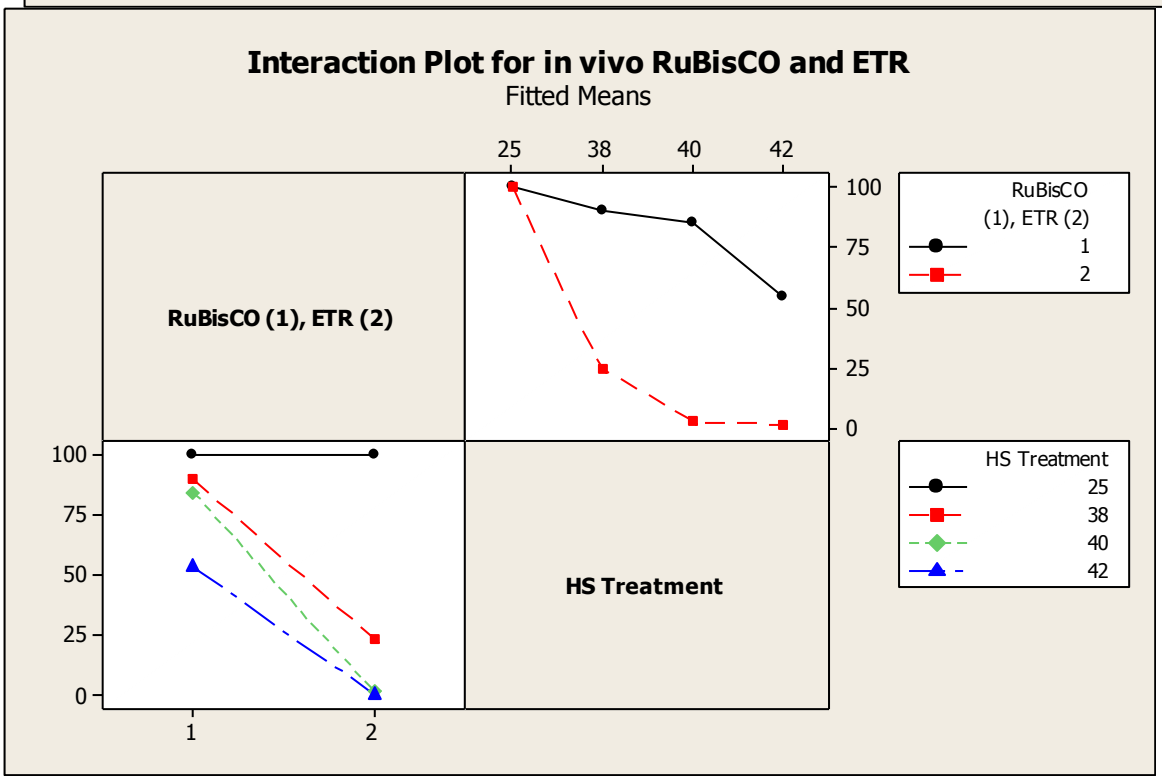
Interaction Plot for in vivo RuBisCO and ETR
Fitted Means
RuBisCO (1), ETR (2)
HS Treatment
RuBisCO (1), ETR (2)
1
2
HS Treatment
25
38
40
42

Figure A 4-9: General Linear Model: Log *in vivo* RuBisCO Activity *versus* Extraction Buffer, Leaf condition

Factor	Type	Levels	Values
Extraction Buffer	fixed	2	1(- Mg2+), 2(+ Mg2+)
Leaf condition	fixed	3	Dark @ 22°C, Light @ 22°C, Light @ 38°C

Analysis of Variance for Log, using Adjusted SS for Tests

Source	DF	Seq SS	Adj SS	Adj MS	F	P
Extraction Buffer	1	0.22889	0.20991	0.20991	75.03	0.000
Leaf condition	2	0.27927	0.26954	0.13477	48.17	0.000
Extraction Buffer*Leaf condition	2	0.27253	0.27253	0.13626	48.71	0.000
Error	11	0.03077	0.03077	0.00280		
Total	16	0.81145				

S = 0.0528928 R-Sq = 96.21% R-Sq(adj) = 94.48%

Grouping Information Using Tukey Method and 95.0% Confidence

Extraction Buffer	Leaf condition	N	Mean	Grouping
2	Light @ 22°C	3	3.840	A
2	Dark @ 22°C	3	3.803	A
1	Light @ 22°C	3	3.775	A
2	Light @ 38°C	2	3.730	A
1	Light @ 38°C	3	3.700	A
1	Dark @ 22°C	3	3.223	B

Means that do not share a letter are significantly different.

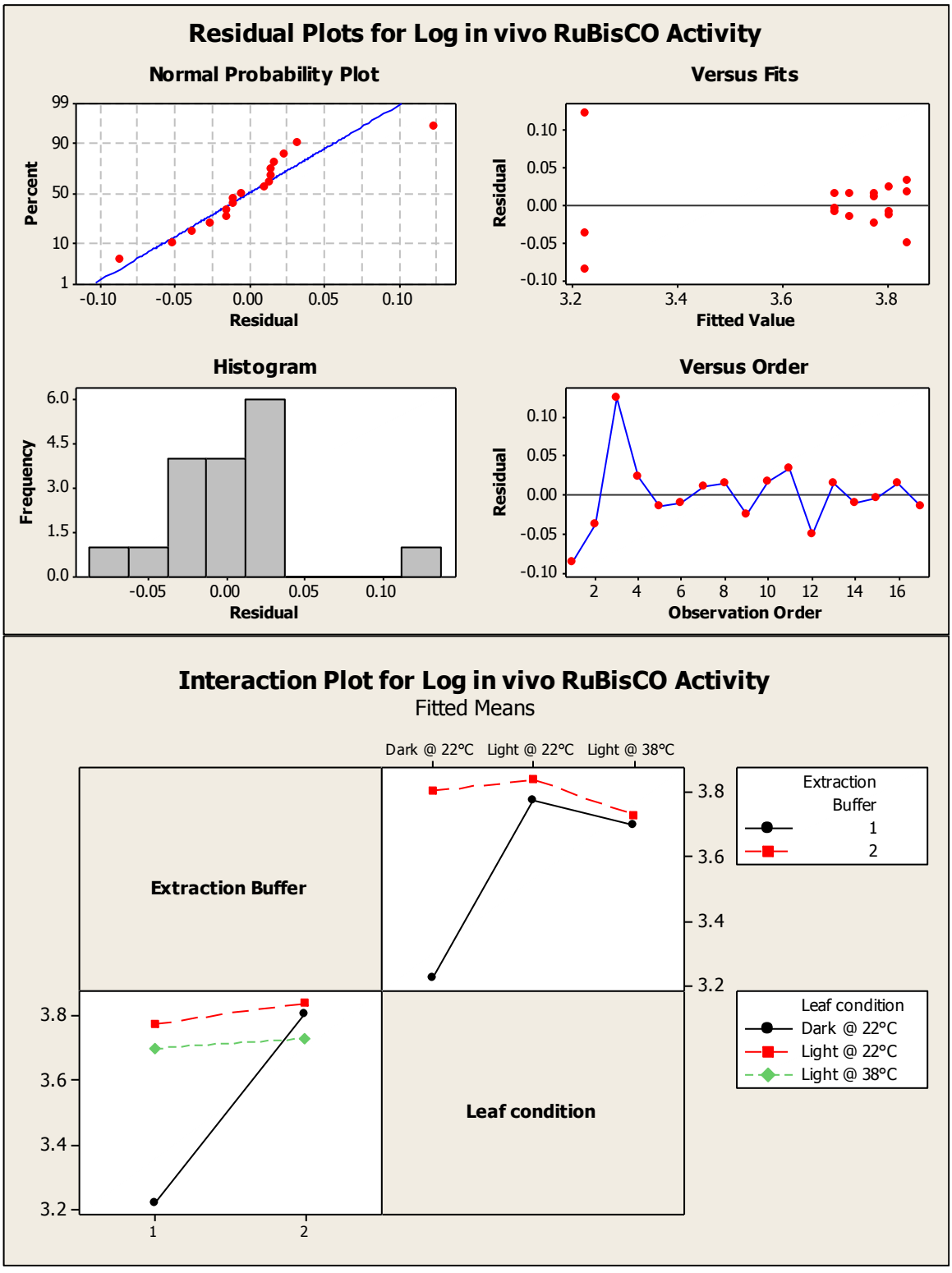
Residual Plots for Log in vivo RuBisCO Activity
Normal Probability Plot
Percent
Residual
Versus Fits
Residual
Fitted Value
Histogram
Frequency
Residual
Versus Order
Residual
Observation Order
Interaction Plot for Log in vivo RuBisCO Activity
Fitted Means
Dark @ 22°C
Light @ 22°C
Light @ 38°C
Extraction Buffer
Leaf condition
Extraction Buffer
1
2
Leaf condition
Dark @ 22°C
Light @ 22°C
Light @ 38°C

Figure A 4-10: General Linear Model: Log *In vivo* RuBisCO Activity *versus* Extraction Buffer, Leaf condition

Factor	Type	Levels	Values
Extraction Buffer	fixed	2	1(- DTT), 2(+DTT)
Leaf condition	fixed	3	Dark @ 22°C, Light @ 22°C, Light @ 38°C

Analysis of Variance for Log, using Adjusted SS for Tests

Source	DF	Seq SS	Adj SS	Adj MS	F	P
Extraction Buffer	1	0.000600	0.000020	0.000020	0.01	0.920
Leaf condition	2	0.024471	0.026645	0.013323	6.96	0.011
Extraction Buffer*Leaf condition	2	0.003830	0.003830	0.001915	1.00	0.399
Error	11	0.021041	0.021041	0.001913		
Total	16	0.049942				

S = 0.0437358 R-Sq = 57.87% R-Sq(adj) = 38.72%

Grouping Information Using Tukey Method and 95.0% Confidence

Extraction Buffer	Leaf condition	N	Mean	Grouping
1	Light @ 22°C	3	3.858	A
2	Light @ 22°C	3	3.840	A
1	Dark @ 22°C	3	3.833	A
2	Dark @ 22°C	3	3.803	A
2	Light @ 38°C	3	3.771	A
1	Light @ 38°C	2	3.730	A

Means that do not share a letter are significantly different.

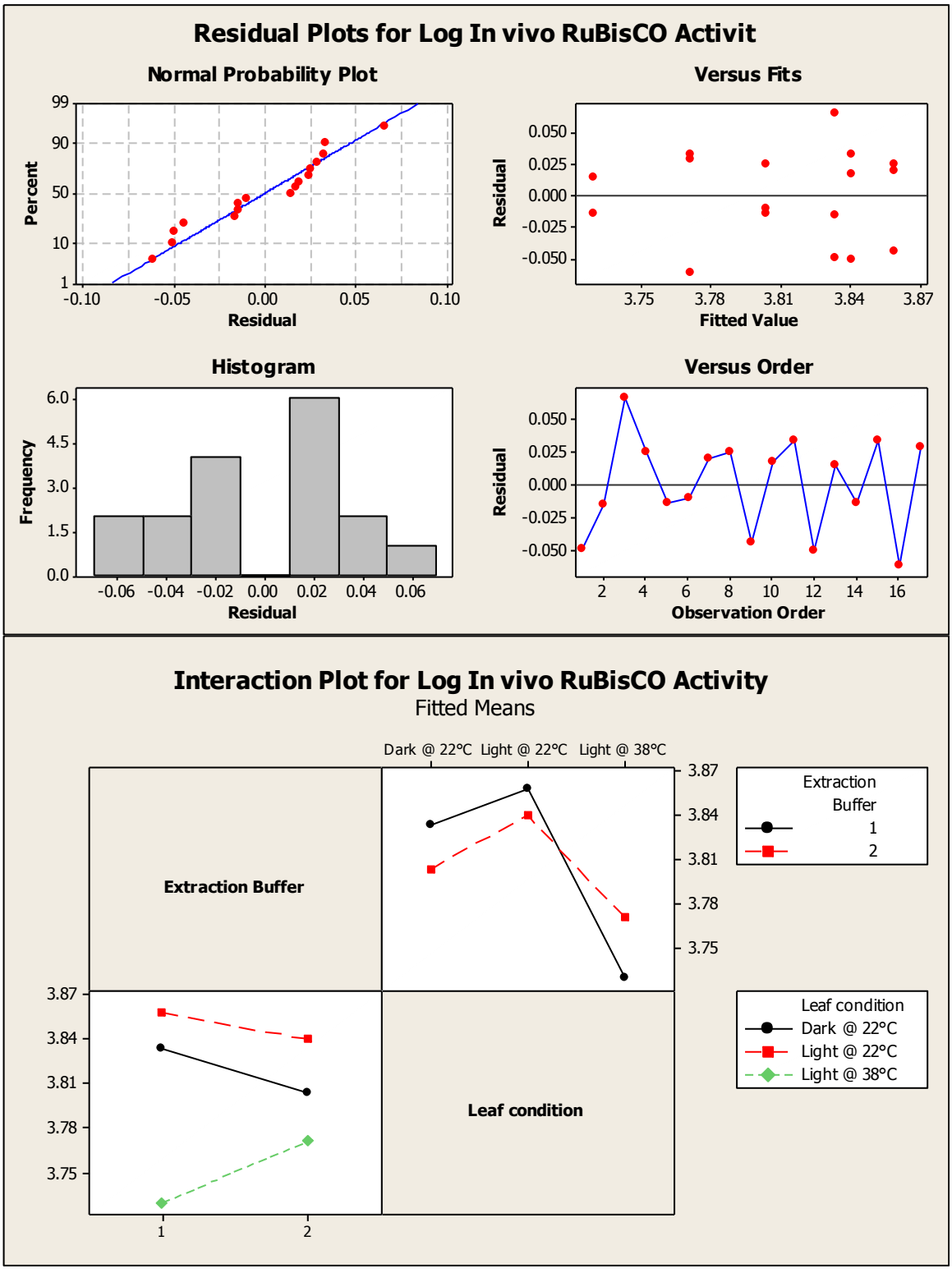
Residual Plots for Log In vivo RuBisCO Activit
Normal Probability Plot
Percent
Residual
Versus Fits
Residual
Fitted Value
Histogram
Frequency
Residual
Versus Order
Residual
Observation Order
Interaction Plot for Log In vivo RuBisCO Activity
Fitted Means
Dark @ 22°C
Light @ 22°C
Light @ 38°C
Extraction Buffer
Leaf condition
Extraction Buffer
1
2
Leaf condition
Dark @ 22°C
Light @ 22°C
Light @ 38°C

Figure A 4-11: General Linear Model: Ri5PI and PRK Activity *versus* HS Treatment

```
Factor        Type   Levels  Values
HS Treatment  fixed       4  25, 36, 38, 40


Analysis of Variance for Ri5PI and PRK Activity, using Adjusted SS for Tests

Source        DF  Seq SS  Adj SS  Adj MS      F      P
HS Treatment   3   35456   35456   11819  16.35  0.001
Error          8    5782    5782     723
Total         11   41237


S = 26.8829   R-Sq = 85.98%   R-Sq(adj) = 80.72%


Grouping Information Using Tukey Method and 95.0% Confidence

HS
Treatment  N    Mean  Grouping
25         3  158.27  A
36         3  133.01  A
38         3   42.24    B
40         3   34.82    B

Means that do not share a letter are significantly different.
```

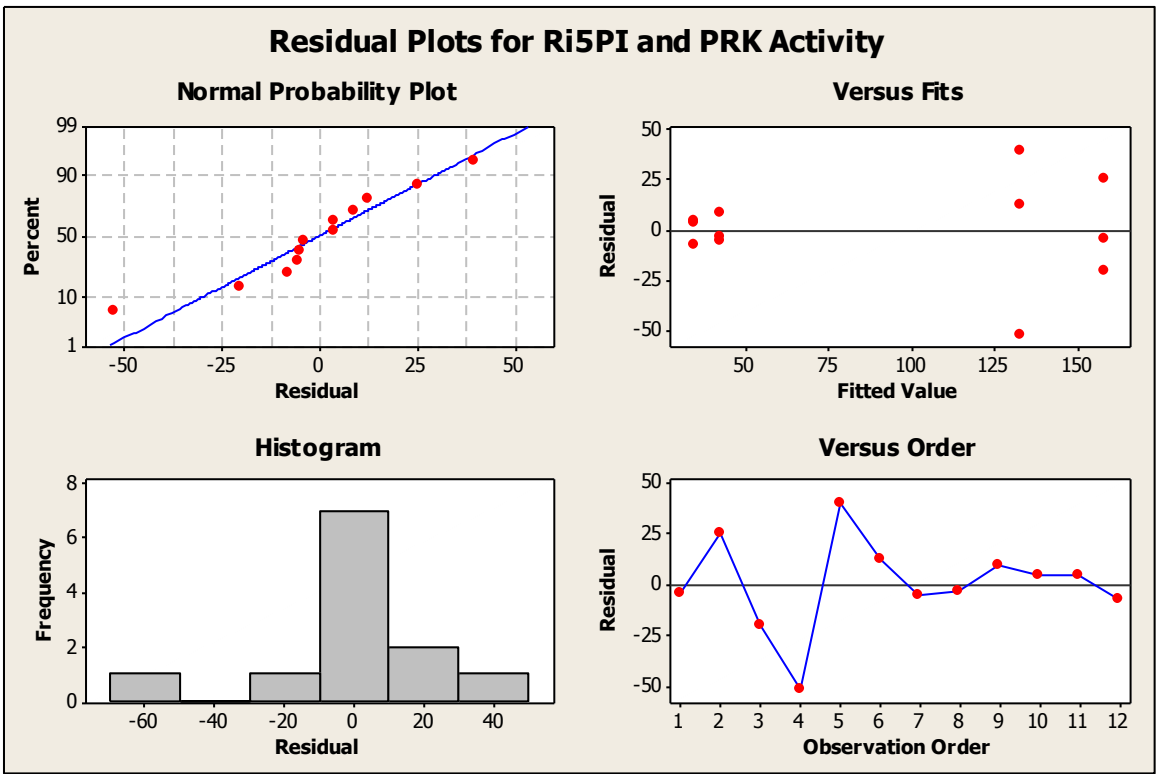

A 4-12: General Linear Model: Assimilation Rate *versus* HS Treatment, CO_2 Concentration

```
Factor             Type   Levels  Values
HS Treatment       fixed       2  25, 38
CO2 Concentration  fixed       2  1(380 µmol CO2. mol-1 air), 2(1000 µmol CO2.
mol-1 air


Analysis of Variance for Assimilation Rate, using Adjusted SS for Tests

Source                          DF  Seq SS  Adj SS  Adj MS       F      P
HS Treatment                     1  744.79  744.79  744.79  374.79  0.000
CO2 Concentration                1   38.09   38.09   38.09   19.17  0.002
HS Treatment*CO2 Concentration   1   53.12   53.12   53.12   26.73  0.001
Error                            8   15.90   15.90    1.99
Total                           11  851.89


S = 1.40968   R-Sq = 98.13%   R-Sq(adj) = 97.43%

Grouping Information Using Tukey Method and 95.0% Confidence

HS         CO2
Treatment  Concentration  N    Mean  Grouping
25         2              3  22.125  A
25         1              3  14.354     B
38         1              3   2.806        C
38         2              3   2.161        C

Means that do not share a letter are significantly different.
```

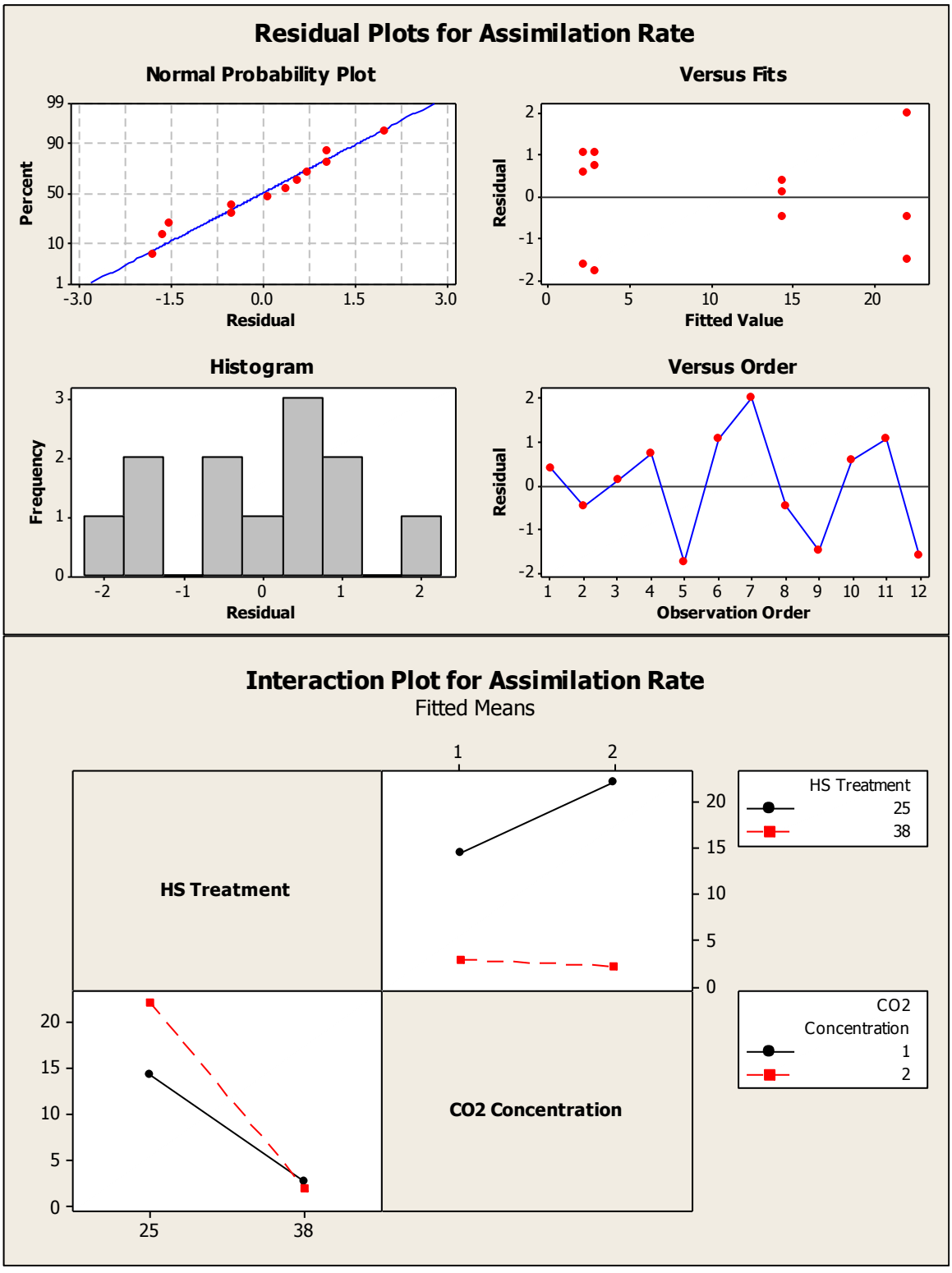
Residual Plots for Assimilation Rate
Normal Probability Plot
Percent
Residual
Versus Fits
Residual
Fitted Value
Histogram
Frequency
Residual
Versus Order
Residual
Observation Order
Interaction Plot for Assimilation Rate
Fitted Means
HS Treatment
CO2 Concentration
HS Treatment
25
38
CO2 Concentration
1
2

Figure A 5-1: General Linear Model: ATP level *versus* Dark or Light

```
Factor          Type   Levels  Values
Dark or Light   fixed       3  Dark (3hr), Light (20min), Light (3min)


Analysis of Variance for ATP level, using Adjusted SS for Tests

Source          DF  Seq SS  Adj SS  Adj MS      F      P
Dark or Light    2  55.798  55.798  27.899  50.49  0.000
Error            6   3.315   3.315   0.553
Total            8  59.113


S = 0.743328   R-Sq = 94.39%   R-Sq(adj) = 92.52%


Grouping Information Using Tukey Method and 95.0% Confidence

Dark or Light  N   Mean  Grouping
Light (20min)  3  7.939  A
Light (3min)   3  7.603  A
Dark (3hr)     3  2.497     B

Means that do not share a letter are significantly different.
```

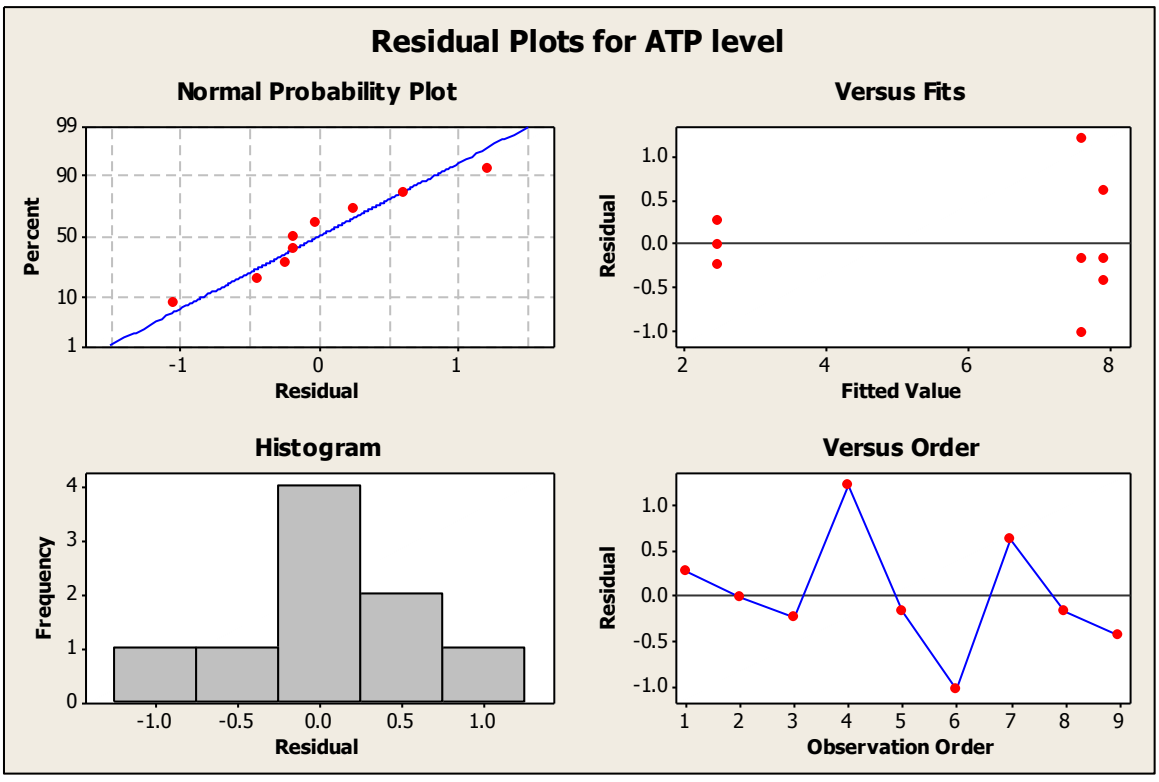

Figure A 5-2: General Linear Model: ATP Level *versus* HS Treatment

```
Factor         Type   Levels  Values
HS Treatment   fixed       4  25, 36, 38, 40


Analysis of Variance for ATP Level, using Adjusted SS for Tests

Source         DF  Seq SS  Adj SS  Adj MS      F      P
HS Treatment    3  73.035  73.035  24.345  47.41  0.000
Error          12   6.163   6.163   0.514
Total          15  79.197


S = 0.716624   R-Sq = 92.22%   R-Sq(adj) = 90.27%


Grouping Information Using Tukey Method and 95.0% Confidence

HS
Treatment  N    Mean  Grouping
25         4  5.4742  A
36         4  5.1285  A
40         4  1.2855     B
38         4  0.8115     B

Means that do not share a letter are significantly different.
```

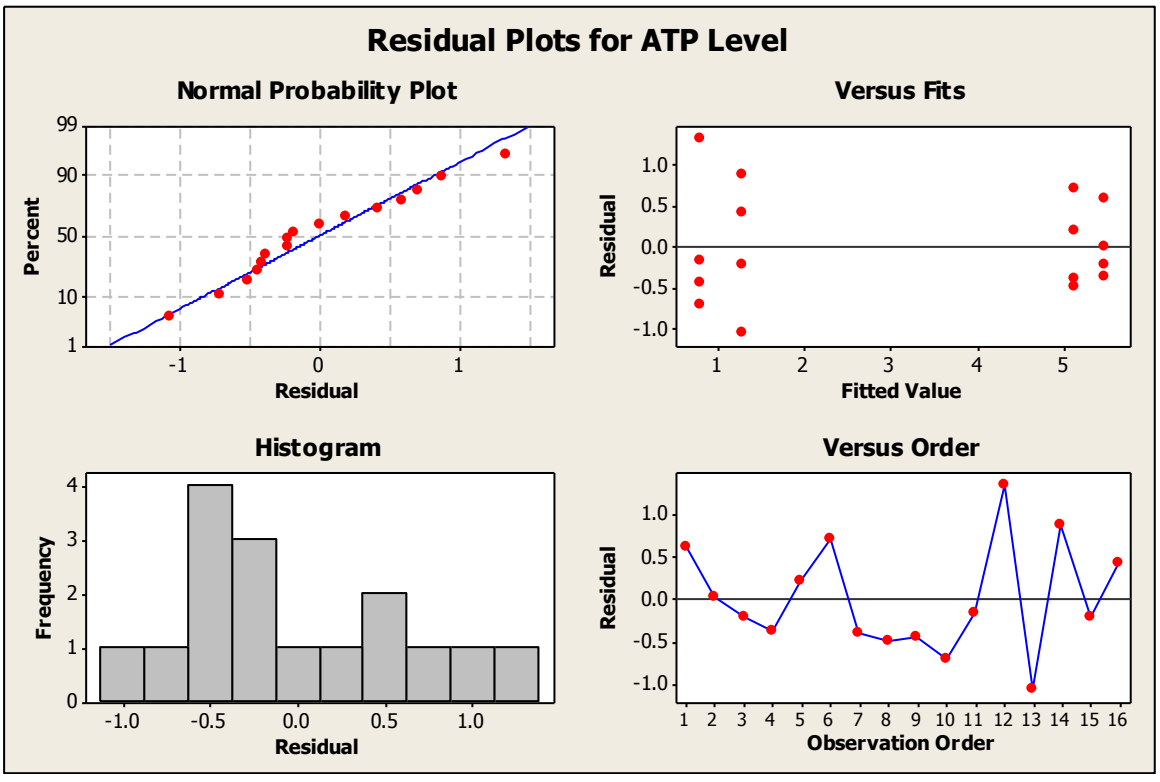

Figure A 5-3: General Linear Model: *in vivo* ETR for ATP *versus* HS Treatments

```
Factor          Type   Levels  Values
HS Treatments   fixed       4  25, 36, 38, 40


Analysis of Variance for in vivo ETR for ATP, using Adjusted SS for Tests

Source          DF  Seq SS  Adj SS  Adj MS       F      P
HS Treatments    3   31092   31092   10364  459.37  0.000
Error           12     271     271      23
Total           15   31362


S = 4.74983   R-Sq = 99.14%   R-Sq(adj) = 98.92%


Grouping Information Using Tukey Method and 95.0% Confidence

HS
Treatments  N     Mean  Grouping
25          4  107.749  A
36          4   91.384     B
38          4   22.296        C
40          4    3.967           D

Means that do not share a letter are significantly different.
```

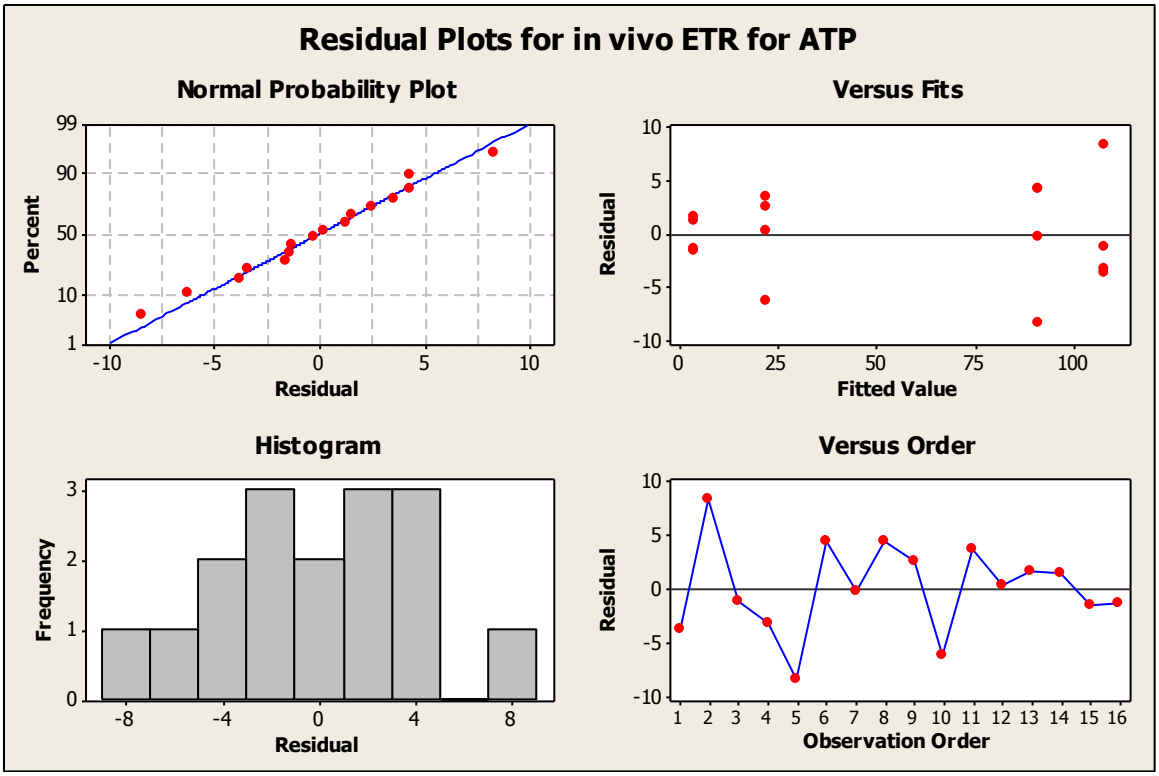

Figure A 5-4: General Linear Model: (t½) barley *versus* HS @ 38°C

```
Factor      Type   Levels  Values
HS  @ 38C   fixed       3  0, 3, 24


Analysis of Variance for (t½ ) barley, using Adjusted SS for Tests

Source      DF  Seq SS  Adj SS  Adj MS      F      P
HS  @ 38C    2   30169   30169   15084  32.35  0.001
Error        6    2798    2798     466
Total        8   32966


S = 21.5935   R-Sq = 91.51%   R-Sq(adj) = 88.68%


Grouping Information Using Tukey Method and 95.0% Confidence

HS  @
38C     N    Mean  Grouping
 3      3  177.99  A
24      3   68.34    B
 0      3   45.27    B

Means that do not share a letter are significantly different.
```

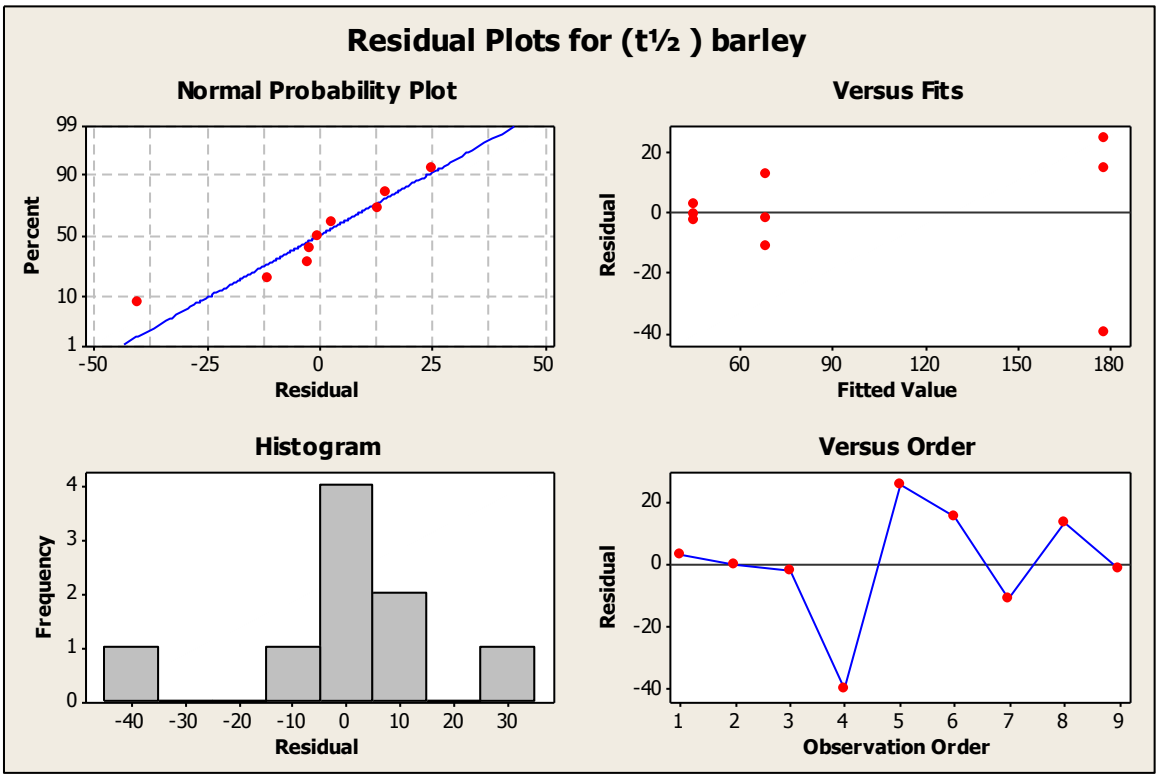

Figure A 5-5: General Linear Model: (t½) barley *versus* HS @ 40°C

```
Factor     Type   Levels  Values
HS @ 40C   fixed       3  0, 3, 24


Analysis of Variance for (t½) barley, using Adjusted SS for Tests

Source     DF  Seq SS  Adj SS  Adj MS      F      P
HS @ 40C    2   27276   27276   13638   7.43  0.024
Error       6   11016   11016    1836
Total       8   38292


S = 42.8487   R-Sq = 71.23%   R-Sq(adj) = 61.64%


Grouping Information Using Tukey Method and 95.0% Confidence

HS @
40C   N     Mean  Grouping
 3    3  180.10  A
24    3  111.15  A B
 0    3   45.27    B

Means that do not share a letter are significantly different.
```

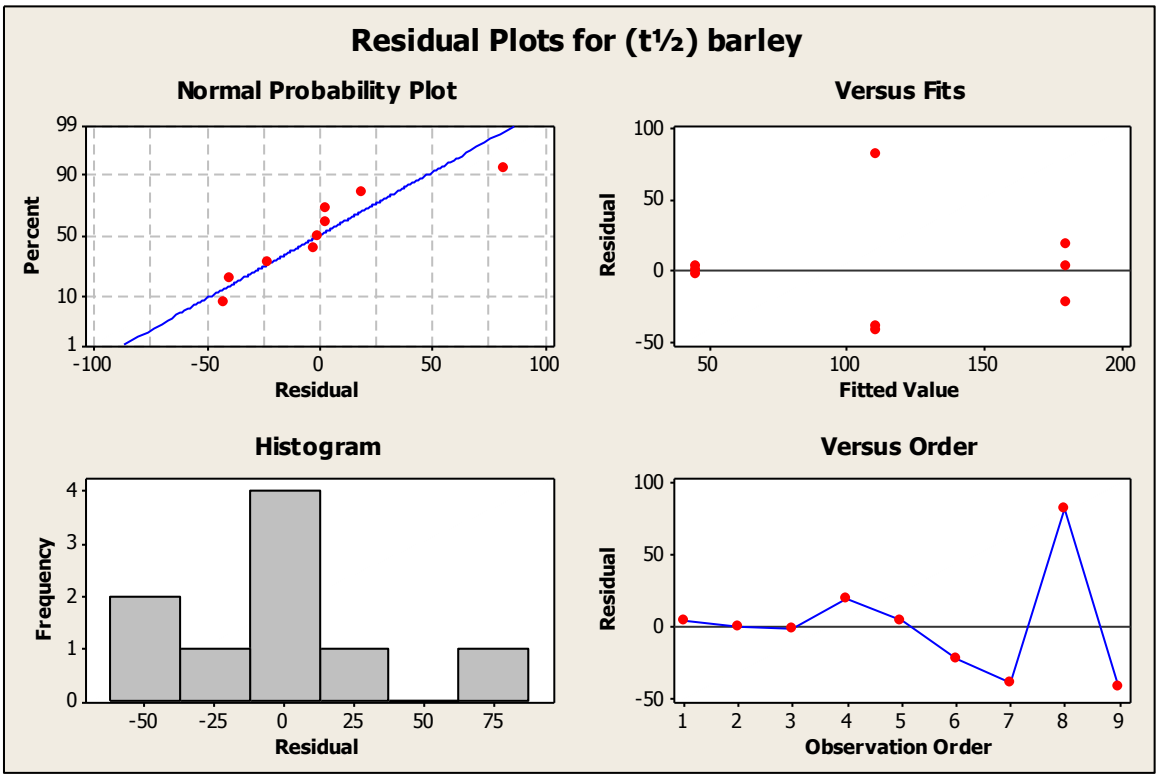

Figure A 5-6: General Linear Model: Yucca (t½) *versus* HS @ 38°C

```
Factor     Type   Levels  Values
HS @ 38C   fixed       3  0, 3, 24


Analysis of Variance for Yuuca (t½), using Adjusted SS for Tests

Source     DF  Seq SS  Adj SS  Adj MS      F      P
HS @ 38C    2  4090.6  4090.6  2045.3   3.34  0.106
Error       6  3675.9  3675.9   612.7
Total       8  7766.6


S = 24.7519   R-Sq = 52.67%   R-Sq(adj) = 36.89%


Grouping Information Using Tukey Method and 95.0% Confidence

HS @
38C   N   Mean  Grouping
 3    3  96.05  A
24    3  54.72  A
 0    3  47.75  A

Means that do not share a letter are significantly different.
```

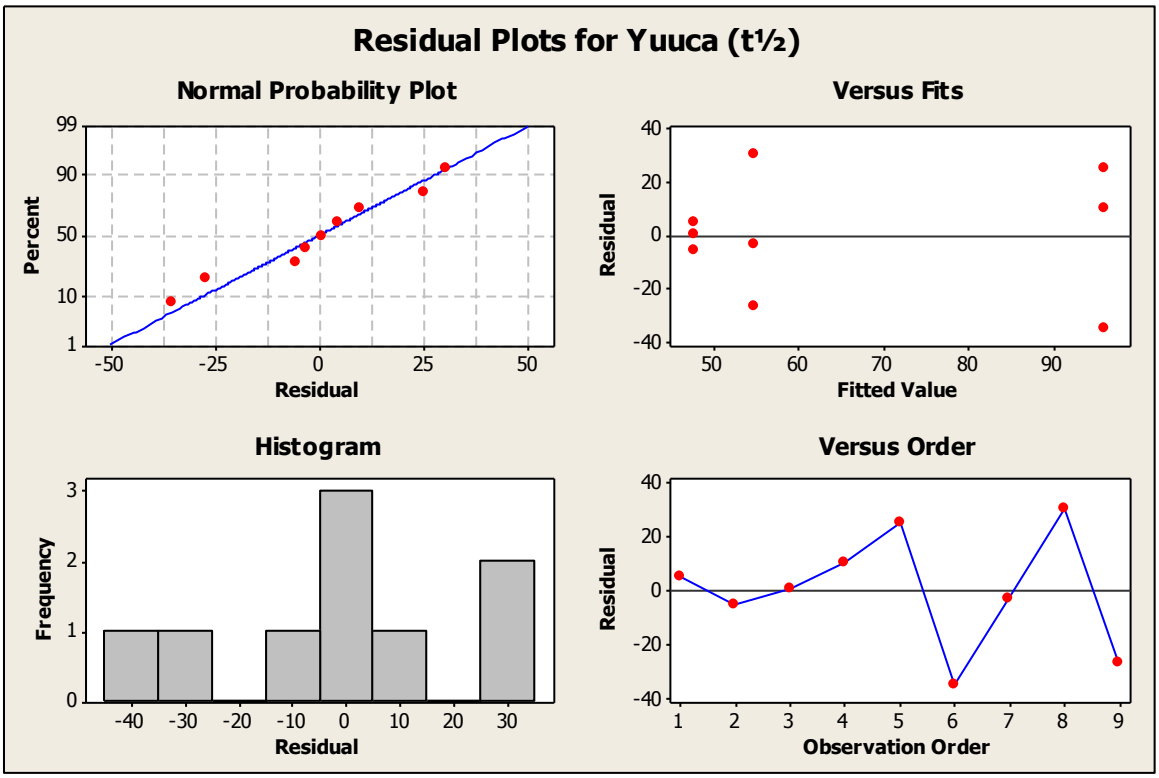

Figure A 5-7: General Linear Model: Yucca (t½) *versus* HS @ 40°C

```
Factor     Type   Levels  Values
HS @ 40C   fixed       3  0, 3, 24


Analysis of Variance for Yucca (t½), using Adjusted SS for Tests

Source     DF   Seq SS  Adj SS  Adj MS      F      P
HS @ 40C    2   9976.3  9976.3  4988.2   7.71  0.022
Error       6   3882.0  3882.0   647.0
Total       8  13858.3


S = 25.4362   R-Sq = 71.99%   R-Sq(adj) = 62.65%


Grouping Information Using Tukey Method and 95.0% Confidence

HS @
40C   N    Mean  Grouping
 3    3  119.81  A
24    3   50.72     B
 0    3   47.75     B

Means that do not share a letter are significantly different.
```

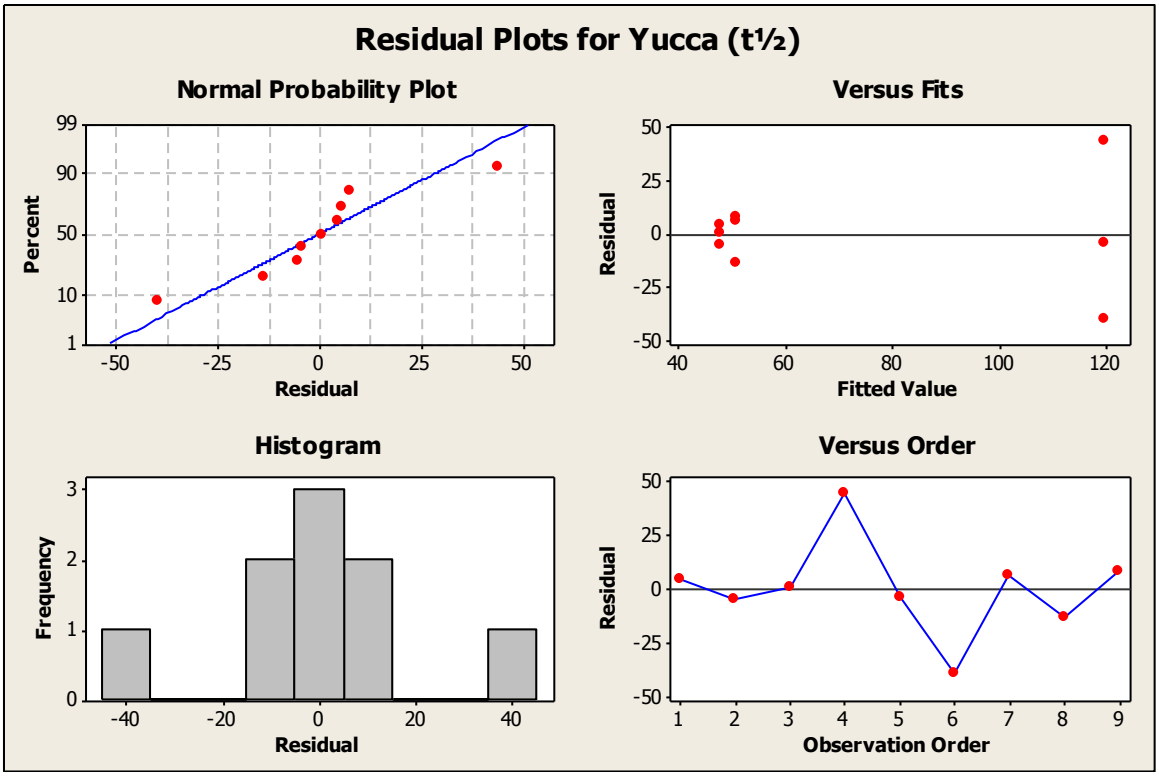

Figure A 5-8: General Linear Model: barley NPQ *versus* HS @ 38°C

```
Factor     Type   Levels  Values
HS @ 38C   fixed       3  0, 3, 24


Analysis of Variance for barley NPQ, using Adjusted SS for Tests

Source     DF   Seq SS   Adj SS   Adj MS     F      P
HS @ 38C    2  0.02956  0.02956  0.01478  0.19  0.832
Error       5  0.38837  0.38837  0.07767
Total       7  0.41793


S = 0.278701   R-Sq = 7.07%   R-Sq(adj) = 0.00%


Grouping Information Using Tukey Method and 95.0% Confidence

HS @
38C   N   Mean  Grouping
 3    3  1.536  A
 0    3  1.492  A
24    2  1.381  A

Means that do not share a letter are significantly different.
```

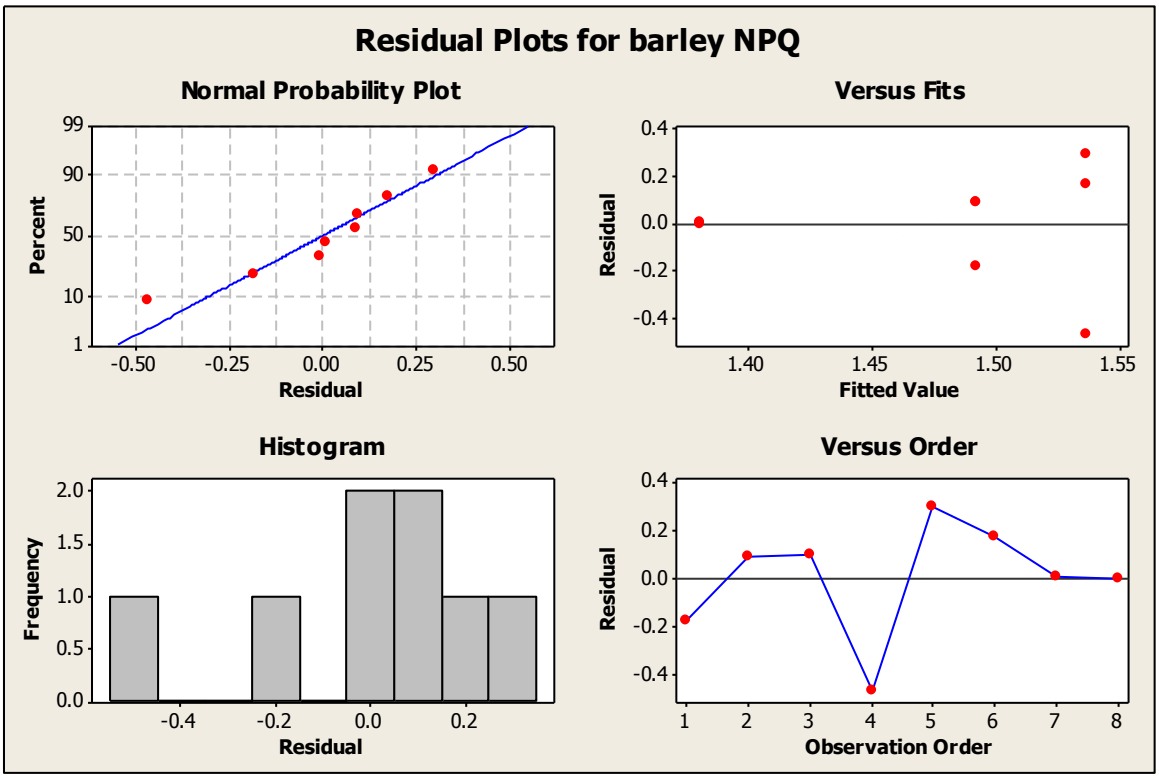

Figure A 5-9: General Linear Model: barley NPQ *versus* HS @ 40°C

```
Factor     Type   Levels  Values
HS @ 40C   fixed       3  0, 3, 24


Analysis of Variance for barley NPQ, using Adjusted SS for Tests

Source     DF   Seq SS   Adj SS   Adj MS      F      P
HS @ 40C    2  0.07041  0.07041  0.03521   0.93  0.466
Error       4  0.15146  0.15146  0.03786
Total       6  0.22187


S = 0.194587   R-Sq = 31.74%   R-Sq(adj) = 0.00%


Grouping Information Using Tukey Method and 95.0% Confidence

HS @
40C   N   Mean  Grouping
 3    2  1.734  A
24    2  1.578  A
 0    3  1.492  A

Means that do not share a letter are significantly different.
```

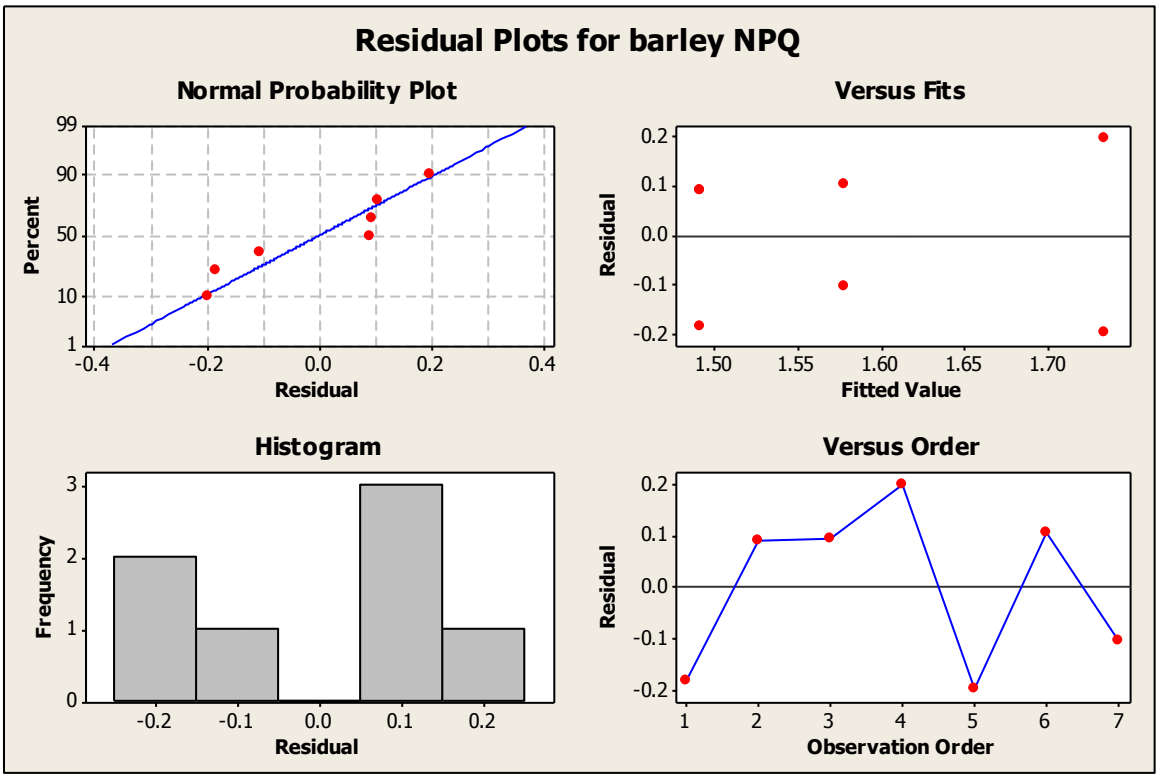

Figure A 5-10: General Linear Model: Log Yucca NPQ *versus* HS @ 38°C

```
Factor     Type   Levels  Values
HS @ 38C   fixed       3  0, 3, 24


Analysis of Variance for Log NPQ, using Adjusted SS for Tests

Source     DF     Seq SS     Adj SS     Adj MS      F      P
HS @ 38C    2  0.058424   0.058424   0.029212   3.76  0.057
Error      11  0.085539   0.085539   0.007776
Total      13  0.143963


S = 0.0881832   R-Sq = 40.58%   R-Sq(adj) = 29.78%


Grouping Information Using Tukey Method and 95.0% Confidence

HS @
38C   N     Mean  Grouping
 3    5   0.3699  A
24    4   0.2546  A
 0    5   0.2238  A

Means that do not share a letter are significantly different.
```

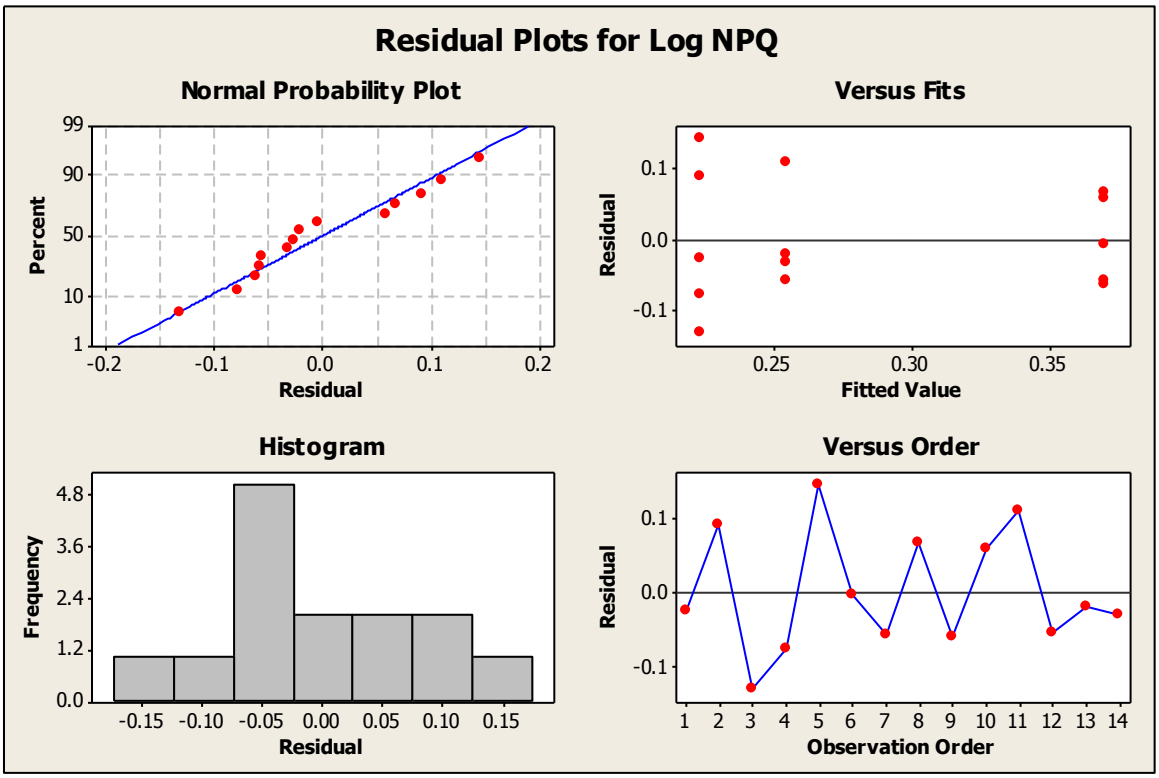

Figure A 5-11: General Linear Model: Yucca NPQ *versus* HS @ 40°C

```
Factor     Type   Levels  Values
HS @ 40C   fixed       3  0, 3, 24


Analysis of Variance for YuccaNPQ, using Adjusted SS for Tests

Source     DF  Seq SS  Adj SS  Adj MS     F      P
HS @ 40C    2  0.7375  0.7375  0.3688  2.22  0.165
Error       9  1.4963  1.4963  0.1663
Total      11  2.2338


S = 0.407745   R-Sq = 33.02%   R-Sq(adj) = 18.13%


Grouping Information Using Tukey Method and 95.0% Confidence

HS @
40C   N   Mean  Grouping
 3    4  2.019  A
 0    5  1.723  A
24    3  1.363  A

Means that do not share a letter are significantly different.
```

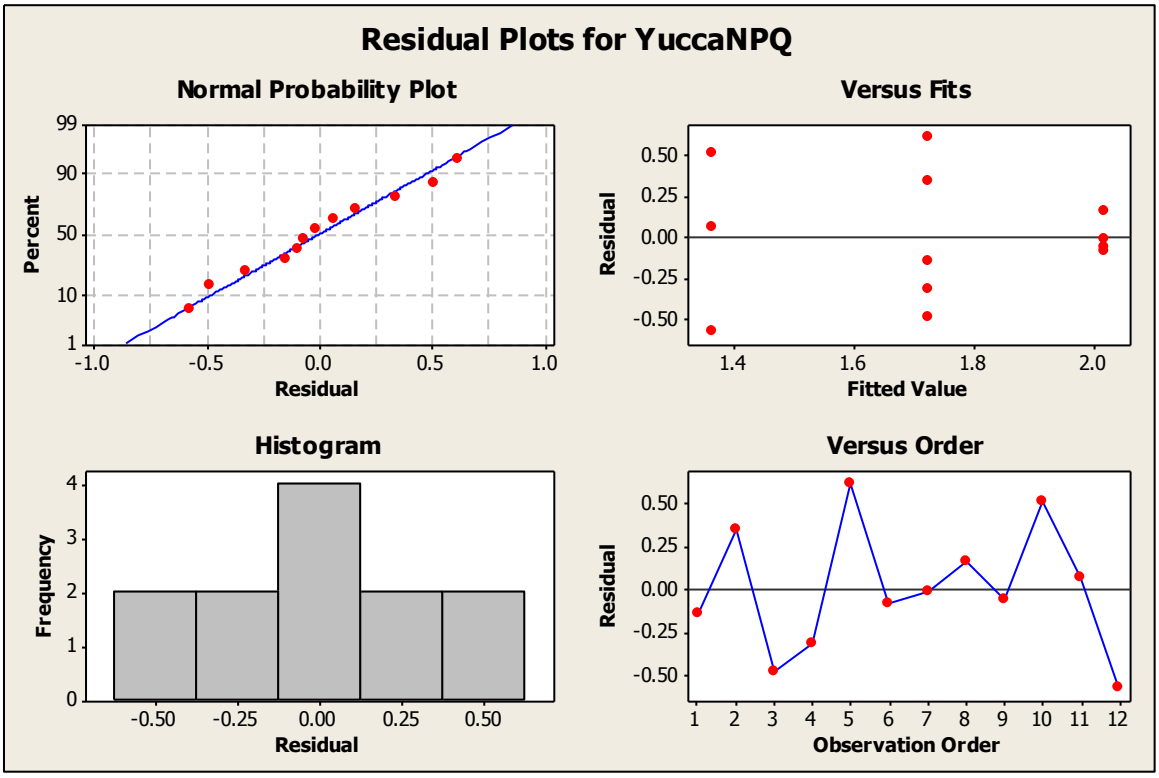

8 List of References

Addanki, S., J. F. Sotos and P. D. Rearick (1966). "Rapid determination of picomole quantities of ATP with a liquid scintillation counter." Analytical Biochemistry **14**(2): 261-264.

Al-Khatib, K. and G. M. Paulsen (1999). "High-temperature effects on photosynthetic processes in temperate and tropical cereals." Crop Science **39**(1): 119-125.

Allen, J., N. Holmes, M. Hipkins and N. Baker (1986). "Electron transport and redox titration." Photosynthesis: energy transduction: a practical approach: 103-141.

Armond, P. A., O. Björkman and L. A. Staehelin (1980). "Dissociation of supramolecular complexes in chloroplast membranes A manifestation of heat damage to the photosynthetic apparatus." Biochimica et Biophysica Acta (BBA)-Biomembranes **601**: 433-442.

Arrivault, S., M. Guenther, A. Ivakov, R. Feil, D. Vosloh, J. T. Van Dongen, R. Sulpice and M. Stitt (2009). "Use of reverse-phase liquid chromatography, linked to tandem mass spectrometry, to profile the Calvin cycle and other metabolic intermediates in Arabidopsis rosettes at different carbon dioxide concentrations." The Plant Journal **59**(5): 826-839.

Ashraf, M. and M. Hafeez (2004). "Thermotolerance of pearl millet and maize at early growth stages: growth and nutrient relations." Biologia plantarum **48**(1): 81-86.

Assmann, S. M. and K.-i. Shimazaki (1999). "The multisensory guard cell. Stomatal responses to blue light and abscisic acid." Plant Physiology **119**(3): 809-816.

Baker, N. R. (2008). "Chlorophyll Fluorescence: A Probe of Photosynthesis In Vivo." Annual Review of Plant Biology **59**(1): 89-113.

Bednarz, C. W. and M. W. van Iersel (2001). "Temperature response of whole-plant CO2 exchange rates of four upland cotton cultivars differing in leaf shape and leaf pubescence." Communications in Soil Science and Plant Analysis **32**(15-16): 2485-2501.

Bernacchi, C. J., A. R. Portis, H. Nakano, S. von Caemmerer and S. P. Long (2002). "Temperature response of mesophyll conductance. Implications for the determination of Rubisco enzyme kinetics and for limitations to photosynthesis in vivo." Plant Physiology **130**(4): 1992-1998.

Berry, J. and O. Bjorkman (1980). "Photosynthetic Response and Adaptation to Temperature in Higher Plants." Annual Review of Plant Physiology **31**(1): 491-543.

Bird, I. F., M. J. Cornelius and A. J. Keys (1977). Effects of Temperature on Photosynthesis by Maize and Wheat. Journal of Experimental Botany. **28:** 519-524.

Bjorkman, O., H. A. Mooney and J. Ehleringer (1975). "Photosynthetic responses of plants from habitats with contrasting thermal environments." Carnegie Inst Wash Yearb **74**: 743-748.

Bosco, C. D., L. Lezhneva, A. Biehl, D. Leister, H. Strotmann, G. Wanner and J. Meurer (2004). "Inactivation of the Chloroplast ATP Synthase γ Subunit Results in High Non-photochemical Fluorescence Quenching and Altered Nuclear Gene Expression in Arabidopsis thaliana." Journal of Biological Chemistry **279**(2): 1060-1069.

Bugg, M. W., J. Whitmarsh, C. E. Rieck and W. S. Cohen (1980). "Inhibition of Photosynthetic Electron Transport by Diphenyl Ether Herbicides." Plant Physiology **65**(1): 47-50.

Bukhov, N., S. C. Sabat and P. Mohanty (1990). "Analysis of chlorophyll a fluoresence changes in weak light in heat treated Amaranthus chloroplasts." Photosynthesis Research **23**(1): 81-87.

Bukhov, N., C. Wiese, S. Neimanis and U. Heber (1999a). "Heat sensitivity of chloroplasts and leaves: Leakage of protons from thylakoids and reversible activation of cyclic electron transport." Photosynthesis Research **59**(1): 81-93.

Bukhov, N. G., C. Wiese, S. Neimanis and U. Heber (1999b). "Heat sensitivity of chloroplasts and leaves: leakage of protons from thylakoids and reversible activation of cyclic electron transport." Photosynthesis Research **59**(1): 81-93.

Carmo-Silva, A. E. and M. E. Salvucci (2011). "The activity of Rubisco's molecular chaperone, Rubisco activase, in leaf extracts." Photosynthesis Research **108**(2-3): 143-155.

Ceccarelli, S., S. Grando, M. Maatougui, M. Michael, M. Slash, R. Haghparast, M. Rahmanian, A. Taheri, A. Al-Yassin and A. Benbelkacem (2010). "Plant breeding and climate changes." The Journal of Agricultural Science **148**(6): 627.

Cen, Y.-P. and R. F. Sage (2005). "The Regulation of Rubisco Activity in Response to Variation in Temperature and Atmospheric CO2 Partial Pressure in Sweet Potato." Plant Physiology **139**(2): 979-990.

Cleland, W. W., T. J. Andrews, S. Gutteridge, F. C. Hartman and G. H. Lorimer (1998). "Mechanism of Rubisco: The Carbamate as General Base x." Chemical Reviews **98**(2): 549-562.

Crafts-Brandner, S. and R. Law (2000). "Effect of heat stress on the inhibition and recovery of the ribulose-1, 5-bisphosphate carboxylase/oxygenase activation state." Planta **212**(1): 67-74.

Crafts-Brandner, S. J. and M. E. Salvucci (2000). "Rubisco activase constrains the photosynthetic potential of leaves at high temperature and CO2." Proceedings of the National Academy of Sciences **97**(24): 13430-13435.

Crafts-Brandner, S. J. and M. E. Salvucci (2002). "Sensitivity of Photosynthesis in a C4 Plant, Maize, to Heat Stress." Plant Physiol. **129**(4): 1773-1780.

Crafts-Brandner, S. J., F. J. van de Loo and M. E. Salvucci (1997). "The two forms of ribulose-1, 5-bisphosphate carboxylase/oxygenase activase differ in sensitivity to elevated temperature." Plant Physiology **114**(2): 439-444.

Cunningham, S. and J. Read (2002). "Comparison of temperate and tropical rainforest tree species: photosynthetic responses to growth temperature." Oecologia **133**(2): 112-119.

Dunwell, J. M. (2000). "Transgenic approaches to crop improvement." Journal of Experimental Botany **51**(suppl 1): 487-496.

Easterling, W., P. Aggarwal, P. Batima, K. Brander, J. Bruinsma, L. Erda, M. Howden, F. Tubiello, J. Antle and W. Baethgen (2007). Food, fibre and forest products. Climate Change 2007: Impacts, Adaptation and Vulnerability. Contribution of Working Group II to the Fourth Assessment Report of the Intergovernmental Panel on Climate Change. C. O. Parry ML, Palutikof JP, Linden PJvd, Hanson CE. Cambridge, UK, Cambridge University Press**:** 273-313.

Ehlers, J. and A. Hall (1998). "Heat tolerance of contrasting cowpea lines in short and long days." Field crops research **55**(1): 11-21.

Enami, I., M. Kitamura, T. Tato, Y. Isokawa, H. Ohta and S. Kato (1994). "Is the primary cause of thermal inactivation of oxygen evolution in spinach PS II membranes release of the 33 kDa protein or of Mn? Biochim." Biophys. Acta **186**.

Evans, J. and F. Loreto (2000). Acquisition and diffusion of CO2 in higher plant leaves. In 'Photosynthesis: physiology and metabolism'.(Eds RC Leegood, TD Sharkey, S von Caemmerer) pp. 321–351, Kluwer Academic Publishers: The Netherlands.

Evans, J. R. (2013). "Improving Photosynthesis." Plant Physiology **162**(4): 1780-1793.

Evans, J. R., S. Caemmerer, B. A. Setchell and G. S. Hudson (1994). "The relationship between CO2 transfer conductance and leaf anatomy in transgenic tobacco with a reduced content of Rubisco." Functional Plant Biology **21**(4): 475-495.

FAO (2009). Expert Meeting on How to Feed the World in 2050. 24-26 June. http://www.fao.org/docrep/012/ak542e/ak542e00.htm. Rome, Food and Agriculture Organization of the United Nation

FAO (2010). FAO cuts wheat production forecast but considers supplies adequate. http://www.fao.org/news/story/tr/item/44570/icode/en/ (accessed December 2013).

Farquhar, G., S. v. von Caemmerer and J. Berry (1980). "A biochemical model of photosynthetic CO2 assimilation in leaves of C3 species." Planta **149**(1): 78-90.

Farquhar, G. D., S. Caemmerer and J. A. Berry (1980). "A biochemical model of photosynthetic CO2 assimilation in leaves of C3 species." Planta **149**(1): 78-90.

Farquhar, G. D. and T. D. Sharkey (1982). "Stomatal conductance and photosynthesis." Annual Review of Plant Physiology **33**(1): 317-345.

Feller, U. (2006). "Stomatal opening at elevated temperature: an underestimated regulatory mechanism." Gen. Appl. Plant Physiology, Special Issue: 19-31.

Feller, U., S. J. Crafts-Brandner and M. E. Salvucci (1998). "Moderately High Temperatures Inhibit Ribulose-1,5-Bisphosphate Carboxylase/Oxygenase (Rubisco) Activase-Mediated Activation of Rubisco." Plant Physiology **116**(2): 539-546.

Flood, P. J., J. Harbinson and M. G. Aarts (2011). "Natural genetic variation in plant photosynthesis." Trends in plant science **16**(6): 327-335.

Flores, S. and D. R. Ort (1984). "Investigation of the apparent inefficiency of the coupling between photosystem II electron transfer and ATP formation." Biochimica et Biophysica Acta (BBA)-Bioenergetics **766**(2): 289-302.

Gardemann, A., M. Stitt and H. W. Heldt (1982). "Regulation of spinach ribulose 5-phosphate kinase by 3-phosphoglycerate." FEBS Letters **137**(2): 213-216.

Gardemann, A., M. Stitt and H. W. Heldt (1983). "Control of CO2 fixation. Regulation of spinach ribulose-5-phosphate kinase by stromal metabolite levels." Biochimica et Biophysica Acta (BBA) - Bioenergetics **722**(1): 51-60.

Gibon, Y., H. Vigeolas, A. Tiessen, P. Geigenberger and M. Stitt (2002). "Sensitive and high throughput metabolite assays for inorganic pyrophosphate, ADPGlc, nucleotide phosphates, and glycolytic intermediates based on a novel enzymic cycling system." The Plant Journal **30**(2): 221-235.

Gotoh, E., Y. Kobayashi and M. Tsuyama (2010). "The post-illumination chlorophyll fluorescence transient indicates the RuBP regeneration limitation of photosynthesis in low light in Arabidopsis." FEBS Letters **584**(14): 3061-3064.

Greer, D. H. and M. M. Weedon (2012). "Modelling photosynthetic responses to temperature of grapevine (Vitis vinifera cv. Semillon) leaves on vines grown in a hot climate." Plant, Cell & Environment **35**(6): 1050-1064.

Gresser, M. J., J. A. Myers and P. D. Boyer (1982). "Catalytic site cooperativity of beef heart mitochondrial F1 adenosine triphosphatase. Correlations of initial velocity, bound intermediate, and oxygen exchange measurements with an alternating three-site model." Journal of Biological Chemistry **257**(20): 12030-12038.

Haldimann, P. and U. Feller (2004). "Inhibition of photosynthesis by high temperature in oak (Quercus pubescens L.) leaves grown under natural conditions closely correlates with a reversible heat-dependent reduction of the activation state of ribulose-1, 5-bisphosphate carboxylase/oxygenase." Plant, Cell & Environment **27**(9): 1169-1183.

Haldimann, P. and U. R. S. Feller (2005). "Growth at moderately elevated temperature alters the physiological response of the photosynthetic apparatus to heat stress in pea (Pisum sativum L.) leaves." Plant, Cell & Environment **28**(3): 302-317.

Hangarter, R. P. and N. E. Good (1982). "Energy thresholds for ATP synthesis in chloroplasts." Biochimica et Biophysica Acta (BBA)-Bioenergetics **681**(3): 397-404.

Harrison, E. P., H. Olcer, J. C. Lloyd, S. P. Long and C. A. Raines (2001). "Small decreases in SBPase cause a linear decline in the apparent RuBP regeneration rate, but do not affect Rubisco carboxylation capacity." Journal of Experimental Botany **52**(362): 1779-1784.

Hasanuzzaman, M., K. Nahar, M. Alam, R. Roychowdhury and M. Fujita (2013). "Physiological, Biochemical, and Molecular Mechanisms of Heat Stress Tolerance in Plants." International Journal of Molecular Sciences **14**(5): 9643-9684.

Havaux, M. (1993). "Characterization of thermal damage to the photosynthetic electron transport system in potato leaves." Plant Science **94**(1): 19-33.

Hisabori, T., E.-I. Sunamura, Y. Kim and H. Konno (2013). "The chloroplast ATP synthase features the characteristic redox regulation machinery." Antioxidants & redox signaling **19**(15): 1846-1854.

Horton, P. and A. Hague (1988). "Studies on the induction of chlorophyll fluorescence in isolated barley protoplasts. IV. Resolution of non-photochemical quenching." Biochimica et Biophysica Acta (BBA)-Bioenergetics **932**: 107-115.

Hozain, M. d. I., M. E. Salvucci, M. Fokar and A. S. Holaday (2010). "The differential response of photosynthesis to high temperature for a boreal and temperate Populus species relates to differences in Rubisco activation and Rubisco activase properties." Tree Physiology **30**(1): 32-44.

Hurwitz, J., A. Weissbach, B. L. Horecker and P. Z. Smyrniotis (1956). "SPINACH PHOSPHORIBULOKINASE." Journal of Biological Chemistry **218**(2): 769-783.

Huxman, T. E., E. P. Hamerlynck, M. E. Loik and S. D. Smith (1998). "Gas exchange and chlorophyll fluorescence responses of three south-western Yucca species to elevated CO2 and high temperature." Plant, Cell & Environment **21**(12): 1275-1283.

IPCC (2001). Climate change 2001: Impacts, adaptation and vulnerability. Contribution of Working Group II to the Third Assessment Report of the Intergovernmental Panel on Climate Change. Cambridge.

IPCC (2007a). Climate Change 2007: Working Group I: The Physical Science Basis, http://www.ipcc.ch/publications_and_data/ar4/wg1/en/contents.html

IPCC (2007b). Fourth Assessment Report. Intergovernmental Panel on Climate Change Secretariat. Geneva, Switzerland.

Kane, H. J., J.-M. Wilkin, A. R. Portis and T. John Andrews (1998). "Potent Inhibition of Ribulose-Bisphosphate Carboxylase by an Oxidized Impurity in Ribulose-1,5-Bisphosphate." Plant Physiology **117**(3): 1059-1069.

Katiyar-Agarwal, S., M. Agarwal and A. Grover (2003). "Heat-tolerant basmati rice engineered by over-expression of hsp101." Plant molecular biology **51**(5): 677-686.

Kemp, P. R. and G. J. Williams III (1980). "A Physiological Basis for Niche Separation Between Agropyron Smithii (C" 3) and Bouteloua Gracilis (C" 4)." Ecology: 846-858.

Keys, A. J. and M. A. Parry (1990a). "Ribulose bisphosphate carboxylase/oxygenase and carbonic anhydrase." Methods in plant biochemistry **3**: 1-14.

Keys, A. J. and M. A. J. Parry (1990b). 1 - Ribulose Bisphosphate Carboxylase/Oxygenase and Carbonic Anhydrase. Methods in Plant Biochemistry. L. E. A. P.J, Academic Press. **Volume 3:** 1-14.

Kim, K. and A. R. Portis (2005). "Temperature dependence of photosynthesis in Arabidopsis plants with modifications in Rubisco activase and membrane fluidity." Plant and cell physiology **46**(3): 522-530.

Kim, K. and A. R. Portis Jr (2006). "Kinetic analysis of the slow inactivation of Rubisco during catalysis: effects of temperature, O2 and Mg++." Photosynthesis Research **87**(2): 195-204.

Kim, S.-H., D. C. Gitz, R. C. Sicher, J. T. Baker, D. J. Timlin and V. R. Reddy (2007). "Temperature dependence of growth, development, and photosynthesis in maize under elevated CO2." Environmental and Experimental Botany **61**(3): 224-236.

Kimmich, G. A., J. Randles and J. S. Brand (1975). "Assay of picomole amounts of ATP, ADP, and AMP using the luciferase enzyme system." Analytical Biochemistry **69**(1): 187-206.

Knight, S., I. Andersson and C.-I. Brändén (1990). "Crystallographic analysis of ribulose 1,5-bisphosphate carboxylase from spinach at 2·4 Å resolution: Subunit interactions and active site." Journal of molecular biology **215**(1): 113-160.

Kobza, J. and G. E. Edwards (1987). "Influences of leaf temperature on photosynthetic carbon metabolism in wheat." Plant Physiology **83**(1): 69-74.

Kubien, D. S. and R. F. Sage (2008). "The temperature response of photosynthesis in tobacco with reduced amounts of Rubisco." Plant, Cell & Environment **31**(4): 407-418.

Kumar, A., C. Li and A. R. Portis Jr (2009). "Arabidopsis thaliana expressing a thermostable chimeric Rubisco activase exhibits enhanced growth and higher rates of photosynthesis at moderately high temperatures." Photosynthesis Research **100**(3): 143-153.

Kurek, I., T. K. Chang, S. M. Bertain, A. Madrigal, L. Liu, M. W. Lassner and G. Zhu (2007). "Enhanced thermostability of Arabidopsis Rubisco activase improves photosynthesis and growth rates under moderate heat stress." The Plant Cell Online **19**(10): 3230-3241.

Larcher, W. (2003). Physiological plant ecology: ecophysiology and stress physiology of functional groups, Springer.

Law, R. D. and S. J. Crafts-Brandner (1999). "Inhibition and Acclimation of Photosynthesis to Heat Stress Is Closely Correlated with Activation of Ribulose-1,5-Bisphosphate Carboxylase/Oxygenase." Plant Physiology **120**(1): 173-181.

Lawson, T., S. Caemmerer and I. Baroli (2011). Photosynthesis and Stomatal Behaviour. Progress in Botany 72. U. E. Lüttge, W. Beyschlag, B. Büdel and D. Francis, Springer Berlin Heidelberg. **72:** 265-304.

Leegood, R. C. (1990). 2 - Enzymes of the Calvin Cycle. Methods in Plant Biochemistry. L. E. A. P.J, Academic Press. **Volume 3:** 15-37.

Lilley, R. M. and D. A. Walker (1974). "An improved spectrophotometric assay for ribulosebisphosphate carboxylase." Biochimica et Biophysica Acta (BBA) - Enzymology **358**(1): 226-229.

Lobell, D. B. and G. P. Asner (2003). "Climate and management contributions to recent trends in US agricultural yields." Science **299**(5609): 1032-1032.

Lobell, D. B., W. Schlenker and J. Costa-Roberts (2011). "Climate trends and global crop production since 1980." Science **333**(6042): 616-620.

Lobell, D. B., A. Sibley and J. I. Ortiz-Monasterio (2012). "Extreme heat effects on wheat senescence in India." Nature Climate Change **2**(3): 186-189.

Loka, D. and D. Oosterhuis (2010). "Effect of high night temperatures on cotton respiration, ATP levels and carbohydrate content." Environmental and Experimental Botany **68**(3): 258-263.

Long, S. P. and D. R. Ort (2010). "More than taking the heat: crops and global change." Current opinion in plant biology **13**(3): 240-247.

Loreto, F., P. C. Harley, G. Di Marco and T. D. Sharkey (1992). "Estimation of Mesophyll Conductance to CO2 Flux by Three Different Methods." Plant Physiology **98**(4): 1437-1443.

Lorimer, G. H., M. R. Badger and T. J. Andrews (1976). "The activation of ribulose-1, 5-bisphosphate carboxylase by carbon dioxide and magnesium ions. Equilibria, kinetics, a suggested mechanism, and physiological implications." Biochemistry **15**(3): 529-536.

Lorimer, G. H. and H. M. Miziorko (1980). "Carbamate formation on the .epsilon.-amino group of a lysyl residue as the basis for the activation of ribulosebisphosphate carboxylase by carbon dioxide and magnesium(2+)." Biochemistry **19**(23): 5321-5328.

Loza-Tavera, H., E. Martínez-Barajas and E. Sánchez-de-Jiménez (1990). "Regulation of Ribulose-1,5-Bisphosphate Carboxylase Expression in Second Leaves of Maize Seedlings from Low and High Yield Populations." Plant Physiology **93**(2): 541-548.

Lu, Z., J. Chen, R. G. Percy and E. Zeiger (1997). "Photosynthetic rate, stomatal conductance and leaf area in two cotton species (Gossypium barbadense and Gossypium hirsutum) and their relation with heat resistance and yield." Functional Plant Biology **24**(5): 693-700.

LujÁN, R., F. LledÍAs, L. U. Z. M. MartÍNez, R. Barreto, G. I. Cassab and J. Nieto-Sotelo (2009). "Small heat-shock proteins and leaf cooling capacity account for the unusual heat tolerance of the central spike leaves in Agave tequilana var. Weber." Plant, Cell & Environment **32**(12): 1791-1803.

Makino, A. and R. F. Sage (2007). "Temperature response of photosynthesis in transgenic rice transformed with 'sense'or 'antisense'rbcS." Plant and cell physiology **48**(10): 1472-1483.

Medlyn, B., C. Barton, M. Broadmeadow, R. Ceulemans, P. De Angelis, M. Forstreuter, M. Freeman, S. Jackson, S. Kellomäki and E. Laitat (2001). "Stomatal conductance of forest species after long-term exposure to elevated CO2 concentration: A synthesis." New Phytologist **149**(2): 247-264.

Mills, J., M. Hipkins and N. Baker (1986). "Photophosphorylation." Photosynthesis: energy transduction: a practical approach: 143-187.

Mills, J. D. and P. Mitchell (1982). "Modulation of coupling factor ATPase activity in intact chloroplasts. Reversal of thiol modulation in the dark." Biochimica et Biophysica Acta (BBA)-Bioenergetics **679**(1): 75-83.

Milos, P., M. Bloom and H. Roy (1985). "Methods for studying the assembly of ribulose bisphosphate carboxylase." Plant Molecular Biology Reporter **3**(1-2): 33-42.

Mitome, N., T. Suzuki, S. Hayashi and M. Yoshida (2004). "Thermophilic ATP synthase has a decamer c-ring: indication of noninteger 10: 3 H+/ATP ratio and permissive elastic coupling." Proceedings of the National Academy of Sciences of the United States of America **101**(33): 12159-12164.

Mitsuo, N., I. Takeru and B. Chance (1962). "Studies on bacterial photophosphorylation III. A sensitive and rapid method of determination of photophosphorylation." Biochimica et biophysica acta **59**(1): 177-182.

Mittler, R. and E. Blumwald (2010). "Genetic engineering for modern agriculture: challenges and perspectives." Annual review of plant biology **61**: 443-462.

Monteith, J. and M. Unsworth (2007). Principles of environmental physics, Access Online via Elsevier.

Moore, B. and J. R. Seemann (1994). "Evidence that 2-carboxyarabinitol 1-phosphate binds to ribulose-1, 5-bisphosphate carboxylase in vivo." Plant Physiology **105**(2): 731-737.

Mott, K., F. Denne and J. Powell (1997). "Interactions among stomata in response to perturbations in humidity." Plant, Cell & Environment **20**(9): 1098-1107.

Murakami, Y., M. Tsuyama, Y. Kobayashi, H. Kodama and K. Iba (2000). "Trienoic fatty acids and plant tolerance of high temperature." Science **287**(5452): 476-479.

Muschak, M., L. Willmitzer and J. Fisahn (1999). "Gas-exchange analysis of chloroplastic fructose-1, 6-bisphosphatase antisense potatoes at different air humidities and at elevated CO2." Planta **209**(1): 104-111.

Nash, D., M. Miyao and N. Murata (1985). "Heat inactivation of oxygen evolution in photosystem II particles and its acceleration by chloride depletion and exogenous manganese." Biochimica et Biophysica Acta (BBA)-Bioenergetics **807**(2): 127-133.

NOAA (2011). NOAA National Climatic Data Center, State of the Climate: Global Hazards for July 2010. published online August 2010, retrieved on December 3, 2013 from http://www.ncdc.noaa.gov/sotc/hazards/2010/7.

Nobel, P. S. and S. D. Smith (1983). "High and low temperature tolerances and their relationships to distribution of agaves." Plant, Cell & Environment **6**(9): 711-719.

Olcer, H., J. C. Lloyd and C. A. Raines (2001). "Photosynthetic capacity is differentially affected by reductions in sedoheptulose-1, 7-bisphosphatase activity during leaf development in transgenic tobacco plants." Plant Physiology **125**(2): 982-989.

Parry, M. A., M. Reynolds, M. E. Salvucci, C. Raines, P. J. Andralojc, X.-G. Zhu, G. D. Price, A. G. Condon and R. T. Furbank (2011). "Raising yield potential of wheat. II. Increasing photosynthetic capacity and efficiency." Journal of Experimental Botany **62**(2): 453-467.

Parry, M. A. J., P. J. Andralojc, J. C. Scales, M. E. Salvucci, A. E. Carmo-Silva, H. Alonso and S. M. Whitney (2013). "Rubisco activity and regulation as targets for crop improvement." Journal of Experimental Botany **64**(3): 717-730.

Pastenes, C. and P. Horton (1996). "Effect of high temperature on photosynthesis in beans (I. Oxygen evolution and chlorophyll fluorescence)." Plant Physiology **112**(3): 1245-1251.

Paul, M. J., S. P. Driscoll, P. J. Andralojc, J. S. Knight, J. C. Gray and D. W. Lawlor (2000). "Decrease of phosphoribulokinase activity by antisense RNA in transgenic tobacco: definition of the light environment under which phosphoribulokinase is not in large excess." Planta **211**(1): 112-119.

Paul, M. J., J. S. Knight, D. Habash, M. A. Parry, D. W. Lawlor, S. A. Barnes, A. Loynes and J. C. Gray (1995). "Reduction in phosphoribulokinase activity by antisense RNA in transgenic tobacco: effect on CO2 assimilation and growth in low irradiance." The Plant Journal **7**(4): 535-542.

Peet, M., S. Sato and R. Gardner (1998). "Comparing heat stress effects on male-fertile and male-sterile tomatoes." Plant, Cell & Environment **21**(2): 225-231.

Peng, S., J. Huang, J. E. Sheehy, R. C. Laza, R. M. Visperas, X. Zhong, G. S. Centeno, G. S. Khush and K. G. Cassman (2004). "Rice yields decline with higher night temperature from global warming." Proceedings of the National Academy of Sciences of the United States of America **101**(27): 9971-9975.

Pons, T. L. and R. A. Welschen (2003). "Midday depression of net photosynthesis in the tropical rainforest tree Eperua grandiflora: contributions of stomatal and internal conductances, respiration and Rubisco functioning." Tree Physiology **23**(14): 937-947.

Portis, A. R. (1992). "Regulation of Ribulose 1,5-Bisphosphate Carboxylase/Oxygenase Activity." Annual Review of Plant Physiology and Plant Molecular Biology **43**(1): 415-437.

Portis Jr, A. R. (2003). "Rubisco activase–Rubisco's catalytic chaperone." Photosynthesis Research **75**(1): 11-27.

Price, G. D., J. R. Evans, S. von Caemmerer, J.-W. Yu and M. R. Badger (1995). "Specific reduction of chloroplast glyceraldehyde-3-phosphate dehydrogenase activity by antisense RNA reduces CO2 assimilation via a reduction in ribulose bisphosphate regeneration in transgenic tobacco plants." Planta **195**(3): 369-378.

Quick, W. P., M. M. Chaves, R. Wendler, M. David, M. L. Rodrigues, J. A. Passaharinho, J. S. Pereira, M. D. Adcock, R. C. Leegood and M. Stitt (1992). "The effect of water stress on photosynthetic carbon metabolism in four species grown under field conditions." Plant, Cell & Environment **15**(1): 25-35.

Quick, W. P. and M. Stitt (1989). "An examination of factors contributing to non-photochemical quenching of chlorophyll fluorescence in barley leaves." Biochimica et Biophysica Acta (BBA) - Bioenergetics **977**(3): 287-296.

Radin, J. W., Z. Lu, R. G. Percy and E. Zeiger (1994). "Genetic variability for stomatal conductance in Pima cotton and its relation to improvements of heat adaptation." Proceedings of the National Academy of Sciences **91**(15): 7217-7221.

Raines, C. A. (2003). "The Calvin cycle revisited." Photosynthesis Research **75**(1): 1-10.

Ralph, P., C. Wilhelm, J. Lavaud, T. Jakob, K. Petrou and S. Kranz (2010). Fluorescence as a Tool to Understand Changes in Photosynthetic Electron Flow Regulation. Chlorophyll a Fluorescence in Aquatic Sciences: Methods and Applications. D. J. Suggett, O. Prášil and M. A. Borowitzka, Springer Netherlands. **4:** 75-89.

Reddy, V., D. Baker and H. Hodges (1991). "Temperature effects on cotton canopy growth, photosynthesis, and respiration." Agronomy journal **83**(4): 699-704.

Robinson, S. P. and A. R. Portis jr (1988). "Release of the nocturnal inhibitor, carbyarabinitol-1 -phosphate, from ribulose bisphosphate carbylase/oxygenase by rubisco activase." FEBS Letters **233**(2): 413-416.

Robinson, S. P. and A. R. Portis Jr (1989). "Adenosine triphosphate hydrolysis by purified Rubisco activase." Archives of Biochemistry and Biophysics **268**(1): 93-99.

Rokka, A., L. Zhang and E. M. Aro (2001). "Rubisco activase: an enzyme with a temperature-dependent dual function?" The Plant Journal **25**(4): 463-471.

Rollins, J., E. Habte, S. Templer, T. Colby, J. Schmidt and M. von Korff (2013). "Leaf proteome alterations in the context of physiological and morphological responses to drought and heat stress in barley (Hordeum vulgare L.)." Journal of Experimental Botany **64**(11): 3201-3212.

Rott, M., N. F. Martins, W. Thiele, W. Lein, R. Bock, D. M. Kramer and M. A. Schöttler (2011). "ATP Synthase Repression in Tobacco Restricts Photosynthetic Electron Transport, CO2 Assimilation, and Plant Growth by Overacidification of the Thylakoid Lumen." The Plant Cell Online **23**(1): 304-321.

Rundle, S. J. and R. Zielinski (1991). "Organization and expression of two tandemly oriented genes encoding ribulosebisphosphate carboxylase/oxygenase activase in barley." Journal of Biological Chemistry **266**(8): 4677-4685.

Rutner, A. C. (1970). "Spinach 5-phosphoribose isomerase. Purification and properties of the enzyme." Biochemistry **9**(1): 178-184.

Sage, R. F. (2002). "Variation in the kcat of Rubisco in C3 and C4 plants and some implications for photosynthetic performance at high and low temperature." Journal of Experimental Botany **53**(369): 609-620.

Sage, R. F. and D. S. Kubien (2007). "The temperature response of C3 and C4 photosynthesis." Plant, Cell & Environment **30**(9): 1086-1106.

Sage, R. F. and T. D. Sharkey (1987). "The effect of temperature on the occurrence of O2 and CO2 insensitive photosynthesis in field grown plants." Plant Physiology **84**(3): 658-664.

Sage, R. F., D. A. Way and D. S. Kubien (2008). "Rubisco, Rubisco activase, and global climate change." Journal of Experimental Botany **59**(7): 1581-1595.

Salvucci, M. E. and S. J. Crafts-Brandner (2004a). "Inhibition of photosynthesis by heat stress: the activation state of Rubisco as a limiting factor in photosynthesis." Physiologia Plantarum **120**(2): 179-186.

Salvucci, M. E. and S. J. Crafts-Brandner (2004b). "Relationship between the Heat Tolerance of Photosynthesis and the Thermal Stability of Rubisco

Activase in Plants from Contrasting Thermal Environments." Plant Physiology **134**(4): 1460-1470.

Salvucci, M. E., B. P. DeRidder and A. R. Portis (2006). "Effect of activase level and isoform on the thermotolerance of photosynthesis in Arabidopsis." Journal of Experimental Botany **57**(14): 3793-3799.

Salvucci, M. E., K. W. Osteryoung, S. J. Crafts-Brandner and E. Vierling (2001). "Exceptional Sensitivity of Rubisco Activase to Thermal Denaturation in Vitro and in Vivo." Plant Physiology **127**(3): 1053-1064.

Sassenrath, G. F., D. R. Ort and A. R. Portis Jr (1990). "Impaired reductive activation of stromal bisphosphatases in tomato leaves following low-temperature exposure at high light." Archives of Biochemistry and Biophysics **282**(2): 302-308.

Schrader, S. M., R. R. Wise, W. F. Wacholtz, D. R. Ort and T. D. Sharkey (2004). "Thylakoid membrane responses to moderately high leaf temperature in Pima cotton." Plant, Cell & Environment **27**(6): 725-735.

Schreiber, U. and J. A. Berry (1977). "Heat-induced changes of chlorophyll fluorescence in intact leaves correlated with damage of the photosynthetic apparatus." Planta **136**(3): 233-238.

Shahwani, M. N. (2011). Studies on abiotic stress tolerance in Hordeum vulgare L. genotypes from arid and temperate regions. . PhD thesis, University of Glasgow.

Sharkey, T. and S. Schrader (2006). HIGH TEMPERATURE STRESS. Physiology and Molecular Biology of Stress Tolerance in Plants. K. V. Madhava Rao, A. S. Raghavendra and K. Janardhan Reddy, Springer Netherlands**:** 101-129.

Sharkey, T. D. (2005). "Effects of moderate heat stress on photosynthesis: importance of thylakoid reactions, rubisco deactivation, reactive oxygen species, and thermotolerance provided by isoprene." Plant, Cell & Environment **28**(3): 269-277.

Sharkey, T. D., M. R. Badger, S. von Caemmerer and T. J. Andrews (2001). "Increased heat sensitivity of photosynthesis in tobacco plants with reduced Rubisco activase." Photosynthesis Research **67**(1-2): 147-156.

Sharkey, T. D. and R. Zhang (2010). "High Temperature Effects on Electron and Proton Circuits of Photosynthesis." Journal of Integrative Plant Biology **52**(8): 712-722.

Sinsawat, V., J. Leipner, P. Stamp and Y. Fracheboud (2004). "Effect of heat stress on the photosynthetic apparatus in maize (Zea mays L.) grown at control or high temperature." Environmental and Experimental Botany **52**(2): 123-129.

Spreitzer, R. J. and M. E. Salvucci (2002). "Rubisco: structure, regulatory interactions, and possibilities for a better enzyme." Annual review of plant biology **53**(1): 449-475.

Srivastava, A., B. Guissé, H. Greppin and R. J. Strasser (1997). "Regulation of antenna structure and electron transport in Photosystem II of< i> Pisum sativum</i> under elevated temperature probed by the fast polyphasic chlorophyll< i> a</i> fluorescence transient: OKJIP." Biochimica et Biophysica Acta (BBA)-Bioenergetics **1320**(1): 95-106.

Stitt, M., J. Lunn and B. Usadel (2010). "Arabidopsis and primary photosynthetic metabolism–more than the icing on the cake." The Plant Journal **61**(6): 1067-1091.

Stitt, M., W. P. Quick, U. Schurr, E. D. Schulze, S. R. Rodermel and L. Bogorad (1991). "Decreased ribulose-1,5-bisphosphate carboxylase-oxygenase in transgenic tobacco transformed with 'antisense' <i>rbcS</i&gt." Planta **183**(4): 555-566.

Stitt, M. and D. Schulze (1994). "Does Rubisco control the rate of photosynthesis and plant growth? An exercise in molecular ecophysiology." Plant, Cell & Environment **17**(5): 465-487.

Stitt, M., W. Wirtz and H. W. Heldt (1980). "Metabolite levels during induction in the chloroplast and extrachloroplast compartments of spinach protoplasts." Biochimica et Biophysica Acta (BBA) - Bioenergetics **593**(1): 85-102.

Stitt, M., W. Wirtz and H. W. Heldt (1983). "Regulation of Sucrose Synthesis by Cytoplasmic Fructosebisphosphatase and Sucrose Phosphate Synthase during Photosynthesis in Varying Light and Carbon Dioxide." Plant Physiology **72**(3): 767-774.

Stock, D., A. G. Leslie and J. E. Walker (1999). "Molecular architecture of the rotary motor in ATP synthase." Science **286**(5445): 1700-1705.

Sulpice, R., H. Tschoep, M. Von Korff, D. Bussis, B. Usadel, M. Hohne, H. Witucka-Wall, T. Altmann, M. Stitt and Y. Gibon (2007). "Description and applications of a rapid and sensitive non-radioactive microplate-based assay for maximum and initial activity of D-ribulose-1,5-bisphosphate carboxylase/oxygenase." Plant, Cell & Environment **30**(9): 1163-1175.

Sun, W., M. Van Montagu and N. Verbruggen (2002). "Small heat shock proteins and stress tolerance in plants." Biochimica et Biophysica Acta (BBA)-Gene Structure and Expression **1577**(1): 1-9.

Tang, Y., X. Wen, Q. Lu, Z. Yang, Z. Cheng and C. Lu (2007). "Heat Stress Induces an Aggregation of the Light-Harvesting Complex of Photosystem II in Spinach Plants." Plant Physiology **143**(2): 629-638.

Tay, A., A. Abdullah, M. Awang and A. Furukawa (2007). "Midday depression of photosynthesis in Enkleia malaccensis, a woody climber in a tropical rainforest." Photosynthetica **45**(2): 189-193.

Teixeira, E. I., G. Fischer, H. van Velthuizen, C. Walter and F. Ewert (2013). "Global hot-spots of heat stress on agricultural crops due to climate change." Agricultural and Forest Meteorology **170**: 206-215.

Usuda, H. (1985). "The activation state of ribulose 1, 5-bisphosphate carboxylase in maize leaves in dark and light." Plant and cell physiology **26**(8): 1455-1463.

Von Caemmerer, S. (2000). Biochemical models of leaf photosynthesis, CSIRO publishing.

von Caemmerer, S., J. R. Evans, G. S. Hudson and T. J. Andrews (1994). "The kinetics of ribulose-1, 5-bisphosphate carboxylase/oxygenase in vivo inferred from measurements of photosynthesis in leaves of transgenic tobacco." Planta **195**(1): 88-97.

Vu, J. C. V., L. H. Allen and G. Bowes (1984). "Dark/Light Modulation of Ribulose Bisphosphate Carboxylase Activity in Plants from Different Photosynthetic Categories." Plant Physiology **76**(3): 843-845.

Wahid, A., S. Gelani, M. Ashraf and M. Foolad (2007). "Heat tolerance in plants: an overview." Environmental and Experimental Botany **61**(3): 199-223.

Walters, R. and P. Horton (1991). "Resolution of components of non-photochemical chlorophyll fluorescence quenching in barley leaves." Photosynthesis Research **27**(2): 121-133.

Wang, P., W. Duan, A. Takabayashi, T. Endo, T. Shikanai, J.-Y. Ye and H. Mi (2006). "Chloroplastic NAD(P)H Dehydrogenase in Tobacco Leaves Functions in Alleviation of Oxidative Damage Caused by Temperature Stress." Plant Physiology **141**(2): 465-474.

Wang, W., B. Vinocur, O. Shoseyov and A. Altman (2004). "Role of plant heat-shock proteins and molecular chaperones in the abiotic stress response." Trends in plant science **9**(5): 244-252.

Warren, C. and E. Dreyer (2006). "Temperature response of photosynthesis and internal conductance to CO2: results from two independent approaches." Journal of Experimental Botany **57**(12): 3057-3067.

Warren, G. (1998). "Spectacular increases in crop yields in the United States in the twentieth century." Weed Technology **12**(4): 752-760.

Weis, E. (1981). "Reversible heat-inactivation of the Calvin cycle: a possible mechanism of the temperature regulation of photosynthesis." Planta **151**(1): 33-39.

Werneke, J. M., J. M. Chatfield and W. L. Ogren (1989). "Alternative mRNA splicing generates the two ribulosebisphosphate carboxylase/oxygenase activase polypeptides in spinach and Arabidopsis." The Plant Cell Online **1**(8): 815-825.

Wise, R. R., A. J. Olson, S. M. Schrader and T. D. Sharkey (2004). "Electron transport is the functional limitation of photosynthesis in field-grown Pima cotton plants at high temperature." Plant, Cell & Environment **27**(6): 717-724.

Wong, S., I. Cowan and G. Farquhar (1979). "Stomatal conductance correlates with photosynthetic capacity."

Wood, T. (1970). "Spectrophotometric assay for d-ribose-5-phosphate ketol-isomerase and for d-ribulose-5-phosphate 3-epimerase." Analytical Biochemistry **33**(2): 297-306.

Wu, H., Z. Ding, L. Li, Y. Jing and T. Kuang (2006). "Expression of the large isoform of ribulose-1, 5-bisphosphate carboxylase/oxygenase activase gene driven by rbcS promoter in Oryza sativa enhances the photosynthetic capacity." Photosynthetica **44**(2): 208-214.

Wu, H., L. Li, Y. Jing and T. Kuang (2007). "Over-and anti-sense expressions of the large isoform of ribulose-1, 5-bisphosphate carboxylase/oxygenase activase gene in Oryza sativa affect the photosynthetic capacity." Photosynthetica **45**(2): 194-201.

Yamori, W., K. Hikosaka and D. A. Way (2014). "Temperature response of photosynthesis in C3, C4, and CAM plants: temperature acclimation and temperature adaptation." Photosynthesis Research **119**(1-2): 101-117.

Yamori, W., K. Noguchi, Y. T. Hanba and I. Terashima (2006). "Effects of internal conductance on the temperature dependence of the photosynthetic rate in spinach leaves from contrasting growth temperatures." Plant and cell physiology **47**(8): 1069-1080.

Yamori, W., K. Noguchi, Y. Kashino and I. Terashima (2008). "The Role of Electron Transport in Determining the Temperature Dependence of the Photosynthetic Rate in Spinach Leaves Grown at Contrasting Temperatures." Plant and Cell Physiology **49**(4): 583-591.

Yamori, W., K. Noguchi and I. Terashima (2005). "Temperature acclimation of photosynthesis in spinach leaves: analyses of photosynthetic components and temperature dependencies of photosynthetic partial reactions." Plant, Cell & Environment **28**(4): 536-547.

Yamori, W., K. Suzuki, K. Noguchi, M. Nakai and I. Terashima (2006). "Effects of Rubisco kinetics and Rubisco activation state on the temperature dependence of the photosynthetic rate in spinach leaves from contrasting growth temperatures." Plant, Cell & Environment **29**(8): 1659-1670.

Yamori, W. and S. von Caemmerer (2009). "Effect of Rubisco Activase Deficiency on the Temperature Response of CO2 Assimilation Rate and Rubisco Activation State: Insights from Transgenic Tobacco with Reduced Amounts of Rubisco Activase." Plant Physiology **151**(4): 2073-2082.

Yang, N.-C., W.-M. Ho, Y.-H. Chen and M.-L. Hu (2002). "A Convenient One-Step Extraction of Cellular ATP Using Boiling Water for the Luciferin–Luciferase Assay of ATP." Analytical Biochemistry **306**(2): 323-327.

Yang, X., X. Chen, Q. Ge, B. Li, Y. Tong, A. Zhang, Z. Li, T. Kuang and C. Lu (2006). "Tolerance of photosynthesis to photoinhibition, high temperature and drought stress in flag leaves of wheat: A comparison between a hybridization line and its parents grown under field conditions." Plant Science **171**(3): 389-397.

Yeoh, H.-H., M. R. Badger and L. Watson (1981). "Variations in Kinetic Properties of Ribulose-1,5-bisphosphate Carboxylases among Plants." Plant Physiology **67**(6): 1151-1155.

Yordanov, I., S. Dilova, R. Petkova, T. Pangelova, V. Goltsev and K. Kuss (1986). "Mechanisms of the temperature damage and acclimation of the photosynthetic apparatus." Photobiochemistry and photobiophysics.

Yoshida, M., N. Sone, H. Hirata, Y. Kagawa and N. Ui (1979). "Subunit structure of adenosine triphosphatase. Comparison of the structure in thermophilic bacterium PS3 with those in mitochondria, chloroplasts, and Escherichia coli." Journal of Biological Chemistry **254**(19): 9525-9533.

Zhang, J. H., W. D. Huang, Y. P. Liu and Q. H. Pan (2005). "Effects of Temperature Acclimation Pretreatment on the Ultrastructure of Mesophyll Cells in Young Grape Plants (Vitis vinifera L. cv. Jingxiu) Under Cross-Temperature Stresses." Journal of Integrative Plant Biology **47**(8): 959-970.

Zhang, N., R. P. Kallis, R. G. Ewy and A. R. Portis (2002). "Light modulation of Rubisco in Arabidopsis requires a capacity for redox regulation of the larger Rubisco activase isoform." Proceedings of the National Academy of Sciences **99**(5): 3330-3334.

Zhang, N. and A. R. Portis (1999). "Mechanism of light regulation of Rubisco: a specific role for the larger Rubisco activase isoform involving reductive activation by thioredoxin-f." Proceedings of the National Academy of Sciences **96**(16): 9438-9443.

Zhang, N., P. Schürmann and A. R. Portis Jr (2001). "Characterization of the regulatory function of the 46-kDa isoform of Rubisco activase from Arabidopsis." Photosynthesis Research **68**(1): 29-37.

Zhang, R. and T. Sharkey (2009). "Photosynthetic electron transport and proton flux under moderate heat stress." Photosynthesis Research **100**(1): 29-43.

Zhang, Z. and S. Komatsu (2000). "Molecular cloning and characterization of cDNAs encoding two isoforms of ribulose-1, 5-biosphosphate carboxylase/oxygenase activase in rice (Oryza sativa L.)." Journal of Biochemistry **128**(3): 383-389.